EXTENSIONS OF QUANTAL PROBLEMS

by

Emel ACAR

A THESIS SUBMITTED FOR THE DEGREE

OF

DOCTOR OF PHILOSOPHY

THE UNIVERSITY OF SHEFFIELD

School of Mathematics and Statistics

Department of Probability and Statistics

March 2000

Extensions of Quantal Problems

by

Emel Acar

Summary

A problem which arises in many different contexts is whether a given set of data can be regarded as integral multiples of some basic unit (or quantum), observed subject to small errors. Typically, the value of the quantum has to be deduced from the data. This thesis is concerned with the investigation of problems in the analysis of such basic quantal models as well as the extensions required to investigate more complex quantal problems motivated by problems in Biology. These concern lateral rootlet spacings in plants such as onions, tomatoes and ferns and arise in data provided by agricultural research stations in Badajoz, Spain, and Long Ashton, UK.

The first chapter begins with a review of the historical development of quantal problems (notably in relation to atomic weights and megalithic yards) and early approaches to their analyses. The second chapter presents the fundamental statistical tool of quantogram analysis developed by Kendall and an alternative Bayesian approach provided by Freeman in their analyses of the 'megalithic yard problem', establishing various statistical properties of the first of these. The comparative power of statistics for testing for pure and shifted quantality are investigated in the following chapter. Chapter 4 introduces the various sets of data on rootlet spacings with some initial analyses and the following chapter applies basic quantal analyses to these sets, identifying deficiencies in the models in their inability to handle the particular data structures. As a consequence, various extended quantal models are proposed. The first of these, a *hierarchical* quantal model, allows for closely related samples to have distinct but 'close' values of a quantum, perhaps at various levels, analogous to one-way or hierarchical linear models. The second, a *regression* quantal model, allows the value of a quantum to change 'slowly' with a covariate (e.g. the position along the parent root). Various computationally intensive algorithmic techniques and graphical tools for their analysis are proposed and applied in Chapter 6. Chapter 7 returns to the Bayesian formulation and applies MCMC methods to the analysis, adapting the approach to cover the extended quantal models. Throughout, new techniques for analysis are illustrated and validated on simulated data before application to the data on rootlet spacings. Chapter 8 summarises and concludes the thesis.

Acknowledgements

I would like to express my deepest thanks to my supervisor, Dr. Nick Fieller, for his thoroughly insightful guidance, enthusiastic involvement, encouragement and support throughout this study. I am also grateful to him for his patience and friendship during the difficult times of my stay in Sheffield. The contributions of the Ministry of National Education of the Turkish Republic must particularly be emphasised for generously sponsoring this research via one of the most prestigious scholarships they provided for me. I am also indebted to the staff in the Ministry for their helpful and friendly approach towards myself. I cannot fail to extend my gratitude to Dr. Pedro Llorett who provided the onion data set as well as Dr. Peter Barlow, who kindly helped to clarify the biological aspects of the research problem, for providing the tomato and fern data sets. I am also grateful to Prof. Clive Anderson not only for his useful suggestions but also for providing the relevant computer program.

A special gratitude goes to my family for their patience and unfailing support during this study. I have also learned from friends among whom I can mention particularly Mike Preston for his help in programming and his constant friendship. I also take pleasure in thanking Alexandra Schmidt for her warm friendship and her valuable comments and discussions at final stages of the study. I am also grateful to Mark Pilling for his generous help whenever I needed. To Jose Ferreira, Sofia Caires, Maged Messeh, Rick Munro and Hyun Ku Yeun, I sincerely thank for their help on various matters, useful discussions, friendships and also for the social events. I would like to mention also Sofia Lopes with whom I had friendly chats during the share of the same office. Not to forget my friends back home Nilüfer Metin and Arzu Şahım who supported me through the letters and phone calls which kept me going.

Emel ACAR, March 2000

Dedicated to my Mother and Father.
Annem ve Babam'a armagan edilmistir.

CONTENTS

CHAPTER 1:

Introduction and Background 1

1.1. Introduction 1

1.2. Examples in the Literature 2

1.3. Outline of Thesis 7

CHAPTER 2:

Theoretical Background 10

2.1. Introduction 10

2.2. Statistical Description of Quantality 11

2.3. The Classic Data Sets 12

2.4. Quantal Models 14

2.4.1. The Pure Quantum Model 14

2.4.2. The Shifted Quantum Model 15

2.5. Previous Methods of Analysis 16

2.5.1. von Mises' Method 16

2.5.2. Broadbent's Method 18

2.6. Kendall's Method: Quantogram Analysis 20

2.6.1. Cosine Quantogram 20

2.6.1.1. A Likelihood Ratio Test for Pure Quantality 23

2.6.2. Modular Quantogram 24

2.6.2.1. A Likelihood Ratio Test for Shifted Quantality 25

2.6.3. Quantogram Graphs 27

2.6.4. Range and Resolution of the Search (q_{min}, q_{max}) 30

2.6.5. Assessing Significance Probabilities 32

2.6.6. Testing the Significance of the β effect 35

2.6.7. Estimation Methods for the β effect 36

2.7. Freeman's Method: A Bayesian Approach 38

2.8. Basic Properties of the Test and Estimation Procedures 41

2.8.1. Half–Normal Probability Plots 41

2.8.2. Some Features of Suprema 43
2.8.2.1. Fitting the G.E.V. Distribution 43
2.8.2.2. A Natural Scale for Gridsearch 47
2.8.2.3. The Effect of the Underlying Distribution 49
2.8.3. The Effect of Random Number Generator 50
2.8.4. The Effect of Autocorrelation 54
2.9. Summary 58

CHAPTER 3:
Power of Significance of Test Statistics 59
3.1. Introduction 59
3.2. The von Mises Distribution 60
3.3. Comparison of the Power of the Test Statistics 62
3.3.1. Critical Values for Pure Quantality 63
3.3.2. Power Calculations for Pure Quantality 65
3.3.3. Power Calculations for Shifted Quantality 68
3.4. The Effect of Sample Size 70
3.5. Concluding Comments 76

CHAPTER 4:
Lateral Root Spacing 77
4.1. Introduction 77
4.2. Data 79
4.2.1. The Onion Data Set 81
4.2.2. The Tomato Data Set 83
4.2.3. The Fern Data Set 83
4.3. Preliminary Analyses 84
4.3.1. Preliminary Analyses on the Onion Data Set 84
4.3.2. Preliminary Analyses on the Tomato Data Set 88
4.3.3. Preliminary Analyses on the Fern Data Set 92
4.4. Concluding Remarks 94

CHAPTER 5:

Quantality of Lateral Roots 96

5.1. Introduction 96

5.2. The Scope and Objectives 97

5.3. The Nature of Quantality for Spacings.. 98

5.4. Initial Quantogram Analyses 100

5.4.1. Practical Considerations 100

5.4.1.1. The Range of Gridsearch.. 100

5.4.1.2. The Accuracy of Measurements 102

5.4.1.3. Assessment of the Significance 104

5.4.2. Quantogram Analyses on the Onion Data Set 105

5.4.2.1. Unrounding the Onion Data Set 109

5.4.2.2. Analyses of Spacings and Positions 114

5.4.3. Quantogram Analyses on the Tomato Data Set 116

5.4.3.1. Analyses of Spacings on the Left and Right Series.......... 117

5.4.3.2. Analyses of Spacings on the Total Series........................ 119

5.4.3.3. Analyses of Positions of the Left, Right and Total Series 120

5.4.4. Quantogram Analyses on the Fern Data Set 122

5.4.5. Issues of Multiple Testing.. 125

5.5. Extended Quantal Models 126

5.5.1. Hierarchical Quantal Models 126

5.5.2. Regression Quantal Models 128

5.6. Discussion 129

CHAPTER 6:

Approaches to Constructing Extended Quantal Models........................... 131

6.1. Introduction 131

6.2. Combining Weak Quantality.. 133

6.2.1. Proposal of a New Aggregate Test Statistic 133

6.2.2. Fisher's Combined Test.. 135

6.2.3. The Power of the Two Combination Procedures.......................... 136

6.2.4. An Algorithmic Approach for Implementing the New Test Statistic 143

6.3. Hierarchical Quantal Models for Onion Roots....... 146
6.3.1. Analyses of Raw Spacings on the Rank and Total Series....... 146
6.3.2. Analyses of Positions on the Rank and Total Series....... 148
6.4. Hierarchical Quantal Models for Tomato Roots....... 150
6.4.1. Analyses of Raw Spacings on the Left, Right and Total Series.... 151
6.4.2. Analyses of Positions on the Left, Right and Total Series....... 156
6.5. One–way Anova Type of Residual Analyses....... 161
6.5.1. Introduction....... 161
6.5.2. Residual Analyses on the Simulated Data....... 163
6.5.3. Residual Analyses on the Root Spacings....... 173
6.6. Overall Conclusions for Onion and Tomato Roots....... 180
6.7. Constructing Regression Quantal Models....... 182
6.7.1. Detection of the Structure: Residual Analyses....... 182
6.7.2. Analysis of the Fern Data using Regression Quantal Model....... 186
6.8. Concluding Remarks....... 188

CHAPTER 7:
A Bayesian Approach....... 191
7.1. Introduction....... 191
7.2. Markov Chain Monte Carlo (MCMC) Method....... 193
7.2.1. Gibbs Sampling Method....... 194
7.2.2. Metropolis–Hastings Method....... 195
7.2.3. Implementation: The BUGS Software....... 195
7.2.4. Monitoring Convergence: The CODA Software....... 197
7.3. Refinements of Freeman's Bayesian Analysis using MCMC....... 198
7.3.1. Critical Review....... 198
7.3.2. Prior Specifications....... 200
7.3.3. Posterior Distributions....... 201
7.3.3.1. Uniform Prior on Standard Deviation (σ)....... 209
7.4. Hierarchical Bayesian Models for Structural Quantality....... 212
7.4.1. Model Specifications for Hierarchical Quantality....... 213
7.4.2. The Assumption of Exchangeability....... 215
7.4.3. A Simulation Study....... 215

7.4.4. Model Criticism 224
7.5. Applications to the Root Spacings 225
7.6. Conclusions 230

CHAPTER 8:
Summary and Conclusions 233
8.1. Introduction 233
8.2. New Features of Existing Methodology 235
8.3. Methodological Developments 236
8.4. Suggestions for Practical Use 238
8.5. Possibilities for Further Research 239

APPENDICES 241
A. List of the Computer Programs 242
B. Results of Initial Quantogram Analyses on Onion Roots 243
C. Results of Initial Quantogram Analyses on Tomato Roots 250
D. Results of Simple and Regression Quantality Search on Fern Roots 256
E. Additional Results of Hierarchical Quantality Search 259
F. Data Sets 262

REFERENCES 276

LIST OF FIGURES

2.1. An example of the Cosine Quantogram graph 29

2.2. Plot of peak cosine quantogram value against number of points (N) searched 31

2.3. Plot of estimated quantum against number of points (N) searched 32

2.4. Half – Normal plot of the circle diameters 42

2.5. Empirical density of supremum values 45

2.6. Probability plot of extreme values 46

2.7. Q–Q plot of extreme values for G.E.V. distribution 46

2.8. Histogram of the 1000 $\hat{\tau}_i$ values 48

2.9. Scatter plot of $\phi(\hat{\tau}_i)$ against $\hat{\tau}_i$ 48

2.10. Empirical densities of the suprema when underlying distribution is Exponential, Gamma, Beta, h-Normal and Uniform (dotted line) 49

2.11. Empirical densities of the supremum values 57

3.1. Power of two test statistics for Pure Quantality 67

3.2. Power of two test statistics for Shifted Quantality when κ=1 69

3.3. Power of $\phi(\tau)$ for Shifted Quantality with respect to κ 70

3.4. Sample size effect on the power of $\phi(\tau)$ for Pure Quantality 71

3.5. Sample size effect on the power of $\chi(\tau)$ for Pure Quantality 71

3.6. A plot of differences between powers of $\phi(\tau)$ and $\chi(\tau)$ Pure Quantality. 72

3.7. Power of $\phi(\tau)$ for Pure Quantality; — regardless of estimated quantum, - - - when estimated quantum is within [0.95–1.05] 74

3.8. Power of $\chi(\tau)$ for Pure Quantality; — regardless of estimated quantum, - - - when estimated quantum is within [0.95–1.05] 75

4.1. A picture of a tomato root bearing laterals and potential budding cells...... 80

4.2. Circumferential positioning of roots of Onion, Tomato and Fern 81

4.3. Schematic representation of the data from one root on onions 82

4.4. Boxplots of combined rank series and total series of onion roots 87

4.5. Boxplots of left and right series on the tomato roots 90

4.6. Boxplots of total series on the tomato roots 91

4.7. Boxplots of fern root spacings 93

5.1. Cosine Quantogram graph for the C1 root 108
5.2. Cosine Quantogram graph for the W5 root 108
5.3. Cosine Quantogram graph for the S6 root 109
5.4. Results of gridsearch on the C1 root after 'unrounding' 111
5.5. Results of gridsearch on the W5 root after 'unrounding' 112
5.6. Results of gridsearch on the S6 root after 'unrounding' 113
5.7. Histograms for theseries of the CT1 root 124
6.1. Powers of T^* and T^F for hierarchical quantality, k=3 and n=50 140
6.2. Plots of residuals when range=0.0544; (a) σ_2=0.00001; $\hat{q}$=5.4407, (a)' reproduction of (a), and (b) σ_2=0.05; $\hat{q}$=5.4407 168
6.3. Plots of residuals when range = 0.272; (a) σ_2 = 0.01; $\hat{q}$=5.4407, (b) σ_2 = 0.272; $\hat{q}$=5.4407 169
6.4. Plots of residuals when range=0.544; (a) σ_2=0.00001; $\hat{q}$=5.4555, (b) σ_2=0.55; $\hat{q}$ = 5.4318 170
6.5. Plots of residuals when range = 1.36; (a) σ_2=0.1; $\hat{q}$ = 2.7218, (b) σ_2=0.5; $\hat{q}$ = 4.8169 171
6.6. Plots of residuals when range=2.72; (a) σ_2 = 0.1; $\hat{q}$ = 4.0916, (b) σ_2=1.5; $\hat{q}$ = 4.0966 172
6.7. Residual plots for treatment groups of onions 174
6.8. Residual plots of Wild type roots 176
6.9. Residual plots of Naa treated Wild type roots 177
6.10. Residual plots of Gib-1 Mutant type roots 178
6.11. Residual plots of Naa treated Gib-1 Mutant type roots 179
6.12. Plot of residuals versus i^{th} observation when σ = 0.00001 184
6.13. Plot of residuals versus i^{th} observation (a) when the length of the root is longer and ε_i =0, (b) σ=0.0001 and (c) σ=0.001 185
6.14. Residual plot for the total series of CT4 186
7.1. A simple graphical model 196
7.2. Log–posterior as a function of q and σ 199
7.3. Graphical representation of simple quantal model in BUGS 202
7.4. Convergence monitoring plots and kernel density plots of each variable for the Good Rings data (n=16) 204
7.5. Plots of Z-scores and autocorrelations between sample values 205

7.6. Trace of first 1000 iterations for q (4th run in table 7.3)............................ 208

7.7. Trace of 501:5500 iterations for q (5th run in table 7.3)............................ 208

7.8. Kernel plot of 501:5500 iterations for q (5th run in table 7.3)................... 208

7.9. Trace of the chains for q and σ (run 4)... 211

7.10. Graphical representation of the Hierarchical Bayesian model for the hierarchical quantality 216

7.11. (a) Convergence monitoring plots and kernel density plots of each variable in Hierarchical Bayesian model for run 1 in table 7.7.................. 220

7.11. (b) Convergence monitoring plots and kernel density plots of each variable in Hierarchical Bayesian model for run 1 in table 7.7.................. 221

7.12. Plots of autocorrelations for each variable in Hierarchical Bayesian model for run 1 in table 7.7. 222

7.13. Convergence monitoring plots for q when (a) WR1–L; run 1, (b) WR1–L; run 2, (c) WR1–R are used 227

7.14. Convergence monitoring plots of q for run 1 (σ_q=0.01) and run 2 (σ_q=1).. 229

B1. Gridsearch results from the Control group onion roots (combined rank series) after 'unrounding' with U(-0.5, 0.5) variate 245

LIST OF TABLES

2.1. The data sets of circle diameters 13

2.2. Results of Quantogram analyses on stone circles (increment=0.0001)....... 35

2.3. Estimated critical values with 95% C.I. and observed significance probabilities for $\phi(\hat{\tau})$ and $\chi(\hat{\tau})$ using different random generators........... 54

2.4. The estimated critical values for $\phi(\tau)$ when data are autocorrelated 57

3.1. Estimated 5% critical values for $\phi(\tau)$ and $\chi(\tau)$ 65

3.2. Estimated powers of $\phi(\tau)$ and $\chi(\tau)$ with respect to κ........ 67

3.3. The total variation of δ with respect to κ and n........ 73

4.1. Number of laterals on each rank and total series of onion roots 85

4.2. Mean distance (± s.e.) and first order autocorrelation between successive laterals in the Control group........ 86

4.3. Mean distance (± s.e.) and first order autocorrelation between successive laterals in the Weak–treated group and Strong–treated group 86

4.4. Mean value (± s.d.) of number of laterals, mean spacings and autocorrelation coefficients per root for Wild type........ 88

4.5. Mean value (± s.d.) of number of laterals, mean spacings and autocorrelation coefficients per root for Gib–1 Mutant 89

4.6. Mean value (± s.d.) of number of laterals, mean spacings and autocorrelation coefficients per root in Ferns........ 92

5.1. The subsidiary peaks produced by the W5 root 107

5.2. The subsidiary peaks produced by the S6 root........ 107

5.3. Results of gridsearch on the C1 root unrounded with a variate U(–a, a) 111

5.4. Results of gridsearch on the W5 root unrounded with a variate U(–a, a) ... 112

5.5. Results of gridsearch on the S6 root unrounded with a variate U(–a, a)..... 113

5.6. Ranges of gridsearch (in terms of q) according to data types and treatment groups........ 114

5.7. Gridsearch results on the treated roots of onions 115

5.8. Gridsearch results using positions of rank and total series on treated roots 116

5.9. Ranges (in terms of q) of search with respect to different data and tomato types 116

5.10. Gridsearch results using right and left series on WR roots 118

5.11. Gridsearch results using right and left series on GR roots 118
5.12. Gridsearch results using right and left series on NWR roots 119
5.13. Gridsearch results using right and left series on NGR roots 119
5.14. Gridsearch results using total series on WR & NWR roots 120
5.15. Gridsearch results using total series on GR & NGR roots 120
5.16. Gridsearch results using positions of L, R & T series on WR roots 121
5.17. Gridsearch results using positions of L, R & T series on GR roots 121
5.18. Gridsearch results using positions of L, R & T series on NWR roots 122
5.19. Gridsearch results using positions of L, R & T series on NGR roots 122
5.20. Gridsearch results using L R & T series on Fern roots 123
5.21. Gridsearch results using positions of L, R &T series on Fern roots........... 124
6.1. The simulated powers of T^* and T^F when $n_1=n_2=n_3=n$; n=50,100............. 141
6.2. Maximum likelihood estimates (s.e.) of parameters of G.E.V................... 142
6.3. Results of hierarchy level 1 analyses for rank series of Control, Weak and Strong–treated roots.. 146
6.4. Results of hierarchy level 2 analyses for rank series of Strong–treated roots.. 147
6.5. Results of hierarchy level 3 analyses for rank series of Strong–treated roots.. 147
6.6. Results of hierarchy level 1 analyses for positions of rank series on the Weak and Strong–treated roots 148
6.7. Results of hierarchy level 2 analyses for positions of rank series on the Strong–treated roots 149
6.8. Results of hierarchy level 3 analyses for positions of rank series on the Strong–treated roots 149
6.9. Results of hierarchy level 1 analyses for positions of total series on the Control, Weak–treated and Strong–treated roots 150
6.10. Results of hierarchy level 1 analyses for Wild, Naa treated Wild, Gib–1 and Naa treated Gib–1 type roots (left and right series used) 151
6.11. Results of hierarchy level 1 analyses for Wild, Naa treated Wild, Gib–1 and Naa treated Gib–1 type roots (total series used).................................. 152
6.12. Results of hierarchy level 2 analyses for Wild type roots and also results of level 3 analyses for their corresponding L, R & T series........................ 154
6.13. Results of hierarchy level 2 analyses for Naa treated Wild type roots and also results of level 3 analyses for their corresponding L, R & T series..... 154

6.14. Results of hierarchy level 2 analyses for Gib–1 Mutant roots and also results of level 3 analyses for their corresponding L, R & T series 155

6.15. Results of hierarchy level 2 analyses for Naa treated Gib–1 roots and also results of level 3 analyses for their corresponding L, R & T series 156

6.16. Results of hierarchy level 1 analyses for Wild, Naa treated Wild, Gib–1 and Naa treated Gib–1 groups (positions of left and right series used)....... 157

6.17. Results of hierarchy level 1 analyses for Wild, Naa treated Wild, Gib–1 and Naa treated Gib–1 groups (positions of total series used)................... 157

6.18. Results of hierarchy level 2 analyses for Wild roots and also results of level 3 analyses for their L, R & T series (positions used)......................... 158

6.19. Results of hierarchy level 2 analyses for Naa treated Wild roots and also results of level 3 analyses for their L, R & T series (positions used).......... 159

6.20. Results of hierarchy level 2 analyses for Gib–1 roots and also results of level 3 analyses for their L, R & T series (positions used)......................... 159

6.21. Results of hierarchy level 2 analyses for Naa treated Gib–1 roots and also results of level 3 analyses for their L, R & T series (positions used) .. 160

6.22. Considered range of quantum values varying around $q_2 \approx 5.44$................. 164

6.23. Results of 2–D gridsearch on the Fern roots 188

7.1. Posterior summaries of each parameter (run 1)... 202

7.2. Diagnostics of the estimates of the parameters from CODA (run 1) 203

7.3. Posterior summaries and convergence diagnostics for different runs 207

7.4. Posterior summaries and convergence diagnostics for different runs when integers are given discrete Uniform prior.. 210

7.5. Posterior summaries and convergence diagnostics when integers are given a truncated Poisson prior 211

7.6. Posterior summaries and convergence diagnostics for different runs when integers are given a Binomial prior 212

7.7. Posterior summaries and their diagnostic test results for different runs when τ_q ~ Gamma(160000, 400) 219

7.8. Posterior summaries and their diagnostic test results for different runs when τ_q ~ Gamma(400000, 625) 223

B1.1. Full results of gridsearch for Control root spacings 244

B1.2. Full results of gridsearch for Weak–treated root spacings 246

B1.3. Full results of gridsearch for Strong–treated root spacings........................ 247

B2.1. Full results of gridsearch for Weak–treated root positions 248

B2.2. Full results of gridsearch for Strong–treated root positions 249

C1.1. Full results of gridsearch for Wild type tomato roots 251
C1.2. Full results of gridsearch for Wild type, Naa treated tomato roots 252
C1.3. Full results of gridsearch for Gib–1 Mutant type tomato roots 242
C1.4. Full results of gridsearch for Gib–1 Mutant type, Naa treated tomato roots 253
C2.1. Full results of gridsearch for Wild type tomato positions 253
C2.2. Full results of gridsearch for Wild type, Naa treated tomato positions....... 254
C2.3. Full results of gridsearch for Gib–1 Mutant type tomato positions 255
C2.4. Full results of gridsearch for Gib–1 Mutant type, Naa treated tomato positions 255
D1.1. Full results of gridsearch for Fern root spacings 257
D1.2. Full results of gridsearch for Fern root positions 257
D2.1. Full results of 2D gridsearch for Fern root positions 258
E1. Results of hierarchy level 2 analyses for Wild type roots and also level 3 analyses for their corresponding L and R series 260
E2. Results of hierarchy level 2 analyses for Gib–1 Mutant roots and also level 3 analyses for their corresponding L and R series 261
E3. Results of hierarchy level 2 analyses for Gib–1 Mutant roots and also level 3 analyses for their corresponding L and R series (positions used).... 261
F1.1. Control group root spacings (mm) 262
F1.2. Weakly–treated group root spacings (mm) 265
F1.3. Strongly–treated group roots spacings (mm) 266
F2.1. Wild type tomato root spacings (cm) 268
F2.2. Gib–1 Mutant type tomato root spacings (cm)... 270
F2.3. Wild type, Naa treated tomato root spacings (cm) 272
F2.4. Gib–1 Mutant type, Naa treated tomato root spacings (cm) 274
F3.1. Fern root spacings (cm) 275

CHAPTER 1.

Introduction and Background

1.1. Introduction

Many scientific questions can be investigated by statistical analysis of relevant data. In particular, the development, analysis and use of statistical models is a fundamental aspect of many scientific studies. Modelling is establishing a relationship between theory, data and reality. A scientific theory is reflected in a statistical model, data are collected and the model is assessed in relation to the data. Sometimes the model is very specific and describes very precisely the form of data anticipated (e.g. that two variables are linearly related), sometimes it is less so.

Many statistical models specify very precisely the form of any potential data: distributional form, relationship with covariates and correlation structure may all be specified except for a small number of estimably parameters. Other models are less prescriptive. This thesis is concerned with the investigation of problems which give rise to models which only partially describe the form of any data collected, that is, they describe only some structural feature without necessarily completely specifying the full distributional form. Examples of problems within the scope of this work are whether builders of megalithic stone circles used a standard unit of measurement, whether atomic weights of nuclei reflect composition of different numbers of identical fundamental particles, whether roots on plants have a systematic sequence of potential budding cells which may (or may not) eventually produce secondary rootlets, whether red-shifts of galaxies reveal a lattice structure of the universe.

In all of these widely differing examples data are available (diameters of stone circles, weights of nuclei, spacing between roots, redshifts and coordinates of galaxies). However, the scientific theories of interest suggest only a partial description of the structure of the data. The common feature of all these examples is that the data are integral multiples of some underlying base unit (or quantum) which is typically unknown before the analysis begins. We term such a model for the data *a quantal model*.

We describe some of these examples in greater detail in later sections and give more precise formulations of quantal models and various extensions and refinements of them. We show how these models can be assessed statistically and investigate the importance and effects of various simplifying assumptions used in analyses.

1.2. Examples in the Literature

The earliest realisation of the problem was in 1815 by Prout, a medical practitioner and chemist, who believed that atomic weights of chemical elements are whole number multiples of the atomic weight of hydrogen. A century later the matter was first tackled with the aid of statistical techniques by a statistician (von Mises, 1918) and had become a scientific issue. In 1918, the structure of atoms was still not well understood however it was observed that there was not a smooth continuum in atomic weights. Later discoveries proved that the reason for this is due to the fact that there has to be an integral number of neutrons and protons in atoms that contribute most to atomic weights but this was not known at the time of von Mises.

Almost twenty years later, Svedberg (1939) investigated the distribution of the molecular weights of proteins and deduced an approximate rule that ‘law of simple multiples....If we choose 17 600 as the unit, the majority of the proteins may be divided into eleven classes with molecular weights which are multiples of this unit by factors containing powers of 2 and 3’, which claims to define a well established protein structure. His hypothesis was further investigated by Johnston et al. (1945) using some function and they concluded, however, that Sverberg’s hypothesis receives no support from the evidence.

In the mid 1950s, Grant (1952) proposed the theory that the observed energy levels of atomic nuclei were integer multiples of a particular energy for each nucleus. The quantum proposed by Grant was based on inspection of the data.

Hammersley & Morton (1954) conjectured that the problem of assigning a probability level to a quantum was beyond the present analytic resolution, and offered a Monte Carlo method to test the supposed grouping.

Broadbent (1955, 1956) illustrated some data sets that suggest a quantum hypothesis by the occurrence of regularly spaced modes. He gave a rigorous method of handling the case of the problem in which an estimate of the quantum is required. In addition, he improved the Monte Carlo solution to test whether the apparent grouping is a coincidence or not. His method has been extensively used by archaeologists (Thom, 1955, 1967) and cosmologists (Grieve and et al, 1985). He also considered the situations in which a quantum model applies after the variate is transformed. For example, he showed that Brook’s law (Fowler, 1909) as stated for the insect Ostracoda, that ‘during early growth, each stage increases at each moult by a fixed percentage of its length, which is approximately constant for its species and sex’ and Przibram’s rule (Wigglesworth, 1942) that ‘the weight doubles at each instar, and each moult all linear dimensions are multiplied by $\sqrt[3]{2}$’ would take the form of quantum model when the logarithms of the weights or lengths are taken.

Quantal problems came to the notice of statisticians with Thom's interpretation of the method of construction of the megalithic stone circles in the British Isles (1955, 1967). There are a large number of these megalithic stone structures and the stones appear to lie on, or close to, the circumference of a circle or ellipse. He measured the diameters of 211 such circles from Scotland, England and Wales and made the most notable data set available. He was concerned with the reasons for the erection of these structures, discussing such matters as the possible astronomical significance of various alignments of the stones and he proposed the theory that the society in megalithic times possessed a unit of length in a way that many of the dimensions of the megalithic sites could be expressed as integer multiples of a megalithic yard which he claimed to be 2.72 ft, or almost equivalently integer multiples of 5.44 ft. There have been many investigations of his theory and it has become the most famous example in the literature. His conclusions on the various astronomical orientations and alignments of the stones in relation to the rising or setting of sun, moon or bright stars have been justified in the archeoastronomical studies of many Megalithic sites (Ruggles, 1984). Thom's interpretation of the 'Megalithic Yard' has also caused confusion and from time to time it has been discussed in various short papers (Olson, 1980; Stewart,1993; Salisbury, 1994; Kirk, 1994).

The problem was tackled, and an attractive solution (cosine quantogram analysis, to be defined in greater detail later) was proposed by Kendall (1974) in the context of the 'megalithic yard' problem. In outline, the method can be described as bootstrapping the empirical characteristic function of the data. He could thus conclude that although the evidence that there is a quantum of 5.44 is less conclusive than one would wish, it is nevertheless strong enough at least to justify the expense of an improved and more accurate survey of the sites.

Later, Freeman (1976) continued Kendall's analysis by considering a Bayesian approach to the problem. It was aimed at examining the possible values of the megalithic quantum rather than at proving or refuting any particular value. His results confirmed Kendall's results which indicated that much of the evidence for the megalithic yard resides almost entirely in the data from Scotland.

There are some other applications concerning ancient mensuration systems (Hewson, 1980; Petruso, 1978, 1981, 1992). Interest is in how systems of measurement of length, volume or weight have developed in societies. Particular interest is in the development of systems around Aegean. It is of interest to know whether there was a fundamental unit of length in use in one society that became adopted by others. This would reflect on patterns of cultural influence. For example, is there a 'Minoan foot' and if so is it related to Spartan and Doric feet? Is there a common unit that might gradually take the place of local units just as some of the metric system has replaced some national units in Europe in the past. Again, whether there was a Troy ounce or Greek pint in societies are other interesting examples in such studies.

Rottländer (1996, 1997) showed that the very beginning of the use of standard measures dates back to a far earlier time than has previously been believed. He found strong evidence that the units of the ell of Nipur in Mesopotamia and the megalithic yard had spread out all over the world from one single region of origin before transformations lead to the manifold units of the first century BC. The units of length were not repeatedly invented at different places and at different times. For example, it is remarkable that 16 cubits of the unit of the ell of Nipur are most precisely as long as ten megalithic yards and at the same time equal to 28 Roman feet.

In addition to such problems, another quantal problem arose in a study of the migration patterns of inter-glaciation Devensian horses. In teeth excavated from caves at Kent's Cavon and Wookey Hole there is substantial evidence in support of apparent periodicities in horse tooth wear stages (i.e. quantal crown heights) that point to seasonal exploitation of the animals in the area which is likely to be the result of just seasonal presence of the horses which were then predated upon by carnivores living in the caves (Turner & Fieller, 1981). A similar problem arises with the seasonal migration pattern of red deer as revealed by the crown heights of their teeth (Klein et al. 1981).

More recently, unsuspected regularities of galactic red-shifts have become a considerable controversy among cosmologists (Tifft and Cocke, 1984; Guthrie and

Napier, 1991). They speculated that redshifts of certain galaxies have a periodic structure but gave, however, an unconvincing statistical assessment of significance. A more rigorous statistical analysis was given by Knox (1994) using extended quantal models to tackle the question of whether, nucleus to nucleus, the redshifts of spiral galaxies exhibit a quantal property. Evidence in favour of quantality obtained from these studies might suggest that the universe has a "lattice" structure rather than the Hubble model of the expanding universe.

It is also noteworthy that Fieller (1993) stated that an unexpected quantal problem arises in tree-rings obtained from timbers of the Sweet Track in the Somerset Levels. The data are not the widths of the rings but their actual numbers in a variety of timbers of different species. Rather than dating of these species, archaeologists are concerned with learning something about the woodland management practices of builders of the track. Particular interest is in answering the question whether the number of rings provide any evidence of regular coppicing. Such information gives additional insight into the level of sophistication of the society at that time.

He also pointed that another application of quanta hunting concerns Roman field systems in Libyan Wadis (Fieller et al., 1990; Gilbertson et al., 1993). The field systems are mainly linear sequences of fields which are separated by parallel walls across the wadi (i.e. dry valleys). Supposing that the sizes of the fields might be optimal in some circumstances, this might be revealed by some regularity in the spacings of walls.

Turning now to the examples which have been the motivation for the current work of this thesis, some theories in developmental biology predict quantality within the rhythm of lateral roots production in some plants (Barlow & Adam, 1988). For instance, spacing problems in tomato roots were tackled with the aid of quantogram analysis and it was found that some series of the roots had a quantal tendency (Newson et al, 1993a), which suggests that the root may be viewed as being segmented. It was anticipated that such information would alter the knowledge about how roots develop.

The present project concerns in particular the quantality of spacing in onion, tomato and fern roots. That is whether the secondary rootlets on these plants are systematically spaced out along the parent roots. If a quantum could be shown to be a feature of the observed roots, then it would be possible to identify potential budding cells in position on the parent root, which would support the segmental view of the root on plants. Consequently, it would help Biologists to understand the process of growth and differentiation of organs. Due to the hierarchical structure of the data set on onion roots, we are now required to develop an analogy to linear models with an hierarchical structure of quantal models (see section 5.5), which is what distinguishes this study from the previous studies. We also use these techniques to re-examine the data (previously analysed by Newson et al, 1993a) provided by Barlow (with further additions for the current study) as well as further data supplied by Lloret (1998).

In the following section we will outline the structure of the thesis.

1.3. Outline of Thesis

This thesis places the quantal problems in its broadest context by imposing different dimensions to quantality that have been suggested by the current data sets. It contains comprehensive definitions of problems and analyses concerning quantality. In addition, it suggests new extensions to quantal models to construct what we have named ‘hierarchical quantal models’ and ‘regression quantal models’. It is hoped that the suggested models and approaches could be applied to cases similar to the quantality of spacing problems.

We begin in the next section with a general description of the concept of quantality in statistical terms by giving an initial formulation of the basic quantal models. It is continued with a review of the various approaches towards the solution of such problems, emphasising similarities and differences between them. Then the most effective method among those, “cosine quantogram analysis”, is introduced in more detail. A fuller description of the well–known Megalithic Yard problem is given to establish various basic properties of the test statistics. Some aspects of the performance of the testing procedure under the violation of assumption of independence are finally outlined here.

Chapter 3 is concerned with a comparison of the power of the test statistics available in relation to two kinds of quantality. Various aspects and results of this comparative study based on simulations are demonstrated and performance of test statistics under certain conditions is discussed.

Chapter 4 presents the full description of the current new quantal problem on spacings of lateral roots of various plants: onions, tomatoes and ferns. This section involves not only a general examination of structure of the data but also an exploration of basic statistical properties of the data. This section prepares for the identification of ideas developed in later chapters.

Again, motivated by the Biological questions, the following chapters are devoted to the investigation of quantal pattern in root spacings and development of new models which would take into account the structure of this new problem.

In Chapter 5 we therefore identify full aspects of the current problem by means of the basic quantogram analyses initially carried out on individual root series. The prime objective of this part is to show that there is a need to extend basic quantal models to the cases where quantality can not be expressed by a common quantum and it is rather variable either within a hierarchy of different roots, plants and treatments – that is a hierarchical quantal model, or along the same root – that is a regression quantal model. The formulation of these newly proposed models is demonstrated and the analytical problems within extensions are discussed.

Chapter 6 develops the methodology for the assessment of structural, both 'hierarchical' and 'regression', quantality. Various approaches are here suggested to quantify the considerations in constructing the proposed models. Our first approach for the detection of such quantality is to perform some residual analyses, using an analogue of that for one–way Anova models. Simulated hierarchical and regression quantal data are here used to demonstrate visually the effect of the existence of structural quantality and observed patterns are compared with the ones obtained from the current data sets. Secondly, we illustrate an algorithmic approach to recognise any hierarchical system of quantum and combine the evidence from different sets of data by an composite test. For the investigation of regression-like behaviour, we use only the fern data sets and the assessment is made by performing two-dimensional quantogram analyses.

Chapter 7 presents a Bayesian Approach. The first part of this chapter is devoted the critical review of previous Bayesian analysis for the basic quantal models. Then refinements have been achieved by means of MCMC methods within the framework of a new package program called BUGS, Bayesian Inference Using Gibbs Sampling. The subsequent part develops Hierarchical Bayesian models in order to consider new forms of quantality proposed within the scope of this study.

Finally, Chapter 8 demonstrates the overall conclusions and gives some directions for future work.

The bulk of this thesis is concerned with the evaluation of the suggested quantogram analyses and the analyses of the algorithmic approaches which can only be carried out numerically. Computer programs to perform the analyses and also the simulation studies have been written in FORTRAN 77 (version 3.5). Bayesian estimation problems have been dealt within the BUGS package program Windows version 1.1 and 1.2. The essential programs written are listed in Appendix A. Other appendices contain the data sets used and mathematical results of the quantogram analyses.

CHAPTER 2.

Theoretical Background

2.1. Introduction

In this chapter we present the basic statistical problem considered in the thesis. Section 2.3 gives a guide to the classic data sets which have generated interest in the problem and in section 2.4 we present formal models for expressing quantality. We give a historical outline of various approaches proposed for investigating it (in section 2.5) and concentrate on the technique developed by Kendall (1974) in section 2.6, providing comments on his development and showing that Kendall's method can be formulated as a likelihood ratio approach. In section 2.7 we describe briefly, a Bayesian approach as given by Freeman (1976) and which is extended in Chapter 7. Section 2.8 describes a study of various properties of Kendall's procedure such as the sensitivity of the test to the underlying 'non–quantal' distribution used to model the data, the null distribution of the test statistic and whether it is better or 'more natural' to base the analysis in terms of the quantum itself or the 'frequency measure' of the reciprocal of the quantum. This section extends initial studies by Kendall (1974) and Kent (1976), and shows that the null distribution of Kendall's test statistic is better represented by a three parameter Generalized Extreme Value distribution than by a two parameter Gumbel distribution.

The final two sections are devoted to more general purposes. The first considers an investigation of whether or not any specific random number generator used for simulating non–quantal random samples fails to generate samples random enough for the purpose of testing for quantality. The second is concerned with the question of whether or not the violation of the assumption that data points are independent (e.g. possibly serially autocorrelated root spacings) would have a substantial effect on the appraisal of significance of quantality in the testing process.

2.2. Statistical Description of Quantality

A statistical problem which appears in many branches of science is to determine whether a given set of data is *quantal*. That is, can some given data set plausibly be regarded as (unknown) integer multiples, subject to a random error, of some (unknown) underlying quantum value.

In most cases, the data reveal their quantal feature by the occurrence of regularly spaced modes. Therefore, a quantal hypothesis arises from a study of the data. For example, the experimenter observes his data to appear to be grouped about equally spaced modes. There is usually no independent evidence of the positions of these groups. It may be that the body of scientific knowledge and his prior belief is neither strongly for nor strongly against even the quantum hypothesis itself, though often there is a scientific theory available that would predict (or at least account for) the quantality. Thus he comes to a statistician and asks the question of whether the apparent grouping is a coincidence arising purely by chance or does it indicate some physical reality? For instance, biologists observe that distances between lateral roots on tomato roots or distances between leaves of fern plants are evenly spaced out, suggesting that a fundamental distance plays a role in lateral root branching process.

Another encounter with some quantal data set may come from investigating its histogram. It is known that several histograms of the same data could be drawn with different starting values and class interval widths. We may somehow end up with a histogram that reveals some groupings. The question whether this may (or may not) be merely an artefact of our particular choice of class intervals in the histogram also leads to a quantal hypothesis.

It is important to distinguish two possible cases of quantal problems. The first one occurs when we have *a priori* knowledge that a quantum of a particular value may exists and we have in fact an idea of its value which needs to be verified. We believe that this is not usually the situation in which we find ourselves.

Secondly, if an exploratory analysis is undertaken to search for an underlying quantum then any value within a range would be acceptable. In this case, the quantum is not known in advance and we may have in fact no idea beforehand that such a quantum exists. If it exists, its value must be deduced from the data and a testing procedure must be carried out to test whether to accept the quantum hypothesis.

2.3. The Classic Data Sets

Before describing statistical models for quantality and the early methods of analysis it is convenient for reference to describe in some detail the various data sets that generated interest in the problems.

Atom Weights: Weights of atomic masses were analysed by von Mises in 1918 (von Mises, 1918). He had available the atomic weights of the 21 metals and also (as then known) of the 24 lightest elements except Hydrogen which was used as a base unit. The data can be found in Tables 1 and 2 respectively in his paper.

Megalithic Yard: The Megalithic Yard data were collected by Thom (1955) and several subsets of the total data set were analysed by Thom (1955), Kendall (1974) and Freeman (1976). The complete data are given in Tables 5.1 and 5.2 of Thom (1967). The data can be divided into two main areas: Scotland and England & Wales. The diameters are given in feet and stated to be "±1 ft or better" in Table 5.1 and "diameters known with less accuracy" in Table 5.2. These are referred to as the "good" and "other" diameters, respectively. These tables also include diameters of some egg shaped layouts. The complete breakdown of the total 211 diameters is illustrated in Table 2.1.

Table 2.1. The data sets of circle diameters

Data	good circles	good rings	all circles	good circles&rings	all data
Scotland	66	16	109	82	127
England&Wales	46	17	60	63	84
Total	112	33	169	145	211

The Ashanti Weights: Hewson (1980) analysed in total 2859 Ashanti weights, commonly called goldweights, from the collections of the Department of Ethnography of the British Museum. There are two basic forms of the goldweights; a geometric form and figurative form. 1208 of the total number were the geometric type and 1651 of the figurative type. Each object was weighted to an accuracy of ± 0.001gr.

Devensian Horse Teeth: The measurements are the crown heights of horse teeth from the period of the Devensian galciation excavated from two sites, i.e. caves. There are a total of 18 sets of measurements, each set corresponding to a particular tooth (e.g. right first molar or left second pre–molar) from a particular site. The sample sizes range from 30 to 180. The data were made available by Turner (1980).

2.4. Quantal Models

The quantality of a data set can be represented by two basic models which we term the Pure Quantum Model and the Shifted Quantum Model.

2.4.1. The Pure Quantum Model

The pure quantum model for a given set of data $\{x_i\}_{i=1}^{n}$ is

$$X_i = m_i q + \varepsilon_i \text{ ; } i = 1, 2, ..., n \text{ ; } m_i \in \text{N and } 0 \le \varepsilon_i < q \tag{2.1}$$

where q is the quantum, m_i are integer multipliers, the integer parts of $\frac{X_i}{q}$ and ε_i is an error term, with either ε_i or $(q - \varepsilon_i)$ "small" for some q which has to be *deduced from the data*. The $\frac{\varepsilon_i}{q}$ are the fractional part of $\frac{X_i}{q}$, i.e. ε_i is the remainder when X_i is divided by q.

Note that some authors prefer to formulate the model as above but with $-q/2 \le \varepsilon_i < q/2$ and $|\varepsilon_i|$ "small". That is, the closest multiple of q to X_i is taken. There is of course no essential difference in the formulation and we may for convenience use either. Essentially the errors can be thought of as circular variables with the 'wrap–around' being absorbed by the multipliers of q.

It can be seen that apparently this model has more parameters than observations – n values of m, q and however many are needed to specify the distribution of the ε_i, i.e. at least n+1 for n observations. The essence of the model however is in the "smallness" of each ε_i or q – ε_i and it is this aspect that can be tested more formally. Once it is established, then a value of q, $\hat{q}$, may be obtained and this then determines ***all*** the unknown m_i. Thus, in actuality the m_i are not independent parameters and the model is not overspecified.

It may be noted that if in model (2.1) all the m_i are equal (to 1 say) then intuitively one would not regard the data as being "quantal". It is only when the m_i cover several different values that it seems reasonable to consider quantal models. This observation has implications in the discussion of the practical examples in chapter 4.

2.4.2. The Shifted Quantum Model

A variant on the basic quantal problem is the 'shifted quantal problem'. That is can a set of data plausibly be regarded as integral multiples of some underlying quantum plus a fixed constant? Mathematically,

$$X_i = \beta + m_i\, q + \varepsilon_i\,; \qquad \text{i = 1, 2,...., n;} \tag{2.2}$$

where $m_i \in$ N , $0 \le \beta <$ q and $0 \le \varepsilon_i <$ q with again either ε_i or (q $-\varepsilon_i$) "small" for some q. Typically, both q and β have to be deduced from the data.

Shifted quantality is equivalent to pure quantality subject to a common additive correction β. The shifted model is appropriate if the data are systematically biased. In the context of megalithic yard problem, for example, this might arise if the circles had been laid out with the centres of the stones lying on a circle of diameter an integral number of megalithic yards, but the diameters had only been measured from the outermost points of stones. Therefore, interior diameters might be pure quantal but exterior diameters are shifted quantal with shift β ≅ width of the stones, assuming stones to be of uniform thickness. This slight uncertainty about whether measurements should be taken from innermost points of the stones or the outermost points or somewhere in between was raised in the paper by Freeman (1976) and subsequent discussion.

Again, an alternative formulation with $-q/2 \le \varepsilon_i < q/2$ is possible. In this case, note that this adjustment will change the range of the parameter β to $-q/2 \le \beta < q/2$.

2.5. Previous Methods of Analysis

Quantal problems have been recognised by many authors who made various attempts at extracting evidence of this feature from data. Kendall's methodology provided a satisfactory solution to these problems appearing in many different areas. This thesis therefore will focus on his method which we term 'quantogram analysis'. However, it is believed that, as he affirms himself, he was inspired by pioneer work of von Mises and Broadbent. Therefore, we begin with describing these earlier analyses so that not only the differences can be emphasised but also how the methodology has developed can be understood.

2.5.1. von Mises' Method

Initially, von Mises (1918) tackled the matter with the aid of the statistical techniques available at that time when he observed a remarkable "integer–like" behaviour in atomic masses of the chemical elements. He investigated the deviations of measured atomic weights from integral values, i.e. the remainders when divided by some quantum value. He developed the well–known distribution, namely the von Mises distribution, discussing the fact that linear Gaussian distribution would give misleading results for such problems with a circular structure.

His procedure is essentially to roll up the line of any sequence of measurements on the perimeter of a circle with a circumference of 1 by indicating the multiplicity of the points each time. Noticing that they cluster around the "0" point played the leading role in answering the repeatedly occurring question of whether the atomic weights of elements can be regarded as a sequence of multiples of integers forming a unit, which is overlapped by a certain mean variation of errors. In order to treat the problem of this "integerness" (i.e. the "true" value of observed quantities is an integer), von Mises developed an error–theory as follows:

Suppose a number of points on the circumference of a circle through the arch lengths ($\theta_1, \theta_2, ..., \theta_n$) are given. The vector mean is defined by

$$\bar{x} = \frac{1}{n}\sum_{i=1}^{n} cos\,\theta_i\ , \qquad \bar{y} = \frac{1}{n}\sum_{i=1}^{n} sin\,\theta_i$$

However it is more convenient to express this vector in polar co–ordinates. Let $\bar{r}$ and $\bar{x}_0$ be a solution of the equations

$$\bar{x} = \bar{r}\ cos\ \bar{x}_0 \quad \text{and} \quad \bar{y} = \bar{r}\ sin\ \bar{x}_0$$

The well known solution is given by

$$\bar{r} = \left(\bar{x}^2 + \bar{y}^2\right)^{1/2} \quad \text{and} \quad \bar{x}_0 = arctan\frac{\bar{y}}{\bar{x}}$$

Then he asks for such a distribution f(ξ), where ξ is an "error of observation" (i.e. $\xi_i = \theta_i - \theta_0$), that the ratio of *a posteriori* to the *a priori* probability (the likelihood function) of a "true value" θ_0 upon n observations $\theta_1, \theta_2,...,\theta_n$ is to be maximum for that θ_0 given by $\bar{x}_0$ which satisfies an equation of the form

$$\sum_{j=1}^{n} \sin\left(\theta_j - \bar{x}_0\right) = 0\,.$$

This functional relationship has the solution

$$f\left(\xi\right) = Ce^{\kappa cos \xi}$$

where C is based on the Bessel function of the first kind and κ is the precision parameter (Gumbel et al., 1958). If κ here is large, the errors are clustered around "0" and the closer the possible errors (ξ) are, the smaller C becomes.
The function can be redefined as

$$C\,e^{\kappa n\,\bar{r}\,cos\left(\bar{x}_0 - \mu_0\right)}$$

If the points are evenly distributed on the circle, the density at each point is $1/_{2\pi}$. Assuming that μ_0=0 so as to simplify the case, he ended up with the criteria for the "integerness" as follows:

$$K = 2\pi C e^{\kappa n \bar{r} \cos \bar{x}_0}$$

Therefore, he states that if K is considerably larger than 1, then the assumption that the "true" value of the observed quantity is an integer is accepted.

Although the technique for deriving the test statistic appears to have similarities with the construction of likelihood ratio tests, the procedure is essentially informal; there was nor formal definition or assessment of 'considerably larger' in terms of a significance test or posterior odds, it was left to intuitive interpretation. We show in 2.6.1.1 and 2.6.2.1 that Kendall's method can be regarded as an approximation to a likelihood ratio test.

2.5.2. Broadbent's Method

Broadbent's approach to extracting any quantal feature of a data set is entirely different in style. Suppose a set of data can be expressed by the shifted model 2.2. Broadbent considers first the case when β and q are hypothesised or known *a priori* and then looking at the residuals z_i. He starts by estimating each m_i by the integer value $\hat{m}_i$ which minimises the residuals

$$z_i = y_i - \beta - \hat{m}_i q$$

such that $|z_i| < q/2$.

If the assumption that there is a definite known single value of q from which the data are supposed to have arisen were true, the z_i's would be expected to cluster fairly close to 0. Whereas if it were false they should be spread unimodally or rectangularly over the whole range from –q/2 to q/2. Therefore, Broadbent (1955) proposed the following test statistic

$$\frac{s^2}{q^2} = \frac{1}{nq^2} \sum_{i=1}^{n} z_i^2, \qquad z_i = \min_{\hat{m}_i} |y_i - \beta - \hat{m}_i q| \tag{2.3}$$

Under the null hypothesis of non–quantality, z_i have an approximately uniform distribution in the interval [–q/2, q/2]. The moment generating function of the uniform density is:

$$\int_{-q/2}^{q/2} \frac{e^{tx}}{q}\,dx = \sum_{i=0}^{\infty}\frac{(1/2\,tq)^{2i}}{(2i+1)!}$$

Therefore, the kth moment is the coefficient of $\frac{t^k}{k!}$ in the expression above and E[$(z_i)^2$] = $q^2/12$; E[$(z_i)^4$] = $q^4/80$ and V[$(z_i)^2$] = $q^4/180$ (Hewson, 1980). Thus, the test statistic

$$\frac{s^2}{q^2} = \frac{\sum z_i^2}{nq^2} \sim N\left(\frac{1}{12}, \frac{1}{180n}\right)$$

A value of s^2/q^2 significantly smaller than 1/12 might therefore be taken to support the quantum hypothesis with given value of q.

When no prior value of q is available, the data have to be used firstly to estimate q and then to assess the significance of the deviations from uniformly distributed errors. It would be clearly misleading to perform first kind of analysis for many values of q and then merely to report the significance level corresponding to the most favourable value. Here Broadbent (1956) uses the quantity

$$\frac{s^2}{\hat{q}^2} = \frac{1}{n\hat{q}^2}\sum_{i=1}^{n} z_i^2, \qquad z_i = \min_{\hat{m}_i}\left|y_i - \hat{\beta} - \hat{m}_i\hat{q}\right| \tag{2.4}$$

Regarded as a function of $\hat{q}$, this has a large number of local minima but it seems natural to consider the minimum for different values of q. However, it is not possible to determine its sampling distribution under the rectangular hypothesis, so Monte Carlo simulations are utilised. Since computer power was not well provided in 1956, the simulations performed by Broadbent were somewhat inadequate by modern standards. It was thus not possible to obtain an accurate significance level for any given data set and especially not for values of n in excess of 100. In 1976, however, Freeman was able to compare Broadbent's method with the one Kendall used for the 211 circle diameters. He concluded that the significance levels for the Broadbent's method when q is not known in advance could only be determined very approximately. When there is a definite known single value of q, he points out that Kendall regarded significance levels quoted for this type of analysis as highly misleading.

Due to the reason that Kendall's method is more powerful and adaptable, it has been decided to use his methodology as a basis to develop quantal models for the present problem. Its power lies in that it permits the use of likelihood based procedures which offer more powerful estimation methods and a wide choice of aspects to examine. Hence we will give all details of the quantogram analysis as well as some features of it we found when re–analysing the megalithic yard problem in following sections.

2.6. Kendall's Method: Quantogram Analysis

2.6.1. Cosine Quantogram

Suppose that we are to investigate stone circles for pure quantality with *a particular quantum q* given in (2.1). It is therefore assumed that the value of q is known in advance for convenience.

In order to illustrate the test statistic to detect quantality, Kendall (1974) carries out an imaginary experiment. At this stage, it is appropriate to follow his way of explaining how to construct his test statistics. In this experiment, he supposes that there exist the following tools at hand, firstly a wheel of circumference q with an origin marked on its circumference, and secondly a long transparent tape carrying a scale (e.g. of feet) with one end represented the zero point.

If X_i (i = 1,...,n) are measured in turn by starting always from the zero point and marking the tape at the other end of the measured length X_i, we will end up with a transparent tape with n marks on it. Then the zero point of the tape is attached to the origin of the wheel and the tape is wrapped around it until all the marks lie upon it. Clearly the marks will be visible due to transparency. Note that the measurements are not laid end to end along the tape, but overlap because they all start from the same zero point. Marking the measurements cumulatively would also be possible in other situation as we will see later when we consider the spacings between rootlets. However, this would introduce another aspect of quantality and we will return to this later. It is easy to see the inspiration of von Mises in Kendall's account.

If the data were *exactly* quantal with quantum q, then all the marks would be lying on the top of one another and coincide with the zero point, in other words all ε_i in the model (2.1) would be equal to zero. In reality however, due to errors made in measurement and recording the data, the exactly quantal data set is unlikely to occur, but we should expect errors to be clustered around the zero point in the presence of that particular q. On the other hand, if there is no quantality of magnitude q (or any fraction or multiple of q), then the marks will be distributed randomly and uniformly around the wheel. That means the error component is very large.

In order to analyse the quantality at quantum q, we must assess, using a suitable test statistic, how well the marked points of the tape are clustered about the origin of the wheel. If the position of the marks are transformed into angular terms, using angular displacement θ_i in radians i.e. $\theta_i = 2\pi X_i \pmod{2\pi}$, then an appropriate 'score' for high clustering could be obtain by using $\cos\theta_i$ due to its property of taking the value +1 at the origin and falling to –1 in both directions away from the origin.

Therefore, a natural measure of clustering will be of the form $\sum_{i=1}^{n}\cos\theta_i$, normalised in some manner to remove the size n dependence, and the test statistic is given by

$$\phi(q) = \sqrt{\frac{2}{n}}\sum_{i=1}^{n} cos\left(\frac{2\pi x_i}{q}\right) = \sqrt{\frac{2}{n}}\sum_{i=1}^{n} cos\left(\frac{2\pi\varepsilon_i}{q}\right) \tag{2.5}$$

Again, the similarity with von Mises is apparent.

For technical reasons which we illustrate in section 2.8.2.2, it is convenient to work in terms of $\phi(\tau)$ where τ =1/q that can be thought of as a measure of frequency.

$\phi(\tau)$ takes a very high value if q has been correctly chosen and the errors are nearly zero. If there is no quantal effect at all in the data (i.e. the errors are uniformly distributed), or if the quantum has been wrongly chosen, then the contributions of the cosines will largely cancel out, and $\phi(\tau)$ will be small and may be either positive or negative. Negative values are also possible if X_i is concentrated around odd multiples of q/2 and avoids even multiples.

In the absence of a quantum, for fixed τ, not too small τ values (i.e. not too big q values) and not too small n, it can be shown that $\phi(\tau)$ is asymptotically an ordinary Gaussian random variable with zero mean and unit standard deviation as follows:

$$E\left[cos\frac{(2\pi x_i)}{q}\right] = \int_{-q/2}^{q/2} \frac{1}{q} cos\left(\frac{2\pi x}{q}\right) dx = 0$$

and

$$E\left[cos^2\left(\frac{2\pi x_i}{q}\right)\right] = \int_{-q/2}^{q/2} \frac{1}{q} cos^2\left(\frac{2\pi x}{q}\right) dx = \frac{1}{2}$$

Therefore, for large n, by the Central Limit Theorem the sum of cosines will be approximately normally distributed with mean zero and variance n/2 and the result for $\phi(\tau)$ follows immediately.

For large data sets, hence, this distributional result allows us a feel for which values of $\phi(\tau)$ will indicate significant quantality, i.e. (regarding τ as fixed)

$$P[\phi(\tau) \geq +2] = 0.0228$$

$$P[\phi(\tau) \geq +3] = 0.00135$$

$$P[\phi(\tau) \geq +4] = 0.000032$$

2.6.1.1. A Likelihood Ratio Test for Pure Quantality

The cosine quantogram of the data could also be regarded as a likelihood ratio test statistic. Since the quantality of data depends upon the distribution of errors, i.e. non–quantal if they are evenly distributed, we can show that Kendall's cosine quantogram function is equivalent to testing for uniformity of the errors. Representing the distribution of the errors by a frequently used error–distribution on the circle namely the von Mises distribution with location parameter zero (i.e. VM(0, κ) as suggested by Kendall (see section 3.2 for the details of the von Mises distribution), a Likelihood Ratio Test for quantality can be formulated as testing for the null hypothesis

$$H_0\!: \ \kappa = 0, \quad \text{(i.e. } \frac{2\pi\varepsilon_i}{q} \sim U(0, 2\pi)\text{)},$$

against

$$H_1\!: \ \kappa_1 > 0, \quad \text{(i.e. } \frac{2\pi\varepsilon_i}{q} \sim VM(0, \kappa_1)\text{, where } \kappa_1 > 0\text{)}$$

The density function of the von Mises distribution with zero mean is

$$f(\theta) = \frac{\exp[\kappa \cos(\theta)]}{2\pi I_0(\kappa)}, \quad 0 < \theta < 2\pi, \quad \kappa > 0$$

So under H_0, the likelihood function is

$$L_0 = \frac{1}{(2\pi)^n}$$

and under H_1,

$$L_1 = \frac{e^{n\kappa_1 \overline{C}}}{\left(2\pi I_0(\kappa_1)\right)^n},$$

where

$$\overline{C} = C/n, \qquad C = \sum_{i=1}^{n} cos\,\frac{2\pi\varepsilon_i}{q},$$

Then, the likelihood ratio test for testing H_0 against H_1 is the ratio

$$\lambda = \frac{L_0}{L_1} = \frac{I_0(\kappa_1)^n}{e^{n\kappa_1\overline{C}}}$$

Since the hypotheses are simple, the best critical region by the Neyman–Pearson lemma is

$$e^{-n\kappa_1\overline{C}}\, I_0(\kappa_1)^n < c$$

hence

$$\overline{C} > \left(log\, c - n\,log(\kappa_1)\right) / \,n\kappa_1 \;=\; c^*$$

where c^* is a constant and determined from the size α, $0< \alpha <1$, according to the relation

$$Pr\left(\overline{C} > c^* \mid H_0\right) = \alpha$$

and this test is known to be uniformly most powerful test (Mardia, 1972), since the critical region does not depend on κ, except that $\kappa > 0$. Hence the most powerful test of H_0: $\kappa = 0$ versus H_1: $\kappa = \kappa_1$, where $\kappa_1 > 0$ becomes the uniformly most powerful test of H_0: $\kappa = 0$ versus H_1: $\kappa > 0$. For large n, $\overline{C}$ is distributed approximately as $N\left(0, (2n)^{-1}\right)$ suggested by Durand et al. (1957) below it can be seen to be equivalent to Kendall's cosine quantogram function:

$$Pr\left((2n)^{1/2}\,\overline{C} > c\right) = Pr\left(\sqrt{\frac{2}{n}}\,\sum_{i=1}^{n} cos\left(\frac{2\pi\varepsilon_i}{q}\right) > c\right) = \alpha$$

2.6.2. Modular Quantogram

Returning to the wheel experiment, the shifted model would be revealed if the marks still coincide but no longer lie on the top of the zero point. They would distribute closely around a point beta, distance β around the origin of the wheel (the sign of β depending on which way around the wheel the tape was wrapped).

A test statistic advocated by Kendall for shifted quantality is essentially the empirical characteristic function of the data, based upon a summation of sines as well as cosines:

$$\chi(\tau) = \frac{1}{2}\left\{\left(\sqrt{\frac{2}{n}}\sum_{i=1}^{n}\cos(2\pi x_i \tau)\right)^2 + \left(\sqrt{\frac{2}{n}}\sum_{i=1}^{n}\sin(2\pi x_i \tau)\right)^2\right\} \tag{2.6}$$

$$= 1 + \frac{1}{n}\sum_{i \neq j}\sum \cos\left(2\pi\left(x_i - x_j\right)\tau\right)$$

This is equivalent to testing the differences between all pairs of observations for pure quantality. $\chi(\tau)$ needs more computation within extra sines and squares but it gives *protection* if the data were in fact shifted quantal.

It can be shown that $\chi(\tau)$ has asymptotically an exponential distribution with unit parameter for fixed q, and not too small n. Therefore, probabilities for significant shifted quantality at a fixed q can be obtained as follows:

$$P[\chi(\tau) \geq x] = e^{-x}$$

$$P[\chi(\tau) \geq 5] = 0.0067$$

$$P[\chi(\tau) \geq 10] = 0.000045$$

It can be seen that the values of $\phi(\tau)$ and $\chi(\tau)$ which give 'significant' results are on totally separate scales, and no comparisons can be made between them.

2.6.2.1. A Likelihood Ratio Test for Shifted Quantality

It can also be shown that the Modular Quantogram could be represented as a LRT for shifted quantality. Suppose now that μ is not known in the null hypothesis of non–

quantality so that under the alternative, κ and μ are both unknown. Therefore we obtain the likelihood ratio test for testing the null hypothesis

$$H_0\colon\ \kappa = 0 \quad \left(\text{i.e. } \frac{2\pi\varepsilon_i}{q} \sim U(\mu, \mu + 2\pi)\right),$$

against

$$H_1\colon\ \kappa > 0, \quad \left(\text{i.e. } \frac{2\pi\varepsilon_{\mathrm{i}}}{\mathrm{q}} \sim \mathrm{VM}(\mu,\ \kappa), \text{ where } \mu \text{ and } \kappa \text{ are unknown}\right)$$

Under H_0 the likelihood function is again

$$L_0 = \frac{1}{(2\pi)^n}$$

whereas under H_1, using the maximum likelihood estimates of μ and κ, it becomes

$$max\ L_1 = \frac{e^{n\hat{\kappa}\overline{R}}}{\left(2\pi I_o(\hat{\kappa})\right)^n}$$

where

$$\overline{R}^2 = \overline{C}^2 + \overline{S}^2, \qquad \overline{S} = \frac{1}{n}\sum sin\frac{2\pi\varepsilon_i}{q}, \qquad \overline{C} = \frac{1}{n}\sum cos\frac{2\pi\varepsilon_i}{q}$$

and

$$A(\kappa) = \frac{I_1(\kappa)}{I_0(\kappa)}$$

MLE $\hat{\kappa}$ of κ is the solution of

$$\hat{\kappa} = A^{-1}\left(\overline{R}\right)$$

Consequently, the likelihood ratio statistic is given by

$$\lambda = \left\{I_0(\hat{\kappa})\right\}^n exp\left(-n\hat{\kappa}\overline{R}\right)$$

and reject H_0, if $\lambda < c$, where c is determined from the size α, $0< \alpha <1$, according to the relation

$$\sup P(\lambda < c \mid H_0) = \alpha$$

Since λ is a monotonically decreasing function of $\overline{R}$ and $\hat{\kappa}$, and $\hat{\kappa}$ is a monotonically increasing function of $\overline{R}$ (Mardia, 1972), the critical region $\lambda < c$ reduces to $\overline{R} > c$ where the size α of the test is attained by choosing c so that

$$Pr\left(\overline{R} > c \mid H_0\right) = \alpha$$

For large n, $2n\overline{R}^2$ is approximately distributed as chi–square with 2 degrees of freedom. That is

$$\left(\sqrt{\frac{2}{n}}\sum_{i=1}^{n}\cos\left(\frac{2\pi\varepsilon_i}{q}\right)\right)^2 + \left(\sqrt{\frac{2}{n}}\sum_{i=1}^{n}\sin\left(\frac{2\pi\varepsilon_i}{q}\right)\right)^2 \sim \chi^2_{(2)}$$

Using the variate relationships (i.e. $\frac{1}{2}\chi^2_{(2)} \sim E_X(1)$), once again we end up with the function Kendall proposed for shifted quantality:

$$\frac{1}{2}\left(\sqrt{\frac{2}{n}}\sum_{i=1}^{n}\cos\left(\frac{2\pi\varepsilon_i}{q}\right)\right)^2 + \left(\sqrt{\frac{2}{n}}\sum_{i=1}^{n}\sin\left(\frac{2\pi\varepsilon_i}{q}\right)\right)^2 \sim E_X(1)$$

2.6.3. Quantogram Graphs

We have so far illustrated the methodology to consider the quantal problems with *a priori* knowledge about what the quantum q is supposed to be, and the test statistics in the above have been demonstrated to test for its existence. We will now consider the case, more common and complicated, where there is no *a priori* reason for adopting a particular value of quantum, however either some underlying theory suggests the existence of a quanta or inspection of the data may reveal evenly spaced groupings. In order to determine the likely values of quantum, it is therefore necessary to consider not the single number $\phi(\tau)$ but rather the range of values of $\phi(\tau)$ as τ is varied. The test statistic now becomes

$$\phi(\hat{\tau}) = \max_{\tau_{min}}^{\tau_{max}}\{\phi(\tau)\}$$

where

$$\hat{\tau} = arg \max_{\tau_{min}}^{\tau_{max}}\{\phi(\tau)\}$$

(or similary $\chi(\hat{\tau})$ in the case of shifted quantality) which defines the best estimate of quantum $\hat{q} = 1/\hat{\tau}$.

The suggested way of obtaining the best candidate for quanta is to work out the test statistic $\phi(\tau)$ [or $\chi(\tau)$] over a plausible prescribed range (τ_{min}, τ_{max}) (i.e.(q_{min}, q_{max})) and plot them over this range. This plot is termed the be *cosine quantogram graph (c.q.g.)* [or *modular quantogram graph (m.q.g.)*]. Although it is perfectly acceptable to plot $\phi(q)$ vs q, the frequency diagram is in more common use and indeed there are good reasons for using τ rather than q and we return to this later.

A cosine quantogram graph is a plot of the sum of cosines and will be wildly fluctuating as seen in Fig 2.1 which exhibits the c.q.g. of all data for the Megalithic Yard example. If there is, however, quantality within the data set with quantum $\hat{q}$ say, a peak appears at $\hat{q}$ which is significantly high against the background noise of the quantogram. The peak of the plot thus gives the best candidate for the unknown quantum within the range (q_{min}, q_{max}). Therefore, the c.q.g. (or m.q.g.) is a convenient illustration of $\phi(q)$ indicating informally how impressive $\hat{q}$ is as a quantum candidate, however the significance of $\phi(\hat{q})$ (or $\chi(\hat{\tau})$) must be assessed by simulation techniques.

Note that if $\hat{q}$ is a possible quantum, then $\hat{q}/2$ and $\hat{q}/3$ and perhaps $2\hat{q}/3$, etc. are likely, but not necessarily, to be good candidates as $\hat{q}$. In general terms, $\frac{\hat{q}}{k}$ may give stronger evidence in favour of quantality than $\frac{r\hat{q}}{k}$ would.

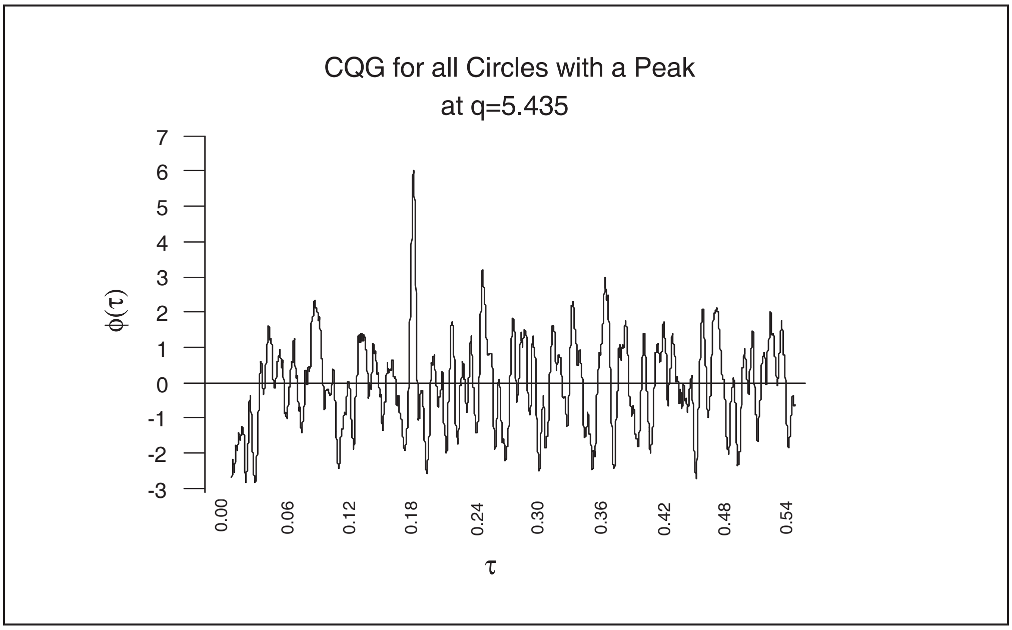

Fig 2.1. An example of the Cosine Quantogram graph

Once one or more values of q which produce a significant peak have been found, then the standard deviation σ about the ε values of clustering can be estimated for each value using the expectation value of the height of the peak at quantum. Incorporating a wrapped Normal distribution for ε, Kendall calculates the expected value as

$$E\left(\phi(\hat{q})\right) = \sqrt{2n}\,\exp\left(\frac{-2\pi^2\sigma^2}{\hat{q}^2}\right) \tag{2.7}$$

which provides an estimate for σ.

2.6.4. Range and Resolution of the Search (q_{min}, q_{max})

The range of q over which the test statistic is evaluated is critical. We do not have to consider the whole range $0 < q < \infty$ and clearly, the choice of very large or very small q values would be irrelevant. Therefore, the range must be truncated in some way, at each end, to prevent an infinitely long process of hunting impossible values. However, if the width of the range [q_{min}, q_{max}] is too narrow then there is a risk of missing the quantum. On the other hand, if it is too wide then the range may include the true value but any significance test for quantality would be weak.

It is logically meaningless to consider values of the quantum either greater than the largest observation or smaller than the accuracy of measurements. The upper end must be chosen on the grounds of efficiency. However, the lower end of the range must be chosen with more care and using common sense is necessary.

It is not possible to determine the maximum of the quantogram analytically and so necessarily it (and its position) must be determined numerically. The number of local maxima increases with both the sample size and the range of search since local maxima, separated by a local minima, could be extremely close together. There is thus no alternative to determining the overall maximum and its position by a gridsearch and so the important issue arises of how fine the gridsearch should be performed over the range (q_{min}, q_{max}). Our approach to the choice of increment will be to start with a reasonably fine gridsearch and then progressively halve it until stability is obtained.

In order to demonstrate the effect of the choice of increment, we perform quantogram analysis on, for example, all circles (n=169) in Scotland and England & Wales. This sample was accepted by Kendall as the main sample throughout his analyses. Here we use again his agreed τ range of search which is [0.09, 0.59] but apply our approach to choose the best increment. The number of points to be searched in the range is calculated as

$$N = \frac{(\tau_{\max} - \tau_{\min})}{incr} + 1 = \frac{0.5}{incr} + 1$$

where *incr* being chosen arbitrarily as 0.01 which gives a reasonable number of points to begin with, and halved continuously until lessening the increment makes no change anymore in the estimate of quantum and its corresponding peak cosine quantogram value. The results for the selected sample are summarised in Figures 2.2 and 2.3.

The circles here represents the estimated quantum values, $\hat{q}$, and their cosine quantogram (i.e. $\phi(\hat{q})$) which were obtained using our approach. The solid circles are used to show Kendall's estimates for the same sample which were $\hat{q}$ =5.442 and $\phi(\hat{q})$ = 4.086. These estimates can be obtained when gridsearch is done with an increment smaller than 0.001. However, the graphs indicate that a finer search changes the both estimates slightly. It can also be seen that they settle at around $\hat{q}$ = 5.428 and $\phi(\hat{q})$ = 4.120 roughly after the increment of 0.0001.

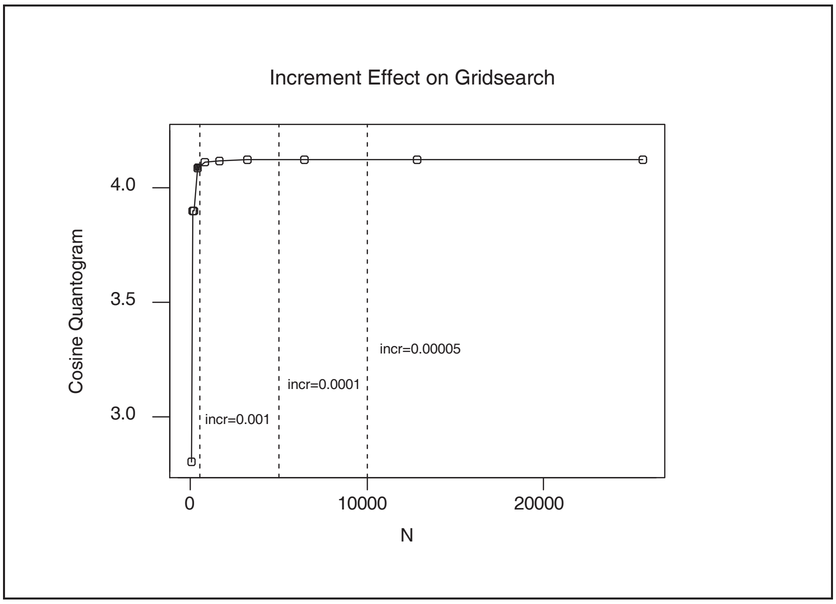

Fig 2.2. Plot of peak cosine quantogram value against number of points (N) searched

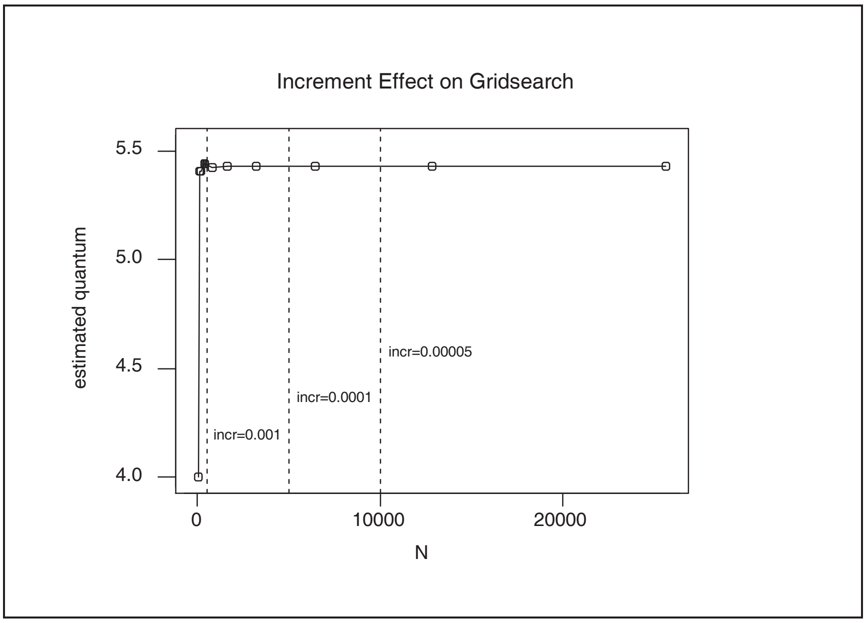

Fig 2.3. Plot of estimated quantum against number of points (N) searched

In addition to the sample used here, other subsets of circles also present similar pictures. Therefore we suggest using the increment of 0.0001 in the search of a quantum for the circle diameters. As a result, the quantogram analyses including the assessment of significance for the data presented in Table 2.1 have been performed using the new increment and the results are presented in a later section.

2.6.5. Assessing Significance Probabilities

Having found the peak in the cosine quantogram (or the modular quantogram) reflecting the evidence in favour of quantality, it is then necessary to asses its significance. We must note here that the null hypothesis is that the data are not quantal. In other words, that the data come from a smooth (but not necessarily uniform) distribution. Rejection of the 'smooth distribution' hypothesis in favour of one that is strongly multimodal with equally spaced modes can be taken as a 'proof' that a quantum actually exists.

Difficulties arise when one requires a significance level for the hypothesis that the data set is non–quantal. If we find our largest peak to be greater than +3, it might be tempting to say that non–quantal hypothesis has been rejected at (say) the 0.135% level. However statistically this is an inadmissible statement because of the fact that we choose the highest peak in the whole τ interval and an appropriate adjustment made to allow for the selection effect. Early workers found it extremely difficult to determine what adjustment was needed.

Broadbent (1955) exemplified the situation by an analogy with the χ^2 goodness of fit test which show that this type of problem is common in statistics. He says: "the agreement between data and hypothesis is measured by χ^2, when the hypothesis is independent of the data the number of degrees of freedom used in the test equals the number of classes used minus one. But if data are used to estimate parameters which the hypothesis does not specify, the χ^2 must be modified. The modification given by Fisher (1924) consists simply in reducing the number of degrees of freedom used in the test by the number of parameters estimated. If the data were used for other purposes, for example, to suggest whether one or another type of distribution be fitted to the data or what the class limits should be, the modification is no longer so simple".

In order to overcome this difficulty, Broadbent in his analysis of quantum hypotheses used Monte Carlo simulations, generating a sample of the same size from a uniform distribution on (0, 1), even if the data were clearly not even approximately uniformly distributed, with the largest observation being equal to 1. Kendall also utilised a simulation technique, which is in fact what is now recognized as a parametric bootstrap technique, but the real data are specifically used in choosing the distribution of the simulated data. Kendall made no adjustment for the fact that the data had been used to suggest the underlying distribution (despite Broadbent's concerns) and indeed apparently no such adjustment is traditional in other applications of parametric bootstrap methods. Later (section 2.8.2.3), we investigate the difference between using uniform distribution for generating the simulations and ones suggested by the data and find that generally any differences are small.

Within the framework of our study, Kendall's simulations therefore will be followed. In other words, parametric or smoothed bootstrap techniques will be used in order to make assessments on how likely the observed quantal tendency will occur at random. The general procedure is to take a 'random' set of data matched to the actual data for basic statistical features such as mean and variance, but not having any quantal structure. Then, we record the maximum of the statistic $\phi(q)$ over the agreed range for q for that facsimile data set, repeating the process for a large number of similar data sets (at least 100), being all independent of one from another. The peak from the original sample can then be compared with the peaks from the simulated samples to estimate the probability that a peak would be at least as large as the observed one if the data were sampled from the proposed non–quantal distribution.

Here we give a summary of results of quantogram analyses performed on the various subsets of circle diameters listed in Table 2.1. The difference between Kendall's analyses and ours stems from the previously drawn conclusion (see section 2.6.4) about the choice of the increment to use in the search of quanta. It has been suggested to use an increment of 0.0001 in quantogram analyses. Therefore, quantogram analyses have been performed over Kendall's τ–range [0.09, 0.59] but with an increment of 0.0001. In addition, the significance of the estimates have been assessed by generating 999 samples from half–Normal distributions (see section 2.8.1). The simulated samples are matched to the actual data sets with respect to their means and variances. For each subsets of circles, a p–value is then calculated as

$$p = \frac{\#\ \left\{\phi(\hat{q}) \geq observed\ peak\right\} + 1}{1000}$$

The results are given in Table 2.2. In comparison with Kendall's results which exist for only a few of the subsets as indicated in the table, one can see that the estimates of quantum values slightly differ, however the significance assessments provide similar p–values for those.

Table 2.2. Results of Quantogram analyses on stone circles (increment=0.0001)

Data	Scotland q	Scotland p	England&Wales q	England&Wales p	Total q	Total p
Good circles	5.440	0.302	4.516	0.289	5.437	0.060 (3)
Good rings	5.440	0.001	2.397	0.524	5.437	0.001
All circles	5.431	0.026 (1)	4.533	0.613 (2)	5.428	0.009 (4)
Good circles&rings	5.440	0.001	5.434	0.328	5.437	0.001
All data	5.437	0.001	5.428	0.307	5.434	0.001

Kendall's results: (1) q=5.435 p=0.021, (2) q=4.53, (3) q=5.435 p=0.068, (4) q=5.442 p=0.0083

Following the remark at the end of section 2.4.1 it may be noted that if for a data set following model (2.1) all the m_i are equal (to m say) then the data will appear to be a sample from a smooth distribution with mean mq and variance equal to that of the ε_i. Consequently the bootstrap technique above will clearly not declare the data to be quantal, which is in agreement with the intuitive idea of a quantal data set.

2.6.6. Testing the Significance of the β effect

If the m.q.g. is plotted and a significantly high peak is found, we can test whether or not β = 0. Redefining $\chi(\tau)$ as

$$\chi(\tau) = \frac{1}{2}\left\{\phi(\tau)^2 + \psi(\tau)^2\right\}$$

where,

$$\psi(\tau)=\sqrt{2/n}\,\sum_{i=1}^{n} sin(2\pi\tau x_i) \qquad (2.8)$$

Under the null hypothesis H_0: β = 0 and for fixed q (i.e. τ)

$$\psi(\tau) \sim N(0,1)$$

Therefore, having obtained the best estimate of the quantum $\hat{q}$ where $\hat{q} = 1/\hat{\tau}$ and

$$\hat{\tau} = arg \max_{\tau_{min}}^{\tau_{max}} \{\chi(\tau)\}$$

in practice, a value of $\psi(\hat{\tau})$ that lies within the range ± 2 can be considered to indicate that β is an unnecessary complication. Otherwise, the β effect is accepted and can be estimated. The estimation procedures are given and discussed in the ensuing section.

2.6.7. Estimation Methods for the β effect

When there appears to be shifted quantality at $\hat{q}$ and $\psi(\hat{\tau})$ is found to be significant, then it is necessary to estimate the β component. The estimation procedures that have so far been used can be summarised as follows:

Least Squares Estimation: the most commonly used method which was proposed by Broadbent. It is equivalent to minimising a function of errors.

$$\hat{\beta} = \frac{\sum_{i=1}^{n}\left(x_i - \hat{m}_i\,\hat{q}\right)}{n}, \qquad \text{where } \hat{m}_i = \left[x_i / \hat{q}\right]$$

[...] meaning “take the nearest integer”.

Although, this provides a good estimate of the β effect when there exists strong quantality, it may not be so if the quantality gets weaker or errors are heavily clustered, since it treats errors on the linear line ignoring the wrap around neighbours of observations from –q/2 to q/2, it can in fact cause misleading, and even wrong, results. Therefore we conclude that it is inappropriate to use ordinary least squares estimate of the shift component. The best estimate could be obtained by the method of maximum likelihood described below. Therefore estimation procedures that have been performed with the least squares method as in analyses of Knox (1994) who suggested shifted quantality of redshifts should be repeated by utilising the maximum likelihood estimation method.

***Maximum Likelihood Estimation*:** in order to estimate the β, Kendall suggested using the maximum likelihood estimation method. In the previous sections, we have explained that testing for pure quantality (β=0) is equivalent to testing whether or not errors come from VM(0, κ). If any shift effect has been suspected, the procedure is altered to testing whether errors come from VM(μ, κ) with μ unspecified. A maximum likelihood estimate of β can be obtained from the m.l.e. of the mean direction, μ, of the von Mises distribution. This is very well–known and given (Mardia, 1972) as follows:

$$\hat{\mu} = \begin{cases} \tan^{-1}\left(\frac{S}{C}\right) & if \;\; C > 0,\ S > 0 \\ \tan^{-1}\left(\frac{S}{C}\right) + \pi & if \;\; C < 0 \\ \tan^{-1}\left(\frac{S}{C}\right) + 2\pi & if \;\; C > 0,\ S < 0 \end{cases}$$

where

$$S = \sum_{i=1}^{n} \sin(\theta_i), \quad C = \sum_{i=1}^{n} \cos(\theta_i) \text{ and } \theta_i = \frac{2\pi x_i}{\hat{q}}$$

This gives a mean direction in the range $0 < \hat{\mu} < 2\pi$. Then the estimate of the shift $\hat{\beta} = \hat{\mu} q/2\pi$ lies within [0, q]. This range can be easily changed to [–q/2, q/2] if necessary.

It is also noteworthy to mention that an estimate of β could be obtained by performing a gridsearch over both q and β. That is to test $\left\{(x_i - \beta_t)\right\}_{i=1}^{n}$ for pure quantality for a grid of trial values $\beta_t \in (0, q_{max})$. Thus, maximizing T((x–β);q) over q and β provides an estimate of quantum and shift. This approach is computationally expensive, however it will also provide a reliable estimate of the shift component.

2.7. Freeman's Method: A Bayesian Approach

Before investigating further properties of Kendall's quantogram approach, we present here the next, in historical terms, approach to the problem as given by Freeman (1976). This is a Bayesian approach and we develop and refine the technique in Chapter 7. His Bayesian method can be given as follows:
under the quantum model (2.2), assuming that the quantum does exist, the data are distributed as

$$p\left(x \mid \beta, q, m, \sigma\right) = N\left(\beta + q\,m, \sigma^2 I_n\right)$$

and the likelihood function is

$$f\left(x_1, \ldots, x_n \middle| m_1, \ldots, m_n, \beta, q, \sigma\right) = \left(\frac{1}{\sqrt{2\pi}\,\sigma}\right)^n exp\left\{-\sum_{i=1}^{n}\left(x_i - \beta - m_i\,q\right)^2 \Big/ 2\sigma^2\right\}$$

Prior ideas about integers m_i can be represented by some common discrete distribution. Freeman chose a discrete uniform distribution to begin with, and also investigated the effect of a Poisson prior for integers. Suppose, an integer therefore comes from a uniform distribution i.e. U(1, N), then the joint prior distribution of n integers assuming that they are, *a priori*, independent is as follows:

$$f\left(m_1, \ldots, m_n \mid N\right) = \frac{1}{N^n}, \quad 1 \le m_i \le N,\ 1 \le i \le n$$

where, as the upper bound must clearly depend on the value of q, $N = \dfrac{k}{q}$ and k is some constant. Defining f(β, q, σ, k) as the joint prior distribution for the three parameters and one hyperparameter, then his resulting posterior is

$$f\left(\beta,q,\sigma,k\mid x\right)\propto\left(\frac{q}{k\,\sigma}\right)^{n}\sum_{m_1=1}^{N}\dots\sum_{m_n=1}^{N}exp\left\{-\sum_{i=1}^{n}\left(x_i-\beta-m_i q\right)^2/2\sigma^2\right\}f\left(\beta,q,\sigma,k\right)$$

$$\propto\left(\frac{q}{k\,\sigma}\right)^{n}\prod_{i=1}^{n}\sum_{m_i=1}^{N}exp\left\{-\sum_{i=1}^{n}\left(x_i-\beta-m_i q\right)^2/2\sigma^2\right\}f\left(\beta,q,\sigma,k\right)$$

He assumed the constant value k to be known as long as $k > x_{max} + I\sigma$ in order to ensure that each sum includes all terms which have a non–zero contribution to make. Here x_{max} denotes the largest observation and I is around 4 or 5.

In addition, he assumed that σ is known even though regarding this is strictly unnecessary since an inverse gamma prior independent of the prior for q could be used. However he prefers to retain σ as a parameter of the posterior for q due to the reason that the posterior still maintains an n–fold multiple sum which cannot be changed into a product as above.

Therefore, assuming k and σ known, he took β = 0 and chose a prior for q to be effectively constant over the range in which likelihood is large. Then the posterior distribution for q becomes

$$f\left(q\middle|x\right)\propto q^n\prod_{i=1}^{n}\sum_{m_i=1}^{N}exp\left\{-\sum_{i=1}^{n}\left(x_i-m_i q\right)^2/2\sigma^2\right\} \tag{2.9}$$

If the assumption of a uniform distribution for the integers m_i is replaced by a truncated Poisson distribution, then again assuming that integers are, *a priori,* independent the joint prior distribution becomes

$$f\left(m_1,\dots,m_n\middle|\mu\right)=\frac{e^{-n\mu}\,\mu^{\Sigma m}}{\left(1-e^{-\mu}\right)^n\prod m_i!},\quad m_i=1,2,\dots,\quad 1\le i\le n$$

where $\mu = k/q$. Thus, the resulting posterior has the form

$$f\left(\beta,q,\sigma,k\mid x\right)\propto \sum_{m_1=1}^{\infty}\cdots\sum_{m_n=1}^{\infty}\frac{exp\left\{-nk/q\right\}exp\left\{-\sum_{i=1}^{n}\left(x_i-\beta-m_iq\right)^2/2\sigma^2\right\}}{\sigma^n\left(1-e^{-k/q}\right)^n\prod m_i\,!\,(q/k)^{\sum m_i}}\,f\left(\beta,q,\sigma,k\right)$$

if β = 0 and σ and k are known

$$f(q|x)\propto\left(\frac{1}{e^{k/q}-1}\right)^n\prod_{i=1}^{n}\sum_{m_i=1}^{\infty}\frac{exp\left\{-\left(x_i-m_iq\right)^2/2\sigma^2\right\}}{(q/k)^{m_i}\,m_i!}$$

Compared with the posterior when a uniform prior is used, he concluded that this posterior reveals similar behaviour which implies that the results of this analysis do not depend crucially on the assumption about the priors of the integers. The choice of σ and k plays an important role in the patterns obtained from both posteriors.

Investigating several subsets of all circles, his results confirmed Kendall's findings such that the evidence in favour of megalithic yard resides almost entirely in the Scottish data set. Freeman also found two other values, 4 and 7.5, which fit the circles almost as well as the yard.

Furthermore, he examined whether taking β=0 seriously influenced the results. A prior for β conditional on q was taken as U(–q/2, q/2) and the joint posterior for β and q was calculated over a limited range (i.e. between 5.34 and 5.54). As a result of this study, he concluded that allowing for non–zero β makes very little difference for again the Scottish data but shows appreciable differences for the English data set.

In the discussion part of Freeman's paper, Silverman demonstrated a connection between Freeman's posterior distributions and Kendall's cosine quantograms, stemming from a close connection between von Mises and wrapped Normal distributions on the circle. Thus, he states that it is not at all surprising that Freeman concluded that Bayes estimates are very close to Kendall's estimates.

We return to this approach in Chapter 7.

2.8. Basic Properties of the Test and Estimation Procedures

In this section, we investigate some of the basic properties of the test and estimation procedures using quantograms. In particular, the dependence of the assessment of significance on the underlying non–quantal distribution used in the analyses, the null distribution of $\hat{q}$ over (q_{min}, q_{max}) and similarly $\hat{\tau}$ over (τ_{min}, τ_{max}) and hence a 'natural' scale of measurement and the empirical limiting distribution of $\phi(\tau)$. Where appropriate illustrations are based on the Megalithic Yard data and in consequence some refinements of Kendall's original analysis are provided.

2.8.1. Half–Normal Probability Plots

Kendall (1974) observed that the stone circle diameters have an half–Normal distribution. He used this in choosing the distribution of the simulated data so as to match the artificial data to the actual circles in all statistical respects.

Before investigating the sensitivity of the analysis to this model assumption, we first investigate whether the circle diameters can indeed be modelled adequately by a half–Normal distribution. For this purpose, we use half–Normal probability plots for an informal test. We illustrate how to obtain such plots below.

If $x \sim N(0, \sigma^2)$, then the variable $| x |$ follows a half–Normal distribution which has a probability distribution function of the exactly the same shape as the right hand half of an $N(0, \sigma^2)$ distribution, but with every ordinate twice as high.

Thus a half–Normal probability plot of a sample is a regular Q–Q plot of the quantiles of the absolute values of the data $| x_1 | \leq \ldots \leq | x_n |$ against the corresponding quantiles of the half–Normal distribution. Quantiles of a half–Normal distribution can be obtained by using the relationship between the cumulative distribution function of the half–Normal and the (full) Normal distribution as follows:

$$\phi_0(|x|) = \phi(x) - \phi(-x)$$

i.e. $$p = 2\,\phi(x) - 1$$

i.e. $$\phi(x) = \frac{p+1}{2}$$

where $\phi(x)$ is the standard normal c.d.f. (Draper and Smith, 1980). Thus using (1+p)/2 in the place of the quantile of the Normal distribution is all needs to be done. In other words, a half–Normal plot will be

$$x_{(i)} \quad \text{vs} \quad \phi^{-1}\left\{\left(\frac{i}{n+1}+1\right)\Big/2\right\}$$

obtained by substituting i /(n+1) for p.

Apart from three points that deviate from the straight line, Fig 2.4 indicates that 211 diameters (i.e. all data) have approximately a half–Normal distribution. The three outliers seen in the figure are found to be from circles placed in the 'less accurate data set' (Thom, 1967; Table 5.2). Kendall (1974) noted that the accurate and less accurate circles indicate the same quantum and the same error.

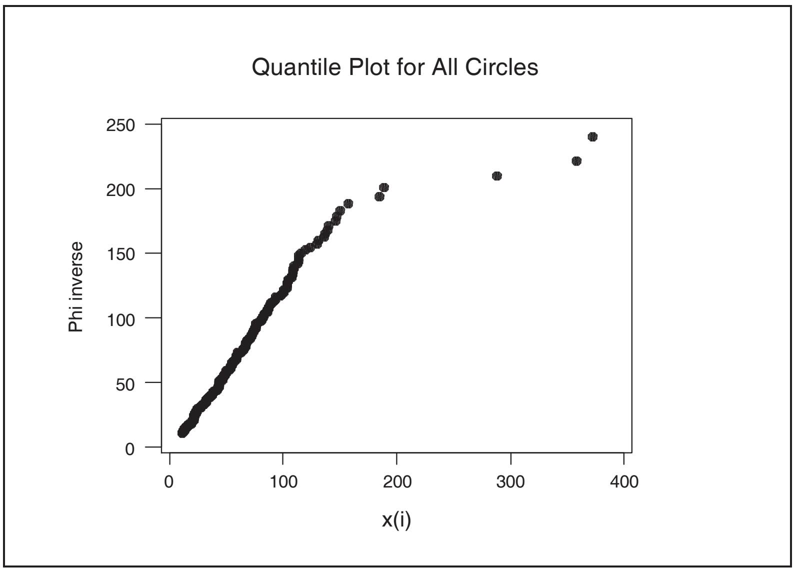

Fig 2.4. Half–Normal plot of the circle diameters

2.8.2. Some Features of Suprema

In this section, we investigate some features of suprema obtained when reassessing the significance of the highest peak appeared to be at 5.435 for 211 circles in the cosine quantogram graph.

Simulation studies were carried out by generating 1000 artificial data sets from a half–Normal distribution that matches the distribution of the circle diameters in the first moments. Both simulation and cosine quantogram analysis were carried out in a FORTRAN program, using the algorithm AS 183 (Wichmann & Hill, 1982). The formula generating the simulated circle diameters was

$$X = 10 + 81.32\,|Z|$$

where Z is an artificial standard Gaussian variable. The numerical coefficients were chosen to match the simulated data sets to the circles with respect to mean and variance. The quantogram analyses were performed over a the τ–range [0.09, 0.59]. Then, the test statistic (i.e. $\underset{\tau_{\min}}{\overset{\tau_{\max}}{Max}}\left\{\phi(\tau)\right\}$) was calculated for each of the independent artificial samples.

So far, some features of suprema of the cosine quantogram, such as the distribution of suprema and the effect of the shape of the simulation distribution on the outcome, have been questioned in preceding analyses of the circles. In the following sections, we present not only some empirical verification of such properties but also some new features of the cosine quantogram analysis.

2.8.2.1. Fitting the G.E.V. Distribution

Kendall points out that the process $\left\{\phi(\tau) : \tau_{min} < \tau < \tau_{max}\right\}$, for not too small n and not too small $\tau_{\min}$, is asymptotically a section of a stationary normalized Gaussian stochastic process. Moreover, a limit theorem of Cramér (Cramér & Leadbetter, 1967) states that the distribution of the supremum of a stationary Gaussian process, as the interval over which we are maximising the function becomes large, converges to a Gumbel distribution.

For samples of size n from the Exponential family, the asymptotic distribution of the largest value, denoted as x[n] (Gumbel, 1958) as $n \to \infty$ is given by the distribution function

$$H(x[n]) = \exp (- \exp (-y)) \tag{2.10}$$

where

$$y = (x[n] - u)/ \alpha$$

The variable y is defined to be the reduced variate which is equivalent to the familiar standardised Gaussian variate. The parameter u and α are location and scale parameters (but not the mean and standard deviation) of the extreme value distribution. Equation (2.10) can be defined as a function of y instead of x. Then, a single reduced extreme value distribution can represent all possible extreme value distributions. The distribution function is as follows

$$H(y) = \exp (- \exp (- y))$$

and the inverse of the distribution function is

$$y = - ln (- ln (H(y))$$

Therefore, a probability plot of ordered extreme values against their expected cumulative relative frequencies (y) can be used as an informal tool in order to detect easily any deviation from a straight line.

For the simulation study of the circles, the supremum values of the cosine quantograms calculated from the 1000 samples each of size 211 drawn from a half–Normal distribution matching that of the stone circles have been obtained and the empirical density of them are given in Fig 2.5.

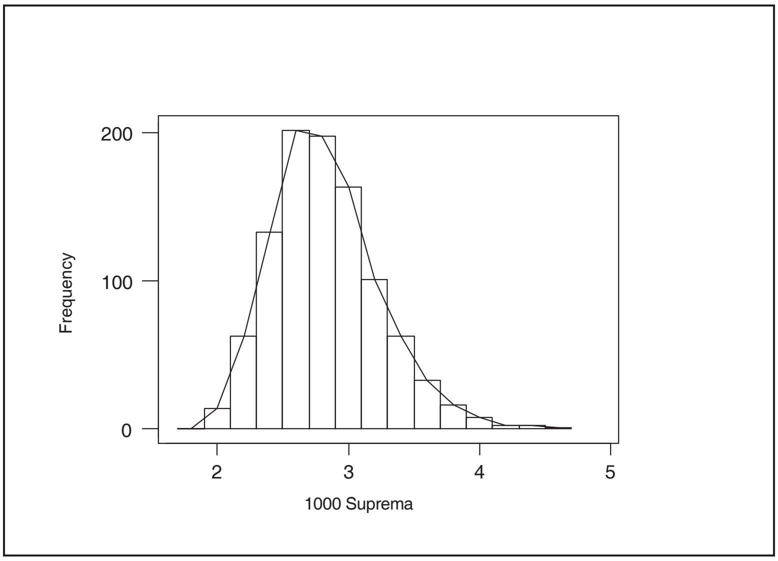

Fig 2.5. Empirical density of supremum values

A program was written to calculate, by the method of maximum likelihood, the estimators of the parameters u and α for the supremum values of cosine quantogram, using the simultaneous equations given by Evans et al. (1993). The estimated values are

$$\hat{u} = 2.635 \quad \text{and} \quad \hat{\alpha} = 0.343$$

A Q–Q plot of the data (Fig 2.6) plotting the ordered values $supr_{(i)}$ (i = 1,2,...,1000) against their expected values (i.e. y= $\hat{u} - \hat{\alpha}\, ln\,(-\, ln\,(\, i/n+1\,))$ shows clear evidence of curvature.

This was investigated further and a Generalized Extreme Value model was fitted. The distribution function of this is the three–parameter function:

$$F(x) = exp\left[-\left(1+\frac{k(x-u)}{\alpha}\right)^{-1/k}\right] \tag{2.11}$$

the third parameter k here enables the fitting procedure to estimate the type automatically. As k approaches zero, this distribution approaches the Gumbel distribution. It is of the Weibull distribution for k less than zero and of the Fréchet distribution for k greater than zero (Embrechts et al., 1997).

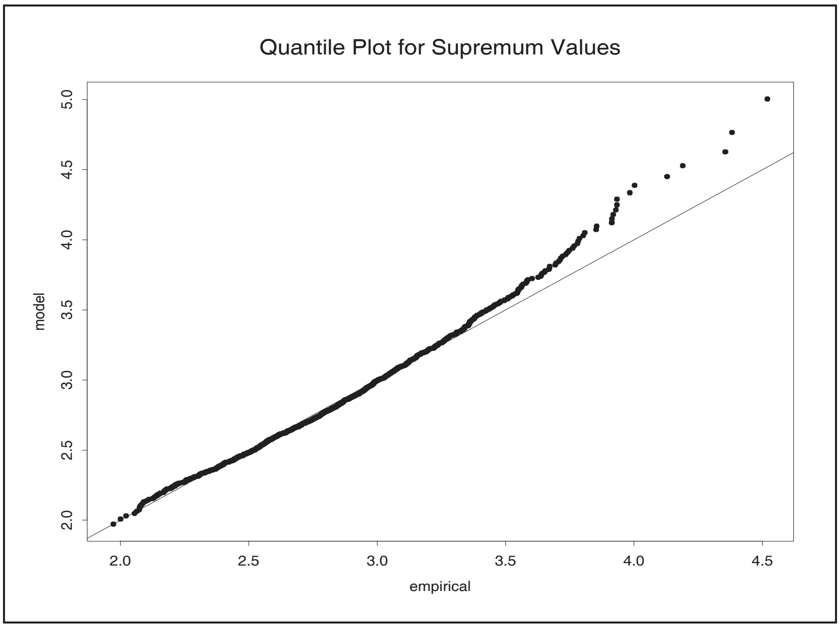

Fig 2.6. Q–Q plot for Gumbel E.V. distribution.

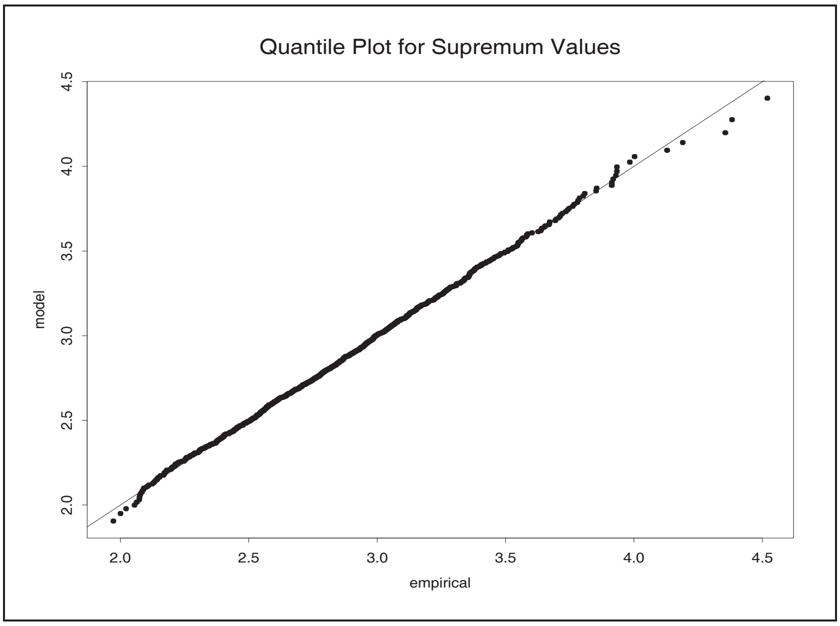

Fig 2.7. Q–Q plot of extreme values for G.E.V. distribution

Maximum likelihood estimates of the parameters for the supremum values of cosine quantograms were found using a program provided by Anderson (pers. comm.) as follows:

$$\hat{u} = 2.6539, \qquad \hat{\alpha} = 0.3508, \qquad \hat{k} = -0.1004$$

The straight line in the Q–Q plot given in Fig 2.7 indicated that a G.E.V. distribution with the parameters above fits better. It should be noted that such an extreme value distribution for supremum of cosine quantogram could be used as an alternative way of assessing the significance of quantal pattern of the data.

2.8.2.2. A Natural Scale for Gridsearch

Two further questions of interest are firstly the distribution of q and τ over (q_{min},q_{max}) and (τ_{min}, τ_{max}) in the null situation, i.e. when the data are not quantal, and secondly whether $\hat{q}$ and $\phi(\hat{q})$ (or $\hat{\tau}$ and $\phi(\hat{\tau})$) are independent in the null situation. If either $\hat{q}$ or $\hat{\tau}$ were uniformly distributed over their ranges then this would be the 'natural' scale to use in for example selecting the range of search and assessing the influence of extending or contracting the range. If $\hat{\tau}$ and $\phi(\hat{\tau})$ were not independent then this might also need to be considered in selecting the range.

Examination of the $\hat{\tau}_i$ obtained in the simulation study above using a Kolmogrov Smirnov Goodness of Fit test for uniformity and the null hypothesis $\hat{\tau}_i \sim U(\tau_{min}, \tau_{max})$ was accepted with P = 0.71 (see Fig 2.8). This clearly excludes the possibility that $\hat{q} \sim U(q_{min}, q_{max})$ and so for many purposes it is 'natural' to work in terms of the 'frequency measure' τ rather than the actual quantum value q.

From the same data Fig 2.9 gives a plot of $\phi(\hat{\tau}_i)$ against $\hat{\tau}_i$. The Spearman Correlation Coefficient for these data is 0.0008 which taken together with the scatter plot indicates no suggestion of dependence between $\hat{\tau}_i$ and $\phi(\hat{\tau}_i)$.

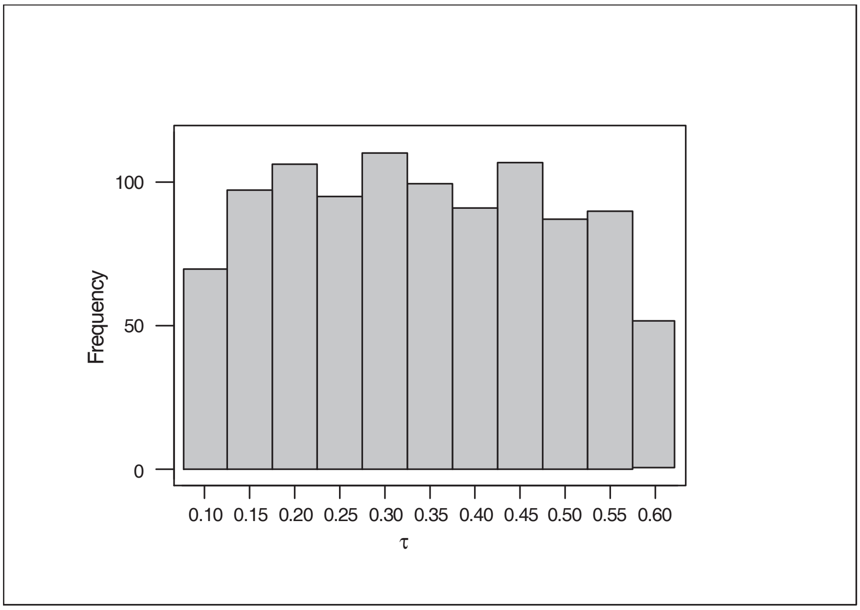

Fig 2.8. Histogram of the 1000 $\hat{\tau}_i$ values

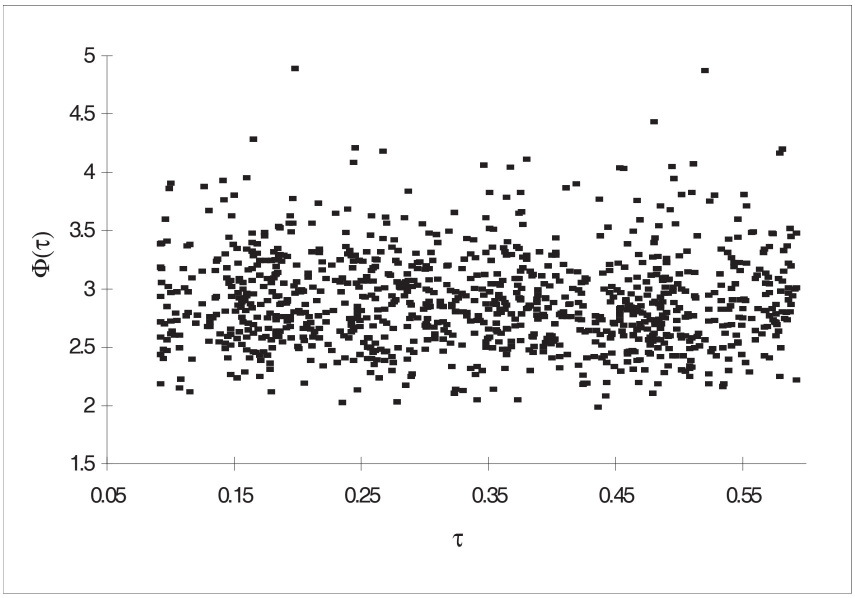

Fig 2.9. Scatter plot of $\phi(\hat{\tau}_i)$ against $\hat{\tau}_i$

2.8.2.3. The Effect of the Underlying Distribution

In both Kendall's and our study on the circles, the simulations are carried out by matching the artificial data sets to the shape of the underlying distribution (i.e. half–Normal). Kendall and Kent in the discussion of Freeman (1976) state that the shape of the simulation distribution has only the slightest noticeable effect on the assessment of significance and that it appears that the distribution of the supremum is similar for a variety of underlying distributions.

Investigating their claim in more detail, we simulated the supremum values from the 1000 samples each of size 211 drawn from other types of underlying smooth distribution, specifically gamma, exponential, beta and uniform as well as half–normal distributions all matched to original data set with respect to mean and variance but not quantality. Then, we compared the distributions of the 1000 supremum values for each and present the results graphically in Fig 2.10. It is remarkable that all the five empirical densities of the supremum values exhibit generally similar behaviour with only the uniform, represented by the broken line, showing any substantial deviation.

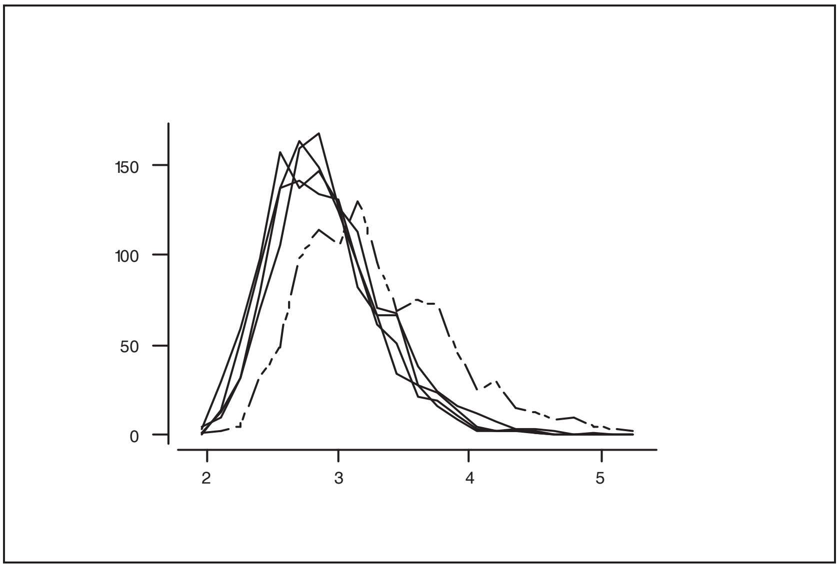

Fig 2.10. Empirical densities of the suprema when underlying distribution is Exponential, Gamma, Beta, h–Normal and Uniform (dotted line)

Kent also points out that the distribution of the supremum values does not depend critically on the exact τ–range. He also mentions that the mean and variance of the limiting Gumbel distribution depend on the underlying distribution X only through EX^2 (see also Kent, 1975). Hence we would not be surprised to find the distribution of the supremum is similar for a wide variety of underlying smooth distribution.

2.8.3. The Effect of Random Number Generator

In statistics, the term 'simulation' describes a wealth of varied and useful techniques, all connected with the mimicking of the rules of a model of some kind. When models are given in a mathematical formulation, but analytic predictions are not possible, then quite often simulation can prove to be a useful tool, not only for describing the model itself but also for investigating how the behaviour of the model may change following a change in the model. It can also be used to gauge the performance of the various techniques.

Simulation techniques depend on generating pseudorandom numbers from a uniform distribution on the interval (0, 1) and converting them to samples from nonuniform distributions. Generated random numbers are required to have some properties such as each element should appear 'equally often', successive numbers should not be correlated and sequences should have a long cycle before repeating. At present, congruential generators form the commonest family of pseudorandom number generators and they have been proved to be satisfactory for most purposes (Ripley, 1983). These are of the form $x_{n+1} = ax_n + b\,(mod\; m)$, where a, b and m are suitably chosen integers, and are referred to as a (a, b; m) congruential generator. Specifying a seed value x_0 allows a sequence $x_1, x_2, \ldots$ of pseudo random numbers to be generated.

Computers are widely used to produce random numbers. Mainframe computers have usually been provided with libraries of sub–routines written by experts. There are also numerous algorithms available for the programmers to use in specific programs. It is always necessary for users and programmers both to be aware of the pitfalls in inadequate algorithms and to know of suitable methods for sampling from normal and other distributions. For example, Neave (1973) demonstrates the effect of using the Box and Muller algorithm with an unsatisfactory multiplicative congruential generator ($131,0;2^{35}$). If the multiplicative constant is small and has a simple binary representation, the tails of the supposedly normal distribution contain spikes and displayed unusual characteristics. For example, he simulated large data sets using the generator mentioned above and observed that frequencies in the intervals $(-\infty, -3.3)$ and $(3.6, \infty)$ were unexpectedly zero.

Hence, one should bear in mind that what is random enough for one application may not be random enough for another. Due to the computer intensive nature of the analyses concerning quantal problems, it is now necessary to investigate whether or not using different random number generators could affect the assessment of quantality by having quantal–like structures in their nature.

For the current investigation, we compare the performances of some random number generators to test for pure and shifted quantality. Our attention is directed to the generators used to generate Uniform and Normal variates. Since there are vast amount of algorithms for these purposes, we had to restrict ourselves to the ones written by experts, which are common in use. Especially, our aim is to investigate the generators to which anyone can have an easy access, such as NAG library routines (1995) and Numerical Recipes (Press et al, 1992). Therefore the following selection of commonly used generators are considered here:

- **RANDOM(dum):** one of the three component generators used by Wichmann and Hill (1982). Call with dum any real number to initialise.
- **G05CAF(dum):** The NAG generator by Numerical Algorithms Group (1995). G05CCF is used to generate a random seed. Call with dum any real number to initialise.
- **RAN0(idum):** "Minimal Standard" generator by Park and Miller (1988) as given in Numerical Recipes in FORTRAN (Press et al. 1992). Call with idum any negative integer to initialise.

- **RAN1(idum):** "Minimal Standard" generator by Park and Miller with Bays–Durham shuffle (see Knuth, 1981) and added safeguards as given in Numerical Recipes in FORTRAN (Press et al. 1992). Call with idum any negative integer to initialise.
- **RAN2(idum):** Long period ($> 2 \times 10^{18}$) random number generator by L'Ecuyer (1988) with Bays–Durham shuffle and added safeguards as given in Numerical Recipes in FORTRAN (Press et al. 1992). Call with idum any negative integer to initialise.
- **RAN3(idum):** A random number generator by Knuth (1981) as suggested for the machines that are poor in arithmetic (i.e. limited to 16–bit integers) in Numerical Recipes in FORTRAN (Press et al. 1992). Call with idum any negative integer to initialise.

The uniform values generated by the above listed generators will be converted to standard Normal variates by means of the Polar Marsaglia–Bray method using a routine named **NRAND** from the library of the Department of Probability and Statistics at Sheffield University. Additionally, the following generators provided by NAG library are considered here to generate from Normal distribution:

- **G05DDF:** generates a random number taken from a Normal distribution. This routine uses Brent's (1974) algorithm, which employs Forsythe's method.
- **G05FDF:** generates a vector of random numbers from a Normal distribution. This routine uses Box–Muller method.

As a pilot sample, all circles in England, Wales and Scotland (n=169) are used for the reason that they were reported by Kendall to be quantal at q = 5.442 with p–value = 0.0083 (in 600 simulations). Therefore we generate non–quantal random samples of size 169 having the same mean and the variance of the pilot sample as

$$Y = 10 + 69.75\,|Z|$$

where z is a standard Normal variate generated using the generators we have listed. Then quantogram analyses for 10000 simulated samples have been carried out over the τ range [0.09, 0.59] with an increment 0.0001.

For both cosine and modular quantograms, then 95% critical values have been calculated by $\phi_{9500}(\hat{\tau})$ [or $\chi_{9500}(\hat{\tau})$] using the ordered values of $\phi_i(\hat{\tau})$ [and $\chi_i(\hat{\tau})$] where i=1,...,10000. In addition, 95% confidence intervals for the critical values have been constructed by means of a rule to construct distribution free confidence intervals for quantiles (David, 1970). It is stated that for n > 10, an approximate 1–α confidence interval for a quantile is obtained by counting off $\frac{1}{2}\sqrt{n}\,u_\alpha$ observations to the left and the right of the sample quantile and rounding out to the next integer, where u_α is the upper $\alpha/2$ significance point of a standard normal variate. Therefore, we obtain a confidence interval as

$$\left(\phi_{9402}(\hat{\tau}), \phi_{9598}(\hat{\tau})\right) \quad \text{or similarly} \quad \left(\chi_{9402}(\hat{\tau}), \chi_{9598}(\hat{\tau})\right)$$

where the values 9402 and 9598 are calculated by applying the rule when α=0.05 as follows:

$$9500 \ \pm \ \frac{1}{2}\sqrt{10000}\,1.96$$

Furthermore, significance probabilities have been estimated by comparing the simulated 10000 values of $\phi(\hat{\tau})$ and $\chi(\hat{\tau})$ with the observed ones which are 4.120 and 8.799 respectively. The results have been summarised in Table 2.3. Examination of this table shows clearly that the assessment of quantality is not affected by the choice of particular generator from this set of commonly used ones.

Table 2.3. Estimated critical values with 95% C.I. and observed significance probabilities for $\phi(\hat{\tau})$ and $\chi(\hat{\tau})$ using different random generators.

Generator	Critical Value (95% C.I.)		P –value	
Normal – Uniform	$\phi(\hat{\tau})$	$\chi(\hat{\tau})$	$\phi(\hat{\tau})$	$\chi(\hat{\tau})$
NRAND – RANDOM	3.627 (3.580, 3.686)	8.343 (8.151, 8.545)	0.0077	0.0321
NRAND – G05CAF	3.631 (3.581, 3.692)	8.294 (8.124, 8.551)	0.0064	0.0336
NRAND – RAN0	3.636 (3.591, 3.691)	8.382 (8.179, 8.606)	0.0075	0.0338
NRAND – RAN1	3.635 (3.583, 3.694)	8.427 (8.236, 8.692)	0.0084	0.0359
NRAND – RAN2	3.638 (3.588, 3.692)	8.355 (8.157, 8.607)	0.0070	0.0337
NRAND – RAN3	3.634 (3.582, 3.691)	8.345 (8.185, 8.625)	0.0074	0.0333
G05DDF	3.624 (3.586, 3.692)	8.376 (8.175, 8.624)	0.0080	0.0332
G05FDF	3.631 (3.573, 3.692)	8.323 (8.123, 8.494)	0.0067	0.0305

2.8.4. The Effect of Autocorrelation

In the assessment of quantality, one of the assumptions about any given data is that the observed values are independently distributed. The foregoing investigations of any quantal effect in the various data sets have raised no doubt about this assumption. As far as root spacings are concerned, however, it has been suggested that there may be some correspondence between them (Lloret, 1998). In order to investigate whether or not the assumption of independency is violated by the root spacings being dealt with in the current study, some preliminary analyses have been carried out (in chapter 4), it has been found that there is some evidence that successive pairs of spacings are autocorrelated, but not in a consistently negative or positive direction from root to root. Although first order correlation coefficients are not great in magnitude (they are between [–0.5, 0.5]), it is perhaps necessary to examine whether such autocorrelation would result in a noticeable change on the assessment of significance of any possible quantal effect.

With this motivation, we carried out a simulation study by generating the artificial, non–quantal data sets from a Markov model (i.e. AR(1)) with an order of magnitude of autocorrelation in the range (–0.5, 0.5). The stationary AR(1) model may be written as

$$y_t = \delta + \phi y_{t-1} + \varepsilon_t$$

where δ is a constant term and ϕ is the autocorrelation coefficient on y_{t-1}. The error term ε_t is then to be white noise with zero mean and variance σ^2 (i.e. $\varepsilon_t \sim N(0, \sigma^2)$, i.i.d.). In addition, given the requirement of the stationarity i.e. $|\phi| < 1$, $E(y_t) = \mu$ and $V(y_t) = \gamma_0$ yields

$$\mu = \frac{\delta}{1-\phi} \qquad \textit{and} \qquad \gamma_0 = \frac{\sigma^2}{1-\phi^2}$$

Assuming that the mean of the series y_t has been subtracted out so that the new series, say Z_t, has a zero mean and variance of γ_0, the first order Autoregressive process can also be represented as weighted linear combination of the present and past terms of a white noise process (Cryer, 1986):

$$Z_t = \varepsilon_t + \phi \varepsilon_{t-1} + \phi^2 \varepsilon_{t-2} + \cdots$$

We illustrate the simulation of AR(1) series of length 100 with $\phi = 0.5$ and $\phi = -0.5$. White noise series is generated according to a normal distribution with zero mean and σ^2 variance. Since the artificial data set has to be matched to the original one with respect to its mean and variance, one of the tomato roots with $\bar{x} = 2.5$ and s = 1.5 has been chosen as a representative of all for this experiment.

Step 1. Set $\phi = 0.5$ (or –0.5) and N = 100 + 51. Decide on σ so that the series has the same variance of s^2 as the selected root.

i.e. $$\sigma = s\sqrt{\left(1-\phi^2\right)}$$

Step 2. Generate $\varepsilon_t \sim N(0, \sigma^2)$ (i.i.d.), t = 1,…, N

Step 3. Set $Z_1 = 0$ and $t = 2$

Step 4. Calculate $Z_t = \phi Z_{t-1} + \varepsilon_t$

Step 5. Set $t = t + 1$

Step 6. Repeat step 4 & 5 50 times

Step 7. Omit the initial 50 transient values in the final series. This 'warming–up' period is necessary because of the recursiveness of the AR defining equations (Cryer, 1986).

Step 8. Since this simulated series has a zero mean, match its mean to the actual one, $\bar{x}$, by adding some constant value to all values of the series. In order to guarantee that the resulting series do not contain any negative values, as the practical experience showed that mean has lesser effect on the quantality, we prefer to add at least 4*s to the final series.

Having generated a Markov series with the autocorrelation coefficient required, it was used to obtain a suprema by performing the quantogram analysis over τ range [0.45, 5] with an increment of 0.001. This process was repeated 1000 times and 95% and 99% critical values were calculated for the cases not only when $\phi = 0.5, -0.5$ but also when artificial data sets were generated from Gamma and h–Normal distributions not having any correlation structure.

Fig 2.11 summarises the results in a graphical form and Table 2.4 presents the critical values estimated. We can see that the autocorrelated samples produced slightly higher critical values at 95% significance level. However, it is believed that this much difference would not cause any distortion. The 99% critical values show a slight variation which could be considered as a random variation. Therefore we can conclude that the autocorrelation between spacings would not result in any problem in the testing procedure.

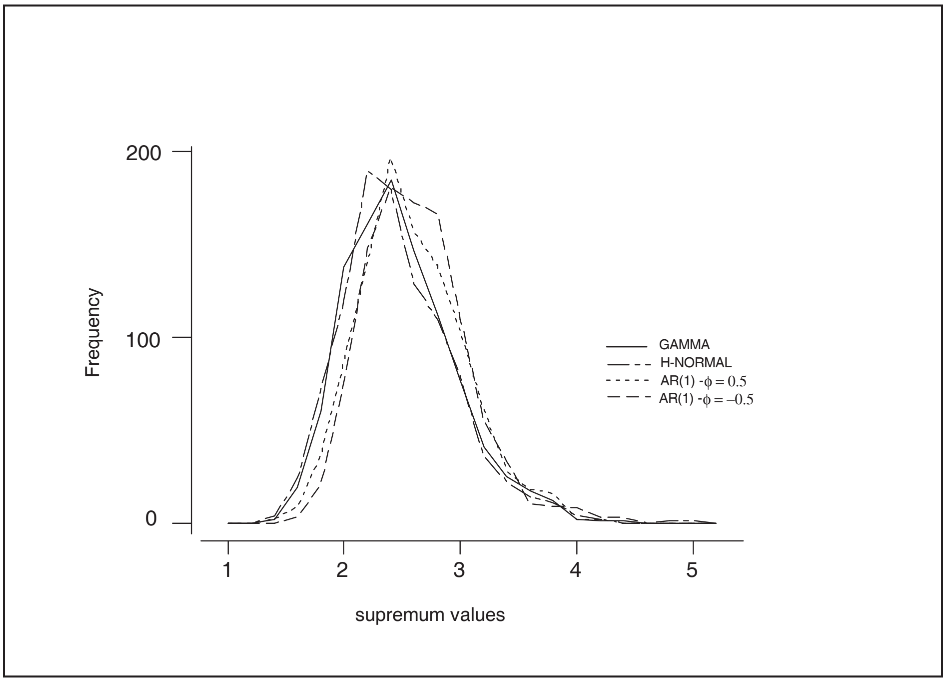

Fig 2.11. Empirical densities of the supremum values

Table 2.4. The estimated critical values for $\phi(\tau)$ when data are autocorrelated.

Dist^n $\alpha \rightarrow$	**0.05**	**0.01**
Gamma	3.338	3.766
H–Normal	3.341	3.836
Markov ($\phi = 0.5$)	3.388	3.793
Markov ($\phi = -0.5$)	3.386	3.891

2.9. Summary

In this chapter, we have demonstrated the basic quantal models, distinguishing between two possible kinds of quantality, “pure” or “shifted”. The essence of the problem is that the underlying quantum (if it exists) is not known in advance and has to be deduced from the data. The earliest statistical method to extract this feature resulted in the foundation of the von Mises distribution which lead to the development of Kendall’s methodology known to be the most efficient method up to now. A review of Broadbent’s method also showed that it is different in style and the estimation of shift effects is not precise as it depends on the least squares estimation method.

Having reviewed the various approaches to solve the problem, we have shown that Kendall’s methodology of so called quantogram analysis is essentially a Likelihood Ratio test that utilises the circular structure of the problem. A further study of Kendall’s procedure revealed that the assessment of the significance of quantality is not influenced by the choice of underlying ‘non–quantal’ distribution. It is also found that the ‘frequency measure’ of the reciprocal of the quantum should be considered as a natural scale to use throughout the analyses. In addition, we have shown that a three parameter Generalized Extreme Value distribution provides a better fit to the null distribution of Kendall’s test statistic as opposed to a two parameter Gumbel distribution.

Noting the computer intensive nature of the problem, we also investigated the effect of different random number generators in the assessment of quantality and found that random numbers generated do not exhibit any hidden quantal structure.

We finally demonstrated that the assessment of quantality remains unaffected when the data points are serially correlated.

CHAPTER 3.

Power of Significance of Test Statistics for Quantality

3.1. Introduction

In this Chapter we further investigate the assessment of pure and shifted quantality with the test statistics available, $\phi(\tau)$ and $\chi(\tau)$ respectively. In section 2.6 we showed that these were likelihood ratio test statistics for the specific alternatives of "pure" and "shifted" quantality respectively and so can be expected to be the most powerful available statistics for moderate sized samples and so these are the only candidates that need to be considered for routine use. Clearly, in many practical situations there may be doubt as to whether any quantality that may be present is "pure" or "shifted" because this depends on the origin of measurement. This arises notably with stone circles where the internal or external diameters that could be examined but only one choice at most would exhibit pure quantality. Similar problems may arise in biological applications where distances are measured from some point on a specimen. Perhaps in physical examples such as atomic weights there might be some scientific theory predicting pure quantality in the available measurements. Thus, in many situations it may be attractive to use $\chi(\tau)$ to investigate quantality rather than $\phi(\tau)$ so as to provide protection against unsuspected 'shifted' quantality. This presumably results in some loss of power over using $\phi(\tau)$ if in fact the quantality is pure (since essentially $\chi(\tau)$ provides an estimate of an extra parameter – the origin of measurement which gives pure quantality) and there will also be some increase in computation. In this chapter we investigate how much power is lost by using $\chi(\tau)$ and how much protection it provides over $\phi(\tau)$ in the presence of shifted quantality.

We begin in section 3.2 with a brief description of the von Mises distribution which plays an important role in the assessment of power of quantogram analyses. Section 3.3 describes a simulation study to evaluate the power of $\phi(\tau)$ and $\chi(\tau)$ for a comparison not only to test for pure quantality but also shifted quantality. The sample size effect on power is also assessed in section 3.4.

3.2. The von Mises Distribution

The power of a test is the probability that the test rejects the null hypothesis when it is false. In a quantogram analysis, the determination of whether to reject or accept the null hypothesis that the data set is *not* quantal depends on the size of the errors (ε_i) referring to models 2.1 and 2.2. In other words, the error component has an important role in assessment of quantality due to the fact that existence of a quantum depends on the magnitude of errors. The more closely clustered they are around 0 or q, the more likely the data are quantal. Similarly, the more they are spread out uniformly between 0 and q, the less likely the data are to exhibit any quantal feature.

Traditionally, measurement (and other) errors are represented by a Gaussian distribution. However, in models 2.1 and 2.2, the Gaussian distribution needs to be modified to produce its 'circular equivalent' because an ε_i very close to q is in practice close to 0 since in the above models increasing ε_i beyond q triggers an increase in m_i by 1 and subtraction of q from ε_i. That is we need to 'wrap' the error distribution round from q to 0. For a given σ, this modification is called the wrapped Gaussian distribution. Our preference, however, is to use another closely related error–distribution on the circle, first introduced by von Mises (1918), which is also in many respects the natural analogue on the circle of the Normal distribution on the real line (Mardia, 1972; Fisher, 1995). It is a symmetric distribution and unimodal.

An angular random variable θ has the von Mises distribution denoted by VM(μ, κ) if its probability density function has the form

$$f(\theta)=\frac{exp\left[\kappa\, cos(\theta-\mu)\right]}{2\pi I_0(\kappa)}, \quad -\pi<\theta<\pi, \quad \kappa>0, \; -\pi<\mu<\pi$$

where $\mathrm{I}_p(\kappa)$ is the modified Bessel function of the first kind and order zero (for further details see Mardia, 1972).

The parameter μ is the mean direction and the parameter κ is known as the concentration parameter and is equivalent to the reciprocal of the variance. This distribution is symmetric about μ and the mode is also μ. In addition, for large κ, the von Mises variate tends to the normal variate N(μ, σ^2) with $\mu = 0$, $\sigma^2 = 1/\kappa$ and for $\kappa \cong 0$, it reduces to the uniform variate U(a, b) with a $= -\pi$, b $= \pi$.

It is also well known (see Stephens, 1963) that the VM(μ, κ) approximates very closely the distribution of the Wrapped Normal with variance σ^2 i.e. WN(μ, σ^2) which will also be used in the thesis. By equating their first trigonometric moments, we have

$$A(\kappa) = e^{-\frac{1}{2}\sigma^2}$$

For any given κ, we can then obtain σ and draw a random sample from $N(\mu, \sigma^2)$ which, with the help of the transformation $x_w = x \pmod{2\pi}$, leads to a random sample from the Wrapped Normal distribution. In order to express this relationship in terms of a quantum, q, the σ should then be replaced by $2\pi\sigma/q$.

In the following sections, a comparative study based on simulations will be carried out to compare the power of two test statistics.

3.3. Comparison of the Power of the Test Statistics

Within the framework of this comparative study, the main concern is directed to the question whether or not the test statistic $\chi(\tau)$ is as good at testing for pure quantality as the test statistic $\phi(\tau)$. So as to compare the power of these, simulation methods have to be used.

Artificial data sets were simulated in the form of the pure quantum model 2.1. The value of the quantum is chosen to be "1" without loss of generality and for reasons of simplicity the sample size is taken to be 50. We describe a limited investigation of the dependence of comparative power on sample size in section 3.4. Integers m_i in 2.1 are generated from a Bi(30, 0.333) which gives similar statistical properties as the integers from the good circles in Scotland.

The errors ε_i in 2.1 were taken as values from $VM(0, \kappa)$ (with various values of κ investigated). An efficient generation of pseudo–random values from $VM(0, \kappa)$ is made by means of the algorithm (Best and Fisher, 1979) based on the envelope–rejection method using the Wrapped Cauchy distribution. It must be noted that this algorithm generates a von Mises variate lying between $\pm\ \pi$. Thus, a simple transformation was needed to convert the numbers so that they lie between $\pm\ \frac{q}{2}$ (i.e. $\frac{-q}{2} \leq \varepsilon < \frac{q}{2}$).

Due to the fact that the 'degree of quantality' depends on the value of κ (i.e. the larger κ, the more the data look quantal), a decision on what values of κ are of most interest must be made first. The lower bound for it has been chosen to be very close to zero, i.e. near uniform so non–quantal data. For the upper bound, taking into the account that the circles were found to be quantal when $\kappa \cong 0.45$ (i.e $\sigma \cong 1.5$ for many subsets of the circles), we will consider the values of κ up to 1.5.

Additionally, the range of the gridsearch for the quantogram analysis has been fixed as $\tau_{min} = 0.75$ and $\tau_{max} = 1.25$ [or equivalently $q_{min} = 0.8$ and $q_{max} = 1.33$] with an increment of 0.001. Again, dependence of comparative power on the range has not been investigated.

In the light of the explanations given above, the following sections will establish necessary computations for assessing the critical region and the power of the two test statistics.

3.3.1. Critical Values for Pure Quantality

When performing a test, one must obtain the critical region for rejecting the null hypothesis. Since samples with different values of κ will have slightly different means and variances, even if generated by 2.1 with identical values of m_i, 5% critical values of $\phi(\tau)$ and $\chi(\tau)$ were calculated separately for each value of κ, and then these estimated values were used in testing each of the 1000 simulated samples constructed for the assessment of power, i.e. fresh critical values were not calculated for each separate sample generated with a common value of κ.

The algorithm for obtaining the critical values is as follows:

Step 1: Generate samples of size 50 in the form of the pure quantum model, in relation to κ varying from 0.05 to 1.5 with an increment of 0.05 and $\kappa_1 = 0.00001$ (31 possible values of κ in the range).

$$x_{ij} = m_i * q + VM(0, \kappa_j), \quad i = 1,\ldots,50; \quad j = 1,2,\ldots,31$$

and calculate the mean $\left(\overline{m}_j\right)$ and the variance $\left(s_j^2\right)$ of each sample.

Step 2: Generate non–quantal samples (y_{ij}) of size 50 from half–Normal distributions having the same mean and variance of x_{ij} as follows:

$$y_{ij} \sim HN(\mu_j, \sigma_j), \quad i = 1,\ldots,50; \ j = 1,\ldots,31$$

i.e. $$y_{ij} = \mu_j + \sigma_j \left|Z_j\right|, \quad i = 1,\ldots,50; \ j = 1,\ldots,31$$

where Z_j are standard Normal variates, $\sigma_j = \dfrac{s_j}{\sqrt{1 - 2/\pi}}$ and $\mu_j = \overline{m}_j - \dfrac{2\sigma_j}{\sqrt{2\pi}}$

***Step 3*:** Perform quantogram analyses for each sample and calculate

$$\hat{\tau} = arg\ Max_{\tau_{min}}^{\tau_{max}}\left[\phi_j(\tau)\right] \text{ and } \hat{\tau} = arg\ Max_{\tau_{min}}^{\tau_{max}}\left[\chi_j(\tau)\right]$$

***Step 4*:** Repeat Step 2 & 3 1000 times for the j^{th} value of κ. Then, repeat Step 1–4 for $(j+1)^{th}$ value of κ until the same process finishes for 31st value of κ.

***Step 5*:** Order the supremum values in increasing order for each κ, e.g.

for κ_1 $$\phi_{1,1}(\hat{\tau}),\ \phi_{2,1}(\hat{\tau}),\ldots,\phi_{950,1}(\hat{\tau}),\ldots,\phi_{1000,1}(\hat{\tau})$$
$$\chi_{1,1}(\hat{\tau}),\ \chi_{2,1}(\hat{\tau}),\ldots,\chi_{950,1}(\hat{\tau}),\ldots,\chi_{1000,1}(\tau)$$

for κ_2 $$\phi_{1,2}(\hat{\tau}),\ \phi_{2,2}(\hat{\tau}),\ldots,\phi_{950,2}(\hat{\tau}),\ldots,\phi_{1000,2}(\hat{\tau})$$
$$\chi_{1,2}(\hat{\tau}),\ \chi_{2,2}(\hat{\tau}),\ldots,\chi_{950,2}(\hat{\tau}),\ldots,\chi_{1000,2}(\hat{\tau})$$

and so on.

Then calculate 5% one–sided critical values (i.e. $\phi_{950,j}(\hat{\tau})$ and $\chi_{950,j}(\hat{\tau})$) for each κ_j (see Table 3.1). It can be seen that there is actually little variation with values of κ in the critical values and perhaps a common value could be used throughout.

Table 3.1. Estimated 5% Critical Values for $\phi(\tau)$ and $\chi(\tau)$

κ	$\hat{\phi}_{950}$	$\hat{\chi}_{950}$	κ	$\hat{\phi}_{950}$	$\hat{\chi}_{950}$
0.00001	3.0651	5.8151	**0.80**	3.0531	5.7259
0.05	3.0083	5.6174	**0.85**	3.0295	5.8012
0.10	3.0708	5.8041	**0.90**	3.1165	5.9210
0.15	3.0405	5.7269	**0.95**	3.0857	5.8604
0.20	3.0589	5.6079	**1.00**	3.0605	5.7556
0.25	3.0877	5.6242	**1.05**	2.9350	5.5483
0.30	3.1037	5.9686	**1.10**	3.1139	5.9882
0.35	3.0701	6.1024	**1.15**	3.0987	5.9446
0.40	3.1048	5.7419	**1.20**	3.0817	5.7944
0.45	3.0106	5.6920	**1.25**	3.1272	6.0269
0.50	3.0748	5.5311	**1.30**	3.0336	5.7240
0.55	3.0261	5.6948	**1.35**	3.1145	5.6389
0.60	3.0301	5.7238	**1.40**	3.0600	5.8392
0.65	3.0800	5.9034	**1.45**	3.0212	5.7729
0.70	2.9972	5.7689	**1.50**	3.0645	5.9810
0.75	3.0512	5.5992			

3.3.2. Power Calculations for Pure Quantality

In the significance–test formalism for quantality, the null hypothesis H_0 is that data are not quantal (i.e. the data come from a smooth distribution) and rejection of H_0 will be used as evidence in favour of pure quantality. Therefore, the power of the cosine and modular quantogram to test for pure quantality is described as

$$\text{Power} = \text{Prob}\{\ \phi(\hat{\tau})\left[or\ \chi(\hat{\tau})\right] \in w \mid H_o\ is\ false\ \}$$

where w is the critical region of size 0.05.

In the process of simulating artificial data sets, the parameter κ is again used to control the degree of quantality. It is expected that test statistics gain more power as κ gets bigger. On the other hand, it has to be noted that even with definitely non–quantal data ($\kappa \cong 0$), the cosine or modular quantogram of the data has peaks of various shapes and sizes since any set of data is bound to give more support to some values of q than to others. In order to evaluate the power, the procedure below is followed:

firstly, for each value of κ, generate artificial data sets from the pure quantal model as in step 1 in section 3.3.1,

$$x_{ij} = m_i * q + VM(0, \kappa_j), \quad i = 1, \ldots, 50; \;\; j = 1, 2, \ldots, 31$$

Then, obtain the most plausible value of τ in the τ range [0.75, 1.25] utilising both the cosine quantogram and the modular quantogram on the x_{ij}.

i.e. $$\hat{\tau} = arg\ Max_{\tau_{min}}^{\tau_{max}} \left[\phi_j(\tau) \right] \quad \text{and} \quad \hat{\tau} = arg\ Max_{\tau_{min}}^{\tau_{max}} \left[\chi_j(\tau) \right]$$

This process was also repeated 999 times for each value of κ and the power was evaluated firstly for $\phi(\tau)$ as

$$\text{Power } (\phi) = \frac{\# \left\{ \phi_j(\hat{\tau}) \geq \phi_{950,j}(\hat{\tau}) \right\} + 1}{1000}$$

and similarly for $\chi(\tau)$ as

$$\text{Power } (\chi) = \frac{\# \left\{ \chi_j(\hat{\tau}) \geq \chi_{950,j}(\hat{\tau}) \right\} + 1}{1000}$$

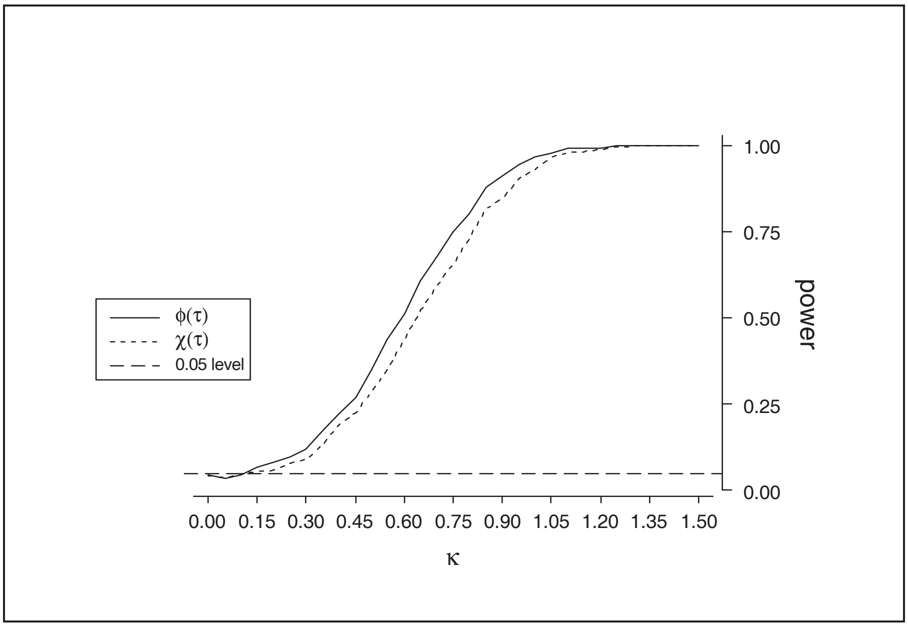

Fig 3.1. Power of two test statistics for Pure Quantality

Table 3.2. Estimated powers of $\phi(\tau)$ and $\chi(\tau)$ with respect to κ.

κ	Power(ϕ)	Power(χ)	κ	Power(ϕ)	Power(χ)
0.00001	0.045	0.042	**0.80**	0.802	0.731
0.05	0.034	0.034	**0.85**	0.880	0.816
0.10	0.044	0.046	**0.90**	0.911	0.847
0.15	0.066	0.054	**0.95**	0.943	0.903
0.20	0.081	0.057	**1.00**	0.966	0.931
0.25	0.097	0.078	**1.05**	0.979	0.965
0.30	0.118	0.089	**1.10**	0.991	0.980
0.35	0.172	0.130	**1.15**	0.992	0.983
0.40	0.219	0.189	**1.20**	0.994	0.989
0.45	0.267	0.225	**1.25**	0.999	0.995
0.50	0.349	0.284	**1.30**	0.999	0.998
0.55	0.437	0.353	**1.35**	0.999	0.999
0.60	0.509	0.438	**1.40**	1.000	0.999
0.65	0.608	0.520	**1.45**	1.000	1.000
0.70	0.680	0.594	**1.50**	1.000	0.999

In Fig 3.1, the power of two test statistics are plotted against κ. It can clearly be seen that there is not much loss in the power of $\chi(\tau)$ to test pure quantality (less than 10% and nearer only 5% for the higher values of κ). This reinforces the general experience.

3.3.3. Power Calculations for Shifted Quantality

Complementary to the previous comparative study for pure quantality is to examine how well (or badly) $\phi(\tau)$ detects shifted quantality by comparison with $\chi(\tau)$. This will show how much protection (i.e. increase in power) is obtained by using $\chi(\tau)$ rather than $\phi(\tau)$. Therefore, the power analysis was re-run by constructing the data from the shifted quantum model 2.2 with the shift β ranging from $-\frac{q}{2}$ up to $\frac{q}{2}$. Note that other components of the model were kept the same as described in the section 3.3.

In this study, the critical values obtained for $\chi(\tau)$ when β=0 (i.e. the pure quantality case) are the same since $\chi(\tau)$ is equivalent to testing the differences of all pairs of observations for pure quantality and so is invariant with respect to β.

On the other hand, the critical values were re–estimated for the test statistic $\phi(\tau)$ by replacing the model in step 1 in section 3.3.1 with the model

$$x_{ij} = \beta_k + m_i * q + VM(0, \kappa_j), \quad i = 1,\ldots,50; \; j = 1,2,\ldots,31; \; k = 1,\ldots,10$$

and re–running the rest of the algorithm for also each value of β in the range [–1/2, 1/2] with an increment of 0.1 (i.e. considering 10 values). It must be noted that the generated values for the error component maintain the same as the magnitude of β changes. Results showed a slight variation among critical values of $\phi(\tau)$ obtained for different values of β. Therefore it is decided to use the critical values computed when $\beta = 0$

The power of the cosine and modular quantogram to test for shifted quantality were computed following the same procedure as in section 3.3.2 except that artificial data sets were generated in the form of the shifted quantum model 2.2 as explained above. Then, the power is plotted against β only over the range of [0,1/2], since the power function is clearly symmetric about $\beta = 0$, and for many levels of quantality (i.e. values of κ). Fig 3.2 gives an example of these plots when $\kappa = 1$. It can be seen that when in fact shifted quantality exists, using $\phi(\tau)$ to examine quantality from data results in a rapid decrease in the power with increasing β as intuition would expect. It has also to be noted that the loss of power of $\phi(\tau)$ becomes more evident as κ increases (Fig 3.3). Furthermore, the β values at which the power of $\phi(\tau)$ is at least as good as the power of $\chi(\tau)$ was plotted (not given here), however no clear patterns emerged.

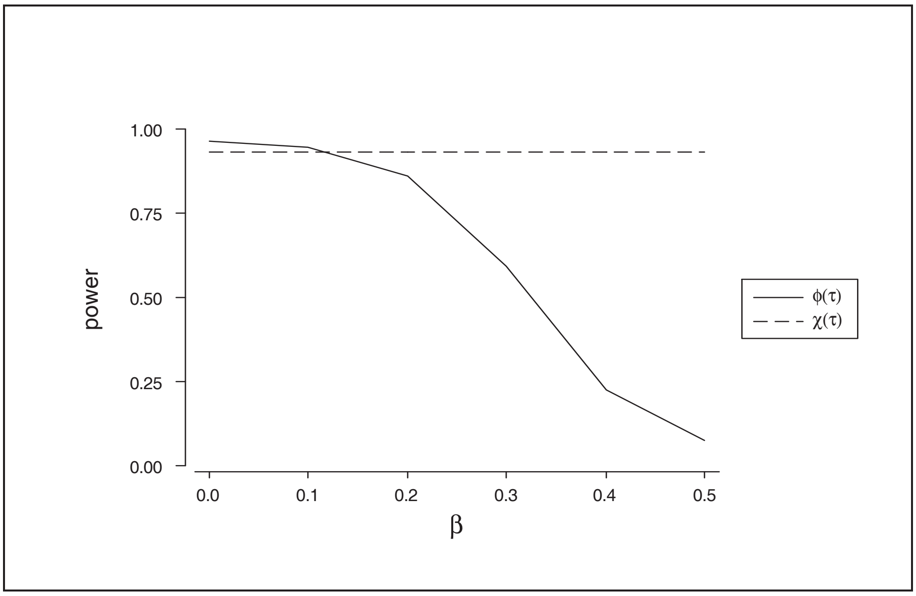

Fig 3.2. Power of two test statistics for Shifted Quantality when κ=1.

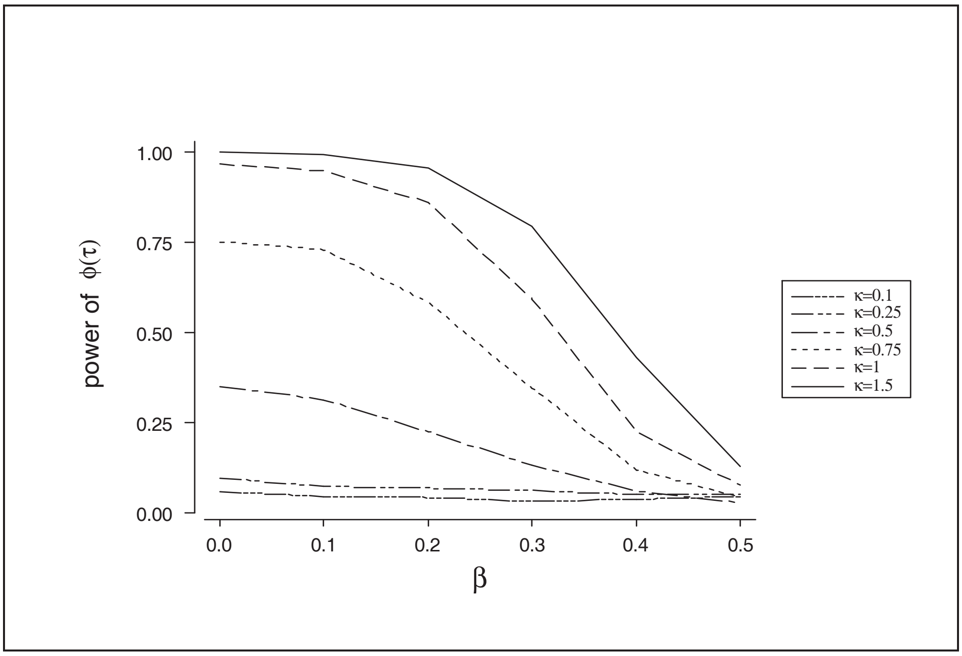

Fig 3.3. Power of $\phi(\tau)$ for Shifted Quantality with respect to κ

3.4. The Effect of Sample Size

Another consideration that may enter into the specification of the testing process for quantality is the effect of sample size on the power of the test. It is anticipated that the power increases as the sample size increases (i.e. that the tests should be consistent). We began our comparative study with a reasonably large value of n, 50. Integers are again generated from B(30, 0.333). To examine the increase in power with sample size, the whole power experiment just for pure quantality was reproduced with different sample sizes. The resulting power of $\phi(\tau)$ for each sample size is plotted in Fig 3.4 and that of $\chi(\tau)$ in Fig 3.5 against κ. It is clear that the power of both test statistics increases steadily as the sample size changes up from 50 to 500.

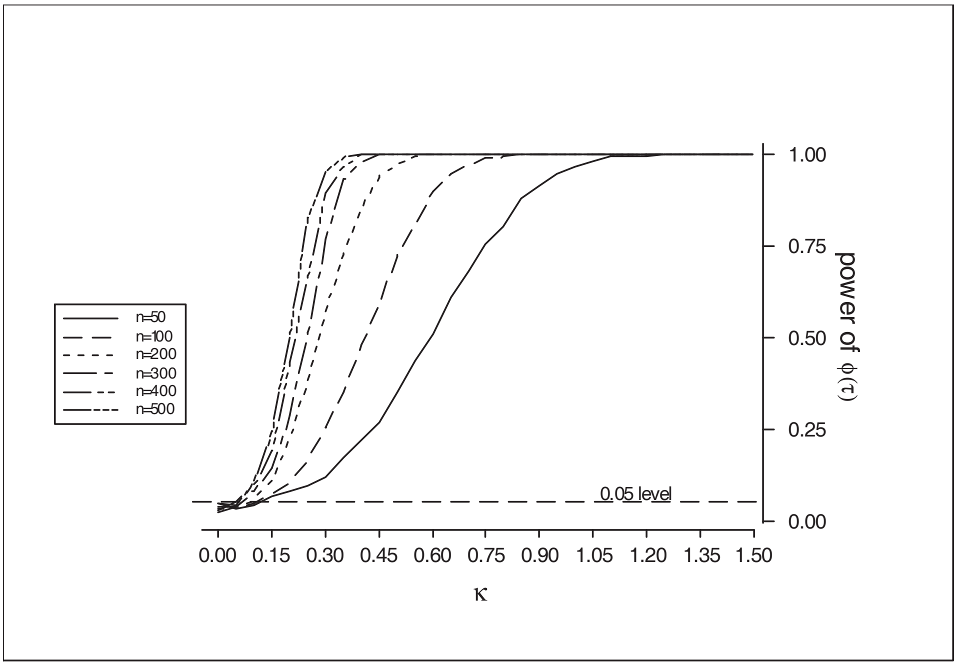

Fig 3.4. Sample size effect on the power of $\phi(\tau)$ for Pure Quantality

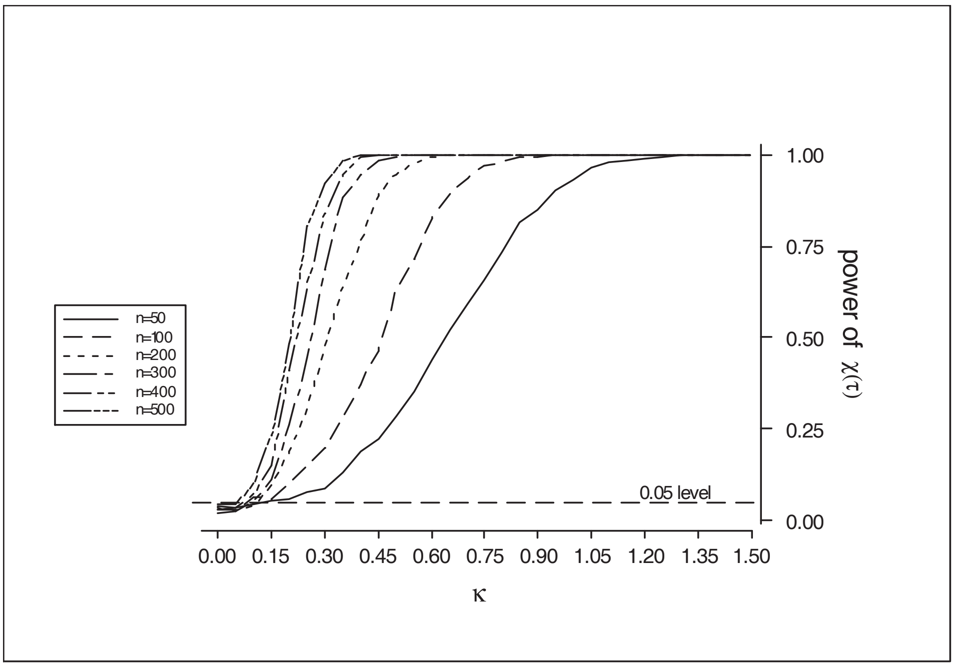

Fig 3.5. Sample size effect on the power of $\chi(\tau)$ for Pure Quantality

These results can be summarized by the difference in power i.e. $$\delta(\kappa, n) = \left\{ Power(\phi(\tau)) - Power(\chi(\tau)) \right\}_{\kappa \cong 0}^{1.5} {}_{n=50}^{500}$$

Figure 3.6 gives a visual presentation of the values of $\delta(\kappa,n)$ which are tabulated in Table 3.3. It is clearly indicated that $\delta(\kappa,n)$ tends to zero as $\kappa \to \infty$ or n $\to \infty$. (The few negative values are probably a reflection of sampling variation rather than indicating that $\chi(\tau)$ is more powerful than $\phi(\tau)$).

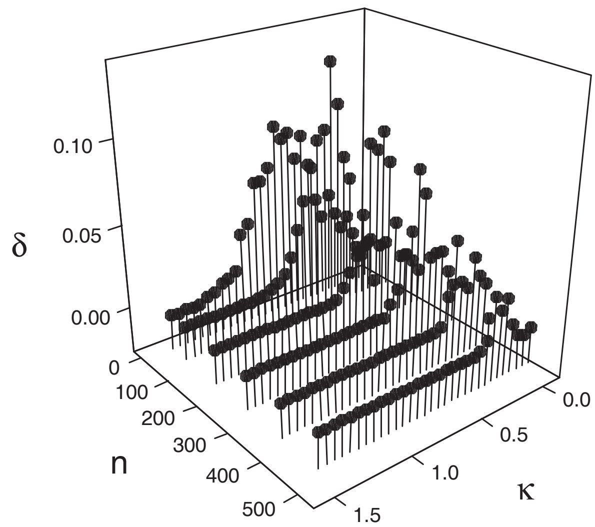

Fig 3.6. A plot of differences between powers of $\phi(\tau)$ and $\chi(\tau)$ Pure Quantality

These illustrate that very little power is lost by using $\chi(\tau)$ rather than $\phi(\tau)$ in testing for pure quantality, especially in larger sample sizes and so, given the substantial protection $\chi(\tau)$ offers in the presence of unsuspected shifted quantality. $\chi(\tau)$ is a better statistic to use in routine situations unless there is substantial *a priori* evidence that any quantality present would be "pure".

Table 3.3. The total variation of δ with respect to κ and n.

	n					
κ	**50**	**100**	**200**	**300**	**400**	**500**
0.00001	0.003	0.007	0.000	0.002	–0.006	0.002
0.05	0.000	0.006	0.008	0.013	0.018	–0.001
0.10	–0.002	–0.016	0.013	0.027	0.024	0.001
0.15	0.012	0.011	0.014	0.027	0.036	0.009
0.20	0.024	0.004	0.037	0.026	0.020	0.026
0.25	0.019	0.011	0.075	0.066	0.025	0.021
0.30	0.029	0.057	0.094	0.081	0.051	0.030
0.35	0.042	0.071	0.085	0.046	0.019	0.006
0.40	0.030	0.104	0.089	0.034	0.002	0.002
0.45	0.042	0.129	0.048	0.014	0.000	0.000
0.50	0.065	0.091	0.024	0.006	↓	↓
0.55	0.084	0.086	0.015	0.000		
0.60	0.071	0.071	0.007	↓		
0.65	0.088	0.052	0.001			
0.70	0.086	0.035	0.000			
0.75	0.094	0.019	↓			
0.80	0.071	0.010				
0.85	0.064	0.006				
0.90	0.064	0.004				
0.95	0.040	0.001				
1.00	0.035	0.001				
1.05	0.014	0.000				
1.10	0.011	↓				
1.15	0.009					
1.20	0.005					
1.25	0.004					
1.30	0.001					
1.35	0.000					
1.40	0.001					
1.45	0.000					
1.50	0.001					

Up to now, we have presented the power assessment for both test statistics regardless of whether or not true the quantum value (i.e. q = 1) has been detected by them. It is possible that the hypothesis of non–quantality is rejected but a value of q ≠ 1 declared as the best candidate for the quantum. Therefore, we extend the analyses such that the power is also calculated as

$$\text{Power } (\phi) = \frac{\#\left\{\phi_j(\hat{q}) \geq \phi_{950,j}(\hat{q}) \textit{ and } 0.95 \leq \hat{q} \leq 1.05\right\} + 1}{1000}$$

and the same formulae applies for the computation of power of $\chi(\tau)$.

Figures 3.7 and 3.8 present the new power of both statistics to test for pure quantality when different sample sizes are considered. In order to make the comparison possible, the new results are given as overlapped with the ones in Figures 3.4 and 3.5 respectively.

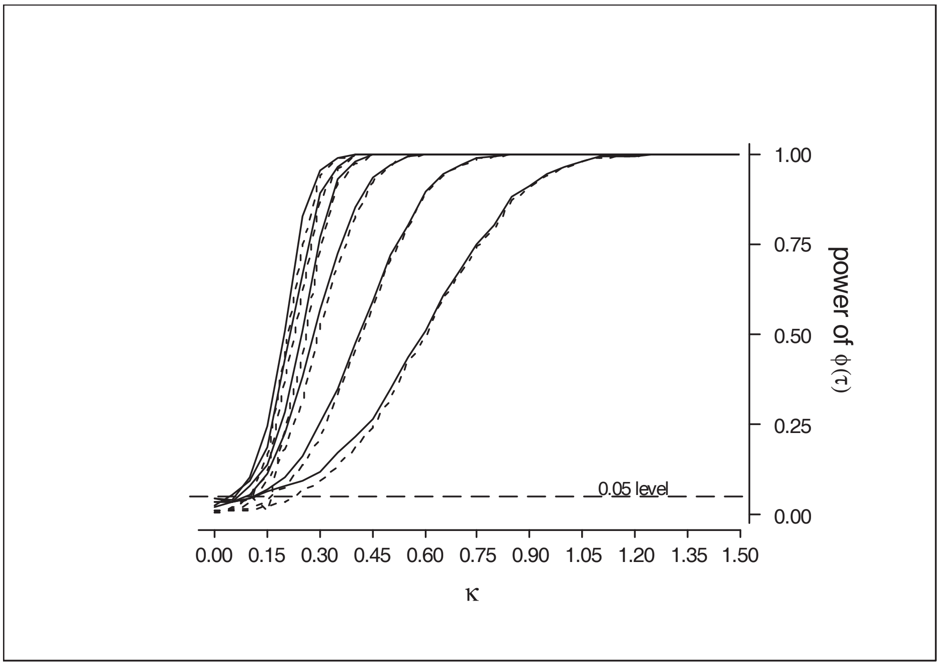

Fig 3.7. Power of $\phi(\tau)$ for Pure Quantality; — regardless of estimated quantum, ... when estimated quantum is within [0.95, 1.05].

Inspection of the graphs indicates that the power of both tests is slightly reduced when there exists no quantality (i.e. κ is small) at the given value of 1. For the κ values assigning weak quantality, there seems to be a slight decrease in the power of $\chi(\tau)$ meanwhile that of $\phi(\tau)$ remains almost the same. That said, the modular quantogram may occasionally provide a different estimate of quantum from the cosine quantogram. When quantality gets stronger, however, this defect almost disappears.

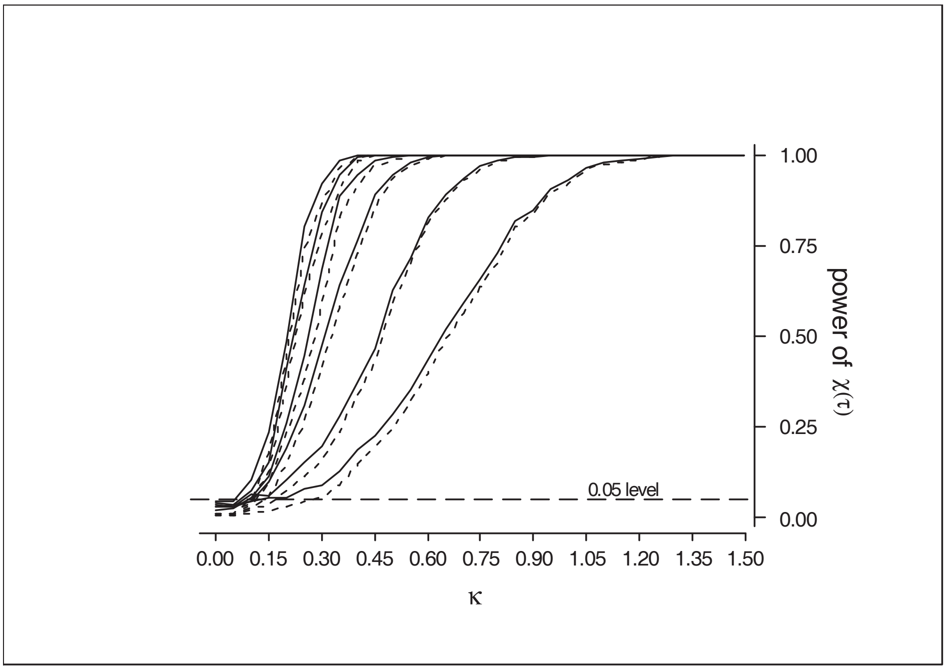

Fig 3.8. Power of $\chi(\tau)$ for Pure Quantality; — regardless of estimated quantum, ... when estimated quantum is within [0.95, 1.05].

3.5. Concluding Comments

This study was motivated by the practical question of how to decide which kind of quantality, "pure" or "shifted" exists for a given set of data. The usual practice is to test, first of all, whether there is any implication of pure quantality and to continue with searching for a shift component. However, the test statistic $\chi(\tau)$ is a modification of the test statistic $\phi(\tau)$ and is expected to show a good performance in testing for the both kinds of quantality. This suggestion leads us to examine the power of $\chi(\tau)$ to test for pure quantality which was the objective of this chapter.

In this chapter, we presented full details of a simulation study performed and concluded that there would be little loss of power if $\chi(\tau)$ instead of $\phi(\tau)$ is used to extract the pure form of quantality. It was further concluded that the amount of loss of power decreases as the sample size increases and when the quantality is strong enough (i.e. κ is big), there remains no difference at all. It is necessary to note that $\chi(\tau)$ may occasionally estimates a different quantum value from $\phi(\tau)$ if there exists only weak quantality. Although this does not change our conclusion that $\chi(\tau)$ could be used to test for pure quantality, it should be born in mind when interpreting the estimated quantum values of weak quantal effect. We also emphasised the fact that this new procedure would increase the computations due to the evaluation of sines as well as cosines. However, it would provide a good protection against shifted quantality.

As a natural extension, we moreover investigated how $\phi(\tau)$ would perform for testing for shifted quantality and it was observed its power decreases rapidly as the shift component (i.e. β) gets bigger. In contrast, the power of $\chi(\tau)$ stays invariant regardless of the magnitude of the shift as it is equivalent to testing the differences of all pairs of observations for pure quantality. In summary, we here advise that one should start analysing the data using the test statistic $\chi(\tau)$ unless there is a reason to believe otherwise. As a result, any existing quantality, pure or quantal, could be easily obtained in one step.

CHAPTER 4.

Lateral Root Spacing

4.1. Introduction

Many aspects of root development on plants require an understanding of the mechanisms leading to the generation of roots. In particular, it is remarked that, to the eye, the lateral roots on a pre–existing root are systematically spaced out. There are however only a few instances that clearly indicate a particular pattern of them. In developmental Biology, the initiation and location of lateral roots have been repeatedly studied in order to provide more information of a general understanding of plant development (e.g. Barlow, 1984). Particular concern is directed to the investigation of the factors, internal or external, which affect the features of root branching. Internal factors include nutritional and hormonal conditions that influence the role of budding cells in activating the root–forming genes which may or not eventually produce a lateral root, as well as the ones that may emanate from already existing lateral roots. External factors include environmental circumstances such as light, temperature and physical forces. With regard to such conditions, various features of lateral root formation and growth have been studied so as to reveal which features are variable and which are constant. Knowledge of what aspects of lateral root development are quantifiable and variable would facilitate the investigation of the factors involved in the plant production. One of the aspects could thus be reflected in the question of whether there is a “fundamental” unit that regulates some rhythmic process of the lateral root production on plants. That is whether the spacing between lateral roots on a root follows some pattern, and is that pattern periodic and quantal. Such quantal feature would suggest that not all lateral roots are separated by a constant distance, but may perhaps, be separated by multiples of a minimum distance.

Measurements of the distance between lateral roots on cultured roots of tomato were investigated (Barlow and Adam, 1988) and it was observed that the distribution of inter–root distances tend to be multimodal, with modes that are multiples of a quantal distance. However, the evidence presented was in a graphic form and not supported by any statistical methods. In a recent publication by Newson et al (1993a), tomato lateral root distribution was re–examined to weigh evidence for quantal tendency in a more systematic fashion, using the statistical method so–called “quantogram analysis” (see chapter 2). As a result, although some of the individual sets of data showed a quantal tendency which is statistically significant at the 10% level, the majority of the data sets did not constitute strong evidence for a general quantal tendency.

If some value of a quantum could be shown to be a feature of the distribution of observed roots, then it would be possible to identify the position of candidate budding cells on the parent root according to their distance from the nearest lateral root. Such information would contribute to the knowledge of cell development and cell differentiation. Moreover, if there are equally spaced budding cells, then the root may be viewed as being segmented (Barlow, 1989), with one candidate cell in each segment, or in particular combinations of segments. If such a segmentation pattern exists, it might help Biologists to understand the process of growth, and a quantal distribution of roots would support this segmental view of the root.

In the present project, spacings in onion, tomato and fern roots are available. The aim of this study is to search for a quantal tendency in onions and to weigh the evidence found for tomatoes in a more systematic fashion, but developing well structured new quantal models. The structure suggested by the data sets available could be hierarchical. That is the magnitude of spacing quanta (if such exists) may vary slightly from root to root, from onion to onion and from treatment to treatment.

Furthermore, the structure of fern roots has always been of great interest to plant anatomists (Lin and Raghavan, 1991). With regard to very regular formation of leaves of fern, it may be expected to find some correspondence between fern leaves and the initiation of lateral roots on its roots (Newson et al, 1993b). The cellular levels of root construction on fern roots bring up the realisation of another type of quantality which allows some spacing quanta for a root that could vary slightly along the root.

In the following section, we present a full description of the data available by showing all biological and structural aspects of the measurements. In Section 4.3, we summarise the data sets by all means of explanatory statistical analyses in order to discover similarities or dissimilarities between roots so that we could shed a light in questions that may arise in a further analysis.

4.2. Data

Data available for the present project consist of measurements of distances between lateral roots on the roots of onion and tomato plants. Selection of these plants for the experiments was made because they are suitable species for investigating the genetic control of root branching and also it is possible to observe roots of them at various stages of their growth and to alter the hormonal and nutritional composition of their growing medium. A small set of roots of fern plants is also available. Before describing the full structure of those data sets in the following sections, it is necessary to provide a general understanding of lateral root branching and positioning on the plants.

Budding cells form in sequence as the parent root grows forwards. That is a new budding cell arises always distal to the next oldest root and never between two pre–existent ones (see Fig 4.1). Lateral roots emerge from potential budding cells and form along the length of a parent root. With the help of this feature, the role of a quantal distribution of laterals becomes clearer. That is if a lateral fails to be produced, the next one on the root forms only after another fundamental distance of root has been produced. Usually, lateral root formation depends on circumferential positioning of the budding cells. Inspection of transverse sections of roots suggested that budding cells favour lateral root initiation at certain sites.

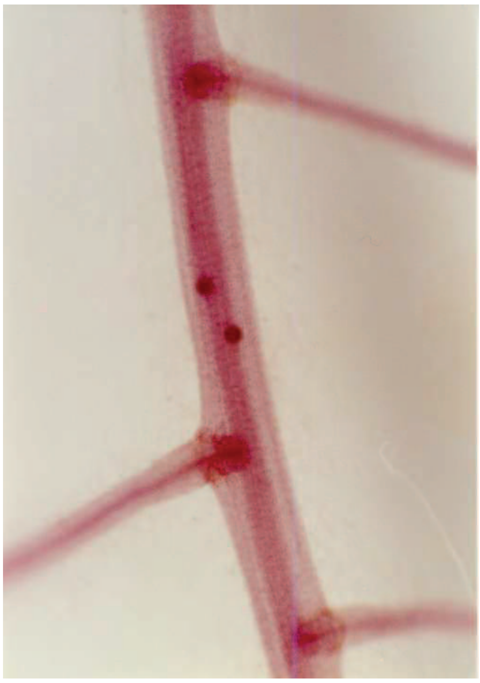

Fig 4.1. A picture of a tomato root bearing laterals and potential budding cells

The onion roots have the feature such that laterals arise in 4–5 lines (i.e. ranks) drawn longitudinally along the root. Imaginary positions of them on the root can be seen in Fig 4.2 (a).

Tomato roots are arranged in two ranks on opposite sides of the root, however they consist of three sub–ranks (see Fig 4.2 (b)). Since the sub–ranks being so close to each other makes the recognition of which sub–rank underlies the laterals very difficult, Biologist consider them as left and right series of laterals. Moreover, Fern roots are also located along two ranks which are again named left and right series (see Fig 4.2 (c)). Note that allocation of series to 'left' and 'right' is arbitrary, not based on any assumed asymmetry.

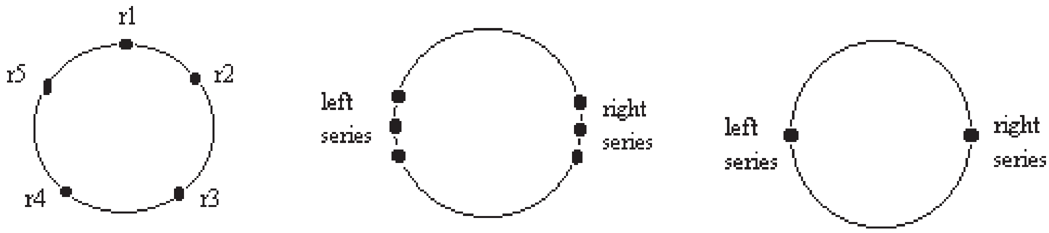

(a) (b) (c)

Fig 4.2. Circumferential positioning of roots of Onion (a), Tomato (b) and Fern (c)

4.2.1. The Onion Data Set

The onion data set was made available by the agricultural research station in Badajoz, Spain via that in Long Aston, UK. The experiment on onions was undertaken in order to investigate any effect of a treatment with Naphthaleneacetic Acid (Naa) on the arrangement of lateral roots in onion by Dr. Pedro Lloret in Badajoz. He measured and studied various aspects of the roots (Lloret et al., 1998) and provided us with the distances between adjacent lateral roots for an investigation of some possible quantal effect on the distribution of spacing. The data set consists of 3 groups of onions: Control, Weak–treated and Strong–treated. Six onion bulbs were used for each of the three groups.

The adventitious roots of the onion bulbs in the control group were grown in tap water under standard conditions. The first day after putting the bulbs in water was considered day zero of the experiment. Only ten roots were allowed to develop from each bulb. When they were 4 days old, 3 roots were harvested from each onion which provided 18 roots for the Control group. Then the roots of the onions in the two treatment groups were immersed for also 4 days in α–naphthaleneacetic acid solution in tap water at a concentration of 0.01 mM or 0.1 mM (i.e. weak and strong Naa treatment respectively) in order to vary their growth rate. At the end of treatment, all roots were returned to tap water until day 6. Then 1–2 roots per onion were harvested, giving 7 roots for the Weak–treated group and 6 roots for the Strong–treated group.

Lateral growth and the initiation of lateral root promordia are studied on each group by measuring the longitudinal distances between lateral roots. In addition, interlateral distances were also obtained by just measuring distances, ignoring the ranks, as each successive lateral root appears along the parent root as a whole. This later gives the total series values (see Fig 4.3). Note that there were occasionally two lateral roots arising from the same root (but in different ranks) at the same distance, giving a distance of zero in total series. In these instances, we will ignore such zero values in the upcoming analyses.

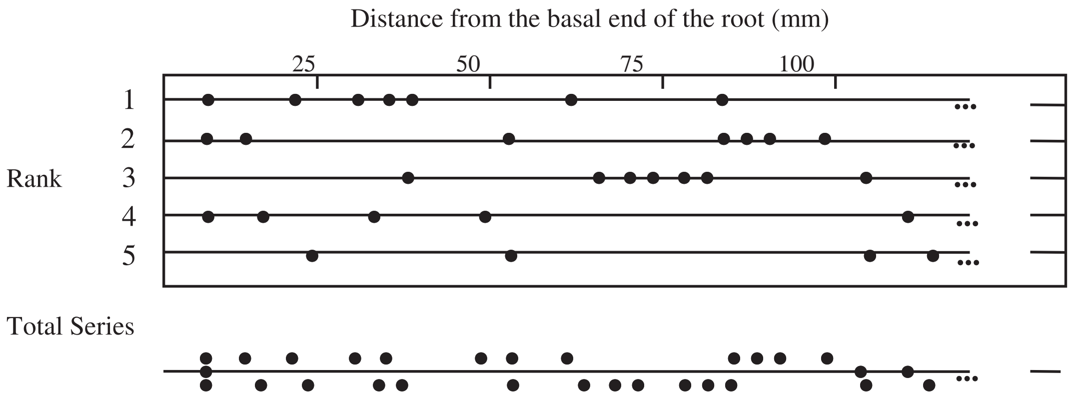

Fig 4.3. Schematic representation of the data from one root on onions (source: Lloret et al., 1998)

For the present project, 1946 spacings in total from 31 roots are available. The distance between laterals along each of the roots has been measured in millimetres to an accuracy of 0.5 mm in the control roots, and to an accuracy of 0.1 mm in the treated roots. We will denote the roots from Control group by C1–C18, the ones from Weak–treated group by W1–W7 and the ones from Strong–treated group by S1–S6. These abbreviations will be accompanied by "r1–r5" in order to refer to the ranks of a specific root.

4.2.2. The Tomato Data Set

The tomato data set was provided by Dr. Peter Barlow, Arable Crops Research Station in Long Ashton. The data were obtained from two types of tomatoes: Wild type and Gib–1 Mutant type. In the experiment, a clone of tomato roots were grown in flasks which contained some sucrose solution at 1.5% that is used as a means of regulating the growth rate. As a part of this experiment, some roots were also given Naa treatment but at a concentration of 0.0005mM. For the whole experiment, 10 roots at 1.5% sucrose level and 4 Naa treated roots of Wild type were used. Additionally, 6 roots at 1.5% sucrose level and 4 Naa treated roots of Gib–1 Mutant type tomatoes were used. Then, the roots were removed from the flasks when they were 8–20 days old and the distances between lateral roots were measured in centimetres and to an accuracy of 0.001 cm.

Therefore, each root consists of the left, right and total series of distances between laterals (see Fig 4.2). Note that again we will ignore any zero distances in the total series. Throughout the analyses concerning tomato roots, we will denote the group of Wild type roots at 1.5% sucrose level by 'WR' and its roots by WR1–WR10. Besides, the group of Naa treated Wild type roots by 'NWR' and its roots by NWR1–NWR4. Moreover, 'GR' and GR1–GR6 will denote the group of Gib–1 Mutant tomatoes at 1.5% sucrose level and its roots. Similarly, the group of Naa treated Gib–1 Mutant roots will be represented by 'NGR' and its roots by NGR1–NGR4. In addition, letters 'L', 'R' and 'T' will denote left, right and total series respectively.

4.2.3. The Fern Data Set

This data set was also provided by Dr. Peter Barlow, Arable Crops Research Station in Long Ashton. The roots were obtained from two type of ferns: *Marsilea quadrifolia* (M–type), *Ceratopteris thalictroides* (C–type). In this data set, only one root of M–type and 4 roots of C–type are available. Again, each root consists of the left, right and total series of distances between laterals. Note that the first type of ferns will be denoted by MQ and the second type by CT1–CT4.

All plants were grown in a greenhouse under fixed normal conditions and roots were cut after some time and analysed under a microscope. Measurements between successive laterals were made in centimetres and to an accuracy of 0.001 cm. Unlike the other data sets available, the fern roots were not exposed to any sort of treatment. Therefore this data set has only a “control” group of 5 roots all together (i.e. 15 series of distances).

Note that both tomato and fern root spacings are given in cm. however the onion root spacings are provided in mm. For the sake of consistency in the forthcoming analyses and results presented, we converted all measurements from tomato and fern roots into mm. The original data for all plants can be found in Appendix F.

4.3. Preliminary Analyses

Before carrying out any analysis concerning quantality of distances, some preliminary analyses were performed in order to explore some important statistical aspects of distances by means of standard statistical summaries. The analyses aim not only to highlight the differences within the roots and different treatment groups but also to investigate any possible autocorrelation between distances.

4.3.1. Preliminary Analyses on the Onion Data Set

To begin with, it is assumed that the process giving rise to the lateral roots on each rank were statistically independent. It must be noted that the sample size in many ranks, mostly in Control and Weak–treated roots, is too small to draw clear statistical conclusions (see Table 4.1). Therefore, the analyses for onion roots have been performed only considering the total and combined rank series of lateral roots.

The primary effect of treatment is not only to decrease the longitudinal distance between successive lateral roots with a noteworthy increase of number of laterals on each rank, but also to distribute them more evenly along the same rank. Mean distances on the total series for Control and Treatment groups given in Tables 4.2 and 4.3 respectively reinforce this conclusion.

This raises a difficulty noted in remarks in section 2.4.1 and 2.6.5. If the effect of the treatment is to stimulate more budding cells to produce laterals, then the integers m_i in model (2.1) will decrease and every budding cell produces one then all m_i become equal to 1 and paradoxically the quantality of the data disappears.

Table 4.1. Number of laterals on each rank and total series of onion roots

Treatment/Root	Rank 1	2	3	4	5	Total series
Control Gr.						
C1	6	9	17	4	3	41
C2	4	7	3	6	1	23
C3	3	3	5	8	7	29
C4	6	10	10	8	4	37
C5	7	10	15	15	8	54
C6	2	2	10	3	6	24
C7	4	0	2	11	10	28
C8	6	7	4	5	3	25
C9	0	7	5	3	1	20
C10	5	4	3	3	1	19
C11	0	4	9	11	3	28
C12	8	7	5	6	4	29
C13	9	5	6	5	4	25
C14	5	12	17	10	10	56
C15	1	12	1	0	3	20
C16	1	4	21	5	0	33
C17	1	0	16	8	7	35
C18	9	2	15	14	12	53
Weak–Treated Gr.						
W1	13	4	6	3	19	49
W2	15	5	11	4	15	51
W3	3	8	3	2	9	27
W4	7	6	16	8	–	40
W5	24	14	12	22	23	94
W6	11	12	4	9	6	40
W7	9	16	7	5	3	39
Strong–Treated Gr.						
S1	24	20	11	8	9	63
S2	58	45	65	32	58	221
S3	24	25	47	24	38	146
S4	16	33	15	32	–	83
S5	31	19	27	19	–	81
S6	116	87	77	94	–	285

Interlateral distances could be variable, either increasing or decreasing along the root. This placement would result in some sort of autocorrelation between successive pairs of lateral roots. This was checked by calculating the first order autocorrelation on just the total series (see Tables 4.2 and 4.3). In the Control roots, the only nominally significant autocorrelation coefficient is obtained from C11, suggesting that short distances tend to be followed by long distances or vice versa. In treated ones, nominally significant result is obtained from roots W3 and S2–4, indicating mainly positive autocorrelation. Noting that 31 autocorrelations have been presented and allowing for multiple testing, the initial conclusion is that there is little evidence overall of autocorrelation except perhaps in the Strong–treated group.

Table 4.2. Mean distance (± s.e.) and first order autocorrelation (t-value) between successive laterals in the Control group

Total	Mean ± s.e.	Autocorr.	Total	Mean ± s.e.	Autocorr.
C1	2.573 ± 0.279	–0.017 (–0.11)	**C10**	3.132 ± 0.500	0.06 (0.28)
C2	3.283 ± 0.418	–0.21 (–1.02)	**C11**	2.589 ± 0.273	–0.5 (–2.63)
C3	2.362 ± 0.332	–0.02 (–0.08)	**C12**	3.052 ± 0.406	0.21 (1.14)
C4	2.135 ± 0.292	–0.08 (–0.47)	**C13**	2.800 ± 0.487	–0.39 (–1.95)
C5	2.046 ± 0.192	–0.11 (–0.77)	**C14**	2.991 ± 0.266	–0.18 (–1.36)
C6	3.604 ± 0.459	0.03 (0.14)	**C15**	4.400 ± 0.683	0.24 (1.07)
C7	3.589 ± 0.394	0.18 (0.95)	**C16**	3.333 ± 0.435	–0.07 (–0.37)
C8	3.180 ± 0.512	0.27 (1.36)	**C17**	3.443 ± 0.439	–0.29 (–1.74)
C9	4.050 ± 0.542	0.15 (0.65)	**C18**	2.962 ± 0.290	0.02 (0.14)

Table 4.3. Mean distance (± s.e.) and first order autocorrelation (t-value) between successive laterals in the Weak–treated group and Strong–treated group

Total	Mean ± s.e.	Autocorr.
W1	1.371 ± 0.235	0.19 (1.34)
W2	1.306 ± 0.208	0.05 (0.39)
W3	2.207 ± 0.432	0.45 (2.35)
W4	2.075 ± 0.335	0.06 (0.37)
W5	0.772 ± 0.068	–0.06 (–0.54)
W6	2.125 ± 0.434	0.17 (1.10)
W7	2.010 ± 0.402	0.06 (0.34)

Total	Mean ± s.e.	Autocorr.
S1	0.434 ± 0.039	–0.12 (–0.98)
S2	0.330 ± 0.016	0.14 (2.04)
S3	0.412 ± 0.024	–0.18 (–2.17)
S4	0.689 ± 0.062	0.35 (3.19)
S5	0.604 ± 0.047	–0.01 (–0.06)
S6	0.256 ± 0.009	–0.03 (–0.57)

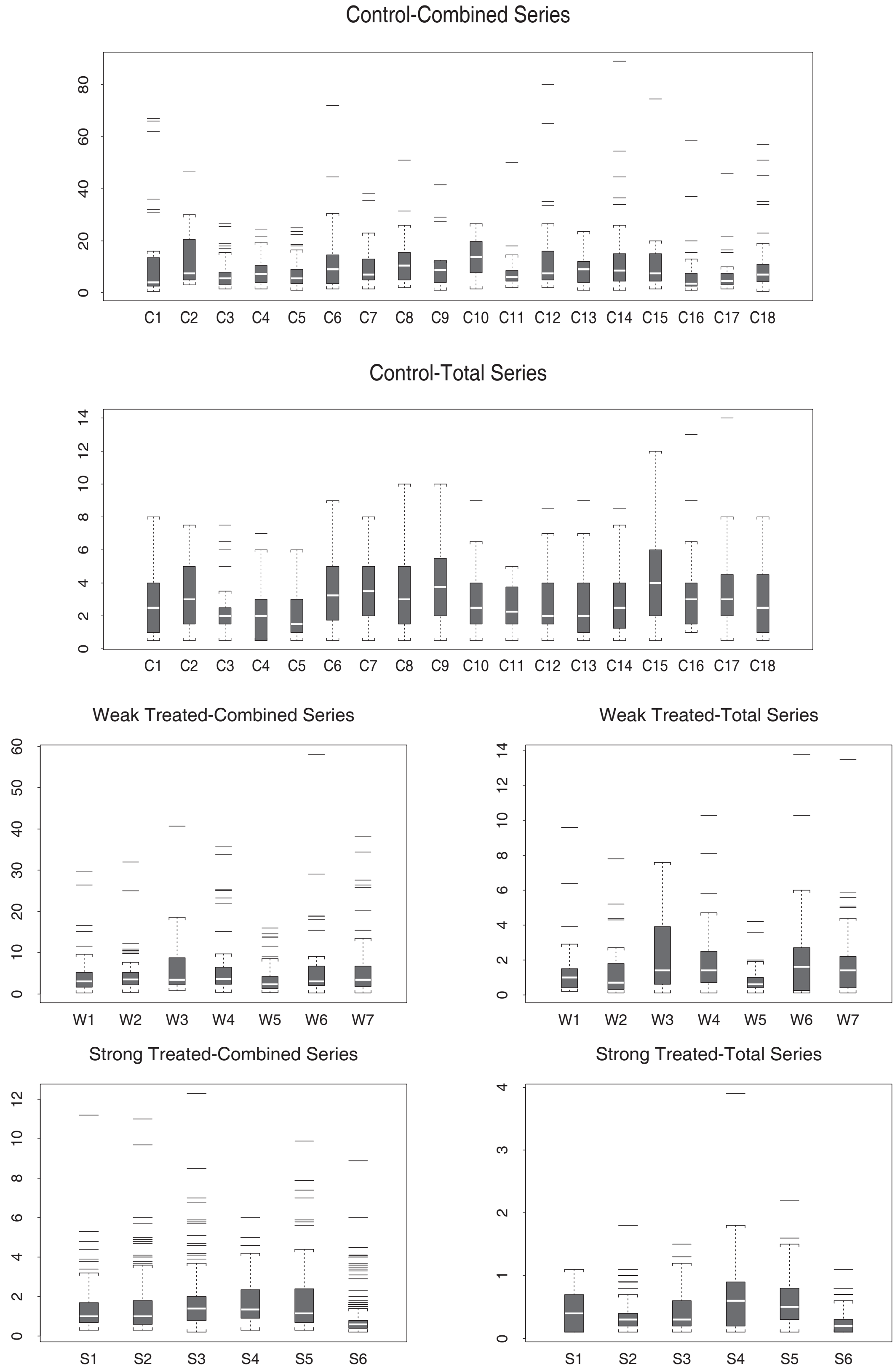

Fig 4.4. Boxplots of combined rank series and total series of onion roots

Fig 4.4 displays, for each treatment group, the boxplots of combined rank series as well as the total series of onion roots. Plots indicate that the roots are not homogenous in their distributions that are being mostly asymmetric. Normality is guaranteed only for a few total series of roots as a whole. The figure also shows that there is a difference in median inter root distance between roots of even the same treatment group. This observable difference is confirmed by a Kruskall–Wallis nonparametric test. Note that difference is less apparent amongst the combined series of treated roots. Treatment group differences in median response are also highlighted in the plots.

4.3.2. Preliminary Analyses on the Tomato Data Set

In the analyses of Tomato roots, the same properties of distances were explored beginning with the Wild type and it was found that whatever regulates the spacing between lateral roots operates uniformly along both left and right series, producing similar distributions of distances (see Table 4.4). The effect of Naa treatment remains the same for tomato roots, promoting the production of lateral roots which are distributed more evenly along the root and decreasing the distances between them.

Table 4.4. Mean value (± s.d.) of number of laterals, mean spacings and autocorrelation coefficients per root for Wild type.

Treatment (# roots)	# Laterals	Mean	A.corr.
Right			
WR (10)	50.9 ± 13.13	3.53 ± 0.73	0.051 ± 0.13
NWR (4)	66.3 ± 20.8	2.55 ± 0.15	0.182 ± 0.08
Left			
WR (10)	55.6 ± 18.86	3.1 ± 0.44	0.131 ± 0.16
NWR (4)	57.3 ± 25.1	3.0 ± 0.31	0.102 ± 0.07
Total			
WR (10)	104.6 ± 31.9	1.77 ± 0.35	0.003 ± 0.16
NWR (4)	123.2 ± 46	1.39 ± 0.06	–0.147 ± 0.05

The first order autocorrelations between successive distances are not of great magnitude, however some nominally significant correlations seem to be produced mainly in left series of the roots, but not in a preferred positive or negative direction. Again this is not surprising given the number of sequences examined.

The total series shows the summation of right and left series of spacing and results in crowding two times as many laterals into one series. Consequently, the total series showed closer spacing of lateral roots than the right and left series of them. The effect of the Naa treatment on the total series remained the same as in the individual series (Table 4.4).

Furthermore, the roots of Gib–1 mutant type tomatoes show a similar result to Wild type roots as far as numbers of laterals and mean spacings are concerned (Table 4.5). However, the picture drawn by Naa treated Gib–1 roots differs from what has been observed so far, the main difference being the surprisingly decreased number of laterals in all series while the mean distance remains similar to the other Naa treated roots.

The analyses of autocorrelation for Gib–1 mutant roots suggested that only in the total series, the majority of short distances are followed by long distances or vice versa. Moreover, the Naa treatment results in some significant autocorrelation between distances (either positive or negative).

Table 4.5. Mean value (± s.d.) of number of laterals, mean spacings and autocorrelation coefficients per root for Gib–1 Mutant.

Treatment(# roots)	# Laterals	Mean	A.corr.
Right			
GR (6)	48 ± 14.1	3.09 ± 0.47	–0.035 ± 0.10
NGR (4)	28 ± 8.29	3.52 ± 0.65	0.177 ± 0.28
Left			
GR (6)	42.2 ± 15.6	3.44 ± 0.31	–0.016 ± 0.13
NGR (4)	27.2 ± 5.12	3.54 ± 0.46	0.16 ± 0.25
Total			
GR (6)	90.2 ± 27.7	1.65 ± 0.14	–0.184 ± 0.2
NGR (4)	55.2 ± 10.2	1.73 ± 0.14	–0.128 ± 0.29

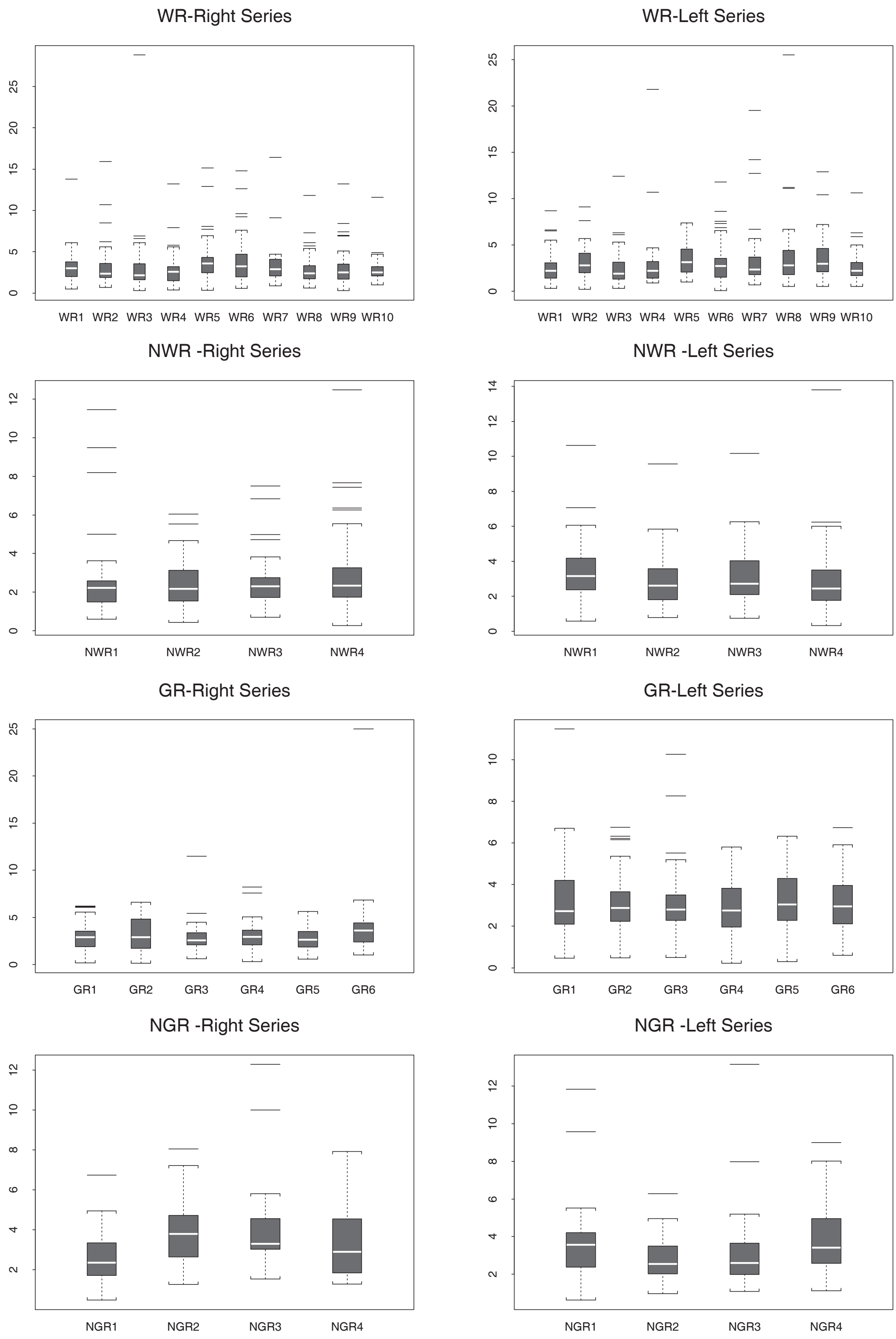

Fig 4.5. Boxplots of left and right series on the tomato roots

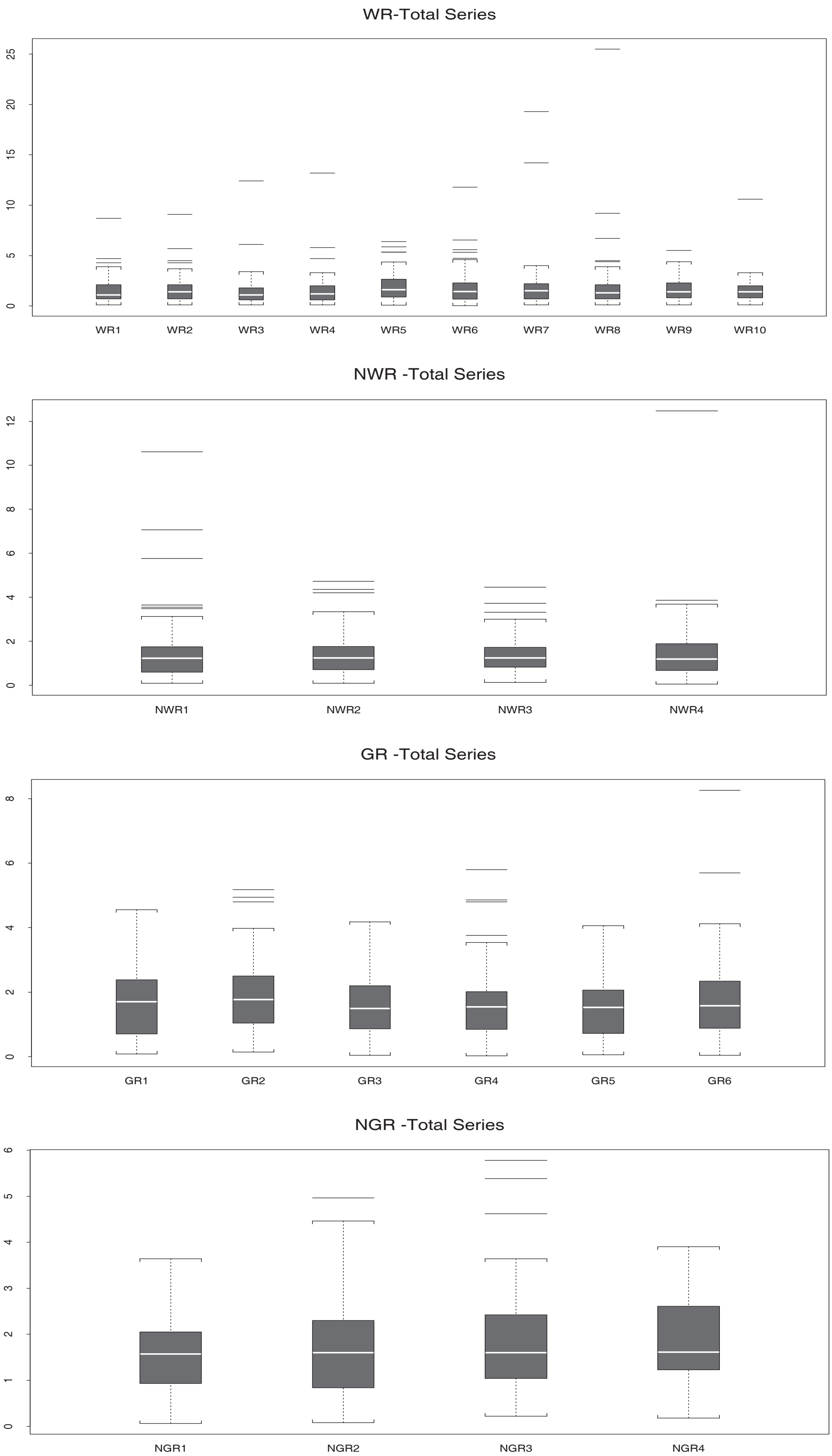

Fig 4.6. Boxplots of total series on the tomato roots

In order to make an overall comparison, the boxplots of spacings on the left and right series of all type of tomato roots are presented in Fig 4.5. It can be seen that most of the tomato roots exhibit similar distributions. The most homogenous root spacings appear in the groups of the Naa treated Wild and Gib–1 mutant roots, which was also indicated by the acceptance of the similarity of roots in median response by K–W tests performed for each group and their series.

Fig 4.6 demonstrates the boxplots of total series on the tomato roots for each plant group. The figure indicates that total series are the most homogenous in their distributions. There appears to be no difference in median inter-root distance between roots of the same plant group. This observation is also verified statistically by a K–W test. However, there exists slight variation of median values amongst the groups.

4.3.3. Preliminary Analyses on the Fern Data Set

Similar analyses have also been performed on the fern data so as to discover some of the aspects of lateralization in fern roots. The results are summarised in Table 4.6. Compared with the root spacings examined so far, the greatest degree of regularity of laterals is observed in the roots of the ferns. This is also indicated by the appearance of relatively large autocorrelation between successive pairs of distances.

Table 4.6. Mean value (± s.d.) of number of laterals, mean spacings and autocorrelation coefficients per root in Ferns.

Series (# roots)	# Laterals	Mean	A.corr.
C – Type			
Right (4)	13.5 ± 1.73	10.3 ± 0.77	0.268 ± 0.34
Left (4)	12.5 ± 1.73	10.8 ± 0.86	0.262 ± 0.31
Total (4)	26.0 ± 3.37	5.4 ± 0.39	–0.17 ± 0.27
M – Type			
Left (1)	97	1.98	0.50
Right (1)	93	2.06	0.29
Total (1)	187	1.03	0.08

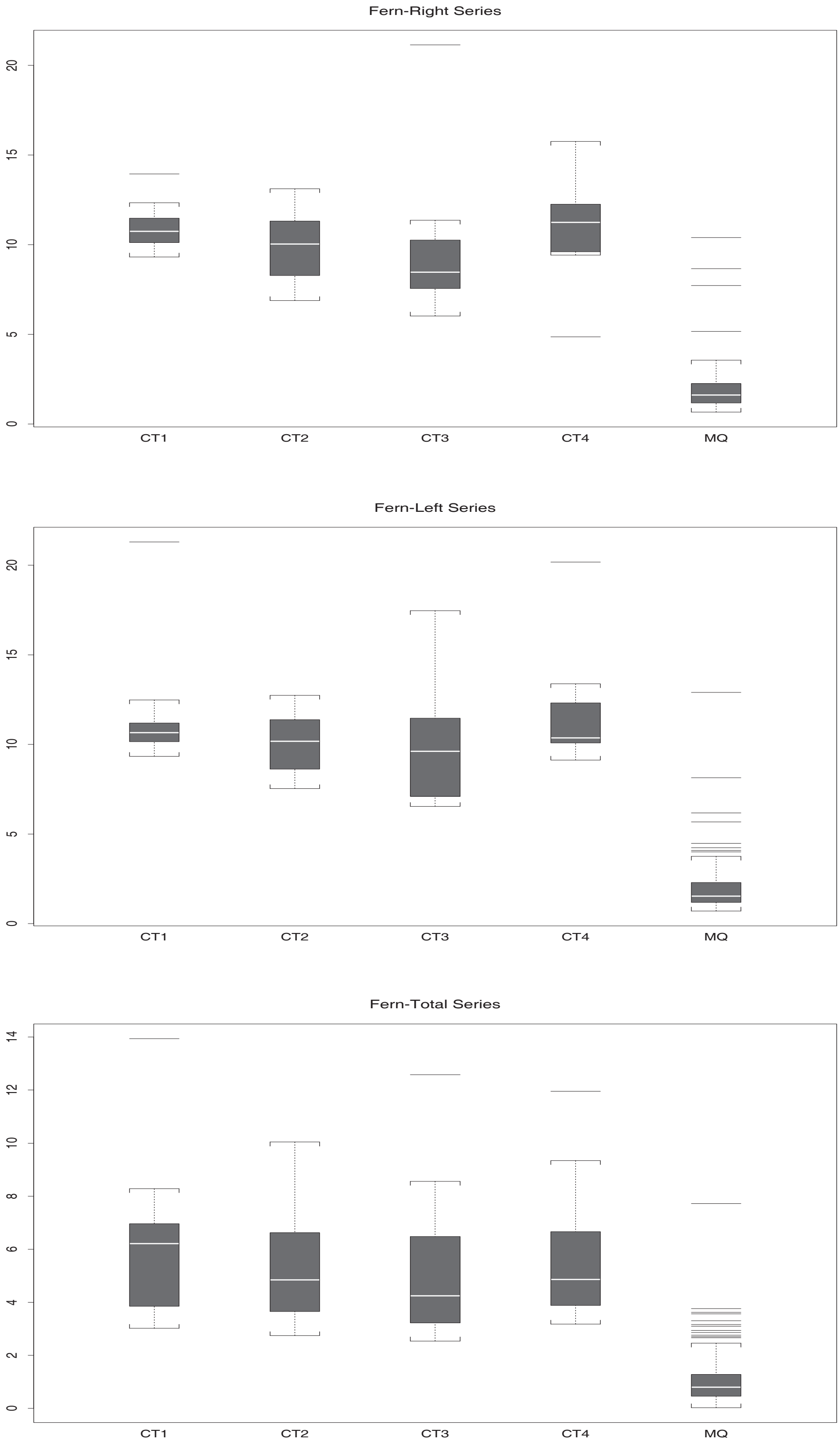

Fig 4.7. Boxplots of fern root spacings

The mean distance of the C–type roots seem to be a lot bigger than other type of roots, however they look similar within and between its left and right series. On the contrary, laterals arise at shorter but very regular intervals from the M–type root and this raises the danger noted in section 4.3.1 that the spacings may be “too quantal” to detect quantality. Except for the left and right series of C–type, the number of laterals is satisfactory to carry out any analyses. As expected, total series bear more spacings, which results in again smaller distances than those on the left and right series.
Fig 4.7 depicts the boxplots of fern root spacings for each root series. The figure shows not only do the fern roots produce higher inter root spacings on average than other type of plants, but M–type fern root differs significantly from the C–type fern roots. Amongst the C-type fern roots, there appear to be difference in median response between only right series of the roots. A K–W test also verified this result.

4.4. Concluding Remarks

This chapter presents the available data sets provided for the current investigation of new forms of quantality. The data are the spacings between lateral roots on the roots of onions, tomatoes and ferns. We have first described some of the aspects of lateral root initiation and development in those plants, and hence compared with the aim of uncovering controls of root branching. Then some statistical features of the spacings were explored by means of standard statistical analyses.
As far as onion roots are concerned, the number of spacings on each rank of Control roots and many of those of Weak–treated roots is too small to draw clear statistical conclusions. Obviously, this fact will remain the same when quantogram analyses need to be performed. We can conclude that we would be obligated to combine individual ranks of each root for those groups. In further analyses, it would then be necessary to assume that distances on different ranks could be pooled to form a common sample. Besides, for tomato roots sample size does not seem to create any problem.
Except for Gib–1 Mutant type tomatoes, Naa treatment creates a competitive mechanism which results in close spacings of laterals along each rank. This raises the

possibility that the magnitude of any quantality may not be constant among the treatment groups, perhaps it is rather variable and being smaller for the treated roots. Although they were not great in magnitude, some roots exhibited serial correlation between successive pairs of spacings. Any analyses concerning quantality require the data to be independently distributed. Hence, the observed autocorrelation endangers the assumption of independency, consequences of which are however further investigated in section 2.8.4 and found not to be serious provided some slight allowance is made in assessment of borderline cases.

CHAPTER 5.

Quantality of Lateral Roots

5.1. Introduction

This chapter provides an introduction to the investigation of any simple quantal tendency, in a practical setting, from the data on spacings of lateral roots presented in the previous section. The aim is to give insight into the current quantal problem we are faced with. To begin with, we consider a general examination of not only the features that arise due to the nature of the roots but also the limitations that are inherent characteristics of the data collection process. Then we will investigate the performance of classical approaches in answering the question of whether the spacings are quantal and show that such methods are limited in resolution when the data records are short and when also the accuracy of the measurements is low.

Throughout the analyses we perform in this chapter, it will be apparent that there is a practical need to extend the basic quantal model to accommodate the structure of the data set being dealt with. We therefore introduce two new quantal models to meet such demands and this illustrates how quantal models can be developed to meet many other specific structures that could arise in other problems. More detailed analyses of these models are deferred to the next chapter.

5.2. The Scope and Objectives

Within the framework of this study, we are mainly concerned with the question of whether spacings between lateral roots on an individual rank series are quantal. If they are, then it is of interest to investigate whether all ranks (or left and right series in the cases of tomatoes and ferns) on roots show quantality, and whether they have the same quantum value.

As far as the onion data set is concerned, however, we know from the exploratory analyses in the previous chapter that only very short sequences on individual ranks are available. Consequently, classical methods of hunting quanta applied separately to individual series may well not detect quantality. Pooling of data from separate short series may mask the evidence of quantality if we expect the spacing quanta (if it exists) to vary from rank to rank on the same root and perhaps also from root to root and further from onion to onion.

In addition, it has also been shown that Naa treatments not only increase the number of lateral roots but also decrease the longitudinal distance between them. Thus it is of interest to examine whether onion roots within the same treatment group tend to have the same quanta, and whether the Naa treatment alters the magnitude of any possible spacing quanta.

Similarly, we might anticipate that any spacing quanta for tomatoes and ferns varies between the series (left, right and total) even though the number of measurements are not so small. If they all indicate the same quantum value, then it is of importance to test whether the quantity is different for the Wild type and the Gib–1 Mutant type. As with the onions, it might also be expected that the Naa treatment could lead to a change in any possible quantum value.

Another interesting feature arising in the nature of the quantality of the spacings is suggested by the total series which define differences between supposedly the target positions of the rootlets regardless of the ranks. Our particular concern is therefore to answer the question of whether it is the raw spacings between rootlets that are quantal or the target positions at which they occur.

In order to quantify these considerations in the context of this study, the following sections are attributed to the initial quantogram analysis on the data sets available. We begin in section 5.3 with a brief discussion about the nature of the quantality expected and an outline of the model selection process with respect to the different types of data sets. Section 5.4 presents a general examination of any possible quantality in its simplest form on the individual rank spacings from onions, tomatoes and ferns. Throughout this part, we will underline practical difficulties such as inadequate accuracy of measurements and quantify the considerations regarding to the quantogram analysis of root spacings. Then in section 5.5 we will endeavour to alter the models by imposing not only a hierarchical but also a regression–like structure on the simple quantal model. The latter have been found more appropriate for the fern roots for reasons explained later in the section.

5.3. The Nature of Quantality for Spacings

One of the important aspects of the current quantality problem is that an individual data set offers three kinds of investigation concerning quantality. The reason for this is that there are three types of measurements obtained from a single root; spacings between laterals on each rank, distances between positions of laterals regardless of ranks (i.e. total series) and target positions of laterals on each rank. The first two have already been described in chapter 4 and the latter comes as a natural extension that will be described here.

With the two types of quantality, pure and shifted, the distinction between the models that may arise according to different types of measurements is here needed and presented below:

Rank (left and right) Series**:** Data are raw spacings $\{X_i\}$ that are the longitudinal distances between successive laterals (see Fig 4.3). They could be either pure or shifted quantal.

Total Series**:** Data are $\{T_i\}$ which are interlateral distances, ignoring the ranks, as each successive lateral appears along the root as a whole (see Fig 4.3). If the rank spacings are pure quantal, then total series are also likely to be pure quantal and similarly, if the rank spacings are shifted quantal then so could the total series be.

Positions of Laterals**:** Data are $\{S_i\}$ which are the positions of the laterals on each rank that are measured from the base of the root, i.e. $S_i = \sum_{k=1}^{i} X_k$. If the spacings are pure quantal then positions would in general relative to the first rootlet but this may not be detected because of the accumulate of errors. i.e. if $X_i = m_i q + \varepsilon_i$ (i=1,...,n), then $S_i = q\sum_{j=1}^{i} m_j + \sum_{j=1}^{i}\varepsilon_j$ and $var\left(S_j\right) = \sum_{j=1}^{i} var\left(\varepsilon_j\right)$. However, if the spacings are shifted quantal then positions may or may not be quantal, either pure or shifted. On the other hand, suppose that S_i are shifted quantal, that is

$$S_i = \beta + m_i q + \varepsilon_i$$

$$S_{i+1} = \beta + m_{i+1} q + \varepsilon_{i+1}$$

then X_i's would be pure quantal (except perhaps X_1) with twice the residual variance, i.e.

$$X_{i+1} = S_{i+1} - S_i = \left(m_{i+1} - m_i\right) q + \left(\varepsilon_{i+1} - \varepsilon_i\right)$$

where $m_{i+1} > m_i$.

From the argument above, one can conclude that it is more likely to observe shifted quantality in positions rather than in actual spacings. In the forthcoming sections, we will therefore consider the cosine quantogram analysis for raw spacings searching for only pure quantality. However we will perform the modular quantogram analysis for the positions in the search of shifted or pure quantality. As we have already shown (see Chapter 3), even if some series of positions exhibit pure quantality, the test statistic for shifted quantality would be good at detecting it as well as the one proposed for pure quantality.

5.4. Initial Quantogram Analyses

5.4.1. Practical Considerations

In the quantogram analyses that have been illustrated so far, we mainly used the data from the Megalithic circles and the range of search for the quantum value used by previous authors. As far as the quantality of rootlet spacings are however concerned, before we begin to carry out any sort of analysis it is necessary to examine some difficulties that may (or may not) arise in practice due to the nature and structure of the data sets. Therefore the following sections will demonstrate our strategy for dealing not only with problems arising with the accuracy of measurements but also for choosing the most appropriate range of the gridsearch.

5.4.1.1. The Range of Gridsearch

To begin with, it should be emphasised that any range must be strictly bounded below by the resolution of the data (see section 2.6.4). A small subset of the tomato data was analysed for quantality by Newson et al. (1993a), so we will initially accept his choice of 0.2 mm which was two times the resolution of the data. Note that the same value will be applied for the fern roots. However, the onion roots may need some adjustments due to the reason that two different accuracies were used in making the measurements (0.1 mm for the treated groups and 0.5 mm for the control group). This will be investigated further later.

The range must be also bounded above by some values of q. Practically, one would expect to observe the quantum within the range between the accuracy of the observations and the smallest observation. For example, in the case of the stone circles, Kendall finally put limits on the range so that the lower bound is the dimension of a single stone (2 ft.) and the upper bound is the diameter of the smallest circle (10 ft.). In our case, however, the smallest observations on onion roots spacings are equal to the accuracies 0.5 mm and 0.1 mm and so we are forced to consider values for the quantum higher than the smallest observation. Therefore, it is necessary to choose a criteria for the upper bound for the spacings. The method suggested by Newson is to take the 95th percentile for the fitted distribution as a strict upper bound for the quanta search. However, it can clearly be seen that this approach has some disadvantages from a practical point of view.

For example, imagine the situation when $q \approx q_{max} \approx X_{[0.95]}$. Then 95% of the measurements would be less than q and as a result 95% of the measurements have their estimated integer multipliers 1 or less (i.e. either 0 or 1). In other words, q is so large (as large as $X_{[0.95]}$) that many of the X_i/q are almost zero, making the contribution of each X to the cosine function equal to its maximum value of 1, which could cause us to accept a spurious value as a quantum.

In order to reduce such an effect, we propose using the median of each sample as an upper bound (i.e. $q_{max} \cong \tilde{x} = median\{x_i\}$) so as to make sure that we have at least half of the observations with the estimated integer multipliers 1 or more. However, the fact that individual roots, even if they are the same type, differ from one to another suggests a further adjustment to this criterion. This is necessary so as to make sure that significance levels estimated over the range are comparable to each other. Therefore, it has been decided to alter the upper bound for the raw spacings of all series as

$$q_{\max} \cong median\{\tilde{x}_j\}; \; j = 1, \dots, k$$

where k is the number of roots from a particular type or group.

As far as positions of the root series are concerned, however, observations are cumulative spacings which allow us to base the criterion for the choice of upper bound onto the smallest positions which are the first observed spacings on root series. Applying q_{max} based on the median of medians for positions would here define an unnecessarily large range of search. As the smallest positions vary from root to root, the upper bound is again adjusted to the median of the smallest observed positions from all type of roots in order to provide a common background for the judgement of the results.

Note that the whole argument concerning the range of gridsearch has been given here in terms of q. This is because it is more sensible and logical to judge such considerations in the value of the real parameter q, but not τ. Throughout the following sections, we will also present the results of quantogram analyses and the ranges of gridsearch, for convenience, in terms of either q or both q and τ. In order to avoid any confusion, it is therefore necessary to emphasise that all quantogram analyses in the previous and also coming sections have been performed strictly over the τ–range (i.e. using a grid equally spaced on the τ scale) noting the result found in 2.8.2.2 that τ is the natural scale for the gridsearch.

5.4.1.2. The Accuracy of Measurements

The major problem concerning the accuracy of measurements in the case of the Onion data set is that measurements were recorded to the nearest 0.1 mm in the treated groups but only to 0.5 mm in the control group.

The consequences of this problem for quantal searches are twofold. First, consider the choice of the range for a gridsearch. The lower bound of the range should be restricted with respect to the accuracy since one cannot hope to distinguish any quantal effect which is, in magnitude, less than the accuracy of measurements. However, for the onion roots we have two different accuracies and that suggests that the use of two separate ranges of search is necessary. We can also perform the gridsearch, following the statement before, at values above 0.5 for the both control and treated roots. Nonetheless, referring to the fact that the treatment decreases the distances between lateral roots, we presumably expect any quantal effect for treated roots to be at a value less than 0.5. Hence we will carry out the quantogram analyses bearing this in mind and try many different ranges of search whenever necessary.

The second consequence is brought about by the choice of the accuracy. In the cosine quantogram analysis, it is likely to detect some quantal effects which are simply artefacts of the accuracy of measurements, especially if the degree of the accuracy is inadequate, as in the control group of onion roots. That resonance of the accuracy “a” with values of trial quantum value which are multiples of “a” will result in strong effects in the quantogram analysis.

A similar but simpler problem came to the notice of Kendall when analysing the diameters of the circles some of which were recorded to the nearest feet or 1/2 feet. During his quantal analysis, he initially searched for the quantum over a very large τ–range [0.05, 2.55] (equivalently q~[0.392, 20]) and naturally picked up strong peaks at 1 and 0.5 feet. One of his approaches to overcoming this problem was to eliminate these what he called ‘factitious’ peaks by reducing the range of the search, mainly by making the τ_{max} smaller (i.e. q_{min} larger), and he ended up with a more appropriate τ–range as [0.1, 0.5] which gives the q range as [2, 10] (note that he altered the range again to τ~[0.09, 0.59] for technical reasons). By this way, he basically left out the artificial effects off the gridsearch.

His second approach was to show that these were artificial peaks, without loosing the true underlying quantality that he was attempting to assess. The method that Kendall used was to add a uniform number to the each diameter from either U(–0.5, 0.5) or U(–0.25, 0.25) depending on whether the accuracy is 1 ft. or 0.5 ft. respectively, and he repeated the analysis with what he termed the ‘unrounded’ data set. This procedure successfully removed the artificial peaks whilst leaving the main peak at around 5.44 relatively unchanged. The reason for this is that the structure which created the artificial peaks was destroyed by the ‘unrounding’ of the data set. However, as real quantal data sets already incorporate an error term, what amounts to slightly altering the error will not destruct the true underlying quantality.

In our situation, we will therefore make use of his methods to eliminate such likely artificial structures created by the accuracies. An alternative way of treating this difficulty could also be to adopt the accuracy "a" into the simulated facsimile data sets to get the same accuracy as the original data set in the process of assessing the significance of them. This approach would reduce the significance of the artificial peaks and make them look just like ordinary ones. However, this method could be useful only as a precaution against accepting an artificial quantal value as the true value. It will not help us to discover true underlying (if there is any) quantality in a given data set.

5.4.1.3. Assessment of the Significance

In the assessment of significance of observed quantal effects from spacings, random non–quantal data sets will be generated from a half–Normal distribution noting the result from section 2.8.2.3 indicating that the actual distribution used is not critical. These random sets will be matched to the actual data with respect to the sample variance and the smallest observation as the practical experience gathered when dealing with tomato spacings suggested that matching also the sample mean would lead to the generation of many values almost equal to "0" and even some negative values. Although random samples are not quantal, as a result of such small values, it is inevitable to observe some factitious peaks which would cause us to generate a naive significance level for the observed peak. As a precaution, without a loss of generality, it is therefore necessary to ensure at least that the smallest observation of a facsimile data set is matched to that of the original sample. Thus, the generating formula is chosen to be

$$Y = \text{constant} + \sigma\ |X|$$

where $X \sim N(0,1)$, σ is the standard deviation of $|X|$ (i.e. $\sigma = \dfrac{s}{\sqrt{(1-2/\pi)}}$, where s is the standard deviation of the original sample) and constant value is the smallest observed spacings of each root series.

In the analyses, the first three highest peaks and their corresponding quantum values have been computed to be able to examine the most suggestive values of quanta. To assess their significance, 999 facsimile samples were generated and estimated the highest peaks (i.e. $\phi(\hat{q})$) are compared with the observed ones. Thus, a p–value is calculated as described in section 2.6.5. Note that it is the modular quantogram to be used for the analysis of positions. For the significance assessment of their peaks, we continue to generate random facsimile samples from the matched half–Normal distribution. An alternative would be to match the distribution of spacings and then cumulate these to mimic the positions. This approach was not investigated further.

5.4.2. Quantogram Analyses on the Onion Data Set

In order to gain a feel for what a gridsearch for the spacings from Onions would produce, some initial quantogram analyses have been performed on some arbitrarily selected roots from each treatment groups, namely the C1, W5 and S6 roots each of which has all their rank spacings combined. Summary statistics of these are as follows:

Root	N	Mean	Median	Min	Max
C1	39	11.94	4	0.5	67
W5	95	3.95	2.3	0.2	16
S6	374	0.76	0.6	0.2	8.9

The search for the quantum has been done over a very wide τ–range [0.2, 5] with an increment of 0.001 for each root so as to decide on what ranges for the gridsearch would be plausible. The Cosine Quantogram graphs for C1, W5 and S6 are displayed in Figures 5.1–5.3 respectively.

In Fig 5.1, one can clearly see that the effect of the accuracy is very strong, which is indicated by the appearance of very large peaks at q=0.5 mm and at q=0.25 mm. Although it is not included in the graph, we must report that the effect of accuracy is prominent at 0.125 and $0.16\dot{6}$ which produce peaks as high as the one at 0.5. The graph presents a perfect symmetric pattern and locations of all the peaks are remotely relatable using the accuracy 0.5 and simple fractions of it, which rises the doubt about the indications of even the moderately high peaks. For example, the subsidiary peaks appearing at q=0.2108, 0.3644 and 0.7962 seem to be directly related neither to each other nor to 0.5 in the first instance. However, their corresponding τ values; 4.744, 2.744 and 1.256 respectively reveals the fact they have a relationship such that 4.744–2.744 = 2 (i.e. q= 0.5); 2.744 + 1.256 = 4 (i.e. q= 0.25) and 4.744 + 1.256 = 6 (i.e. q= $0.16\dot{6}$). This would happen only if the data are composed of the values of 0.5 and any integer, which describes the data sets for control group roots. Therefore, it is clear that having such an inadequate accuracy of measurements makes us unable to observe any true underlying pattern in the data. Which of those peaks may give a true indication of quantality will however be further investigated by 'unrounding' the data later.

In comparison with the C1 root, the pattern produced by the W5 root in Fig 5.2 seems to be more random, however there is not a strong indication of any quantality. On the other hand, the subsidiary peaks listed in Table 5.1, except the one at q=0.2, may be considered as some signs of weak quantality. Although the values up to 0.2 mm have been excluded from the search in order to eliminate the effect of accuracy 0.1 mm, there is still a tendency to produce a peak at 0.2 mm. This is also true for other weak–treated roots. When similar analyses have been performed, it was observed that most of them favoured 0.2 as a quantum. This is clearly an artefact of the measurement accuracy.

As far as strong treated roots are concerned, the selected root, S6, presents a cosine quantogram graph in Fig 5.3 which drastically differs from the previous two roots examined. It is somehow much smoother however with some significantly high quantogram values as listed in Table 5.2. The first quanta in the table should be again treated as a clear effect of the accuracy of measurements for the treated roots. In the graph, one can also notice a sharp increase which seems to be producing a very high peak. Nevertheless, this is not suggestive of any quantality. In fact, this is purely the consequence of choosing the upper bound of the range for the gridsearch too large. As discussed in section 5.4.1.1, searching for a quantum in the range which exceeds the median value causes the data to enter the cosine function as an error by producing "0" integer and eventually to propose a spurious value as quantum. This result highlights the importance of the right choice of the range of search once again and supports our conclusion that the range must be bounded by the median value.

Table 5.1. The subsidiary peaks produced by the W5 root.

q	**τ**	**Peak**
0.2425	4.123	2.864013
0.3623	2.760	2.810213
0.2000	5.000	2.466619
0.3454	2.895	1.836736

Table 5.2. The subsidiary peaks produced by the S6 root.

q	**τ**	**Peak**
0.2019	4.954	5.778864
0.4496	2.224	5.319882
0.4958	2.017	4.622068
0.3758	2.661	1.310617

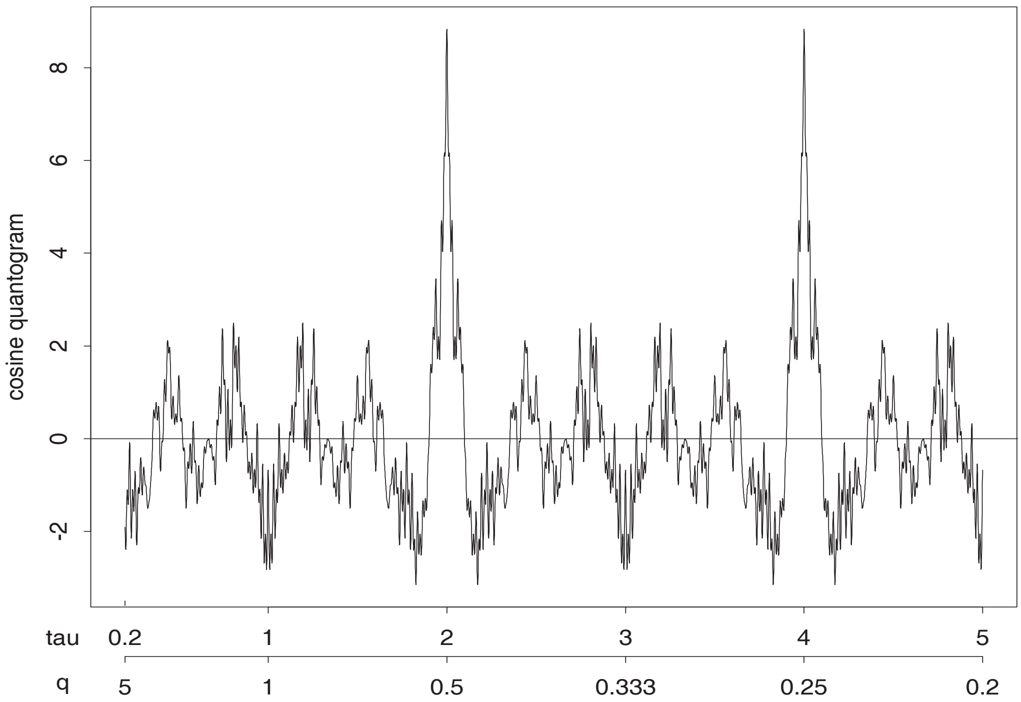

Fig 5.1. Cosine Quantogram graph for the C1 root

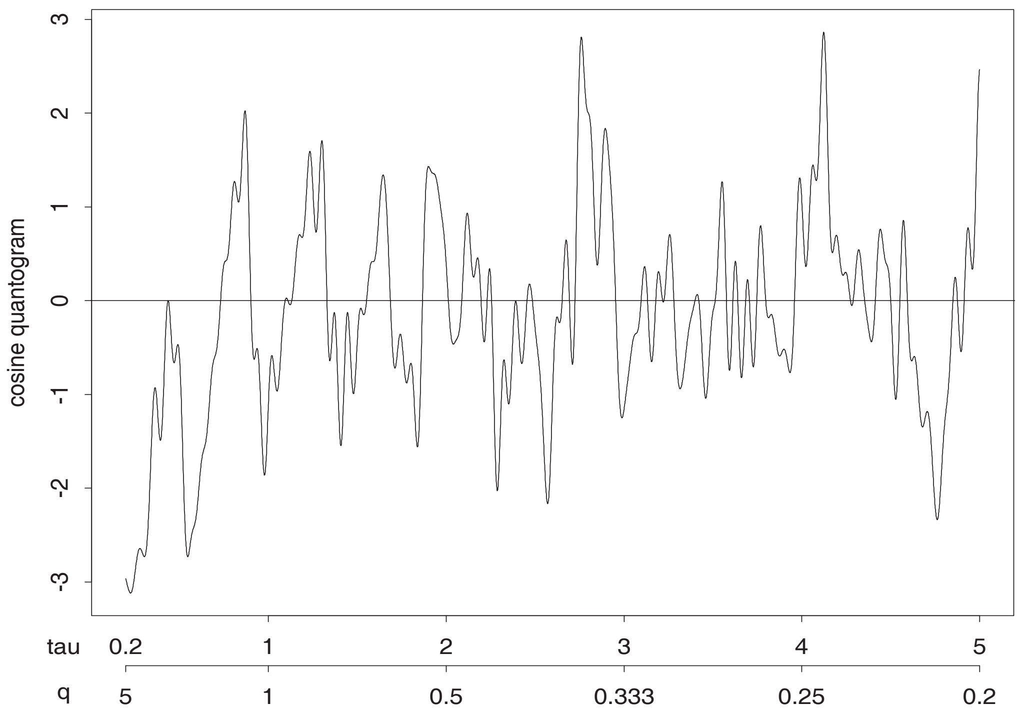

Fig 5.2. Cosine Quantogram graph for the W5 root

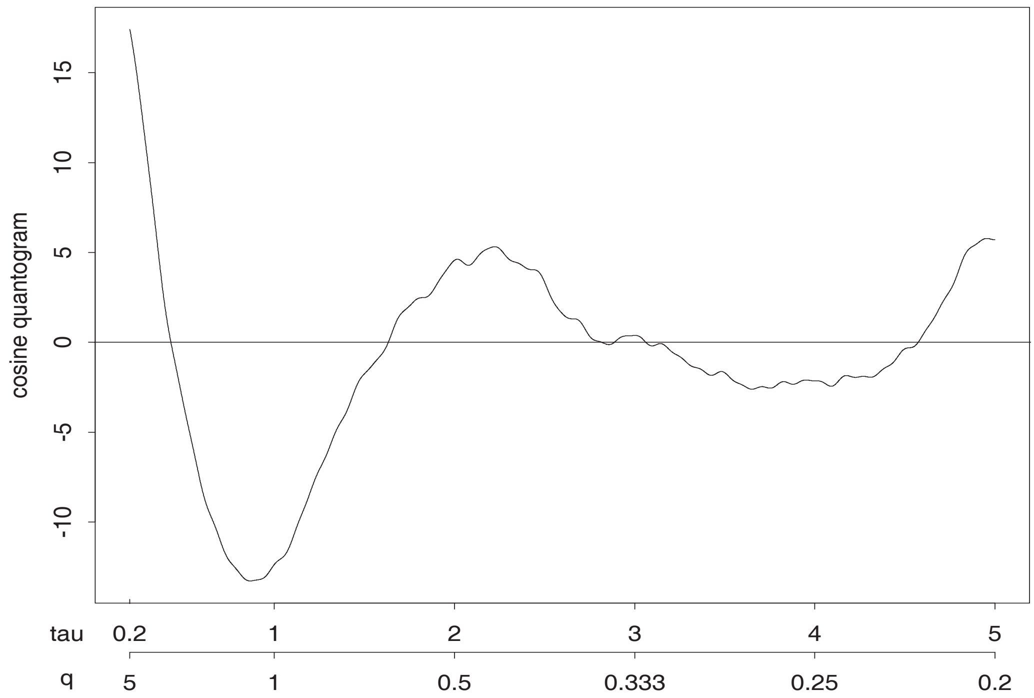

Fig 5.3. Cosine Quantogram graph for the S6 root

5.4.2.1. Unrounding the Onion Data Set

Having observed a very strong resonance of the accuracy 0.5 for Control group roots and some tendency for the treated roots to be quantal (perhaps only weakly), we next investigate whether or not these features are spurious. If they are artificial, the progressive diluting of the structure of the original data set will gradually destroy them, leaving the true effects unchanged. With this motivation, the 'unrounding' method has been considered. Note that the aim here is not to provide a formal significance test of particular values, this analysis is to be regarded as a part of the exploratory stage and, by unrounding, we wish to explore the possible values of any quantum that may be present for the onions.

As a pilot study again we used the roots C1, W5 and S6. To begin with, we have added a uniform value from U(–a, a) with, a first obvious choice, a = 0.25 to all observations of the C1 root. Then a gridsearch over the τ–range [1.111, 5] (or q~[0.2, 0.9]) using the new unrounded data set has been performed. We also repeated this process 100 times recording the maximum peak and the estimated quantum each time. Due to the reason that the effect of accuracy 0.5 is very strong such that even its simple fractions control the locations of peaks, the C1 data set has been unrounded by adding the uniform values with also a = 0.5 and 1. Then 100 gridsearches again have been performed for each. In order to examine the strength of the peaks, a frequency diagram of the estimated quantum values for each of the unrounding variates are obtained as in Fig 5.4. As a result, one can see that the effect of the accuracy 0.5 is reduced by 'unrounding'. More importantly, an appealing result from 'unrounding' is that the most of estimated quantum values lie notably around 0.3.

Similarly, the roots W5 and S6 have been unrounded by adding each observation a uniform value from U(–a, a) with a = 0.05, 0.1 and 0.2. As before, frequency diagrams of the 100 estimated quantum values for each have been obtained and are presented in Figures 5.5 and 5.6 respectively. For the W5 root, estimated quantum values tend to lie most particularly around 0.3. Remembering that the S6 root produced some significant results at around 0.45, unrounding the measurements with the variate a = 0.05 and 0.1 seem to support these values. When a = 0.2 (i.e. 2*accuracy) however, this effect collapses drastically and the effect moves down to the values around 0.3 or 0.2.

In addition, recorded 100 maximum peaks are presented in Tables 5.3–5.5 as N2 = # $\{2 \leq \text{maxima} < 3\}$, and N3 = # $\{\text{maxima} \geq 3\}$. Note that Roman numbers I, II,..., VII represent the intervals [0.2,0.3), [0.3,0.4), [0.4,0.5), [0.5,0.6), [0.6,07), [0.7,0.8), [0.8,0.9] respectively.

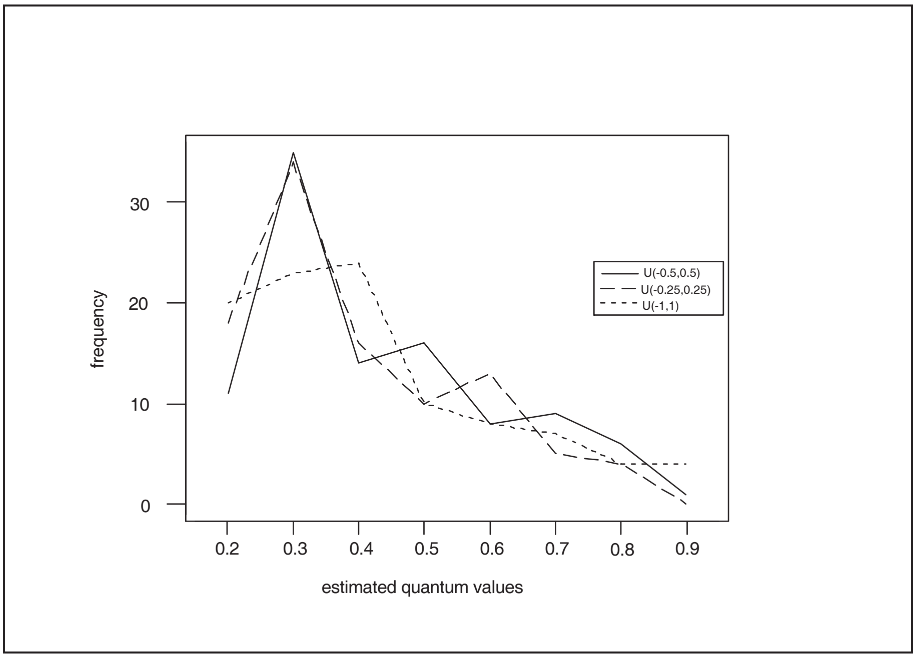

Fig 5.4. Results of gridsearch on the C1 root after ‘unrounding’.

Table 5.3. Results of gridsearch on the C1 root unrounded with a variate U(–a, a)

a	#	I	II	III	IV	V	VI	VII
0.5	**N2**	21	14	9	7	7	2	1
	N3	9	9	7	5	3	2	4
0.25	**N2**	18	13	8	4	7	3	0
	N3	19	10	5	6	3	2	2
0.1	**N2**	14	14	9	6	5	3	3
	N3	16	14	16	2	2	3	3

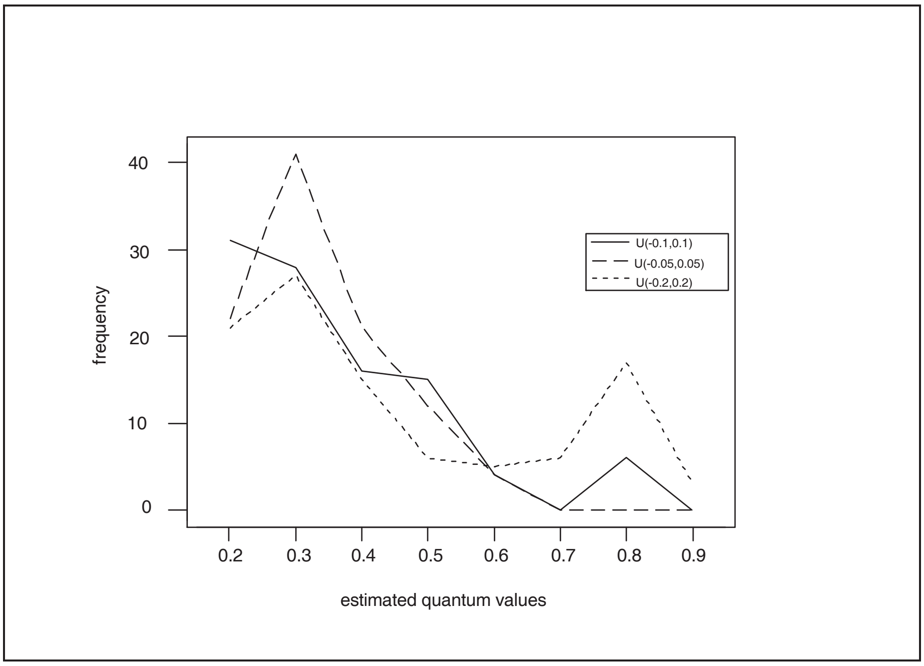

Fig 5.5. Results of gridsearch on the W5 root after 'unrounding'.

Table 5.4. Results of gridsearch on the W5 root unrounded with a variate U(–a, a)

a	#	I	II	III	IV	V	VI	VII
0.05	**N2**	30	22	0	14	0	0	0
	N3	15	11	0	1	0	0	0
0.1	**N2**	38	18	8	7	2	2	4
	N3	5	5	1	1	0	0	0
0.2	**N2**	26	12	8	4	5	6	10
	N3	12	3	2	0	0	0	3

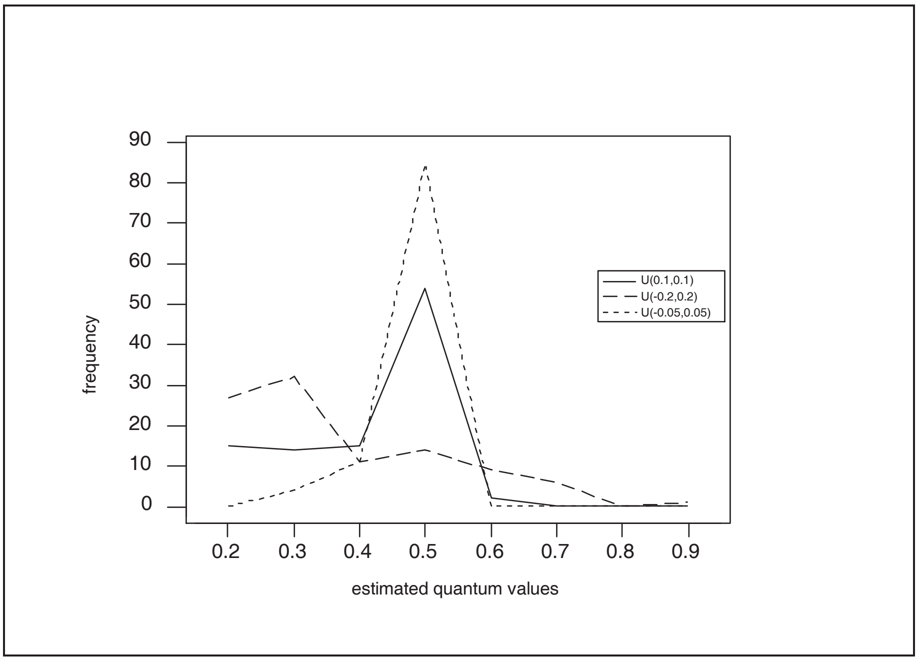

Fig 5.6. Results of gridsearch on the S6 root after 'unrounding'.

Table 5.5. Results of gridsearch on the S6 root unrounded with a variate U(–a, a)

a	#	I	II	III	IV	V	VI	VII
0.05	**N2**	3	0	25	6	0	0	0
	N3	0	1	62	2	0	0	0
0.1	**N2**	12	4	32	13	0	0	0
	N3	3	1	4	6	0	0	0
0.2	**N2**	16	5	5	8	1	1	0
	N3	2	2	2	0	0	0	0

5.4.2.2. Analyses of Spacings and Positions

In addition to the roots investigated above, individual rank and total series of all onion roots of each treatment group as well as their combined rank series have been analysed by means of quantogram analyses. Moreover similar analyses have been performed for the positions of all series. Ranges of the gridsearch for both spacings and the positions can be found in the Table 5.6. Note that all the analyses have been carried out with an increment of 0.001. The upper bounds for the treated roots and also positions of control roots are chosen according to the argument in section 5.4.1.1. For the control group spacings, it is however kept much restricted due to the strong effect of their accuracy. Moreover, the lower bound for treated roots is increased from 0.2 to 0.21 so as to avoid the aforementioned effect of the accuracy which resulted in many treated roots to favour 0.2 as a quantum.

Table 5.6. Ranges of gridsearch (in terms of q) according to data types and treatment groups

Data Type	**C**	**W**	**S**
Rank spacings $\{X_i\}$	[0.55–0.9]	[0.21–3.0]	[0.21–0.9]
Total spacings $\{T_i\}$	[0.55–0.9]	[0.21–1.4]	[0.21–0.6]
Positions $\{S_i\}$	[0.55–4.0]	[0.21–2.5]	[0.21–2.5]

Full results of all the analyses are demonstrated in Appendix B and only significant ones will be presented here. To begin with, it can be concluded that all control group roots are under the strong influence of the accuracy 0.5 so that integral multiples of this value (and half its value 0.25) produce moderately high peaks. Therefore no assessment of significance has been carried out for the observed peaks of the control group roots. However, their combined rank series have been unrounded to the accuracy 0.5 and similar behaviour with the root C1 has been observed for all (see Appendix B).

Significant results obtained for some of the treated roots are shown in Table 5.7. It can be observed that total series present the least tendency to be quantal. Besides Strong treated roots show more evidence of quantality than Weak treated ones. Estimated quantum values for the rank series however do not indicate the same value.

Table 5.7. Gridsearch results on the treated roots of onions

Root–series	$\hat{q}$	$\phi(\hat{q})$	P–value
W1–T	0.2133	3.7851	0.007
W2–r3	0.4032	3.3673	0.064
W5-r5	0.8230	3.1463	0.091
S3–r5	0.4636	3.4833	0.019
S4–r2	0.3527	2.9089	0.112
S5–r3	0.3272	2.9172	0.097
S6–r2	0.5032	3.6225	0.010
S6–r3	0.4502	3.9277	0.002
S6–r4	0.4921	3.4921	0.009

In addition to the raw spacings, any quantal tendency from the positions of the rank and total series has also been investigated by applying modular quantogram analysis and results are given in table 5.8. The control group roots again suggested spurious quantum values and the results remained inconclusive. Positions of the treated rank spacings however provide the most of the evidence in favour mostly of pure quantality. Only few total series again presented nominally significant results.

Table 5.8. Gridsearch results using positions of rank and total series on treated roots.

Root	$\hat{q}$	$\chi(\hat{q})$	$\psi(\hat{q})$	$\hat{\beta}$	P–value
W1–T	1.3580	9.9674	–3.1289	–0.5112	0.028
W5–r1	0.5583	8.2939	–0.2244	—	0.108
S1–r2	0.3920	8.3730	–3.1084	–0.0538	0.033
S2-r3	0.2806	9.9617	4.4345	0.0752	0.041
S3–r4	0.3007	8.4906	–1.2536	—	0.106
S4–T	0.4600	7.3935	–1.7958	—	0.057
S6–r1	0.4221	9.0685	–1.4103	—	0.090
S6–r4	0.5507	10.0936	1.0799	—	0.019

5.4.3. Quantogram Analyses on the Tomato Data Set

The initial search for quantality has also been similarly done for the roots of tomato specimens. The quantogram analyses of all tomato roots have been performed with an increment of 0.001 over the ranges of τ converted from the q–ranges given in Table 5.9. Note firstly that the choice of ranges have been made using the argument in section 5.4.1.1 and also that a pilot study on a randomly selected root has been undertaken in order to choose the best increment for root spacings following the approach illustrated in section 2.6.4.

Table 5.9. Ranges (in terms of q) of search with respect to different data and tomato types

Data Type	Wild	Wild–Naa	Gib1	Gib1–Naa
L & R Spacings $\{X_i\}$	[0.2–2.6]	[0.2–2.4]	[0.2–2.9]	[0.2–3.1]
Total Spacings $\{T_i\}$	[0.2–1.4]	[0.2–1.2]	[0.2–1.5]	[0.2–1.6]
Positions $\{S_i\}$	[0.2–2.5]	[0.2–2.5]	[0.2–2.5]	[0.2–2.5]

The roots showing nominally 'significant' (i.e. $P < 0.1$) results for some of their series of raw spacings and positions with estimated quantum values and their nominal significance probabilities are displayed in tables. The full results for all series are given in Appendix C. It should be emphasised that the P–values quoted here are 'nominal' values obtained by testing each series separately and no allowance has been made for multiple testing and identification of individual series on the basis of their yielding a 'significant' result. At this stage the analysis is still in the exploratory stage. This aspect will be discussed further in section 5.4.5.

5.4.3.1. Analyses of Spacings on the Left and Right Series

The simple quantal tendency has been investigated on the left and right series of tomato roots and results are demonstrated in Tables 5.10–5.13. For the wild type roots, it appears that the estimated quantum values indicate some quantality at around 0.3 ranging roughly from 0.240 to 0.375 except the left series of root WR7, half of whose quantum of 0.749 is however still within the same range. It must be emphasised here that the left series of root WR1 provides the strongest evidence against the non–quantal hypothesis by its first highest peak at $q^{(1)}=0.362$ ($\tau^{(1)}=2.758$) nominally significant at the 2% level and the second highest peak at $q^{(2)}=0.240$ ($\tau^{(2)}=4.158$) also nominally significant at the 5% level. Notice the relationship between those two as $q^{(1)} =1.5*q^{(2)}$.

As far as wild type roots are concerned, it must be pointed out that the quantality of the roots WR1–4 were also analysed by Newson et al. (1993a). In comparison to our results, he agrees with the conclusion that some series of only WR1 and WR3 have the tendency to be quantal and the roots WR2 and WR4 show no sign of being quantal. Some slight differences in the estimates of our quantum values and those of his values are believed to be created by different approaches in the application of cosine quantogram analysis. First of all, the range of gridsearch he chose was larger (see section 5.4.1.1) and the number of candidate points he tested within the range somewhat smaller than the ones we used here. The other major difference is brought about by the zero spacings in the total series of the roots which were included in his analyses however we excluded those from the data for the reasons explained in Chapter 4.

The outcome of the analyses conducted for the Gib–1 Mutant type roots concludes that some indication of quantality is also evident for some quantum values ranging from 0.263 to 0.501 as given in Table 5.11.

Table 5.10. Gridsearch results using right and left series on WR roots

Root	*Series*	$\hat{q}$	$\phi(\hat{q})$	P–value
WR1	*Right*	0.3003	1.9090	0.890
	Left	0.3625	3.5875	**0.011**
WR3	*Right*	0.3032	1.9190	0.871
	Left	0.2636	3.0475	**0.091**
WR7	*Right*	0.7110	2.4517	0.567
	Left	0.7498	3.2928	**0.078**
WR9	*Right*	0.4625	2.0462	0.839
	Left	0.3672	3.0891	**0.097**

Table 5.11. Gridsearch results using right and left series on GR roots

Root	*Series*	$\hat{q}$	$\phi(\hat{q})$	P–value
GR3	*Right*	0.4279	2.6649	0.196
	Left	0.2774	2.9102	**0.097**
GR5	*Right*	0.3282	2.0396	0.821
	Left	0.5014	3.2218	**0.068**
GR6	*Right*	0.2631	3.1041	**0.117**
	Left	0.2801	3.2849	**0.043**

In addition to the results above, only a few Naa treated Wild type roots suggested some quantum values which are 0.529 and 0.315 (see Table 5.12) and only left series of one Naa treated Gib–1 type root proposed the value of 0.869 as a quantum (see Table 5.13).

Table 5.12. Gridsearch results using right and left series on NWR roots

Root	***Series***	$\hat{q}$	$\phi(\hat{q})$	P–value
NWR2	*Right*	0.5084	2.5660	0.183
	Left	0.5292	3.4740	**0.017**
NWR4	*Right*	0.4594	2.7872	0.156
	Left	0.3156	3.0446	**0.075**

Table 5.13. Gridsearch results using right and left series on NGR roots

Root	***Series***	$\hat{q}$	$\phi(\hat{q})$	P–value
NGR2	*Right*	0.2506	2.5020	0.388
	Left	0.8693	2.9241	**0.070**

5.4.3.2. Analyses of Spacings on the Total Series

Proceeding with the investigation of quantality on the total series, we again performed cosine quantogram analyses and results are presented in Tables 5.14 and 5.15. In general one can conclude that there is some, but not strong, evidence of quantality. The quantum values significant at 10% level are again around 0.33 and 0.24 for the raw spacings but they seem to be increased by the Naa treatment for GR types. The second highest peak of the NGR4 arises at 0.320 that is however not found to be significant.

Table 5.14. Gridsearch results using total series on WR & NWR roots

Root	$\hat{q}$	$\phi(\hat{q})$	P–value
WR3–T	0.3360	3.2127	**0.039**

Table 5.15. Gridsearch results using total series on GR & NGR roots

Root	$\hat{q}$	$\phi(\hat{q})$	P–value
GR2–T	0.2470	2.8901	**0.085**
GR5–T	0.5180	2.4304	0.181
NGR3–T	0.3381	2.7466	**0.120**
NGR4–T	1.3353	3.4993	**0.012**

We have so far exhibited quantal tendency in raw spacings and total series of all roots. As a result, it was observed that some series of roots, but not all, revealed some tendency to be quantal in the lateral production. Regardless of the type of tomatoes, an overall, rather surprising, result is observed such that only left and total series of distances exhibit any substantial evidence for the existence of a quantal distribution. The reason for this is not obvious.

5.4.3.3. Analyses of Positions on the Left, Right and Total Series

The study for the existence of any quantality is continued next for the positions of laterals on each series, left, right and total. Again, modular quantogram analyses have been performed for this purpose and the significant results with estimated quantum values and their nominal significance probabilities are displayed in Tables 5.16–5.19. In the cases when shifted quantality exists (i.e. the value of test $\psi(\hat{q})$ is outside the region ± 2), maximum likelihood estimates of shift β is displayed. When no value of β is given, this would mean that the β–effect is not found significant and there appear to be pure quantality for those series.

Table 5.16. Gridsearch results using positions of L, R & T series on WR roots

Root	$\hat{q}$	$\chi(\hat{q})$	$\psi(\hat{q})$	$\hat{\beta}$	P–value
WR1–T	0.4211	9.70928	–3.0232	–0.0506	**0.078**
WR2–T	0.7509	9.86452	4.0555	0.1375	**0.066**
WR6–R	0.5971	10.8340	2.5494	0.0550	**0.070**
WR8–T	0.9925	9.05916	–2.2191	–0.0866	**0.094**

Table 5.17. Gridsearch results using positions of L, R & T series on GR roots

Root	$\hat{q}$	$\chi(\hat{q})$	$\psi(\hat{q})$	$\hat{\beta}$	P–value
GR3–R	0.2114	10.15378	4.1662	0.0396	**0.070**
GR4–R	0.3267	10.80457	–1.8439	–	**0.031**
GR4–T	0.9025	10.92986	–2.8644	–0.3565	**0.042**
GR6–L	0.5742	9.81927	3.9370	0.1871	**0.084**
GR6–T	0.4030	9.73101	–1.9787	–	**0.101**

An overall conclusion drawn from the results is firstly that positions of root series exhibit more evidence in favour of quantal pattern, particularly in the form of shifted quantality. Secondly, right series whose raw spacings did not show any evidence of quantality appear to be quantal in their positions. Most of the support come from positions of right and total series.

Table 5.18. Gridsearch results using positions of L, R & T series on NWR roots

Root	$\hat{q}$	$\chi(\hat{q})$	$\psi(\hat{q})$	$\hat{\beta}$	P–value
NWR1–L	0.7896	9.33241	2.3588	0.0725	**0.094**
NWR1–R	0.2438	9.94706	2.8329	0.0267	**0.074**
NWR2–R	0.7351	10.70794	–4.3155	–0.1405	**0.028**
NWR4–R	0.2149	10.28014	–4.5288	–0.0554	**0.037**

Table 5.19. Gridsearch results using positions of L, R & T series on NGR roots

Root	$\hat{q}$	$\chi(\hat{q})$	$\psi(\hat{q})$	$\hat{\beta}$	P–value
NGR3–R	0.4207	8.17953	–3.8202	–0.1275	0.142
NGR4–R	0.3254	8.21825	1.3526	–	0.151

5.4.4. Quantogram Analyses on the Fern Data Set

The very regular production of leaves on fern plants has raised the question of whether there is some correspondence between the production of leaves and roots. It is therefore of our particular concern to investigate the regularity of fern root production. For this study, only a few roots available from the selected species, C–type and M–type. Our initial inspection indicates that the fern roots distinctively appear to have their spacings very regular. However, this picture creates this phenomena, related to our remarks in 2.4.1 and 2.6.5, where data are too regular and therefore no quantality can be detected. The quantogram analyses we perform on the fern spacings will here present this effect.

The range of gridsearch is chosen as [0.2, 11] and [0.2, 1.5] for rank series (i.e. the left and right) of the C–type and M–type respectively. For the total series, it is

[0.2, 0.5] for the C–type and [0.2, 0.8] for the M–type. In addition, the quantogram analyses of positions are performed over the range of [0.2, 11] for all. Note that the upper bounds are based on the median of the median values as before.

As a result of this study, the quantal tendency is observed only in the CT1 and MQ roots with the values presented in Table 5.20. The left and right series of the CT1 root here appear to be a good example of our previous remarks about spacings being "too quantal". One can clearly see that both series suggest almost the same quantum with high cosine quantogram values, however, the quantality of the right series is rejected meanwhile that of left series is accepted. The reason for this can be found in the histogram graphs of the series in Fig 5.7. The right series have a unimodal distribution with a small variation, which produces integers of "1" for all its spacings in the quantogram analysis and therefore quantality disappears. Although, this is also true for the left series, it has only one spacings giving an integer of "2". The paradox here exists such that if we excluded that observation, then quantality of the root would be rejected. The total series of the CT1 root however gives a good picture of quantal distribution. The M-type fern root remains only suggestive of quantality in its left series. Note that full results are given in Appendix D.

Table 5.20. Gridsearch results using L, R & T series on Fern roots

Root	***Series***	$\hat{q}$	$\phi(\hat{q})$	P–value
CT1	*Right*	10.9890	4.2790	0.525
	Left	10.6383	4.7761	**0.001**
	Total	3.5211	4.9638	**0.001**
MQ	*Right*	0.2268	1.8842	0.913
	Left	1.0137	3.0498	**0.104**
	Total	0.6417	2.3283	0.203

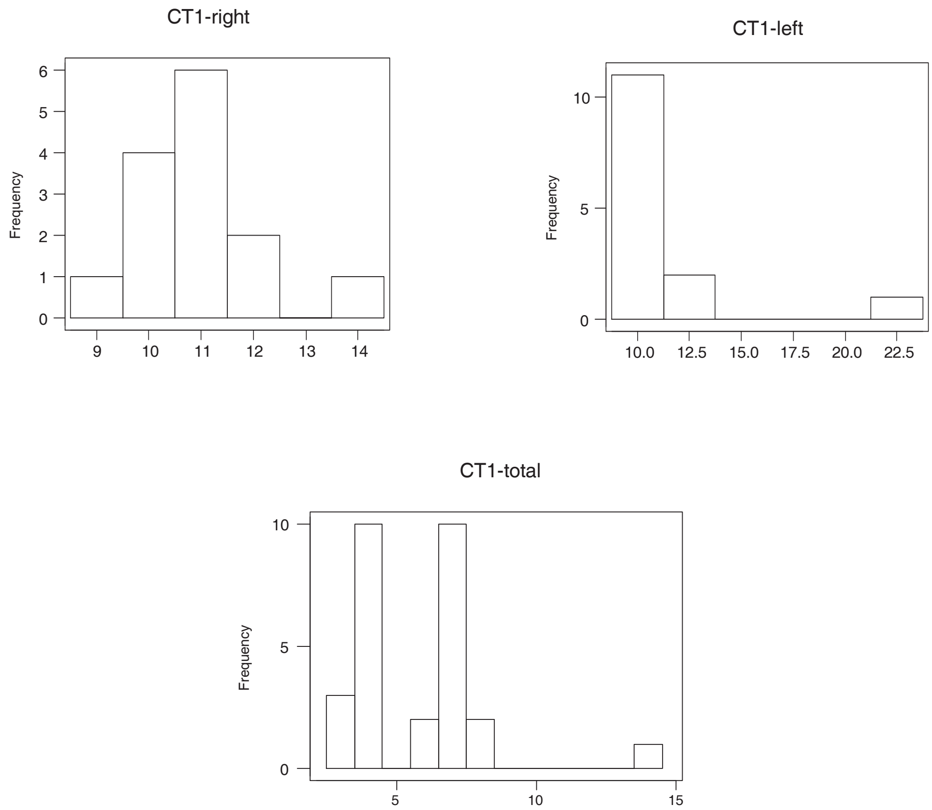

Fig 5.7. Histograms for the series of the CT1 root

Undertaking the similar investigation for the positions of fern roots, the only root that suggested quantality is MQ (see Table 5.21). The right series of the CT1 root here appears to give some signs of shifted quantality. Note that the full results can be found in Appendix D.

Table 5.21. Gridsearch results using positions of L, R & T series on Fern roots

Root	$\hat{q}$	$\chi(\hat{q})$	$\psi(\bar{q})$	$\widehat{\beta}$	P–value
CT1–R	10.7527	8.5441	3.5097	3.6407	0.169
MQ–L	1.1328	10.1017	–1.0720	–	**0.085**

5.4.5. Issues of Multiple Testing

In the search of quantality for roots, we have so far carried out many quantogram analyses and presented the root spacing series found to be “nominally” significant. No adjustment was made for the number of significance tests performed in the hunt for a ‘small P–value’. This could be done by a simple Bonferroni adjustment of using a nominal level of α/k in each of k tests to be able to claim an overall level α for the results of the k tests considered as one overall analysis. Further in performing k tests, in the null situation the number of results nominally significant at the α level is Binomially distributed $B(k, \alpha)$.

In the case of the Wild type of tomatoes, for example, we examined 10 roots each of which had 2 series, left and right. Amongst those 20 hypothesis tested, only four of them were declared significant at the 10% level including one significant result at the 5% level. If the overall significance level α is prespecified as 0.05, one would need at least one result nominally significant at the 0.0025 level. Thus, the Bonferroni adjustment would not declare a result significant at the 0.05 level, although it might be noted that the 4 results nominally significant at the 10% level is slightly higher than the expected value of 2.

Similar conclusions apply to the other types of tomatoes. Of course, these simple Bonferroni adjustments are extremely conservative and so should not be taken as the final analyses of these data sets. In a later chapter we shall consider more refined methods of combining P–values to provide an overall analysis of each data set but in the next section we consider ways of extending quantal models to allow data sets consisting of several separate but related series to be analysed as a single whole and thus avoid the problems of multiple testing that arise when they are examined separately.

5.5. Extended Quantal Models

5.5.1. Hierarchical Quantal Models

Up to now, we have investigated the quantality of the data sets available and our initial analyses suggest that such a feature (if it exists) can not be represented by a common quantum. Having also highlighted the limitations and considerations within the scope of this study, we have however observed that assuming a common quantum value for all the roots does not reveal any evidence of quantality. The absence of evidence may be because combining separate data sets (which might have slightly different quanta) may mask the quantal evidence.

Therefore, it is necessary, at this stage, to extend the existing models so that the new models enable us to assign different quantum values to different rank series, roots and treatment groups. In other words, we need to develop an analogy to linear models with a hierarchical structure imposed so as to allow (in the case of the onions for example) the spacing quanta (if it exists) to vary from rank to rank, from root to root and from treatment group to treatment group. In the case of tomato data we might allow for variation between varieties and treatments and between roots. Assuming that distances between laterals tend to be quantal, a natural extension therefore comes from a simple adjustment of the basic quantum models as follows:

Model 1: suppose the data from one root are X_{ij},

$$X_{ij} = \left(\beta_j\right) + m_{ij} q_j + \varepsilon_j; \quad j = 1,\ldots,k;\ i = 1,\ldots,n_j \tag{5.1}$$

where k is the number of ranks (or series), n_j is the number of distances on the j^{th} rank of the root and q_j is the quantum for j^{th} rank. In addition, the shifted version of the hierarchical model is possible by including the shift components, β_j, assigned to the j^{th} rank and given in brackets in order to present both pure and shifted hierarchical quantum models in 5.1.

In this model, as noticed, the quantum values differ from rank to rank on the same root. However, the variation between them must be somehow restricted. In fact, one should expect the quantum values from individual ranks (or series) to be very "close" to each other, or more specifically varying slightly around a mean value. We will return to discussing what we mean by "close" (which is the essence of the model) later.

If it is apparent that each root in a given treatment group does not share the same quantum, then it is necessary to extend the model for several roots.

Model 2: suppose the data from several roots are $X_{ij\ell}$

$$X_{ij\ell} = \left(\beta_\ell + \delta_{j\ell}\right) + m_{ij\ell} q_{j\ell} + \varepsilon_{ij\ell}; \quad \ell = 1,\ldots,L,\ j=1,\ldots,k_\ell,\ i=1,\ldots,n_{j\ell} \tag{5.2}$$

where L = number of roots, k_ℓ = number of ranks on ℓ^{th} root and $n_{j\ell}$ is the number of distances on the j^{th} rank on the ℓ^{th} root. Again, the shifted version of this second model is represented by two components; $\delta_{j\ell}$, the shift associated with j^{th} rank on the ℓ^{th} root, and β_ℓ, the shift associated with the ℓ^{th} root.

In this model, it must be noted that we allow some variation among quantum values for ranks as well as the roots. In this case, however, it should be expected that $\left\{q_{j\ell}\right\}_{j=1}^{k_\ell}{}_{\ell=1}^{L}$ to vary least with j and more with ℓ. In other words, the variation between estimated quantum values should be less within ranks on the same root than within roots in the different treatment groups.

A major feature of these models is hidden by the statement that the quantum values are very "close" to each other or "varying slightly". It must be emphasised here that this is equivalent to a judgement depending on degrees of belief (i.e. amount of evidence) and has the disadvantage of not being expressed in a precise form. In order to overcome this difficulty, we have to develop some methods so that we could express 'mathematically' how 'close' quantum values could be but still be detectable. The possible approaches will be presented and investigated in later chapters.

5.5.2. Regression Quantal Model

The apparent lack of periodicity in most of the roots examined is perhaps because the rhythm of lateral root production changes as the root grows. This would indicate some variation in the quantal pattern or its periodicity along the root. Such quantal structure may be particularly appropriate in the case of fern roots for reasons connected with their biology (Barlow, pers. comm.). The establishment of a "fundamental distance" for the roots of two water–ferns would have a particular implications for the root development. It would suggest that within the root there are quantal cell divisions where one of the cells of a division gives rise to lateral roots. That is to say that distance between laterals is actually cumulative length of a certain number of variably sized cells rather than being an absolute distance that ignores the cellular structure.

In order to formulate this new quantality, suppose we have distances from a particular series on a root, i.e. X_i, i=1,...,n. Thus, the implication of the spacing quanta varying slightly along the root can be modelled with what we will call a *Regression Quantal Model* as follows:

$$X_i = m_i q_i + \varepsilon_i ; \quad i = 1, \ldots, \mathrm{n} \tag{5.3}$$

where

$$q_i = q + \gamma \, t_i , \tag{5.4}$$

t_i is a covariate, n is the number of spacings and q is the common quantum for all spacings. Within the framework of this study, the positions of laterals on the root could be chosen as a covariate. The function of the parameter γ is to allow q some variation along the root which is assumed to be small with respect to q (i.e. $\gamma\, t_i < q$). As a consequence, the parameter γ should be expected to be very small.

As the quantogram analysis relies on the spacing quanta remaining constant throughout the period of lateral root production, the available methodology needs to be modified for the evaluation of the regression quantal models in relation to the condition (5.4). In the ensuing chapter, the issue of how to assign a certain variability to the spacing quanta is demonstrated and various aspects are explored by means of simulated data and the data from ferns.

5.6. Discussion

This chapter has presented simple (or simplistic) analyses of all roots separately. Some individual root spacings exhibited some evidence of quantality but not of sufficient strength to reach a conclusion after conservative Bonferroni adjustments are made. More evidence obtained from the positions which mainly favoured shifted quantality, however did propose neither the same quantum value nor the same shift. Nevertheless, these initial analyses suggest that more detailed and refined investigations might be profitable.

One can conclude from the results that each rank has its own periodic lateralization, and this varied from rank to rank, and from root to root. However, pooling the rank spacings obliterated any periodicity and also masked the evidence of such variable quantality. Using the expectation that any differences between quanta for different roots would be ‘small’, the basic quantal models are here extended to the cases when underlying quanta is possibly nested within roots, treatments etc., for which we proposed a new model as we named *Hierarchical Quantum Model*.

Another extension has been suggested by interesting features of the Fern roots. First of all, the analyses of C–type Fern roots exhibited an intriguing phenomena whereby visual inspection of lateral root production leaves no doubt about the regularity of the laterals, however the pattern appeared to be too perfect for quantogram analyses. In other words, the laterals are produced very regularly along the root without there being any “gaps”. This is the phenomenon noted in the comments in section 4.3.3. This means that there is no underlying quanta for quantogram to discover. Along with the second feature of Fern roots associated with their biology, a new form of quantality has been brought up with some quanta that is not constant for all root spacings, but (may be) stretched along the individual root. For this new kind of quantality, we formed a new model, namely *Regression Quantum Model*.

In the formulation of extended quantal models, hierarchical and regression, difficulties arise due to the uncertainty about how to specify the underlying argument – quantality being *slightly* variable, either within different groups or along the same root. It is clear that these new models require development of new methodologies and testing procedures. In the coming chapters, we therefore will propose, and follow, a variety of approaches and examine their performances in detecting the new forms of quantality.

CHAPTER 6.

Approaches to Constructing Extended Quantal Models

6.1. Introduction

The study of the existence of regular patterns in spacings from the selected plants highlighted the diverse aspects of quantality by the implication of not only a coherent hierarchical system but also a regression–like pattern in the formation of the roots. Hence, we have laid a foundation for a theory of such structural quantality whose methodological consequences we shall explore in this chapter.

The essence of the current problem is searching for a fundamental distance in spacing that is consistent with a 'sensible' hierarchy of units, in the sense that the magnitude of spacing quanta (if it exists) changes very slightly from root to root, and in fact possibly from also rank to rank but still be detectable. It would be inadmissible to propose a set of quantum values that are irrelevant and far away from each other. However, it is very difficult to incorporate such a prior conviction into the quantogram analysis and express it in a mathematical form. It is evidently necessary to be able to apply some newly acquired techniques to this apparently totally different quantal problem.

In the first part of this chapter, we will therefore develop some methods that would enable us to detect hierarchical quantality in which quantum values are close to each other. One approach is essentially algorithmic. One data set is selected and the best quantum value for it is determined by searching over a wide range, subsequent data sets are examined over a much restricted range of search around this initial value. The evidence from the separate data sets is then combined by either a composite test or by the so-called Fisher's method for combining the significance of independent tests. This algorithmic approach ensures we look for quanta in different data sets that are close together and by recognising the analogy with one–way Anova, we can apply simple ideas of residual analysis.

A second way of expressing the notion that quantal values are close to each other is through a Bayesian formulation which stipulates that the values arise from a distribution whose variance is *a priori* formulated as being very small. This approach is taken up in Chapter 7.

The second part of this chapter concentrates on the formation of Regression Quantal models arising specifically with the certain biology of Fern roots. For this kind of quantality, a difficulty arises with the idea of allocating certain variability to some quantum value supposed to exist along a root. Obviously, the amount of variation should depend on the quantum value and the total length of the root. As the usual quantogram analysis does not take any such restriction into account, we need to modify the approach and extend the analysis to a two dimensional gridsearch so as to estimate the new parameter that controls the variation as well as the quantum.
Note that we will make use of some simulation techniques in the development of above mentioned methodologies.

In section 6.2, we begin with a proposal of a new test statistic in order to combine the amount of information supplied by the data and illustrate that it is as powerful as the well–known Fisher's method. Then an algorithmic approach is illustrated in order to construct a hierarchical quantality with quantum values close to each other. The evidence that is present for the estimated values are then combined by the proposed test statistic and tested using simulation. Section 6.3 and 6.4 summarise the results when this methodology is applied onto onion and tomato roots. Then, an analogy to the one–way Anova is illustrated in section 6.5 employing residual analyses for a visualisation of the structural quantality and it is followed by a demonstration of various patterns of residuals obtained from a simulation study. Finally, section 6.6 deals with the proposal of Regression quantality. Detection of the structure visually is first considered through some residual analyses and how much variation to the quantum is to be allowed is discussed. That is followed by the illustration of estimation procedures for the parameters with a particular application on the Fern data sets. Section 6.7 investigates all evidence obtained for onion and tomato roots so as to draw overall conclusions of quantality. Then, this chapter is closed by making some final remarks.

6.2. Combining Weak Quantality

6.2.1. Proposal of a New Aggregate Test Statistic

When a number of quite independent tests of significance have been performed, it sometimes happens that although few or none of them can be claimed individually as significant, nevertheless the aggregate gives an impression that the probabilities are on the whole lower than would often have been obtained by chance. Then it is desired, taking account only of these probabilities which may be the results from different sources, to obtain a single test based on the product of the probabilities individually observed.

Similarly, when quantogram analyses were performed for example on the tomato roots it was felt an overall result would lead to the acceptance of the quantality, even though few or none of the ranks can be accepted individually as giving significant evidence of quantality by themselves. In other words, if what we call weak quantality over the treatments (or ranks series) could be combined, evidence of some quantal effect on the whole could yet be obtained. We therefore propose a single test of an overall effect as a combination of the individual effects. Suppose we want to combine information over k groups, then the new statistic is proposed to be

$$T^* = \sum_{j=1}^{k} \phi\left(\hat{\tau}_j\right) \tag{6.1}$$

where

$$\hat{\tau}_j = arg \max_{\tau_{min\,j}}^{\tau_{max\,j}} \left\{\phi\left(\tau, \underline{x}_j\right)\right\}$$

which define the best estimates of quantum $\hat{q}_j = 1/\hat{\tau}_j$ for the k groups.

The essence of this test statistic is the advantage of being able to restrict the range of gridsearch for individual groups of roots. This would enable us to start searching for a quantum for one group over a very large range and subsequently search for the others in a much narrower range around the estimated quantum value of the first group. With the aid of this approach, only quantum values close to each other would be selected and the support coming from the data for those could be combined by the new test T^*. The question of whether or not the overall evidence obtained is significant or not could be assessed by Bootstrapping T^*. As a result, we claim that any hierarchical quantality with quantum values close to each other (if exists) could be extracted quite easily using the test statistic above.

Before implementing the new combined test, it must however be tested in order to validate its use for testing hierarchical quantality. As far as the validity of a test is concerned, how powerful it is in rejecting the wrong model should be examined. It is therefore necessary to study the power of the new test and also compare its power with one of the other procedures that are available in the literature for combining independent tests.

6.2.2. Fisher's Combined Test

Statistical procedures for combining independent evidence from several sources has long been an important topic and widely studied in the literature. For a review of these procedures, refer to Hedges and Olkin (1985), and Rosenthal (1978). Although, there is no single method of combining tests which is uniformly best for all problems, at least from the point of view of maximising power, it appears that Fisher's method of combining independent tests is considered to be the optimal one among all other "reasonable" combining procedures (Littell et al, 1971; Marden, 1991). Therefore, we have decided to use it as a criterion by which the new test statistic can be compared. Our reasons for considering this method as a standard are merely its simplicity and its wide acceptance in the literature. The method can be described as follows:

Suppose, we have k independent hypothesis testing problems based on the independent statistics $T^{(1)}, T^{(2)},...,T^{(k)}$ respectively, and wish to combine the statistics into one overall statistic to test the null hypothesis H_0 that all n individual null hypotheses hold. Assuming that each $T^{(i)}$ has a continuous distribution function F_i under its null hypothesis, and that it is appropriate to reject the i^{th} null hypothesis for large values of $T^{(i)}$. Then the p–value for $T^{(i)}$ is simply $P_i = 1 - F_i(T^{(i)})$ and has a Uniform (0,1) distribution under the null. Therefore, the method for combining such probabilities from independent tests is given by Fisher (1950) as

$$T^F = -2\sum_{i=1}^{k}\log_e\left(P_i\right) \sim \chi^2_{2k,\alpha} \tag{6.2}$$

where $\chi^2_{2k,\alpha}$ is the upper α point of the chi–squared distribution on 2k degrees of freedom. Hence, Fisher's test rejects H_0 for large values of T^F.

In order to assess numerically the performance of the new combined test we proposed, whether or not its power is as good as Fisher's combined test is to be investigated. In the ensuing sections, we will therefore carry out a simulation study to compute the power of both tests at variety of degrees of quantality so as to discover if they differ in any direction.

6.2.3. The Power of the Two Combination Procedures

In the formulation of this comparative power study, the artificial data sets were simulated in the form of the hierarchical model 5.1, having assumed that there is not any β effect. For the sake of simplicity, only three sets of data with the size of each 50 were considered. Allowing some, but small, variation among those, the quantum values were arbitrarily chosen to be 0.95, 1.00, 1.05 for the 3 groups respectively. The integers were generated from Bi(30,0.333). The errors in 5.1 were generated from VM(0, κ) with various values of κ in order to vary the degree of quantality. We here consider the values of κ varying from 0.1 to 1.5 with an increment of 0.1 and κ_1=0.00001 (i.e. κ_ℓ; ℓ=1,...,16). In addition, the range of gridsearch is fixed the same for three groups as τ_{min}= 0.75 and τ_{max}= 1.45. The quantogram analyses are performed with an increment of 0.001.

As the evaluation of the Fisher's combined test requires us to know the observed significance levels of individual tests (i.e. $\phi(\tau)$), Monte–Carlo simulations need to be performed to generate these P–values at each degree of quantality. For the same purpose, however, one could also make use of an extreme value distribution. In fact, section 2.8.2.1 concluded that the null distribution of the test statistic $\phi(\hat{\tau})$ can be represented by a three parameter Generalized Extreme Value distribution. As far as time limitations are concerned, it is therefore more advantageous to employ this asymptotic result to calculate the significance probabilities in this comparative study.

To begin with, it is necessary to estimate the parameters of the G.E.V. distribution. The procedure is as follows:

Generate a quantal data set, first with $q_1 = 0.95$ when $\kappa = \kappa_1$.

i.e. $$X_{i1} = m_i q_1 + VM(0, \kappa_1)$$

and calculate its mean and variance. Then generate 2000 non–quantal random data sets from half–Normal distribution matched to X_1 with respect to its mean and variance. Performing quantogram analyses on each, 2000 maximum peaks are obtained and a G.E.V. distribution is fitted to those using maximum likelihood method giving the estimates of three parameters, i.e. u, α, k. Furthermore, we repeated the whole process for other values of κ in order to take into account its contribution to the mean and variance of the original sample. Then, the same analyses are performed for X_2 with $q_2 = 1.00$ and also X_3 with $q_3 = 1.05$. Estimated values of G.E.V. parameters with respect to 3 groups and 16 kappa values are presented in Table 6.2.

The power of Fisher's test, i.e. prob$\{T^F \in w \mid H_0 \text{ is false}\}$ where w is the critical region of size 0.05, is therefore evaluated following the steps below:

STEP 1. Generate quantal data sets of size 50; $X_{j\ell}$, $j = 1, 2, 3$ with $q_1 = 0.95$, $q_2 = 1.00$, $q_3 = 1.05$ and errors from VM$(0, \kappa_\ell)$, $\ell = 1,...,16$.

STEP 2. Perform quantogram analyses on each to estimate their maximum peaks,

i.e. $$T_{j\ell} = \phi_\ell\left(\hat{\tau}_j\right) \text{ where } \hat{\tau}_j = arg \max_{\tau_{min}}^{\tau_{max}}\left\{\phi\left(\tau, \underline{x}_{j\ell}\right)\right\}$$

STEP 3. Calculate significance levels of individual tests as

$$P_{j\ell} = 1 - F\left(T_{j\ell}\right), \qquad j = 1, 2, 3;\ \ell = 1,...,16$$

where F is the distribution function of G.E.V. distribution given as in 2.11. Note that estimated values of three parameters u, α and k for the j^{th} data set and at the ℓ^{th} kappa value are taken from the Table 6.2.

STEP 4. Calculate the Fisher's test as

$$T_\ell^F = -2\sum_{j=1}^{3} log_e\left(P_{j\ell}\right), \quad \ell = 1,\ldots,16$$

STEP5. Power is obtained as

$$\text{Power}_\ell\,(\text{T}^\text{F}) = \frac{\#\left\{\text{T}_\ell^\text{F} \geq \chi^2_{6,0.95}\right\}+1}{1000}, \qquad \ell = 1, ...,16$$

where $\chi^2_{6,0.95} = 12.59$.

For the new test statistic, first 5% critical values need to be simulated. Taking into the account the possibility of any variation between critical values at different degrees of quantality for the new test, even if generated with identical values of m_i, separate critical values for each value of κ are computed. The algorithm for obtaining the critical values is as follows:

STEP 1: Generate 3 samples in the form of the hierarchical quantum model with quantum values $q_1 = 0.95$, $q_2 = 1.00$, $q_3 = 1.05$ as

$$x_{ij} = m_{ij}\, q_j + \varepsilon_{ij},\ i = 1,\ldots,50;\ j = 1, 2, 3$$

with errors $\varepsilon_{ij} \sim \text{VM}(0, \kappa_\ell)$, ℓ=1,...,16. Note that $-\text{q}_\text{j}/2 \leq \varepsilon_\text{ij} < \text{q}_\text{j}/2$ for j =1, 2, 3.

STEP 2: Calculate the mean $\left(\overline{m}_j\right)$ and the variance $\left(s_j^2\right)$ of each sample. Then, generate non–quantal random samples (y_{ij}) of the same size from half–Normal distributions matched to x_{ij} as follows:

$$y_{ij} = \mu_j + \sigma_j \left|Z_j\right|, \quad i = 1,\ldots,50;\ j = 1, 2, 3$$

where Z_j are standard normal variates, $\sigma_j = s_j \Big/ \sqrt{1-2/\pi}$ and $\mu_j = \overline{m}_j - 2\sigma_j \big/ \sqrt{2\pi}$

***STEP 3*:** Perform quantogram analyses for each sample to calculate the new statistics

$$T_{\ell}^{*} = \sum_{j=1}^{3} \phi_{\ell}\left(\hat{\tau}_j\right) \quad \text{where} \quad \hat{\tau}_j = arg \max_{\tau_{min\,j}}^{\tau_{max\,j}} \left\{\phi\left(\tau, \underline{x}_j\right)\right\}$$

***STEP 4*:** Repeat Step2–3 1000 times and order 1000 values of T_{ℓ}^{*} in an increasing magnitude. Then find 5% critical values for the new test statistic i.e. $T_{950,\ell}^{*}$ for the ℓ^{th} value of κ.

In the algorithm above, note that each null distribution was based on half Normal simulations that matched the mean and variance of one particular quantal sample. We did not produce a null distribution for every sample since means and variances of quantal samples generated with the same κ have been found not to vary much. We further investigated the effect of such variation on the critical values by generating a sample of size 100 critical values which had null distributions matched to such slightly varying means and variances, and also by generating another set of 100 critical values which had null distributions matched to a particular mean and variance. As a result, variations among both sets of critical values have been found to be similar.

In order to evaluate the power function of the new test, 3 data sets of size 50 are first generated in the form of the hierarchical model 5.1 as before. Secondly the quantogram analyses have been performed to calculate

$$\phi_{\ell}\left(\hat{\tau}_j\right) \quad \text{and also} \quad T_{\ell}^{*} = \sum_{j=1}^{3} \phi_{\ell}\left(\hat{\tau}_j\right) \quad \text{for j = 1, 2, 3}$$

Having repeated this process 999 times for ℓ^{th} value of κ and the power of T* is evaluated as

$$\text{Power}_{\ell}\,(\text{T*}) = \frac{\#\left\{T^{*} \geq T_{950,\ell}^{*}\right\} + 1}{1000}, \qquad \ell = 1, ..., 16$$

When assessing the optimality of tests, usually the rates at which p–values or the observed significance levels converge to zero when the null hypothesis is false are compared and the procedure that yields the most rapid rate of convergence is judged optimal (Littell et al., 1971). In testing for hierarchical quantality, the simulated powers of the Fisher's test T^F and the proposed competing test T* are summarised visually in Fig 6.1 and also presented in Table 6.1.

Our simulations indicate that the test based on the sum of suprema has some advantage over the Fisher's method based on individual significance of independent tests. On the basis that small significance levels lead to the rejection of the null hypothesis that data are not quantal, the test statistic T* which shows more rapidly increasing power as the degree of quantality gets bigger is here considered superior. Hence it seems reasonable to choose T* for a hierarchical problem such as the present one. The following section will demonstrate how to apply T* to test whether or not the spacings available from plants exhibit any hierarchical quantality.

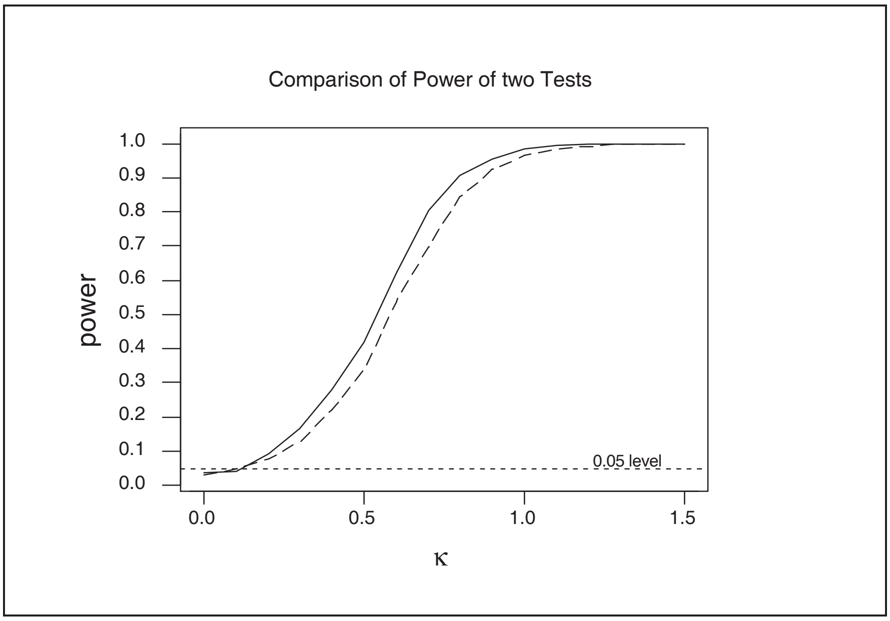

Fig 6.1. Powers of T^* and T^F for hierarchical quantality, k=3 and n=50

Table 6.1. The simulated powers of T* and T^F when $n_1=n_2=n_3=n$; n=50,100

			n	
κ	**Test**	crit.values	50	100
0.00001	T*	8.269	0.039	0.042
	T^F	12.59	0.029	0.037
0.1	T*	8.279	0.041	0.053
	T^F	12.59	0.046	0.053
0.2	T*	8.304	0.093	0.173
	T^F	12.59	0.076	0.126
0.3	T*	8.194	0.165	0.395
	T^F	12.59	0.129	0.306
0.4	T*	8.338	0.267	0.589
	T^F	12.59	0.217	0.532
0.5	T*	8.334	0.418	0.807
	T^F	12.59	0.336	0.720
0.6	T*	8.311	0.621	0.926
	T^F	12.59	0.538	0.905
0.7	T*	8.280	0.804	0.979
	T^F	12.59	0.698	0.966
0.8	T*	8.234	0.908	0.998
	T^F	12.59	0.845	0.996
0.9	T*	8.256	0.956	1.000
	T^F	12.59	0.925	1.000
1.0	T*	8.282	0.985	↓
	T^F	12.59	0.965	
1.1	T*	8.317	0.997	
	T^F	12.59	0.986	
1.2	T*	8.250	0.999	
	T^F	12.59	0.993	
1.3	T*	8.224	1.000	
	T^F	12.59	1.000	
1.4	T*	8.229	↓	
	T^F	12.59		
1.5	T*	8.324		
	T^F	12.59		

Table 6.2. Maximum likelihood estimates (s.e.) for parameters of G.E.V.

	q_1			q_2			q_3		
κ	$\hat{u}$	$\hat{\alpha}$	$\hat{k}$	$\hat{u}$	$\hat{\alpha}$	$\hat{k}$	$\hat{u}$	$\hat{\alpha}$	$\hat{k}$
0.00001	2.048	0.423	–0.110	2.089	0.433	–0.097	2.107	0.435	–0.112
	(0.010)	(0.007)	(0.014)	(0.011)	(0.007)	(0.013)	(0.011)	(0.007)	(0.013)
0.1	2.050	0.424	–0.098	2.087	0.432	–0.105	2.102	0.422	–0.102
	(0.010)	(0.007)	(0.013)	(0.011)	(0.007)	(0.013)	(0.010)	(0.007)	(0.014)
0.2	2.058	0.430	–0.109	2.079	0.430	–0.117	2.092	0.427	–0.093
	(0.011)	(0.007)	(0.013)	(0.011)	(0.007)	(0.013)	(0.011)	(0.007)	(0.014)
0.3	2.070	0.444	–0.113	2.069	0.429	–0.098	2.103	0.415	–0.112
	(0.011)	(0.008)	(0.013)	(0.011)	(0.007)	(0.013)	(0.010)	(0.007)	(0.015)
0.4	2.057	0.438	–0.114	2.075	0.431	–0.094	2.098	0.428	–0.113
	(0.011)	(0.008)	(0.013)	(0.011)	(0.008)	(0.014)	(0.011)	(0.007)	(0.014)
0.5	2.060	0.432	–0.130	2.055	0.433	–0.111	2.103	0.417	–0.121
	(0.011)	(0.007)	(0.012)	(0.011)	(0.007)	(0.012)	(0.010)	(0.007)	(0.013)
0.6	2.052	0.438	–0.122	2.081	0.421	–0.092	2.096	0.414	–0.088
	(0.011)	(0.008)	(0.013)	(0.010)	(0.007)	(0.014)	(0.010)	(0.007)	(0.014)
0.7	2.060	0.432	–0.130	2.066	0.435	–0.107	2.097	0.419	–0.096
	(0.011)	(0.007)	(0.012)	(0.011)	(0.007)	(0.012)	(0.010)	(0.007)	(0.013)
0.8	2.043	0.430	–0.095	2.093	0.421	–0.121	2.095	0.415	–0.077
	(0.011)	(0.007)	(0.014)	(0.010)	(0.007)	(0.014)	(0.010)	(0.007)	(0.014)
0.9	2.035	0.427	–0.097	2.078	0.420	–0.102	2.094	0.427	–0.080
	(0.011)	(0.007)	(0.014)	(0.010)	(0.007)	(0.014)	(0.011)	(0.007)	(0.014)
1.0	2.039	0.435	–0.099	2.077	0.424	–0.105	2.102	0.419	–0.101
	(0.011)	(0.008)	(0.014)	(0.011)	(0.007)	(0.014)	(0.010)	(0.007)	(0.013)
1.1	2.029	0.438	–0.102	2.079	0.426	–0.120	2.105	0.435	–0.094
	(0.011)	(0.008)	(0.012)	(0.010)	(0.007)	(0.012)	(0.011)	(0.008)	(0.013)
1.2	2.049	0.431	–0.096	2.071	0.425	–0.100	2.084	0.424	–0.091
	(0.011)	(0.008)	(0.014)	(0.010)	(0.007)	(0.014)	(0.011)	(0.007)	(0.014)
1.3	2.032	0.435	–0.099	2.067	0.431	–0.100	2.100	0.428	–0.099
	(0.011)	(0.008)	(0.013)	(0.011)	(0.007)	(0.013)	(0.011)	(0.007)	(0.014)
1.4	2.075	0.436	–0.117	2.063	0.419	–0.122	2.101	0.420	–0.129
	(0.011)	(0.008)	(0.014)	(0.010)	(0.007)	(0.013)	(0.010)	(0.007)	(0.014)
1.5	2.074	0.434	–0.117	2.075	0.426	–0.128	2.099	0.414	–0.100
	(0.011)	(0.007)	(0.013)	(0.011)	(0.007)	(0.015)	(0.010)	(0.007)	(0.015)

6.2.4. An Algorithmic Approach for Implementing the New Test Statistic

Having achieved the goal of devising an overall test procedure with good power properties, we can now proceed with the numerical evaluation of overall evidence in favour of hierarchical quantality from the data available.

The nature of the current problem has a 3–level hierarchy. The first is concerned with quantality of treatment groups when all the spacings within the group have been pooled. Having combined all the spacings from the ranks on the same root, the second considers quantality of roots under the same treatment group. Finally, the third level focuses on the quantality of the ranks under the same root. This hierarchy is schematically shown, for example on the Onion data set below:

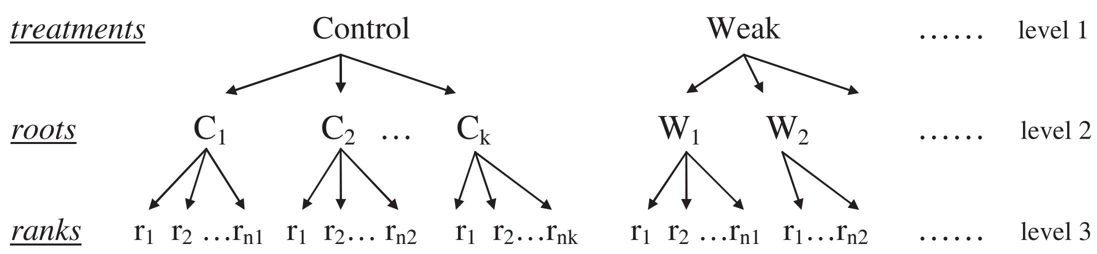

This hierarchy can also be constructed for the tomato data set by replacing treatments with tomato types and their Naa treatment groups (i.e. Wild, Naa treated Wild, Gib–1, Naa treated Gib-1), and also by changing rank series with each roots' left and right series. Note that when the total series are being analysed, this hierarchy is reduced to two levels as each root, onion or tomato, has only one total series.

The motivation for the development of the new test has been to be able to combine weak quantality from different roots with quantum values close to each other. Therefore the prime question of how to obtain quantum values close to each other needs to be answered next. Our solution is to employ an algorithmic approach to analyse the levels that compose the quantal hierarchy. The approach is better described by addressing the current problem in the following setup:

Hierarchy Level 1:

As each treatment group (or tomato type) has different characteristics, we begin the analysis by performing quantogram analyses on each separately over a considerably large range on all the data available from the separate ranks of all roots in that treatment group pooled together. The choice of the large ranges will be discussed and given for each type of plant in their own coming sections. Then, we combine the evidence from different groups by the composite test, T* and assess its significance by means of Monte Carlo simulations.

Hierarchy Level 2:

At this level, the range of gridsearch is narrowed half around the estimated quantum value of, say, the first treatment group obtained at level 1. For each of the roots of the first treatment group, we perform quantogram analyses over this restricted range on the data pooled this time from the separate ranks constituting the root. Then the evidence obtained from independent roots for the resulting set of quantum values is combined by the new test statistic, T*, and significance is assessed by simulations producing a significance probability, P*. Next, the roots of other treatment groups are to be investigated in the same way as described for the first treatment.

Hierarchy Level 3:

Since quantum values of rank series are expected to be much closer to each other, the range is further reduced to half around the estimated quantum values of roots obtained at level 2 within the same treatment group. Quantogram analyses are performed for each individual rank series on the same root over this restricted range and again evidence is combined for each root and tested as before.

The essence of this algorithmic approach is that quantum values of a given hierarchy level bond in a particular way and thereby form an entity at the next higher level. As a result of that, we form a sensible hierarchy that relates one level to another. With the ranges narrowed at each level, we moreover obtain a hierarchy in which quantum values close to each other with a degree of closeness which is low at the beginning of hierarchy but gets higher at a more complex level.

An appealing feature of the proposed testing procedure is that the power increases by pooling data and also by restricting the ranges of gridsearch. However, there is no definite rule for determining by how much to narrow the range. The choice of a range is already a very crucial issue in the quantogram analysis. How much a range could be reduced in the setup above is an open question. Obviously, one must avoid ending up with a very small range as the significance level in such cases would be overestimated. Therefore one must be aware of the risk and should select a judicious choice of the ranges.

In our analyses, the smallest range to be considered will be only one quarter of the original large range chosen at level 1. Notice that the narrowing process is performed in terms of τ–range and the lower, τ_{min}, and upper, τ_{max}, values of the original range are set strict bounds for any outcoming range after the reduction. For example, if the new upper bound exceeds τ_{max}, then the range is moved down in order to make sure the upper bound is equal to τ_{max} again. The same adjustment is considered for the new lower bound as well.

So as not to limit ourselves with the specific choice of the ranges that the strategy above defines, we also approached the problem in a way such that many quantogram analyses over many different ranges for each data set could be carried out and other possible combinations of quantum values could be well investigated. This is achieved not only by trying to reduce the ranges with different proportions but also by guiding higher levels of hierarchy with the second and third indicative quantum values of each group at the level 1. Full details of the significant and marginally significant (i.e. with $P^* <0.05$ and $P^* <0.1$) results from such analyses will be given in Appendix E and also mentioned here briefly whenever necessary.

The following sections will summarise the outcome of these algorithmic procedures when applied to the current data sets.

6.3. Hierarchical Quantal Models for Onion Roots

6.3.1. Analyses of Raw Spacings on the Rank and Total Series

The algorithmic approach with the setup as described before has been applied to first the rank series of onion data set. At the first level, all spacings within the same treatment group are combined and the quantogram analyses over the separate ranges as given in Table 6.3 have been performed for each treatment group. The choice of the ranges here is affected essentially by the inadequate accuracies of the measurements whose strong artificial effects on the quantogram analyses of this particular data set have been explored in Chapter 5. For example, the upper bound τ_{max}=1.92 (i.e. $q_{min}\approx$0.52) for Control and τ_{max}=4.762 (i.e. $q_{min}\approx$0.21) for treated groups were chosen to avoid the influence of the accuracies 0.5 and 0.1 respectively. Any ranges below those values suggested the artefacts of the accuracies as possible quantum values. Moreover, a common lower bound was used on the basis of the fact that it is very unlikely to observe any quantal effect above the value of 2. As a result, an overall quantality with the quantum values given in Table 6.3 is suggested by a P* value significant at 10% level.

Table 6.3. Results of hierarchy *level 1* analyses for rank series of Control, Weak and Strong–treated roots

Group	τ–range	$\hat{\tau}$	$\hat{q}$	$\phi(\hat{q})$	P	P*
C	[0.5, 1.920]	1.349	0.7412	2.3574	0.862	
W	[0.5, 4.762]	4.029	0.2482	2.7390	0.606	0.087
S	[0.5, 4.762]	2.162	0.4625	4.4001	0.002	

Moving onto the analyses of the roots of each treatment group, first the original ranges are narrowed half around their corresponding $\hat{\tau}$ values seen in Table 6.3. For example, the roots of Control group have been analysed using a range calculated as 1.349 ± (1.92 – 0.5)/4 and similarly for the Weak and Strong treated roots. As a result of these level 2 analyses of the hierarchy, the combined evidence for a set of quantum values is found significant only for the S roots as listed in Table 6.4.

Table 6.4. Results of hierarchy *level 2* analyses for rank series of Strong–treated roots

S Roots	$\hat{\tau}$	$\hat{q}$	$\phi(\hat{q})$	P	P*
S1	2.941	0.3400	2.0969	0.596	0.001
S2	1.830	0.5464	1.6372	0.956	
S3	2.181	0.4585	3.4715	0.007	
S4	2.820	0.3546	3.4715	0.011	
S5	3.027	0.3303	2.5481	0.313	
S6	2.224	0.4496	5.3198	0.001	

Table 6.5. Results of hierarchy *level 3* analyses for rank series of Strong–treated roots.

Root	$\hat{q}_1$	$\hat{q}_2$	$\hat{q}_3$	$\hat{q}_4$	$\hat{q}_5$	P*
S3	0.4642 (0.437)	0.4170 (0.307)	0.4555 (0.162)	0.4524 (0.910)	0.4636 (0.015)	0.091
S4	0.2936 (0.325)	0.3527 (0.036)	0.3566 (0.460)	0.3049 (0.496)	–	0.126
S6	0.3879 (0.265)	0.5032 (0.002)	0.4502 (0.004)	0.4921 (0.003)	–	0.001

As described in the third level of hierarchy, the quantality of rank series of S roots is next examined over the ranges reduced again to the half around the estimated quantum values of S1–S6 roots (see Table 6.4). Among all, ranks of only S3 and S6 roots produced significant sets of quantum values as presented in Table 6.5, which suggests quantality at around 0.45. Another suggestive but inconclusive evidence is obtained from the rank series of the S4 root for quantum values varying at around 0.35.

In addition to the analyses of raw spacings on the ranks, the total series of onion roots have also been examined. We have not yet obtained either significant nor suggestive results from any treatment group. Any combination of quantum values obtained has been rejected with high probabilities.

6.3.2. Analyses of Positions on the Rank and Total Series

The positions of the onion root series are now subjected to the investigation of hierarchical quantality. It must be noted that, as far as Control group roots are concerned, analyses have been performed on only positions of their total series.

Table 6.6 gives the results of level 1 analyses with the original range of gridsearch, estimated quantum values and their individual significance probabilities for all combined treated spacings within each treatment. At this stage, it is clear that observed quantality does not provide enough significance. Despite this result, we furthermore conducted level 2 and level 3 analyses on the treated roots and their rank series respectively.

Table 6.6. Results of hierarchy *level 1* analyses for positions of rank series on the Weak and Strong–treated roots.

Type	τ –range	$\hat{\tau}$	$\hat{q}$	$\phi(\hat{q})$	P	P*
W	[0.4, 4.762]	3.234	0.3092	3.14020	0.641	0.617
S	[0.4, 4.762]	3.102	0.3224	3.13935	0.653	

As a result, we obtained some significant hierarchical quantality for the rank series of only the Strong–treated roots as given in Table 6.8. Note that their quantum values are variable around the ones initially estimated from their corresponding roots (see Table 6.7).

Table 6.7. Results of hierarchy *level 2* analyses for positions of rank series on the Strong–treated roots

S Roots	$\hat{\tau}$	$\hat{q}$	$\phi(\hat{q})$	P	P*
S1	2.874	0.3479	2.6123	0.618	0.198
S2	3.117	0.3208	3.0301	0.546	
S3	3.380	0.2958	3.0969	0.439	
S4	2.808	0.3561	3.8280	0.033	
S5	3.105	0.3220	3.1333	0.302	
S6	2.370	0.4219	3.1042	0.461	

Table 6.8. Results of hierarchy *level 3* analyses for positions of rank series on the Strong–treated roots.

Root	$\hat{q}_1$	$\hat{q}_2$	$\hat{q}_3$	$\hat{q}_4$	$\hat{q}_5$	P*
S1	0.3269 (0.139)	0.3907 (0.008)	0.3477 (0.390)	0.3365 (0.238)	0.2927 (0.694)	0.032
S3	0.3043 (0.711)	0.2754 (0.028)	0.3420 (0.749)	0.3005 (0.006)	0.2802 (0.119)	0.015
S4	0.4130 (0.081)	0.3561 (0.143)	0.3436 (0.202)	0.4417 (0.610)	–	0.063
S5	0.3655 (0.324)	0.3247 (0.256)	0.3222 (0.420)	0.2999 (0.087)	–	0.111
S6	0.4219 (0.007)	0.4728 (0.128)	0.3940 (0.061)	0.4803 (0.521)	–	0.004

In addition to the positions on the rank series, we performed the same analyses for the positions on the total series. Results of level 1 analyses can be found in Table 6.9. It can be observed that no significant quantality appears at this stage for the treatment groups. Moreover, the analyses at the level 2 and 3 on their roots did not reveal any evidence in favour of hierarchical quantality either.

Table 6.9. Results of hierarchy *level 1* analyses for positions of total series on the Control, Weak–treated and Strong–treated roots

Type	τ –range	$\hat{\tau}$	$\hat{q}$	$\phi(\hat{q})$	P	P*
C	[0.2, 1.812]	1.771	0.5647	2.63543	0.911	
W	[0.4, 4.762]	2.893	0.3457	3.13003	0.681	0.885
S	[0.4, 4.762]	1.312	0.7622	2.99259	0.794	

6.4. Hierarchical Quantal Models for Tomato Roots

Similarly, hierarchical quanta hunting with the algorithm given before has been considered for the Tomato data set which includes four groups of tomatoes; Wild type (WR), Gib–1 Mutant type (GR), Naa treated Wild (NWR) and Naa treated Gib–1 (NGR) groups. For this set, we are here interested in the construction of two hierarchical models, one for raw spacings of left and right series and the other for total series. If two independent investigations indicate similar quantality, this would reinforce the overall conclusion in the end. Therefore, we will present the results from those two independent analyses in the same table so as to make comparisons between them viable. Note that the same idea applies when positions of left, right and total series are to be analysed. Furthermore, it is necessary to point out that the original τ–ranges of gridsearch to begin level 1 analyses of the algorithm are chosen as [0.4, 5] for both raw spacings and positions of the left and right series. It is however fixed to be [0.8, 5] for the total series of again for both type of measurements. These are considered to be the largest common ranges that could be used for the type of analysis we are confronted with. Throughout the coming sections, note that all the quantogram analyses are being performed with an increment of 0.001.

6.4.1. Analyses of Raw Spacings on the Left, Right and Total Series

Beginning with the analysis of left and right series, each group of tomatoes are individually analysed to start the search for hierarchical quantality. Table 6.10 summarises the results including the original range of gridsearch, estimated quantum values and their individual significance probabilities. The individual tests of significance seem to show some, but weak, tendency to be quantal in WR and GR groups, however Naa treated groups do not suggest any evidence at all. When the evidence from individual tests are next combined, the overall result is still not supported by the combination procedure (i.e. P* > 0.10). Above all, it is noteworthy to assert that estimated quantum values of WR and NWR groups suggest a relationship such that $5\frac{1}{3} \times 0.3605 = 1.92$. Similarly a correspondence between quantum values of GR and NGR groups is also observed such that 7*0.2292=1.61.

Table 6.10. Results of hierarchy *level 1* analyses for Wild, Naa treated Wild, Gib–1 and Naa treated Gib–1 type roots (left and right series used)

Type	τ –range	$\hat{\tau}$	$\hat{q}$	$\phi(\hat{q})$	P	P*
WR	[0.4, 5]	2.774	0.3605	2.67671	0.163	0.227
NWR	[0.4, 5]	0.520	1.9198	2.64451	0.398	
GR	[0.4, 5]	4.368	0.2292	2.79326	0.147	
NGR	[0.4, 5]	0.612	1.6260	2.37102	0.718	

In addition to the analysis of left and right series at level 1, the total series have also been examined and results are demonstrated in Table 6.11. Although each group is analysed independently in the same full range, surprisingly they suggest quantum values close to each other all at around 0.24. Neither separate tests nor the combined evidence from independent tests for those quantum values is however found to be significant.

Table 6.11. Results of hierarchy *level 1* analyses Wild, Naa treated Wild, Gib–1 and Naa treated Gib–1 type roots (total series used)

Type	τ **–range**	$\hat{\tau}$	$\hat{q}$	$\phi(\hat{q})$	**P**	**P***
WR	[0.8, 5]	4.151	0.2409	1.17378	0.869	0.619
NWR	[0.8, 5]	4.245	0.2356	1.04509	0.994	
GR	[0.8, 5]	4.439	0.2252	2.13109	0.331	
NGR	[0.8, 5]	3.851	0.2596	2.76497	0.041	

In comparison with the quantum values given in Table 6.10, one should notice Wild type roots favour the following two values; 0.36 and 0.24. Although this effect does not appear to be significant at this stage, it is intriguing that those two values were also the ones supported most by the initial analyses of the individual root series in Chapter 5. Furthermore, it is notable that not only left and right series but also the total series of Gib–1 type tomatoes suggested almost the same value, ≈0.23.

Despite that the overall results have not been found significant, we take into the account that such findings may nevertheless indicate some quantality. Therefore we continued with analyses of the second and third level hierarchy for each group and a set of quantum values at each level which shows the strongest evidence are listed in tables. For the purposes of simplified comparisons, the table is organised as follows:

The first highlighted column demonstrates the quantum values suggested by the second level analyses for the roots of a particular group, say Wild, from a range narrowed around its initial value from level 1, 0.3605 as given in Table 6.10. It also includes the significance probability (i.e. P^*) of whether or not to accept the combined evidence of those suggested values. Similarly, the second highlighted column summarises the results of second level analyses again but obtained from total series independently.

In addition, the remaining part of the table is devoted to the results of third level analyses which presents the quantum values of the left and right series that are estimated closely at around the quantum values of their corresponding roots in each row. In the same line, a significance probability, P^* is also presented in order to assess the significance of the combined evidence from left and right series of the each root. Note that a significance probability for every quantum value in the table is also produced and presented in brackets.

As far as wild type tomatoes are concerned, the aggregated measure of quantality from 10 Wild roots, even though only a few roots can be claimed individually significant, suggests quantum values as given in Table 6.12 varying around q=0.3605 with an overall P^* of 0.096. Moving onto the level of left and right series, nominally significant combinations of quantum values are obtained for those belonging to the roots WR1 and WR9 with quantum values varying around q=0.3626 and 0.3663 respectively. Although they are inconclusive, there appears to be some evidence from also roots WR3, WR6. An inspection of quantum values obtained for the total initiating the analyses at around 0.2409 (see Table 6.11) however showed no significant evidence.

It must be noted here that Wild type roots distinctively offer another significant result obtained by initiating the second level analyses around 0.2650 which is suggested by the second highest peak of Wild type at level 1. This solution is presented in Appendix E.

Table 6.12. Results of hierarchy *level 2* analyses for Wild type roots and also results of *level 3* analyses for their corresponding L, R & T series

root	$\hat{q}$	$\hat{q}_L$	$\hat{q}_R$	P*	$\hat{q}_T$
WR1	0.3626 (0.345)	0.3625 (0.015)	0.3003 (0.516)	**0.051**	0.2419 (0.310)
WR2	0.3005 (0.656)	0.3004 (0.129)	0.3061 (0.811)	0.268	0.2471 (0.917)
WR3	0.2640 (0.019)	0.2636 (0.036)	0.3032 (0.754)	**0.159**	0.3360 (0.026)
WR4	0.2944 (0.233)	0.2982 (0.917)	0.2637 (0.376)	0.744	0.2159 (0.977)
WR5	0.3087 (0.723)	0.3084 (0.770)	0.3586 (0.763)	0.735	0.2435 (0.704)
WR6	0.2947 (0.024)	0.2952 (0.032)	0.3433 (0.585)	**0.133**	0.2951 (0.186)
WR7	0.3545 (0.783)	0.3750 (0.255)	0.3561 (0.456)	0.311	0.2327 (0.401)
WR8	0.3591 (0.320)	0.3589 (0.883)	0.2960 (0.692)	0.892	0.2142 (0.491)
WR9	0.3663 (0.292)	0.3672 (0.026)	0.4625 (0.548)	**0.089**	0.3311 (0.309)
WR10	0.3124 (0.279)	0.3115 (0.730)	0.3135 (0.416)	0.623	0.2083 (0.778)
P*	**0.096**				0.572

Table 6.13. Results of hierarchy *level 2* analyses for Naa treated Wild type roots and also results of *level 3* analyses for their corresponding L, R & T series

root	$\hat{q}$	$\hat{q}_L$	$\hat{q}_R$	P*	$\hat{q}_T$
NWR1	0.7689 (0.412)	0.7687 (0.440)	0.8095 (0.689)	0.636	0.2420 (0.134)
NWR2	0.5228 (0.061)	0.5292 (0.008)	0.5084 (0.193)	**0.009**	0.2637 (0.661)
NWR3	2.3186 (0.436)	2.1110 (0.518)	2.3776 (0.519)	0.565	0.2958 (0.770)
NWR4	1.9440 (0.230)	1.9581 (0.171)	1.8420 (0.320)	**0.112**	0.3375 (0.446)
P*	**0.093**				0.523

In addition, the evidence in favour of hierarchical quantality obtained from Naa treated WR roots is demonstrated in Table 6.13. The available four roots presented significant overall evidence for q values varying around 1.9298 (see Table 6.10) and also left and right series of two roots, NWR2 and NWR4 were found nominally significant at 5% and 10% respectively. However, the total series provided no evidence to signify their quantum values.

Having pointed out that it may be likely to observe some quantality at around 0.2292 that may be confirmed by all series of Gib–1 Mutant type roots, hierarchical quantal model is constructed around this value as presented in Table 6.14. As a result, we have not found any evidence to suggest such a model from Gib–1 roots, nor from their left and right series, except for GR6 which presents quantum values markedly significant and varying around 0.2777. Moreover, the overall picture remained the same as far as total series of Gib–1 roots are concerned.

A further investigation on Gib–1 roots revealed a significant set of quantum values varying around an initial value of 0.4994 which is the second suggestive quanta obtained at level 1. Full results are listed in Appendix E.

Table 6.14. Results of hierarchy *level 2* analyses for Gib–1 Mutant roots and also results of *level 3* analyses for their corresponding L, R & T series

root	$\hat{q}$	$\hat{q}_L$	$\hat{q}_R$	P*	$\hat{q}_T$
GR1	0.2297 (0.577)	0.2307 (0.681)	0.2136 (0.833)	0.860	0.2641 (0.620)
GR2	0.2466 (0.291)	0.2476 (0.381)	0.2260 (0.340)	0.314	0.2470 (0.054)
GR3	0.2766 (0.742)	0.2774 (0.056)	0.2727 (0.707)	0.293	0.2262 (0.232)
GR4	0.3283 (0.151)	0.3282 (0.152)	0.3239 (0.914)	0.454	0.2205 (0.245)
GR5	0.2716 (0.912)	0.3098 (0.802)	0.2705 (0.520)	0.727	0.2291 (0.422)
GR6	0.2777 (0.603)	0.2801 (0.008)	0.2631 (0.030)	**0.006**	0.2948 (0.554)
P*	0.698				0.245

Moreover, Table 6.15 summarises the results for the roots of NGR group. When the tendency for them to be quantal around the originally indicated value of 1.6260 has been integrated, the evidence on the whole is not found significant. It can however be observed that there is some evidence of hierarchical quantality for the total series around 0.2596 (see Table 6.11).

Table 6.15. Results of hierarchy *level 2* analyses for Naa treated Gib–1 roots and also results of *level 3* analyses for their corresponding L, R & T series

root	$\hat{q}$	$\hat{q}_L$	$\hat{q}_R$	P*	$\hat{q}_T$
NGR1	0.6243 (0.384)	0.7410 (0.961)	0.6258 (0.486)	0.868	0.3118 (0.128)
NGR2	2.2366 (0.532)	0.8693 (0.067)	0.7930 (0.558)	**0.115**	0.3126 (0.236)
NGR3	1.1138 (0.984)	2.1825 (0.889)	1.1190 (0.236)	0.789	0.3381 (0.131)
NGR4	1.3017 (0.483)	1.2952 (0.615)	1.6359 (0.241)	0.398	0.3196 (0.538)
P*	0.704				**0.129**

6.4.2. Analyses of Positions on the Left, Right and Total Series

Referring to the initial quantogram analyses of positions in chapter 5, it should be remembered that the positions of most of the series had a tendency to be shifted quantal with a shift that is brought by the uncertainty about the location of an assumed base line from which positions are measured. That is to say that first measurements of roots are not a natural part of the spacings, therefore come into the model as shift effects. Therefore positions with such a feature could not be fitted a pure hierarchical model in the same way as for the raw spacings. However, if the first measurements (i.e. shift) could be subtracted from all positions, then the resulting new data should no longer be shifted quantal. Then we can proceed with an analysis of the positions in order to search for pure hierarchical quantality by applying the approaches proposed and used so far. Within the framework of this study, we will hence take advantage of this practical solution and apply new ideas on the positions from which the first measurements have been subtracted.

To begin with, we demonstrate the results of level 1 analyses conducted both on left and right positions and on the total positions independently in Tables 6.16 and 6.17 respectively. It can be seen that we again could not obtain significant overall evidence of separate groups from either left and right or total positions. The strongest indication seems to come from Naa treated Gib–1 roots for a value of 0.22.

Table 6.16. Results of hierarchy *level 1* analyses for Wild, Naa treated Wild, Gib–1 and Naa treated Gib–1 groups (positions of left and right series used)

Type	τ –range	$\hat{\tau}$	$\hat{q}$	$\phi(\hat{q})$	P	P*
WR	[0.4, 5]	3.622	0.2760	3.60651	0.479	0.397
NWR	[0.4, 5]	3.139	0.3186	3.28973	0.614	
GR	[0.4, 5]	0.756	1.3224	3.64645	0.370	
NGR	[0.4, 5]	4.498	0.2223	3.68932	0.190	

Table 6.17. Results of hierarchy *level 1* analyses for Wild, Naa treated Wild, Gib–1 and Naa treated Gib–1 groups (positions of total series used)

Type	τ –range	$\hat{\tau}$	$\hat{q}$	$\phi(\hat{q})$	P	P*
WR	[0.8, 5]	1.863	0.5367	3.23394	0.817	0.810
NWR	[0.8, 5]	3.324	0.3008	3.05808	0.902	
GR	[0.8, 5]	4.544	0.2200	3.19184	0.857	
NGR	[0.8, 5]	4.616	0.2166	3.82372	0.121	

In order to test how much these initial values will be supported with what values of quanta by their roots and root series, we next present the results of level 2 and level 3 analyses in the forthcoming tables.

Beginning with Wild type root positions, a proposed hierarchical structure around 0.2760 as seen in Table 6.18 received no support on the whole from their left and right series. The total series produced no significant combination of quantum values around 0.5367 (see Table 6.17) either.

Table 6.18. Results of hierarchy *level 2* analyses for Wild roots and also results of *level 3* analyses for their L, R & T series (positions used)

root	$\hat{q}$	$\hat{q}_L$	$\hat{q}_R$	P*	$\hat{q}_T$
WR1	0.2993 (0.358)	0.2590 (0.205)	0.2525 (0.851)	0.547	0.4214 (0.317)
WR2	0.2948 (0.185)	0.2985 (0.128)	0.2809 (0.801)	0.387	0.7514 (0.014)
WR3	0.2637 (0.658)	0.2630 (0.701)	0.2478 (0.826)	0.878	0.3728 (0.886)
WR4	0.2146 (0.696)	0.2070 (0.742)	0.2168 (0.416)	0.647	1.0289 (0.428)
WR5	0.3508 (0.681)	0.3022 (0.493)	0.3534 (0.866)	0.793	0.9222 (0.766)
WR6	0.2940 (0.623)	0.2547 (0.897)	0.2940 (0.367)	0.734	0.7847 (0.584)
WR7	0.2400 (0.763)	0.2123 (0.697)	0.2268 (0.590)	0.703	0.7133 (0.198)
WR8	0.3484 (0.817)	0.3872 (0.821)	0.3317 (0.167)	0.424	0.5921 (0.182)
WR9	0.3492 (0.771)	0.3618 (0.681)	0.3493 (0.178)	0.399	0.3492 (0.602)
WR10	0.2572 (0.433)	0.2246 (0.181)	0.2859 (0.416)	0.222	0.6450 (0.903)
P*	0.697				0.359

Table 6.19. Results of hierarchy *level 2* analyses for Naa treated Wild roots and also results of *level 3* analyses for their L, R & T series (positions used)

root	$\hat{q}$	$\hat{q}_L$	$\hat{q}_R$	P*	$\hat{q}_T$
NWR1	0.2498 (0.219)	0.2637 (0.016)	0.2439 (0.017)	**0.002**	0.7540 (0.892)
NWR2	0.2389 (0.748)	0.2231 (0.251)	0.2241 (0.549)	0.361	0.7821 (0.771)
NWR3	0.2475 (0.067)	0.2475 (0.874)	0.2476 (0.264)	0.618	0.8950 (0.612)
NWR4	0.4508 (0.896)	0.5563 (0.492)	0.4509 (0.334)	0.433	0.1011 (0.744)
P*	0.352				0.949

An inspection of positions four Naa treated Wild roots indicated that there is no significant combination of quantum values for none of the root series except for NWR1 which has its left and right series significantly quantal at around 0.2498 as seen in Table 6.19.

Table 6.20. Results of hierarchy *level 2* analyses for Gib–1 roots and also results of *level 3* analyses for their L, R & T series (positions used)

root	$\hat{q}$	$\hat{q}_L$	$\hat{q}_R$	P*	$\hat{q}_T$
GR1	0.8909 (0.417)	0.8908 (0.362)	1.3268 (0.397)	0.365	0.2629 (0.445)
GR2	0.9826 (0.346)	1.9893 (0.057)	1.6377 (0.298)	**0.080**	0.2275 (0.475)
GR3	0.9801 (0.816)	0.7616 (0.510)	1.0673 (0.457)	0.501	0.2305 (0.230)
GR4	0.9024 (0.010)	1.1343 (0.372)	0.9023 (0.532)	0.444	0.3277 (0.853)
GR5	0.4984 (0.015)	0.4961 (0.555)	0.4983 (0.362)	0.486	0.2379 (0.943)
GR6	0.4031 (0.063)	0.4032 (0.343)	0.3972 (0.570)	0.450	0.2794 (0.718)
P*	**0.012**				0.826

Moving onto the Gib–1 type roots, level 2 analyses indicated that there exists a set of quantum values varying around 1.3224 with a combined evidence found significant. The values can be seen in Table 6.20. Only the GR2 root received further support from its left and right series at the third level of hierarchy. Moreover, independently analysed total series produced no significant evidence for the existence of its initial value, 0.2200.

As far as positions of Naa treated Gib–1 are concerned, we pointed out that the strongest evidence is received from both left, right and total positions for a value around 0.22 at the level 1 (see Tables 6.16 and 6.17). This remained the same at the second level of hierarchy. Roots bearing their combined left and right positions suggested a set of quantum values variable around 0.2223, meanwhile total positions presented their values around 0.2166. However, individual left and right series indicated no evidence in favour of these values when level 3 analyses were performed. Results can be found in Table 6.21.

Table 6.21. Results of hierarchy *level 2* analyses for Naa treated Gib–1 roots and also results of *level 3* analyses for their L, R & T series (positions used)

root	$\hat{q}$	$\hat{q}_L$	$\hat{q}_R$	P*	$\hat{q}_T$
NGR1	0.2229 (0.517)	0.2039 (0.389)	0.2470 (0.631)	0.539	0.3101 (0.154)
NGR2	0.2223 (0.273)	0.2166 (0.473)	0.2015 (0.204)	0.288	0.2855 (0.477)
NGR3	0.2513 (0.144)	0.2216 (0.492)	0.2513 (0.812)	0.750	0.2695 (0.172)
NGR4	0.2642 (0.115)	0.3083 (0.656)	0.2660 (0.047)	0.211	0.2660 (0.179)
P*	**0.095**				**0.119**

6.5. One–way Anova Type of Residual Analyses

6.5.1. Introduction

It is the intent of this section to provide another way of identifying any hierarchical formation of quantality by means of simple ideas of residual analysis based on analogies with one–way Analysis of Variances. The basic strategy is to employ a model analogous to 1–way Anova, to devise an "analysis of quantality model" and assess the appropriateness of the model in terms of behaviour of the observed residuals. It is well known that analysis of residuals is useful for detecting model inadequacies and outliers. Residuals are widely used in many procedures designed to extract various types of disagreement between data and an assumed model. Graphical techniques are very effective for detecting abnormal behaviour of residuals. If the model is correct and the assumptions are satisfied, the residuals should appear to behave as random variation with zero mean. Any convincing pattern in the residuals would suggest some inadequacy in the model or assumptions.

Suppose that, for example, we have a data set which arises from a one–way Anova model with k factors (i.e. treatments):

$$y_{ij} = \mu + \tau_j + \varepsilon_{ij}, \quad j=1,\ldots,k$$

where μ is thought of as the overall true mean of the k treatments, ε_{ij} is the random error associated with the i^{th} observation in the j^{th} treatment and assumed to be independently and identically distributed as $N(0, \sigma^2)$, and τ_i are defined as the treatment deviations about the true mean, so that $\Sigma\tau_j = 0$.

For such data, suppose we instead and mistakenly fit an overall model ignoring any treatment levels, that is,

$$y_{ij} = \mu + \varepsilon_{ij}$$

We would then expect the residuals from this model to be clustered into k groups, revealing the fact that the fitted model is the wrong model and the true model has a one–way structure. Clearly, the degree of clustering would depend on the magnitude of σ in comparison to the differences between groups in their mean responses. If σ is small relative to the spread of group means then the k clusters will be well separate from each other and easily identifiable. The larger the magnitude of σ the less detectable will be the group structure.

This feature has provided the motivation to utilise an analogy to one–way Anova to detect any hierarchical structure in the quantality of root spacings. Using the same principle, it is therefore of interest to know what would happen if the root spacings come from a one–way quantal model with a different quantum q_j for each rank; that is

$$y_{ij} = m_{ij}\, q_j + \varepsilon_{ij}, \qquad j = 1,\ldots,k;\;\; i = 1,\ldots,n_j \tag{6.3}$$

where $$q_j = q + \delta_j,$$

which satisfies $\sum \delta_j = 0$, and q is the common quantum for all k groups, then, however, we fit an overall model,

i.e. $$y_{ij} = m_{ij}\, q + \varepsilon_{ij} \tag{6.4}$$

As intuition would expect, residuals from this fitted overall model should also cluster into k groups, and this feature if observed in data would imply some grouping in the data and that a wrong model had been fitted.

As far as hierarchical quantal models are concerned, we have so far suggested that there may exist some spacing quanta that varies among ranks, roots, etc. but it is not known how much variation between the quanta is needed so that the hierarchical quantality can be detected. Hence, the awareness of the possible effects of the amount of variation between quantum values is of primary importance when the goal is a thorough understanding of a ‘sensible’ hierarchy of quantum values.

The analogy with one–way Anova models is not perfect. With Anova models, if the residual variance is large in comparison with the difference between group means then the group means will not be detected and the simple model with just a mean term would be preferred to the one–way Anova model. With the one–way quantal model, we may again fail to detect the group structure if the ‘residual variance’ is large but we might not detect any quantality at all and so as well as discarding model 6.3 we would also discard model 6.4.

The small simulation study presented below is designed to investigate this problem: What relative values of residual variance and spread of subgroup quanta (a) mask the detection of the subgroups and (b) mask the presence of any quantality.

The study is limited to 3 subgroups and the various other values for quanta and variances are based on values observed in data from the Megalithic circles so as to be plausible.

6.5.2. Residual Analyses on the Simulated Data

In order to simulate data sets that follow the one–way quantum model in the form of (6.3), the following settings are considered: firstly, it is supposed that there are k=3 groups (i.e. treatments or factors) of size each 100 (i.e. n_j=100, j=1, 2, 3). Then a mean quantum value for the experiment is fixed to be 5.4407 (τ=0.1838) and the integers obtained from circles in the Scotland data set are again used in the one–way quantal data generation. The reason for these choices is that the agreed range of gridsearch for the Megalithic Yard problem is more advantageous for the purpose of the current investigation.

The objective of this study is to find out what sort of variation among quantum values could be considered reasonable. The question could therefore be whether the supposed range of possible quanta from different roots be as much as some fraction of the mean value of the quantum. In order to consider a variety of ranges, the reasonable one–way quantum values are calculated for the cases when they are expected to form a range as large as, say, 1%, 5%, 10%, 25% and 50% of the mean value 5.4407, defining many variations from small to large in magnitude. The calculated quantum values of the first and third group and the ranges of variation they define are listed in Table 6.22. Note that the mean quantum value is always q_2 =5.4407 and the ranges are equal to those given in the table.

Table 6.22. Considered range of quantum values varying around $q_2 \approx 5.44$.

	1%	**5%**	**10%**	**25%**	**50%**
q_1	5.4134	5.3050	5.1686	4.7596	4.0799
q_3	5.4678	5.5772	5.7127	6.1199	6.8027
range	0.0544	0.2722	0.5441	1.3603	2.7228

The core of this study lies within the magnitude of the errors. In other words, a clear visualisation of grouping in the residuals should be dependant on how dispersed are the errors from individual groups. The error term in model (6.3) is therefore generated from a Wrapped Normal distribution i.e. WN(0, σ) and the degree of quantality determined by the value of σ is controlled by the expected value of cosine quantogram as given below:

$$E\left(\cos(2\pi\varepsilon/q)\right) = \sqrt{2n}\ \exp\left\{-\frac{1}{2}(2\pi\sigma/q)^2\right\}$$

As one may notice, the smaller the value of σ in relation to q, the larger is the expected value. That is the data get 'more quantal'. Since the model being dealt with has 3 separate quantum values, the measure of dispersion, σ, is expected to change as the magnitude of quantum values change. In other words, the ratio σ/q plays an important role in determining the height of a peak at q in the cosine quantogram. That is to say that the same degree of quantality at different quanta can be achieved by choosing different σ values. Therefore we obtain the same concentration around zero even though the σ differs from q_1 to q_3.

As the aim here is to investigate the patterns of residuals when various degrees of quantality exist, we will assign σ many values from very small to large in relation to the q being considered. Suppose that σ_1, σ_2 and σ_3 represent the concentration of errors when q_1, q_2 and q_3 are considered respectively.Therefore our strategy here will be to fix a value for σ_2 corresponding to the mean quantum value q_2 = 5.4407 and calculate the relative size of the σ_2 in q_2 (i.e. ratio=σ_2/q_2). Then it is easy to work out the equivalent dispersion parameters for the second and third groups as σ_1 = ratio$\times q_1$ and σ_3 = ratio$\times q_3$ respectively. These values are used to generate errors in the model (6.3) from the wrapped normal distribution as described in section 3.2.

With the model specifications given above, therefore one–way quantal data sets with the quantum values defined in Table 6.22 were generated. This structure was ignored and the data sets were combined and a working model with a common q fitted to obtain the estimates of q as the value maximising the cosine quantogram. All quantogram analyses have been performed over the τ–range as [0.09, 0.59] with an increment of 0.0001. Then residuals are calculated as below:

Actual Model : $y_{ij} = m_{ij}\, q_j + \varepsilon_{ij}$, j=1, 2, 3; i=1, …,100

Working Model: $\hat{y}_{ij} = \widehat{m}_{ij}\, \widehat{q}$

Residuals : $\widehat{\varepsilon}_{ii} = y_{ij} - \widehat{y}_{ij}$

Then, the residuals were analysed graphically using dot plots and specially written (in S–plus) circular plots.

Note that, in each presentation, the diameter of the circle is equal to the estimated common quanta, $\widehat{q}$, which varies from plot to plot. Each circular plot is accompanied by either a linear histogram of the same residuals or a plot of residuals versus the 3 group indexes. It should also be noted that number of classes (i.e. bin intervals) is fixed arbitrarily to 57 for all the circular plots and histograms so that any grouping can be detected easily.

Possible types of patterns that can emerge from the residuals of one–way quantal models are portrayed in Figures 6.2–6.6. When the range of variation is 0.0544 (see

Table 6.22), quantogram analysis of generated data that is very quantal, i.e. σ is very small for all 3 groups, estimates the common quantum value as 5.4407 which is exactly the same as the mean quantum value. Therefore the estimated value provides a good fit for the second group but the true quantum values for the first and third are underestimated and overestimated respectively. A plot of residuals over the full range $\pm$ q/2 however does not show a clear picture of the grouping because all the residuals are very small (see Fig 6.2.a) and groups are too close to each other. Therefore the plot is reproduced considering the range of residuals as the full range. A clear pattern of grouping can be viewed now more clearly in Fig 6.2.a′. Then the analysis is continued for different values of σ_j and as seen in Fig 6.2.b the clear pattern has disappeared for the values of σ_j as large (and more) as the range of variation. A similar result has been obtained when the range is equal to 5% of the mean value as given in Fig 6.3. If the range is equal to 10%, then quantogram analysis is no longer able to estimate a common quantum as exactly equal to the mean value but slightly larger or smaller. However, such small deviation does not prevent the residual plot from demonstrating a clear pattern of grouping when σ_j are very small (Fig 6.4.a). Again Fig 6.4.b shows that the existing pattern vanishes as σ_j get larger.

Interesting pictures have been obtained when the range of the variation among the three quantum values gets even larger. First of all, suppose that the variation is 25% of the mean value and the quantality is strong (σ_j are very small). Then the quantogram analysis underestimates the mean value and proposes a simple fraction of it as the possible common quanta. Fig 6.5.a shows what pattern could be visualised in that case. Although the circular plot itself gives the impression that there are 4 groups, a plot of residuals versus individual group indexes indicates that $\hat{q}$ which was estimated as approximately half of the mean value still fits the second group well, however, the residuals from the first and second groups appear in 4 clusters, which reveals the fact that the quanta is underestimated too much. On the other hand, the plot still gives an indication about what amount of variation exists among the quantum values. In addition, having 4 clusters could be also used as a guide that the fitted common quantum is half of the real mean value.

Secondly, suppose that the variation is around 50% of the mean value and each group is considered quantal at q_j (i.e. σ_j are very small). In this case, it has been observed (see Fig 6.6.a) that the influence of the mean value disappears and the group which has the smallest quanta dominates the results by proposing its quanta as the common quantum. This is very natural because one would intuitively expect the smaller values to fit data better. The plot also shows 3 clusters of residuals and the locations of them again provide the information about amount of the variation that exists. In addition, both Figures 6.5.b and 6.6.b yield the same conclusion that it is difficult to discern the pattern as σ_j get bigger.

The following major conclusion can be drawn from this simulation study. One–way Anova type of residual analysis is a useful tool in recognising the indications of hierarchical quantal models for some given data, under particular circumstances determined by both the residual variance and the range of variation among any quantum values. The patterns of the residuals could be picked quite easily if $\sigma \ll$ range of variation. For the cases when this condition does not hold (i.e. when weaker quantality exists), it is difficult to obtain a clear cut grouping pattern. In that case it could be useful to carry out a formal statistical analysis such as one–way Anova or its non–parametric version for circular residuals to test whether groups differ in their mean response.

The following subsection will present the similar analyses on the current data sets of the root spacings.

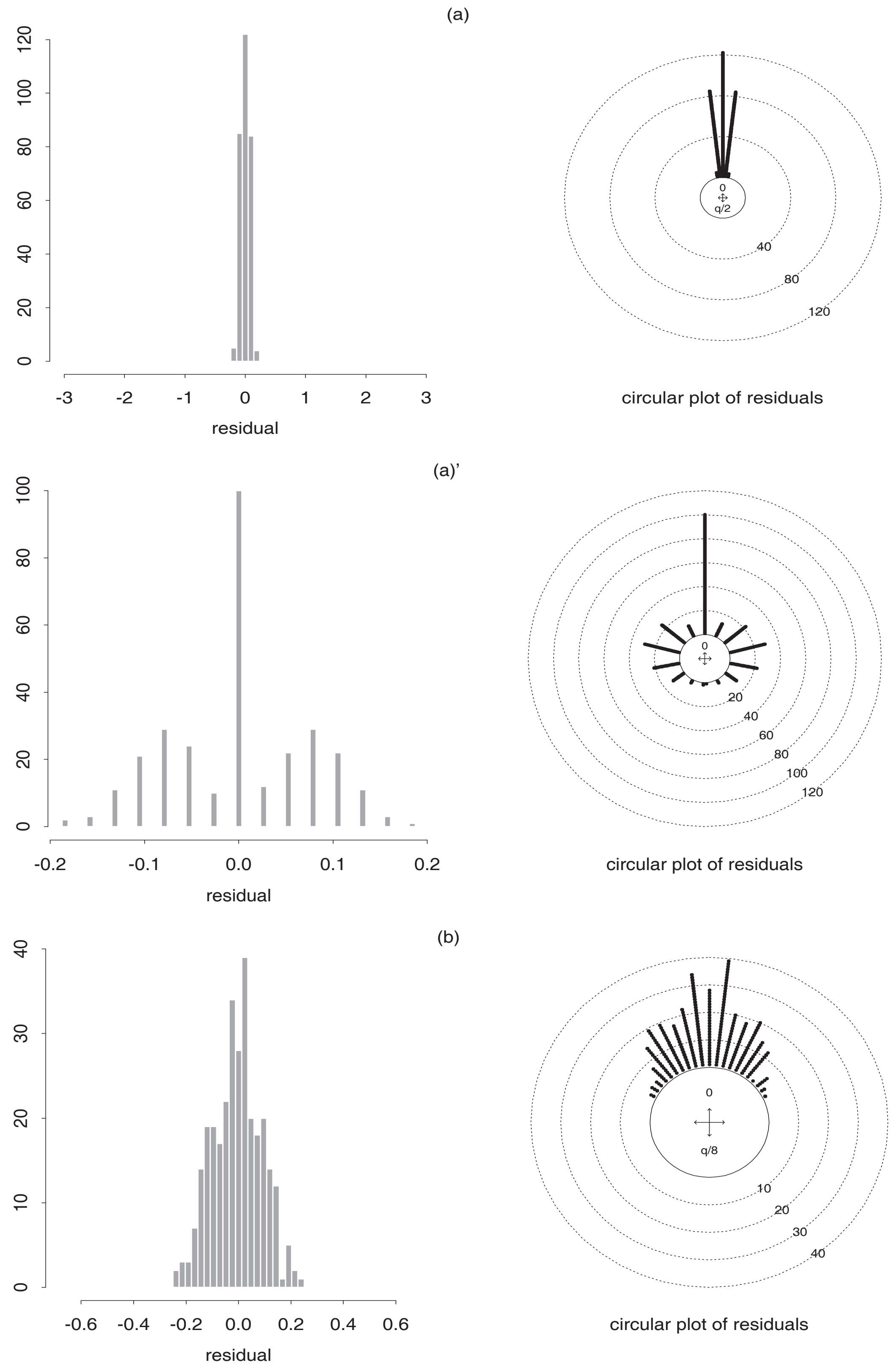

Fig 6.2. Plots of residuals when range=0.0544; (a) σ_2=0.00001; $\widehat{q}$ =5.4407, (a)′ reproduction of (a), and (b) σ_2=0.05; $\widehat{q}$ =5.4407

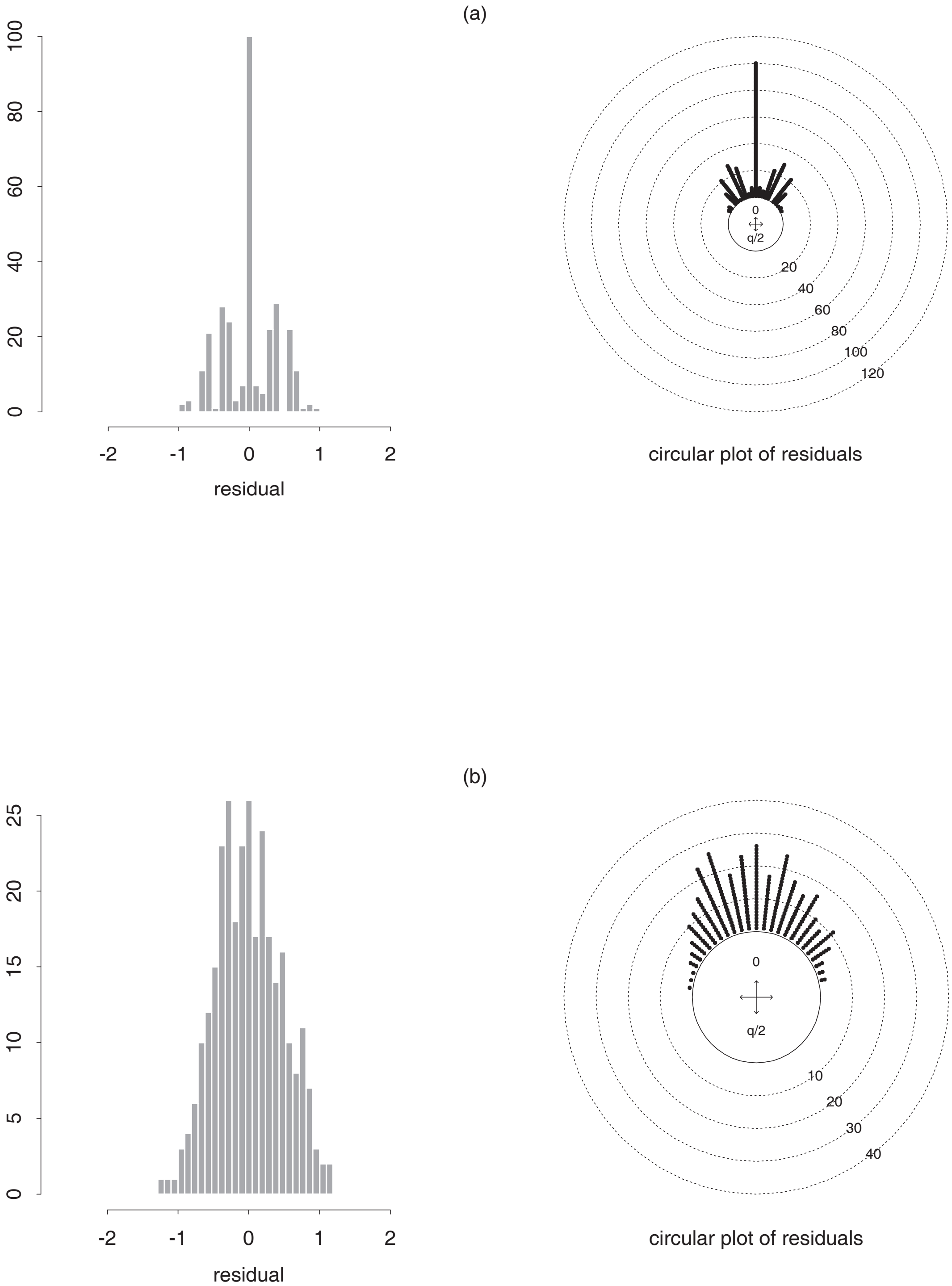

Fig 6.3. Plots of residuals when range = 0.272; (a) σ_2 = 0.01; $\widehat{q}$ =5.4407, (b) $\sigma_2 = 0.272$; $\widehat{q}$ =5.4407

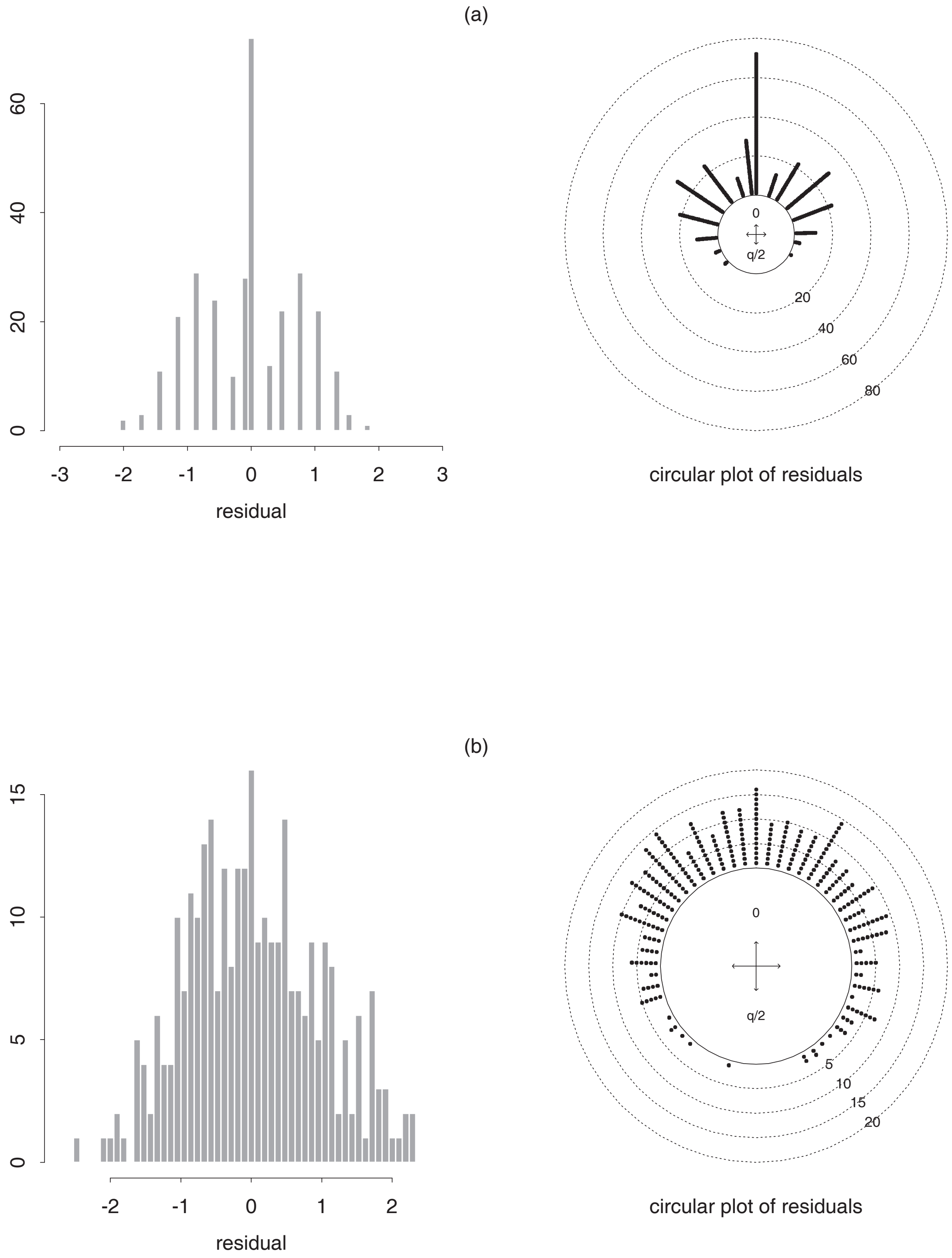

Fig 6.4. Plots of residuals when range=0.544; (a) σ_2=0.00001; $\widehat{q}$ =5.4555, (b) σ_2=0.55; $\widehat{q} = 5.4318$

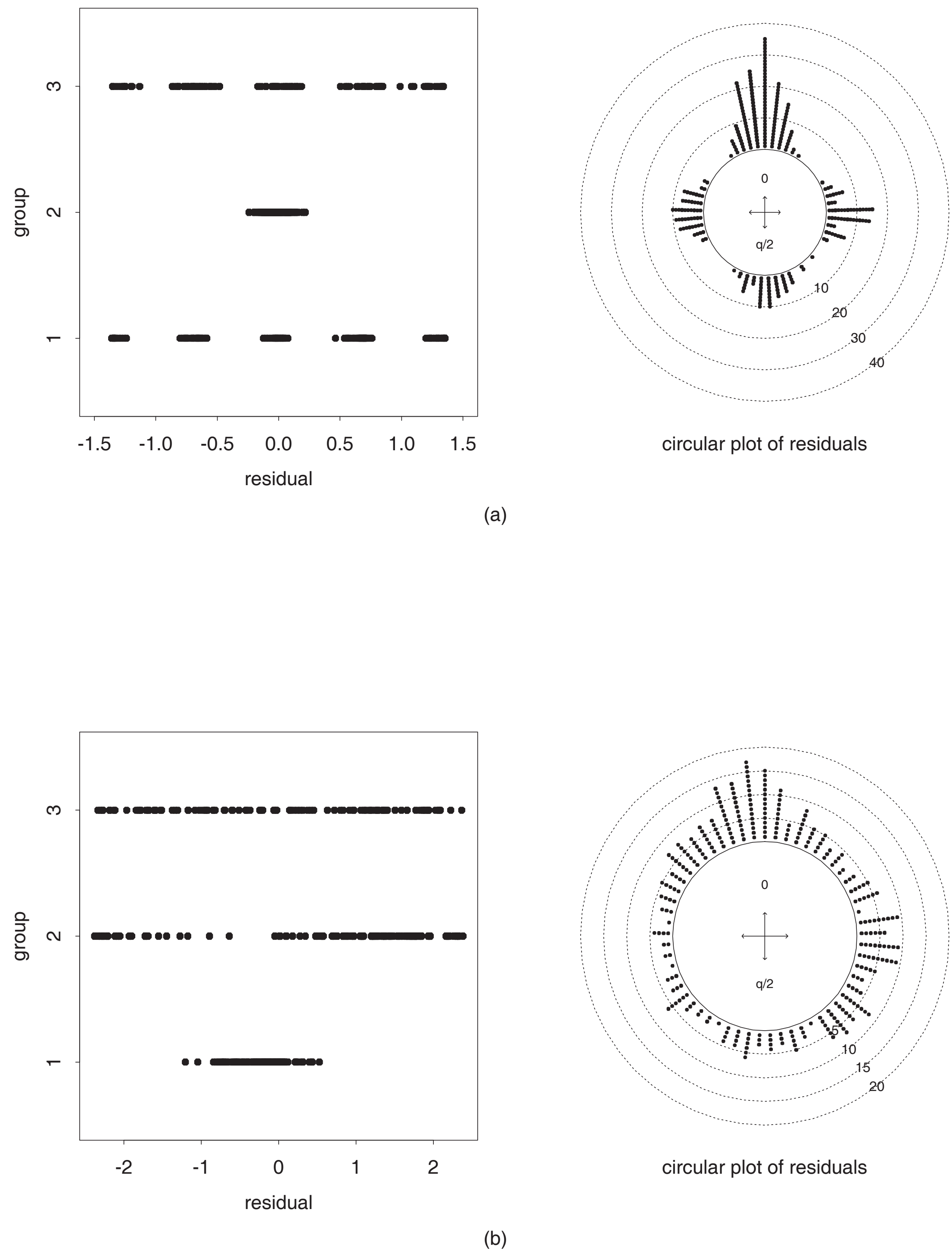

Fig 6.5. Plots of residuals when range = 1.36; (a) σ_2=0.1; $\hat{q}$ = 2.7218, (b) σ_2=0.5; $\hat{q}$ = 4.8169.

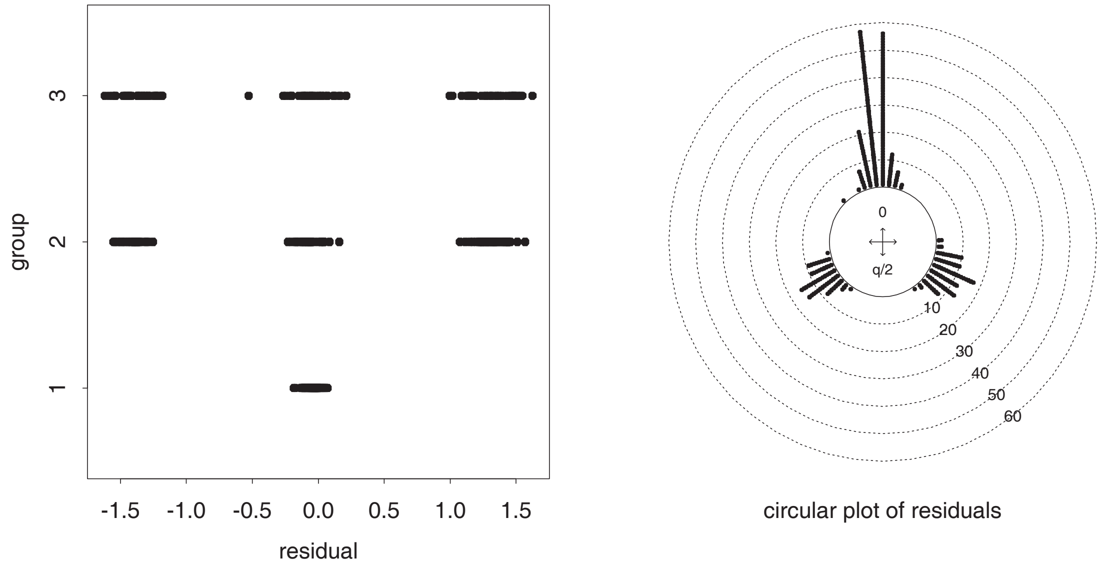

(a)

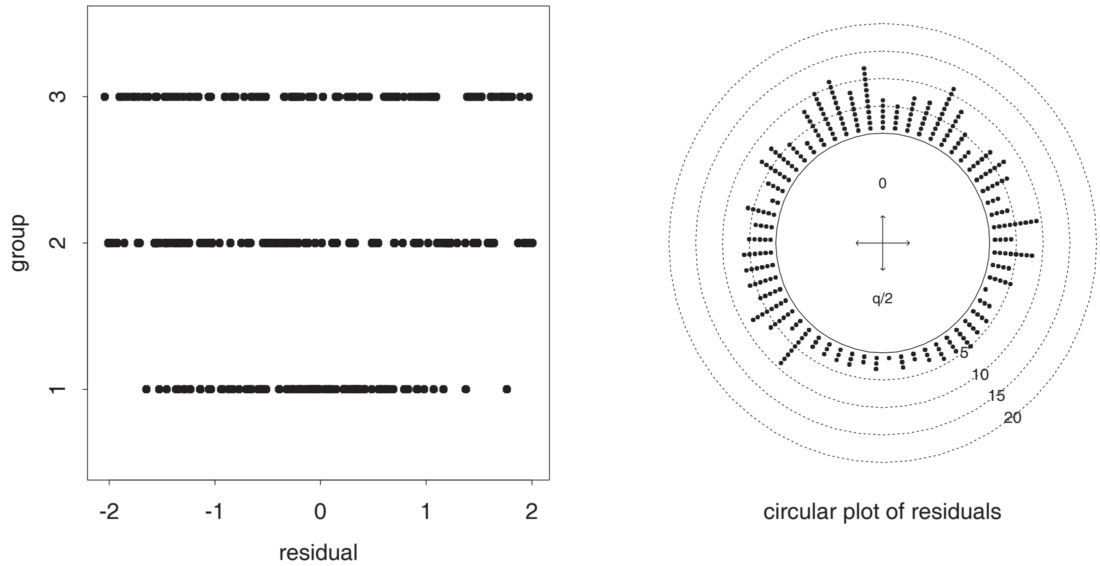

(b)

Fig 6.6. Plots of residuals when range=2.72; (a) $\sigma_2 = 0.1$; $\hat{q} = 4.0916$, (b) $\sigma_2 = 1.5$; $\hat{q} = 4.0966$.

6.5.3. Residual Analyses on the Root Spacings

Having demonstrated the various patterns that can emerge from hierarchical quantal data simulated when different degrees of quantality are considered, it is now necessary to perform similar analyses on the available root spacings from onions and also tomatoes.

Beginning with each group of onion roots, we conducted the quantogram analyses on their combined rank spacings from all roots in order to obtain a common quantum value for each. Then residuals have been obtained and plotted as described before. Each plot that will be presented here shows the common quantum value estimated for that particular group of spacings under investigation. Figure 6.7 displays the plots of Control, Weak–treated and Strong–treated groups.

Once again, the influence of the accuracy 0.5 mm. used for control roots is indicated very clearly by the appearance of three clusters as the common quantum is also very close to a multiple of 0.5. The picture obtained for weak–treated group seems to be more dispersed, however 5 groupings can still be picked out. A plot of residuals versus root indexes however shows that major influence for the existing grouping come from the root W5 and not all the roots support this picture. For example, W6 and W3 may favour the fitted quantum and W7 seems to prefer a larger quantum value. For the strong–treated group, there seems to be sub-groupings which may be caused by the S6 root bearing the majority of the spacings in this group. This is the root that shows a strong tendency to be quantal at around 0.5, mainly due to having most of its spacings equal to 0.5. Note that the total and also rank series of each treatment demonstrate the similar features. Therefore these graphs will not be presented here.

Furthermore, the spacings of tomato roots recived the same analyses and the residual plots have been obtained the same as before. Fig 6.8 illustrates some examples of the obtained features for Wild type tomato spacings.

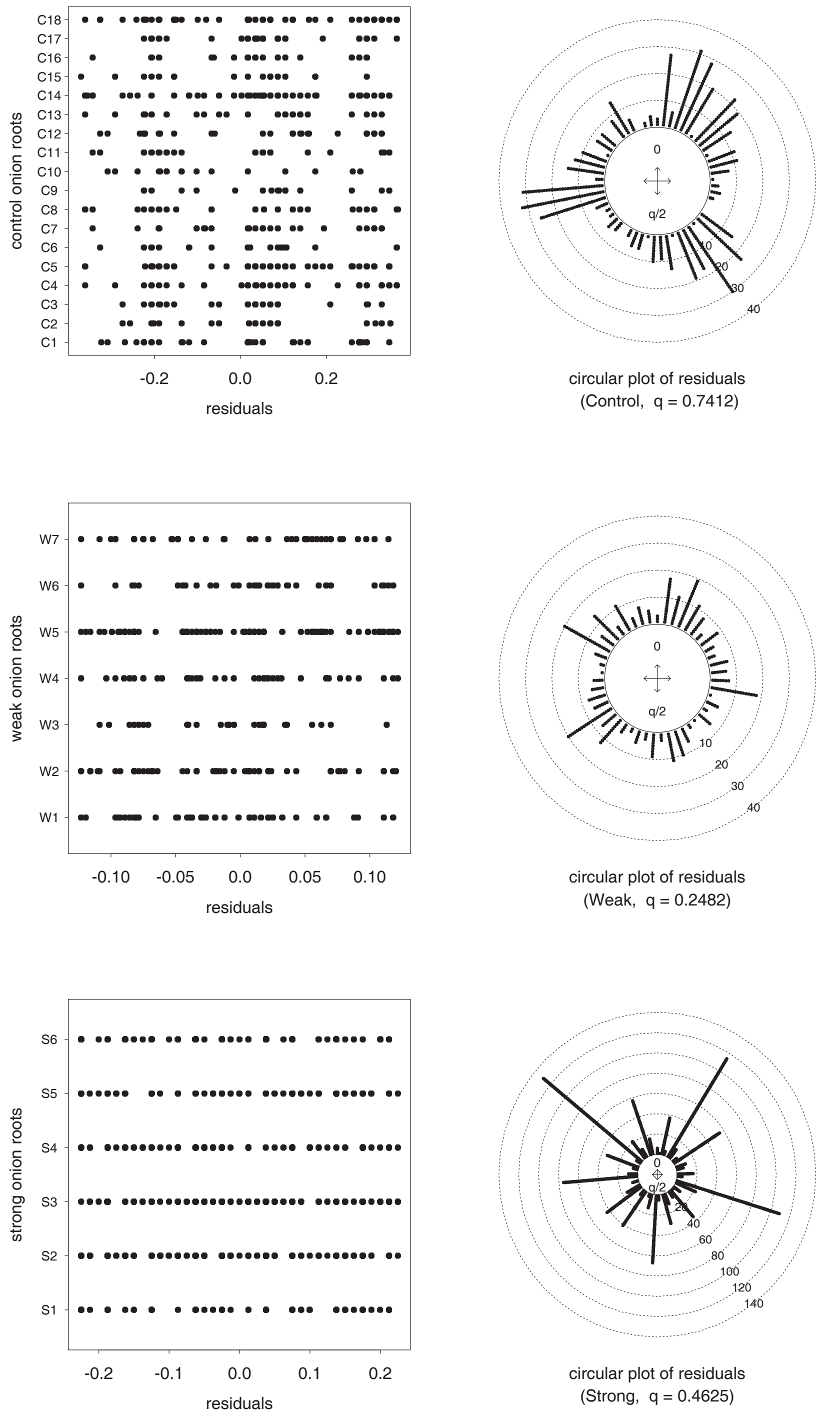

Fig. 6.7. Residual plots for treatment groups of onions.

The first circular plot shows a very clear groupings of residuals obtained for the wild roots. As seen in the plot of residuals versus root indexes, this is however not suggestive of slightly differing quantum effects. In fact, a closer look at the residuals of WR1 shows that they are grouped rather within the root. The location of sub-groups hence gives a sign of another potential quantum value that is 0.24. Note that similar patterns observed for the majority of the roots. Moving onto the left and right series of the wild type roots such as WR3 and WR10, one can see that residuals do not exhibit clear pattern. However, it can still be noticed that left series of the first root favours the fitted common q and additionally, the second root gives a slight indication such that quantum values of its series vary around the fitted common q. An inspection of the residuals obtained for other wild type root series also showed similar results, therefore they are not presented here.

Moreover, the residual plot for the Naa treated Wild roots in Fig 6.9 gives no evidence of any groupings. At the level of their left and right series, the only root that gives any sign of variable quantality is found to be NWR1 for which the present quantality is very weak. Other roots show a similar pattern like NWR4 and that is very diffuse.

In addition, Gib–1 Mutant type roots also do not reveal their residuals with a clear-cut clusters (see Fig 6.10). Therefore, it is very difficult to discern any pattern from the plot. The residuals of GR1 shows that its left series tend to be around the common q unlike its right series which presents groupings within itself. It must be noted here most of the GR type roots display a similar pattern. The most distinctive pattern is obtained for GR2 with root series varying around the fitted common q. However, this effect is also not strong enough to be distinguished in the circular graph.

Furthermore, Fig 6.11 presents the residual plot for the Naa treated Gib–1 roots. It is again observed that there is not a distinctive pattern to suggest any variable quantality. The total series of this type of roots exhibited very strong sub-groupings. A slight evidence of variable quantality can be observed for the left and right series of the roots NGR3 and NGR4. However, again this effect is not very distinct.

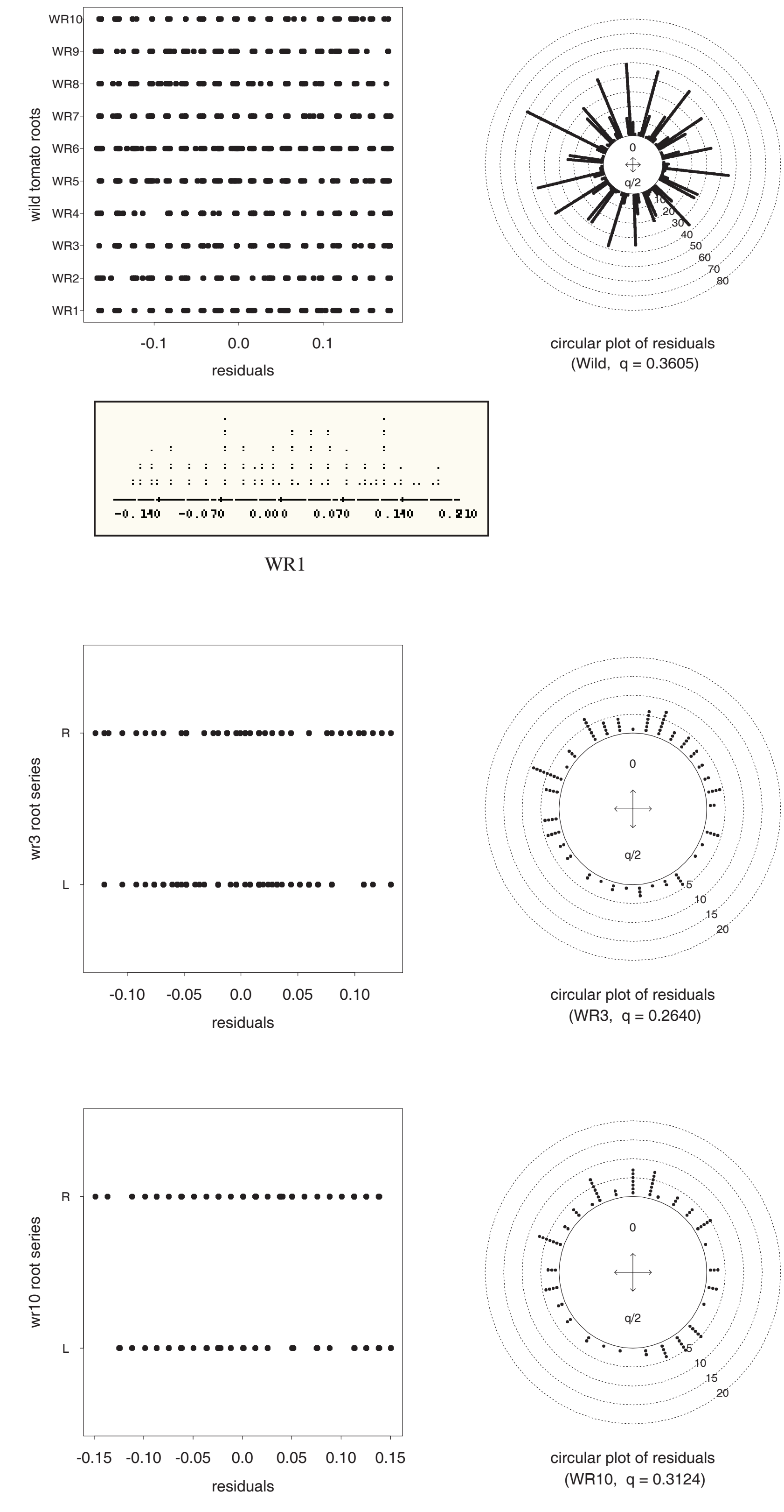

Fig 6.8. Residual plots of Wild type roots

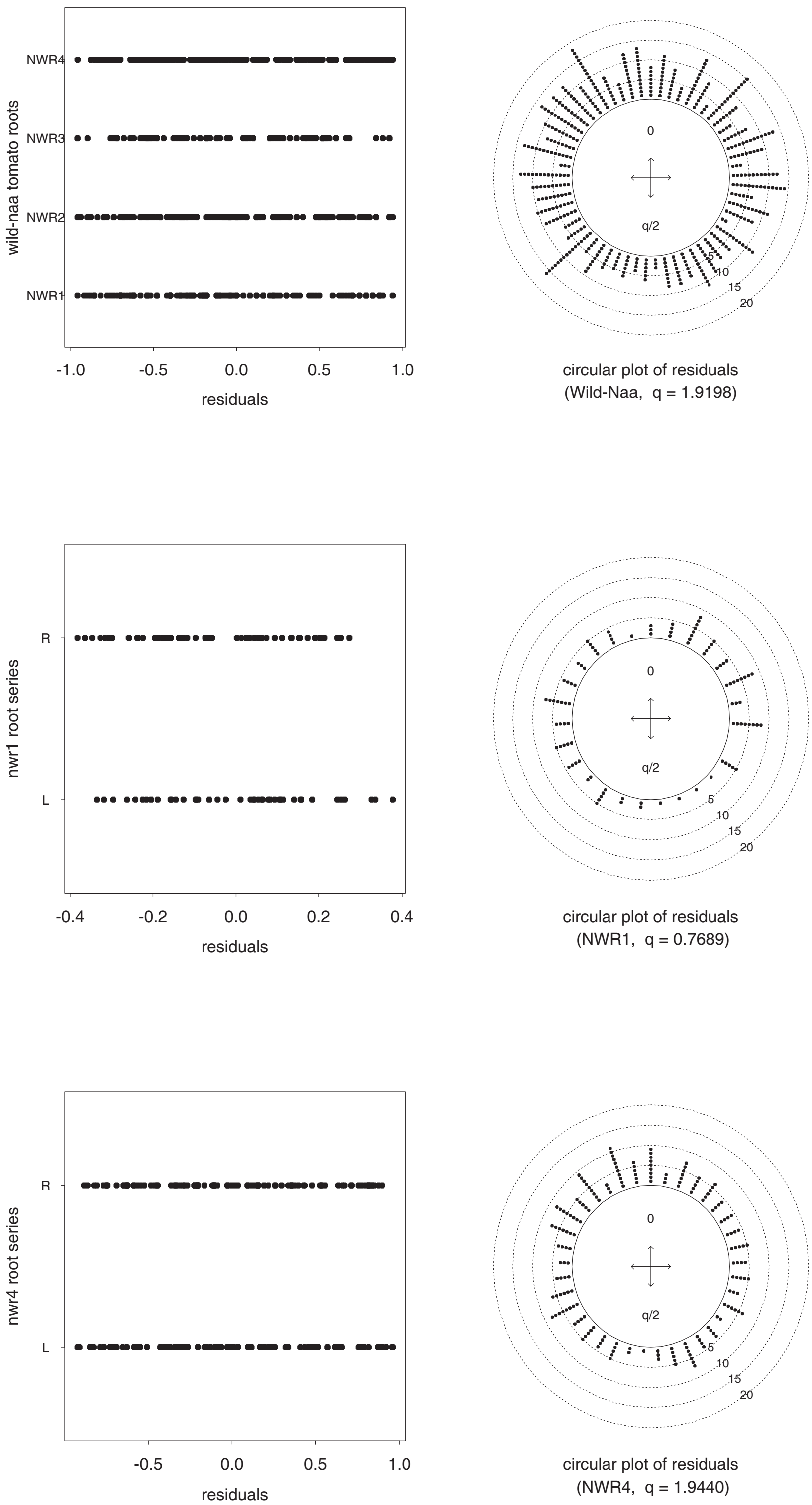

Fig 6.9. Residual plots of the Naa treated Wild type roots

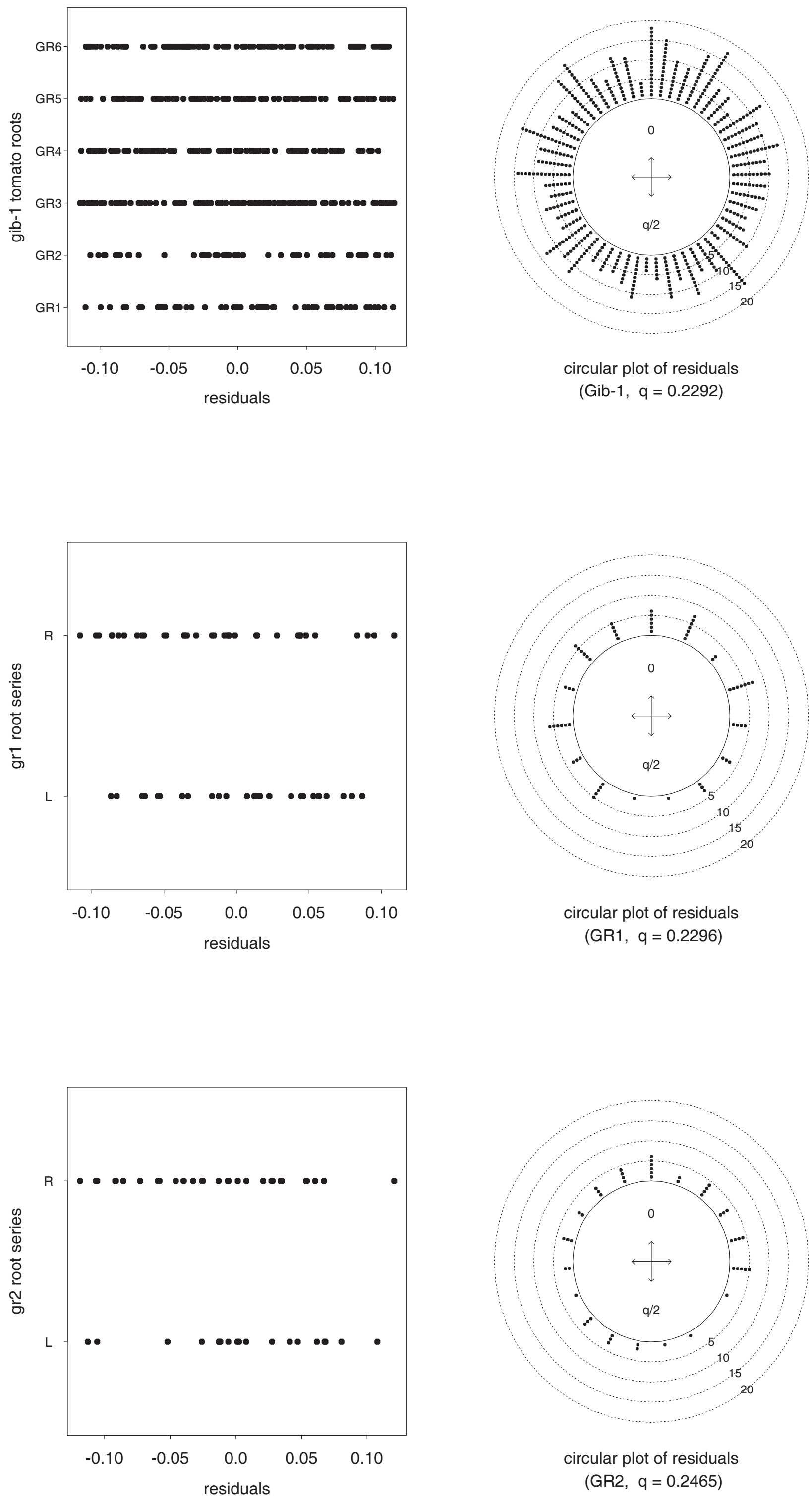

Fig 6.10. Residual plots of Gib-1 Mutant type roots

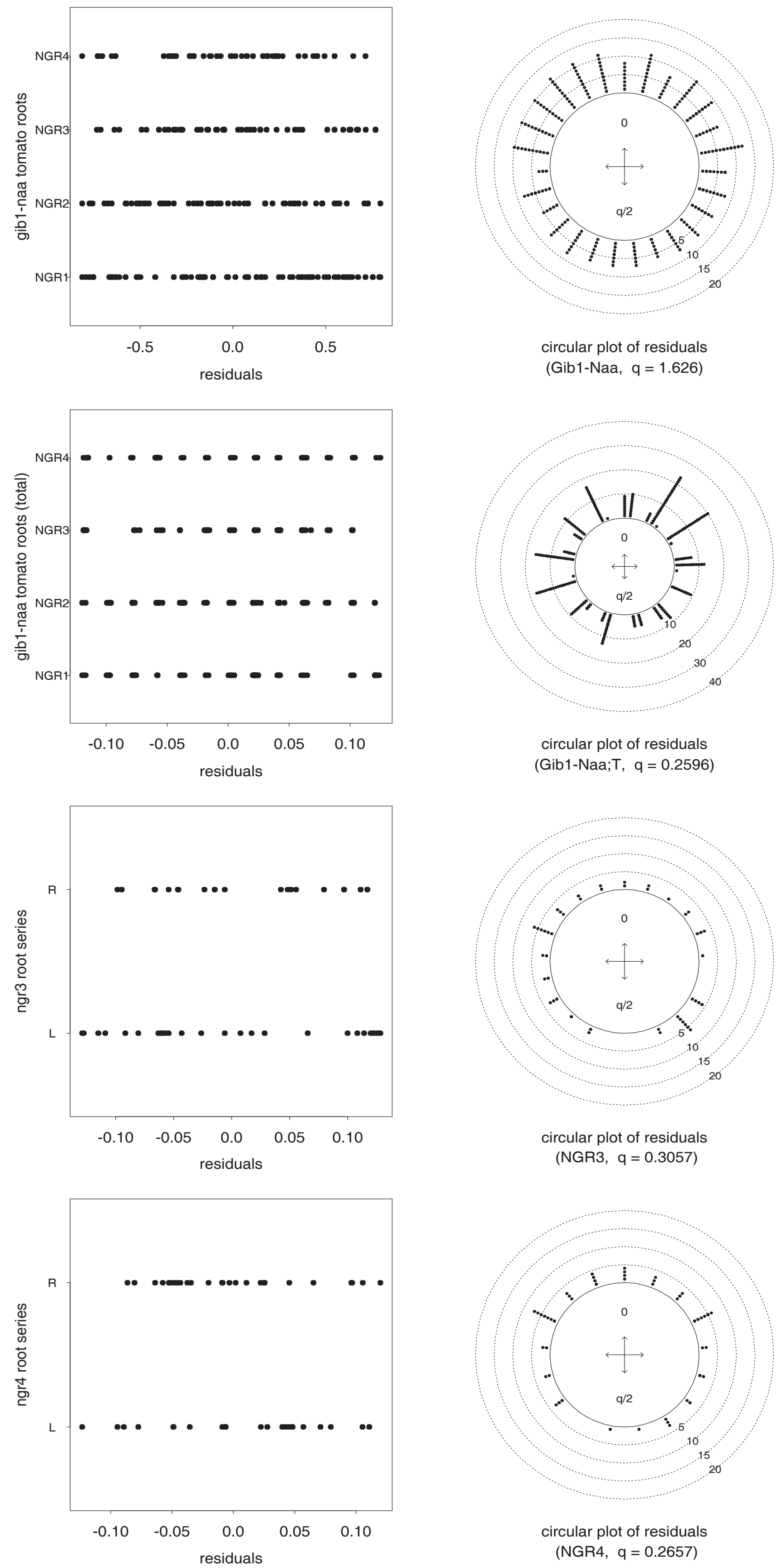

Fig 6.11. Residual plots of Naa treated Gib–1 Mutant type roots

6.6. Overall Conclusions for Onion and Tomato Roots

The current study of quantality has been motivated by the questions of firstly whether or not root spacings exhibit any quantal feature in their distributions and if so, secondly, whether this is the overall picture for all treatment groups of onions or varieties of tomatoes. We have so far searched for not only simple but hierarchical quantality in the root spacings of both plants and exhibited that there is considerable evidence ($P < 0.05$) and suggestions ($0.05 < P < 0.1$) of quantality for the various individual roots. At this stage, it is necessary to assess whether the overall evidence is good enough to draw an overall conclusion of quantality or these are just the results of multiple testing showing a few interesting results. For this purpose, an analysis of the evidence obtained so far is here provided using Fisher's combined test and supported by a Binomial assessment of the number of nominally significant values at the 10% level.

Quantality of Onion Roots : we first note that quantogram analyses on the control group roots suffered from the low accuracy of the measurements. No significance assessment is therefore made for the control roots and results remained inconclusive.

For the treated roots, all the estimated significance probabilities for simple quantality have been integrated by the Fisher's combined test, and the overall evidence lead us to the conclusion that treated onion spacings are not quantal. However, 7 significant results out of 39 hypothesis tests give a $P=0.089$ suggesting some evidence. It must be noted much of the contribution to this result comes from the Strong treatment group. Furthermore, the combining evidence is performed over the P^* values obtained in the search of hierarchical quantality and the overall evidence is significant at the 5% level, but with 4 significant P^* values amongst 15 tests which gives a $P=0.056$. The influence of the Strong treated spacings on the acceptance of a hierarchical quantum model should be emphasised.

In addition, we also examined the combined evidence from the total series in favour of both simple and hierarchical quantality. However, no significant result is obtained for either form of the quantality.

It was further of interest to know whether or not positions of onion roots exhibit any overall tendency to be quantal. Firstly, the combined evidence from the positions of the rank series are found to be neither simple nor hierarchical quantal. However, a closer look at the Strong treated root positions gives some suggestive evidence ($P < 0.1$) of simple form and moreover good evidence ($P < 0.05$) of the hierarchical form on the whole. Secondly, positions of the total series are examined and we found no evidence of quantality.

<u>*Quantality of Tomato Roots*</u>: the assessment of overall evidence of simple quantality is next pursued for tomato roots in the similar way. The combined evidence indicated that tomato root spacings are quantal at the 5% level. Compared with the expected value of 5, 10 out of the 48 hypothesis tests gave a significant result (i.e. P=0.019), also providing the same suggestion. In addition, investigation of the significance probabilities, P^*, estimated from tomato root spacings also revealed good overall evidence ($P < 0.05$) of hierarchical quantality. In all, we observed 6 significant P^* values out of 29 hypothesis tests, which gives some indication (i.e. P=0.064) of hierarchical quantality.

Moreover, the total series produced no evidence to suggest simple quantality and in the same way they showed no tendency to be hierarchical quantal either.

Proceeding with the positions, first we investigated the rank series (i.e. the left and right series). Although 8 significant results at the 10% level among 48 tests give some indication (i.e. P=0.102), the evidence on the whole was not good enough to suggest a quantal distribution. This conclusion remained the same when the evidence for hierarchical quantality was combined. Second the positions of the total series produced mildly interesting number of significant results, i.e. 5 out of 24 giving a P=0.085, and the overall evidence suggested no quantality. Again the hierarchical quantality of positions of the total series received neither good nor suggestive evidence.

6.7. Constructing Regression Quantal Models

6.7.1. Detection of the Structure: Residual Analyses

Having proposed another form of quantality, namely the Regression quantal model as given in section 5.4.2, it is now necessary to investigate how to extract this feature, if it exists, from some given data. As an explanatory stage, it is natural to consider some residual analyses which would reveal indications of any structure visually.

In the search of quantality, for a given set of data, one would typically perform the usual quantogram analysis and estimate the candidate quantum. It is therefore of our particular concern to investigate what would happen if data are in fact regression quantal, however, regardless of this underlying structure, this data are mistakenly fitted a common quantum value, that is

$$\text{Actual model: } X_i = m_i q_i + \varepsilon_i; \quad i = 1,\ldots,n$$

$$\text{where } q_i = q + \gamma\ t_i$$

$$\text{Working model: } X_i = m_i q + \varepsilon_i; \quad i = 1,\ldots,n$$

As the new quantality implies that the value of quantum stretches along the length of the root, the fitted quantum is intuitively expected to be slightly too big for small i and too small for big i. As a result of this effect, one also should expect to observe a distinctive pattern, visually in a plot of residuals (i.e. $\hat{\varepsilon}_i = X_i - \hat{m}_i \hat{q}$) versus i index. However, a clear cut pattern would again depend on the residual variance. If the variance is big we may then fail to detect the structure. In order to investigate what values of variance could give a clear indication of regression quantality, a simulation study is designed.

First, we generate some data that are regression quantal with the covariate t_i chosen as positions along the root by following the procedure given below:

Step 1. Define b such that $b = t_n - t_1$ where t_n = total length of the root, t_1 = first observed spacing. Then arbitrarily choose a value for both q and b. Some care is needed to choose a value for γ. As the variation of q is controlled by the component, $\gamma\, t_i$ added to the common q, its largest value must be much smaller than q. We therefore assign γ such a value that $\gamma b \ll q$.

Step 2. Generate $u_i \sim U(0, b)$, put them in descending order and $t_i = u_{(i)}$

Step 3. Calculate $q_i = q + \gamma\, t_i$

Step 4. Calculate $m_i = [(t_i - t_{i-1})/q_i]$; $i = 2,\ldots,50$ and $m_1 = [t_1/q_1]$. Note that […] means nearest integer.

Step 5. Use the quantum values from step 3 and the integers from step 4 to form regression quantal data, i.e. $X_i = m_i\, q_i + \varepsilon_i$; where $\varepsilon_i \sim WN(0, \sigma^2)$ and $-q_i/2 \le \varepsilon_i < q_i/2$.

For this study, it is decided to generate a regression quantal data set of size 50. The values of q and b are chosen arbitrarily as 0.25 (i.e. $\tau = 4$) and 15 respectively and also γ as 0.00001. Different values of σ for errors ε_i have been considered to be able to observe the effect of the magnitude of errors for this type of quantality. Then we ignored this structure and fitted a common q performing the quantogram analysis over the τ–range ~ [2.5, 10] with an increment of 0.001. Residuals from the fitted model are next obtained and plotted. Figure 6.12 demonstrates the residual plot when errors are generated with σ=0.00001 and common quantum is estimated as $\hat{q}$ = 0.26006 (i.e. $\hat{\tau}$=3.999). The pattern obtained gives a very clear indication of quantality variable along the root. Estimated residuals mostly being negative at the beginning and positive towards the end of the root shows that the simple quantum model with a common q does not provide a good fit. Note that if the length of the root was longer, say b=30, the same analysis on the generated data with all ε_i =0 would produce a fan shaped residual plot as the sample contains more variety of integers as demonstrated in Fig 6.13(a). Here different integer values for m_i correspond to straight lines with different gradients since the residuals from fitting the working model, if the actual model is true, should be $m_i \gamma t_i + \varepsilon_i$. This distinctive feature becomes however sparse when errors get larger.

Figures 6.13(b) and (c) present the residual plots obtained when σ=0.0001 and 0.001 which suggested common quantum values as $\hat{q}$ =0.25012 and 0.25018 ($\hat{\tau}$ =3.998 and 3.997) respectively. Although the implication of the regression quantal model in the first graph can still be observed when moderately large errors are used, it however becomes difficult to discern this pattern if errors have a variation of 0.001 as in the second graph.

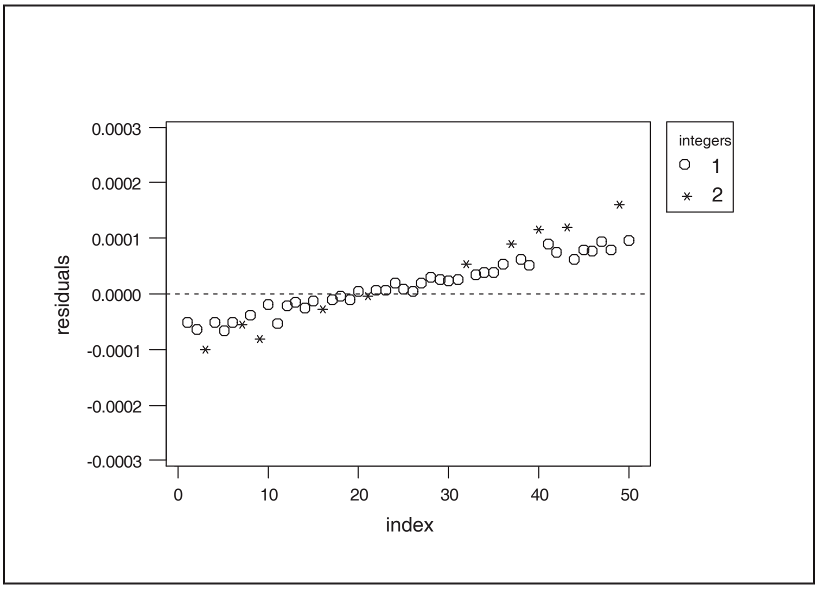

Fig 6.12. Plot of residuals versus i^{th} observation when σ = 0.00001

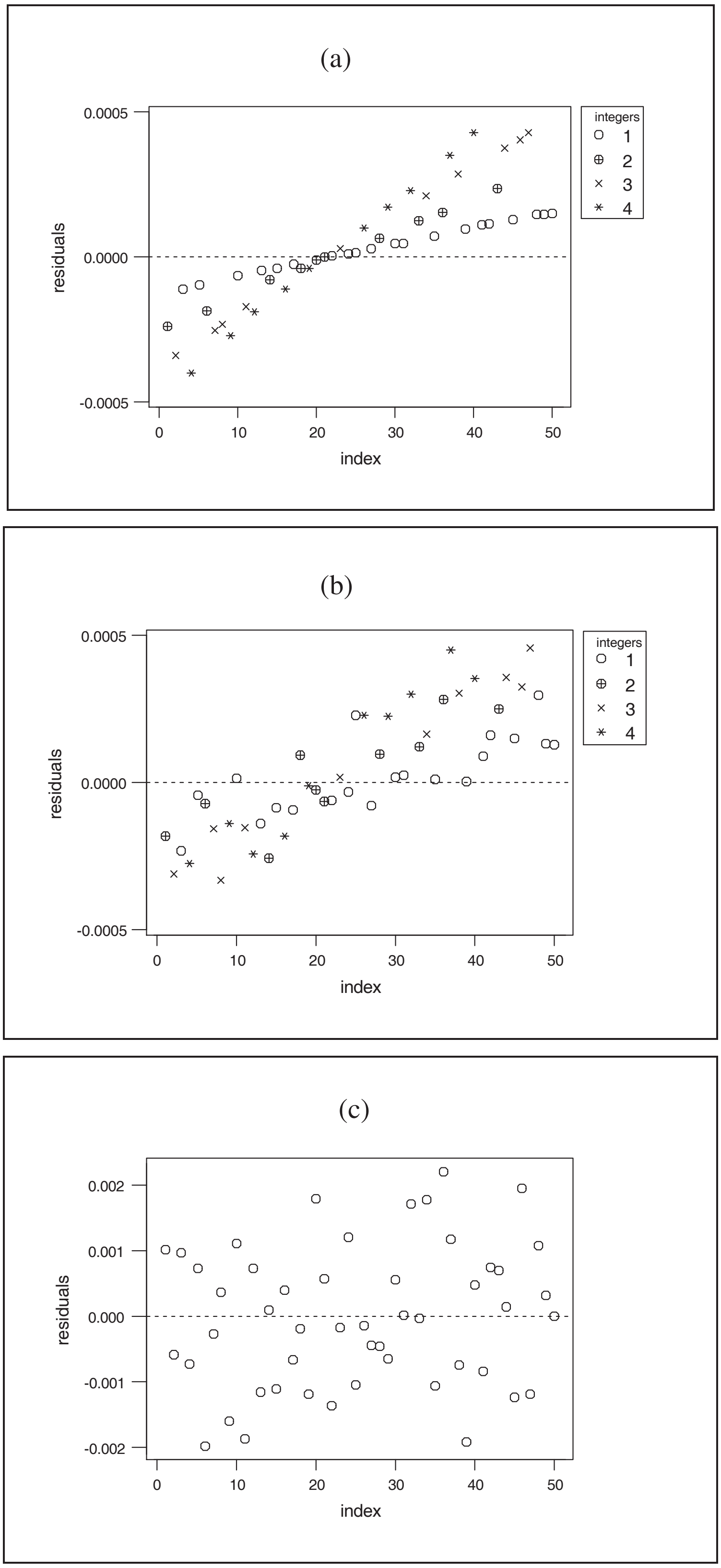

Fig 6.13. Plot of residuals versus i^{th} observation (a) when the length of the root is longer and $\varepsilon_i = 0$, (b) σ=0.0001 and (c) σ=0.001

Up to now, we have demonstrated the patterns that could emerge as an indication of regression quantality on the simulated data. Similarly, the residual plots have also been obtained for Fern root spacings using the common quantum values estimated and presented in table D1.1. An inspection of the patterns however revealed no clear suggestion of regression quantality around those common q values for majority of the root series. Figure 6.14 shows the plot obtained for the total series of CT4 root, which gives the most distinctive pattern, however with a large variance.

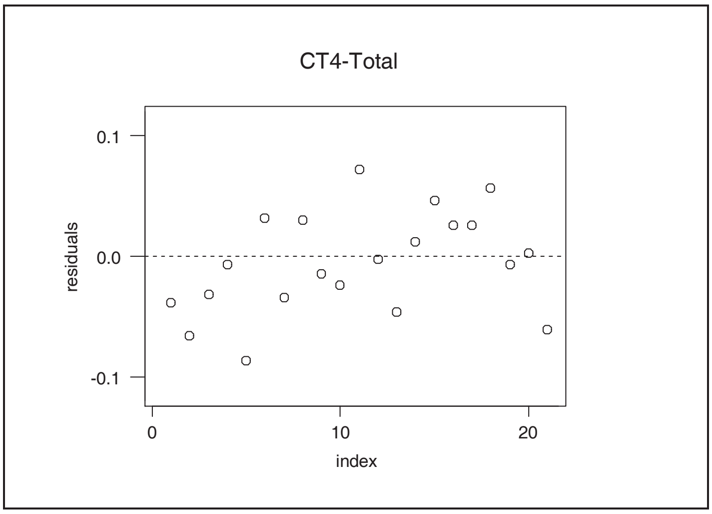

Fig 6.14. Residual plot for the total series of CT4

6.7.2. Analysis of the Fern Data using Regression Quantal Model

Should there exists such quantality that the quantum elongates its magnitude as root grows, one is confronted by the estimation problem of not only quantum itself but also another parameter, γ, that allocates a certain variation to the quantum. It is apparent that this could not be achieved by the ordinary quantogram analysis simply performing a gridsearch for the quantum. However, it could be modified to take into the account the additional parameter. Note that the test statistic $\phi(q)$ changes to a two parameter function, i.e. $\phi(q,\gamma)$. It is therefore essential to perform a second gridsearch for γ over a range being modified simultaneously with respect to every q taken from its range. In other words, a two–dimentional gridsearch needs be executed to maximise the test statistic $\phi(q,\gamma)$. Whether or not the resulting peak at $\hat{q}$ and $\hat{\gamma}$ is significantly high can then be tested again by Monte Carlo simulations.

Before beginning to apply such an analysis on any real data, two important points of the analyses should be explained. The first is concerned with the choice of the range for the gridsearch of the new parameter. We have so far stressed the fact that the right choice of the range is essential to observe the genuine underlying quantal effect. This is also true and crucial for the new parameter as it entirely depends on the quantum value and the total length of the root (i.e. $\gamma << q/b$). Since the total length is fixed for any selected root being investigated, a plausible range for the gridsearch of γ would be between 0 and γ_{max}, where γ_{max} is being modified according to j^{th} value of quantum tested in the grid. In other words, γ_{max} could get values from the least equal to q_{min}/b to the most equal to q_{max}/b. If these modifications are not made, one would get erroneous results.

The second point that arises is the question of how to choose the best increment for the gridsearch of the new parameter. As we have already studied the best increment for the gridsearch of the quantum using the halving method (see section 2.6.4), what needs to be done next is to apply the same method for the new parameter while fixing the best increment chosen for quantum search beforehand.

Having clarified these points, investigation of regression quantality has been conducted for the fern roots available. The two–dimentional quantogram analyses are performed over the τ–range [0.14, 5] (i.e. q~ [0.2, 7]) with an increment of 0.001 to estimate quantum, $\hat{q}$, meanwhile another search is being done over the γ–range of [0, γ_{max}] with an increment of 0.0001 to estimate the new parameter, $\hat{\gamma}$. Note that $\hat{q}$ and $\hat{\gamma}$ are the values that maximise the test statistic $\phi(q,\gamma)$. The significance of the peak observed is then assessed by performing 99 simulations. The roots showing some evidence in favour of regression quantality are presented in Table 6.23. The P-values are nominal since no allowance is made for the selection of the most impressive results. Note that full results can be found in Appendix D.

First of all, it should be born in mind that inclusion of the second dimension to the quantogram analysis increased the time of the computations and put restrictions on the number of simulations that could be performed, and therefore the strength of any conclusions that could be drawn. Looking at the results, one can however observe the tendency for the C–type fern roots (except CT1) to be regression quantal rather than pure quantal. However, it is clear that the M–type fern does not favour this new form and its quantality remained as a weak indication of the pure quantal form.

Table 6.23. Results of 2–D gridsearch on the Fern roots

Root Series	$\hat{\gamma}$	$\hat{q}$	$\phi(\hat{q},\hat{\gamma})$	P–value
CT1–Total	0.0000	3.5273	4.96475	0.02
CT2–Right	0.0107	0.2421	4.22410	0.04
CT2–Left	0.0126	0.2549	3.98247	0.12
CT3–Total	0.0015	0.2577	4.16323	0.05
CT4–Right	0.0150	0.3940	4.01024	0.11

6.8. Concluding Remarks

This chapter has been concerned with the development of new systems of quantality, namely Hierarchical quantality and Regression quantality, proposed as a consequence of the non–constant feature of rhythmic phenomena initially observed for some roots. In pursuing investigations into the construction of hierarchical structure, an immediate difficulty arises with formulating the idea that quantum values should be close to each other as to form a sensible hierarchy. In this chapter, this difficulty is dealt with by proposing some methodological tools that could be used as both formal and graphical test procedures.

The first is achieved by proposing an algorithmic approach to the analysis of levels that compose the hierarchy. In practice, it essentially involves searching for a quantum of one data set, then restricting the range around it to search for the others. This enables us to choose and investigate close quantum values. Then the evidence from separate data sets is integrated by, or into, a new aggregate test and significance is assessed by bootstrapping the new test statistic.

An initial verification of this composite test is done by comparing its power with that of the well–known combination method of Fisher's combined test and it was found that it has better power properties, therefore is considered superior to Fisher's test in our analyses. An overall assessment of the results of the algorithmic search has however been done by means of Fisher's test as this is computationally more feasible.

The second tool proposed for the realisation of hierarchical quantality is achieved by recognising an analogy to the one–way Anova model and applying the ideas of residual analyses. It is therefore concerned with a visualisation of the structure and provides an easy way for an initial investigation of the existence of any pattern. If there exists a hierarchical quantality in a given data set having subgroups, it is shown that a common quantum value fitted wrongly to the data would result in clusters in a residual plot, giving the indication of structural quantality. It is concluded that if the degree of quantality is strong, such indications could be easily picked up. However, if not, then we fail to detect not only the quantality of subgroups but also any quantality at all.

Along with this graphical detection of the structure, note that a good analysis for hierarchical quanta hunting should always try different ranges of search covering many combinations of possible values. Thus this algorithmic approach requires a degree of intuition in the choice of judicious ranges. Then, the final interpretation should be based on the result which gives the best evidence.

Bearing this in mind, we applied the above–mentioned tools on the data sets available. The Strong–treated onion roots provided good evidence in favour of hierarchical quantality at around 0.46. The analyses of Wild type tomato roots also indicated the existence of this new form of quantality primarily at around the value of either 0.36 or 0.24. In addition, positions of both total and rank series of Naa treated Gib1–Mutant type roots showed relatively significant tendency towards the value of 0.22. An assessment of the overall evidence concluded that both tomato roots and treated onion roots provide a good indication of hierarchical quantality.

Within this Chapter, we also dealt with the construction of another new quantality proposal, Regression quantality, which is brought by the nature of the process of root growth that may directly influence the slower, but still rhythmic, generation of lateral roots. Detection of this structure is first investigated by means of some residual analyses. Then the existing simple quantogram analyses are extended such that a second dimension of a gridsearch is also considered to solve estimation problems arising with not only quantum itself but also new parameter which governs how much a quantum can be allowed to stretch along the root.

A particular application of this new methodology has been conducted on the Fern root spacings. As a result, a regression quantal model claimed to provide, especially for the C–type Ferns, a better fit rather than a pure quantal model. However, it is believed that repetition of the same analyses with greater number of simulations would help to draw stronger conclusions.

In general, whether it be hierarchical or regression quantal model, we have provided in this chapter new effective methods not only for inspecting the patterns but also for verifying the existence of any patterns observed in some given data.

CHAPTER 7.

A Bayesian Approach

7.1. Introduction

In the previous chapter, we illustrated the ways of formulating the theory that regularity of lateral root production of plants has a hierarchical form. The kernel of our approaches to the statistical modelling of such structural quantality has so far been the use of descriptive and algorithmic procedures supported by the 'classical' objectives of the significance test formalism, mostly based on simulation methods. Basically, the established methodology aimed to investigate the relative amounts of support supplied by given data sets to various sets of q.

The major complication with the construction of hierarchical quantality has stemmed from our theory that any hierarchical quantality should reveal its quantum values 'close' to each other. As all theories have to be judged in relation to their probability in the light of evidence, the only way to proceed here is through regarding probability as a degree of belief: i.e. subjective measure. In this application it is therefore desirable to introduce well–based subjective probabilities into the argument. At a more theoretical level, it is always instructive to analyse a problem from several points of view.

In this Chapter, we therefore will assess the support in favour of hierarchical quantality by evidence measured from different roots, using a different approach, namely Bayesian analysis. In applied statistical work, Bayesian inference is used partly to make use of the flexible modelling that occurs when treating all unknowns as random variables. The basis of all Bayesian methods is to combine the information provided by the data, x, through the likelihood function $p(x \mid \theta)$, and our beliefs about the model parameters before the observation of the data, expressed through the prior distribution $p(\theta)$, in order to derive the posterior distribution $p(\theta \mid x)$ using Bayes theorem. The posterior distribution is the probability distribution of the quantity of interest θ after observing the data and is given by

$$p(\theta \mid x) = \frac{p(\theta) p(x \mid \theta)}{\int p(\theta) p(x \mid \theta) d\theta}$$

Analytical evaluation of the posterior is easy as long as well known distributions and conjugate priors are used. However, in real life, it is often very difficult to model the situations which arise in practice in that way. Instead, it is often only possible to obtain the posterior up to a normalising constant,

$$p(\theta \mid x) \propto p(\theta) p(x \mid \theta)$$

but there is no easy way of finding the normalising constant. This is even more true when it is necessary to evaluate the marginal density of a single component θ_i of θ. Therefore the practical implementation of Bayesian methods is quite difficult and requires a great amount of computation due to the intractable integrals.

This case was once raised when the Megalithic Yard problem received a Bayesian analysis by Freeman (1976). He pointed out that a quantal model involves more parameters than there are observations. Due to n integers being treated as unknown parameters, integration over q or σ involves n–fold multiple sums. Such a proliferation of unknown parameters makes an exact analytic computations for the posterior distributions unavailable.

However, it is now often possible to obtain inferences using simulation–that is, to summarise a "target" posterior distribution by a sample of random draws from it, rather than analytic calculations. There are now new simulation techniques available for the numerical integration. These techniques are collectively known as Markov Chain Monte Carlo Methods, MCMC, for short (Gamerman, 1997). Hence, it is of our particular interest to facilitate inference about parameters of quantal models, simple or structural, utilising these techniques.

We begin the next section with a brief description of MCMC methods and a general introduction of not only the software package BUGS (Spiegelhalter et al., 1995) which implements the methods, but also CODA (Best et al., 1995) which includes many diagnostic tools to examine BUGS output. Then in section 7.3, we repeat and refine Freeman's analyses on the data of the stone circles by means of MCMC methods within the framework of BUGS. The refinements of his analyses produced here use different prior distributions and the drawbacks of MCMC in the analyses of quantal problems will be outlined. This will be followed by a proposal of a Bayesian model that incorporates our *a priori* beliefs on the structure of hierarchical quantality at stages, that is a hierarchical Bayesian model (section 7.4). The model will be evaluated on the simulated hierarchical quantal data, highlighting the various aspects of the analysis and then applied on some selected roots in section 7.5. The final section will close the chapter with a summary.

7.2. Markov Chain Monte Carlo (MCMC) method

In many applications, until recently, implementing the full complexity and structure of problems was difficult and required the development of specific methodology. Now, MCMC techniques provide a framework within which many complex problems can be analysed. The basic philosophy behind the method is to take a Bayesian approach and carry out the necessary numerical integrations using simulations. MCMC is essentially a technique of Monte Carlo integration using Markov Chains.

Monte Carlo integration draws samples from the required distribution i.e. posterior distribution, and then forms sample averages to approximate expectations. In general, drawing samples from the posterior is not feasible as the posterior can be quite non–standard. However, the samples need not necessarily be independent. They can be generated by any process which draws samples throughout the support of the posterior in the correct proportions. One way of doing this is through a Markov chain having the posterior as its stationary distribution (Spiegelhalter et al, 1995).

A *Markov chain* can be thought of as a model for a system which moves randomly through series of 'states' without having memory where it has been – where it jumps to next depends solely on where it is now. In other words, given the present, past and future are independent. This is an iterative process that changes its distribution at every iteration. As the number of iteration increases, however, the chain will eventually converge from the incorrect starting distribution to a unique stationary (or invariant) distribution which is the posterior distribution of interest (Gamerman, 1997).

The question of how to construct a Markov chain such that its stationary distribution is precisely the distribution of interest is described below.

7.2.1. Gibbs Sampling

The Gibbs sampler is an algorithm which allows the analysis of complex models through decomposition and sampling from full conditional distributions. Suppose we have a vector of parameters $\underline{\theta} = \left(\theta_1, \theta_2, \ldots, \theta_k\right)$. The algorithm starts with a vector of initial values for parameters, say $\underline{\theta}^{(0)}$, and updates each element of $\underline{\theta}^{(0)}$ in turn with a value sampled from its full conditional distribution. For example, the first iteration is performed as below:

$$\begin{array}{lll} \text{begin by sampling} & \theta_1^{(1)} & \sim \left[\theta_1 \middle| \theta_2^{(0)}, \theta_3^{(0)}, \ldots, \theta_k^{(0)}\right] \\ \text{then by sampling} & \theta_2^{(1)} & \sim \left[\theta_2 \middle| \theta_1^{(1)}, \theta_3^{(0)}, \ldots, \theta_k^{(0)}\right] \\ \quad\vdots & & \\ \text{finally by sampling} & \theta_k^{(1)} & \sim \left[\theta_k \middle| \theta_1^{(1)}, \theta_2^{(1)}, \ldots, \theta_{k-1}^{(1)}\right] \end{array}$$

In the second iteration, $\underline{\theta}^{(2)}$ is generated using $\underline{\theta}^{(1)}$ in the place of $\underline{\theta}^{(0)}$ and so on. After k iterations, we obtain a sequence $\underline{\theta}^{(0)}, \underline{\theta}^{(1)}, \ldots, \underline{\theta}^{(k)}$ which has the Markov property and is called a Markov chain.

7.2.2. Metropolis–Hastings Method

The algorithm for the Metropolis–Hastings Method is similar to that of Gibbs sampling except that a realisation is not taken from the appropriate conditional distribution, instead it is taken from a proposal distribution with a particular probability. If it is not accepted with a low probability, then the previous realisation in the chain is used. For technical details of the calculation of the probability and the acceptance rate, we refer the reader to Spiegelhalter et al.(1995).

In the next section, we will introduce a computational system that is capable of specifying a variety of prior distributions for any given model and sampling from the resulting full conditionals. The system is called BUGS (Spiegelhalter et al., 1995), which is an acronym for Bayesian Inference Using Gibbs Sampling. Moreover, it is supplemented by the software CODA which stands for Convergence Diagnosis and Output Analysis Software for Gibbs Sampling output.

7.2.3. Implementation: The BUGS Software

BUGS is a program that carries out Bayesian inference on statistical problems using the simulation technique known as Gibbs Sampling. It assumes a Bayesian or full probability model, in which all quantities are treated as random variables. This system consists of a set of functions that allows specification of models and probability distributions for all its random components (i.e. observations and parameters).

It starts with a graphical representation of the model which reflects conditional independence assumptions. Specifically, a variable (parameter or data) is thought of as a node in a graph, whose local dependencies are specified by the user in directed links. Then each node is conditionally independent, given its parent node, of all the other nodes that are not descendants. For example, the graph in Fig 7.1 provides the relationships between the parameters A, B, C and D in a very simple model. This graph implies that parameter C depends only on the values of A and B. Similarly, parameter D depends on the value of C but conditionally independent of the values of A and B. In other words, knowing the values of A and B, given the value of C, provides no extra information about parameter D. In the subsequent graphs, note that the dotted lines represent deterministic relationships and solid lines represent stochastic relationships. The square boxs are used to show constant values.

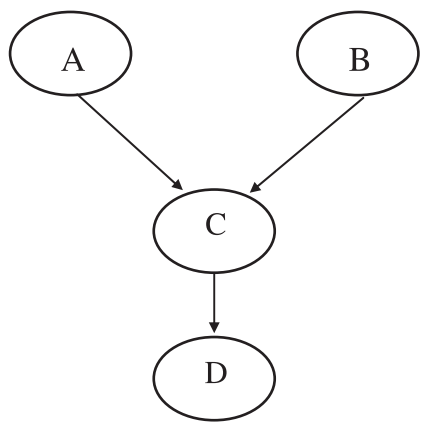

Fig 7.1. A simple graphical model

The probability distribution of observations and prior distributions of the parameters need next to be defined. Under the model specifications, first data are provided, and the unobserved nodes (parameters) are given initial values by either the user or BUGS. Then, the program starts to sample from the full conditional distribution of each variable, updating one at a time given all the others in the model in an iterative process. After a long burn–in, the iterated values should converge to its stationary distribution (posterior). The convergence should however be checked by the diagnostic tools given in CODA. Several methods CODA includes are introduced briefly in the following subsection.

Throughout the analyses of this chapter, note that we will use the windows version of BUGS, namely WinBUGS due to the reason that the Metropolis–Hastings sampler is stated to be more flexible and powerful in WinBUGS.

7.2.4. Monitoring Convergence: The CODA Software

CODA is an output processor for convergence diagnostics and statistical and graphical analysis of BUGS output which contains series of simulated values (i.e. 'chains'). Available convergence diagnostics are

- *Geweke (1992)*: this is based on early and late values of the chain. The convergence diagnostic Z is the difference between the sample mean of first 10% and last 50% of the iterates divided by the asymptotic standard error of their difference. As the chain length$\rightarrow\infty$, the distribution of Z$\rightarrow$N(0, 1) if the chain has converged. Similarly, Z scores can be computed within many segments of the chain and are expected to lie within a 95% probability interval for the N(0, 1) distribution.
- *Gelman and Rubin (1992)*: this is based on two or more parallel chains, each started from different initial values. The test is based on a comparison of the within and between chain variances for each variable, which is used to estimate a "Shrink Factor". A convergent chain should have a shrink factor equal to unity.
- *Raftery and Lewis (1992a)*: this is developed with an argument that it is wasteful and unnecessary to perform several runs, since convergence can be detected from a single long run. It suggests N – the total number of iterations that should be run

for each variable; M – the number of initial iterations to discard as the 'burn–in' and I – the increase in the number of iterations needed to reach convergence due to dependence between samples and k–thinning interval to be used. Raftery and Lewis (1992b) suggest that values of $I > 5.0$ often indicate convergence failure.

- *Heidelberger and Welch (1983)*: this is based on Brownian bridge theory and uses the Cramér–von–Mises statistic to test the null hypothesis that sample values for each variable form a stationary process. It reports whether the test is 'passed' or 'failed' with the number of iterations to keep, the number of initial iterations to discard and the Cramér–von–Mises statistic.
- *Autocorrelations* for each variable in each chain. High autocorrelations within chains indicate slow mixing, possibly poor convergence.
- *Cross–correlations* between variables.

It should be noted that no convergence diagnostic can say with certainty that a Gibbs sample is a representative of the underlying stationary distribution, as this is also stated in the CODA manual (1995). It is therefore suggested to use a combination of diagnostics to assess the convergence.

7.3. Refinements of Freeman's Bayesian Analysis using MCMC

7.3.1. Critical Review

In section 2.7, we briefly explained Freeman's Bayesian Analyses and summarised his findings for the data on the stone circles. In general, one should admit that he tackled the problem in a very efficient way, considering the profound difficulty of modelling a hypothesis of this kind with the computer power available at that time. However, his way of exploring the likely values of a quantum by means of its posterior functions was different in style compared with the Bayesian analyses being performed today by modern standards.

For example, (referring to formulation and notation in section 2.7) firstly, he assumed that σ is known and examined the behaviour of the posterior distribution by considering a grid of quantum values within the range [2, 10] with an increment of 0.05. As a result, he concluded that one should not expect to observe any quantality if σ is greater than 2. Having observed a peak at around 5.45 as well as the others, then he chose a $\chi^2_{(2)}$ prior for σ which gives more weight on values of σ smaller than 2. By this way he estimated σ for q=5.45 when only the region [5.34, 5.54] was explored.

As an example, we reproduced his posterior distribution (2.9) when applied to the good rings in Scotland (n=16) and summarised his results as a 3D representation in Fig 7.2. Note that here we used a grid of σ values over the range [0.5, 2] with an increment 0.1.

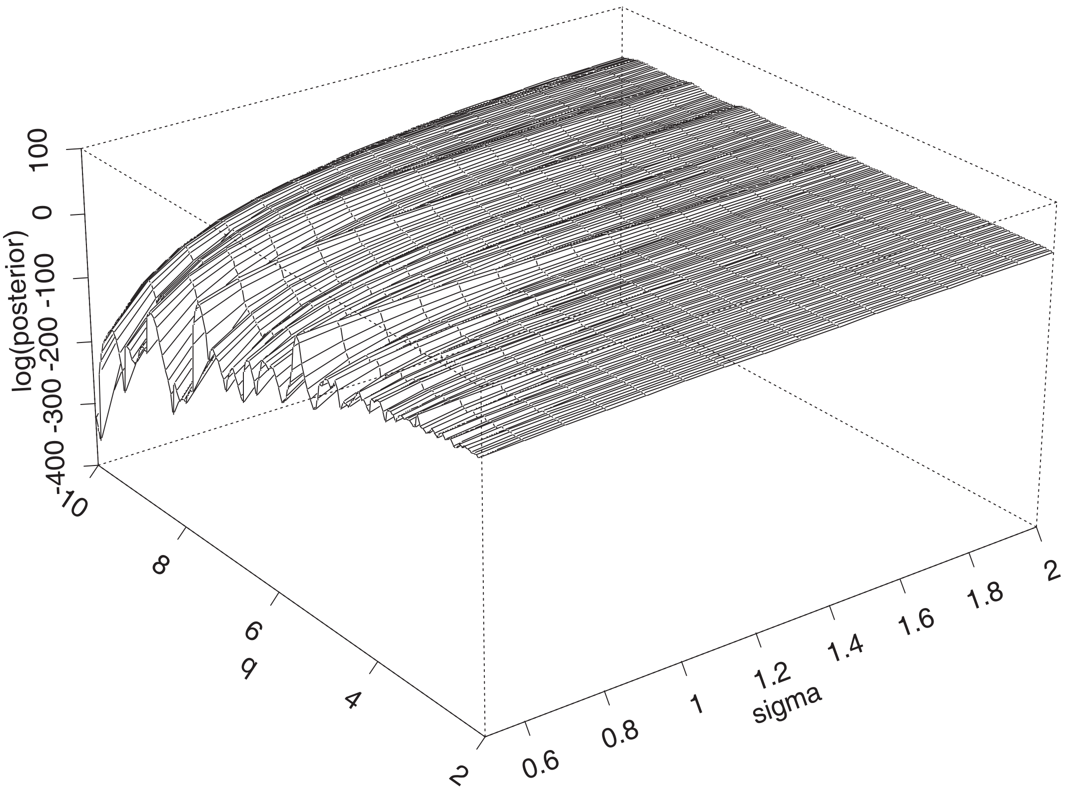

Fig 7.2. Log–posterior as a function of q and σ

Freeman's main conclusions can be clearly seen in this graph. There is no single outstanding peak, the posterior distribution is rather oscillating (see the highest peak at 5.45). The main peak tends to occur at larger values of q as σ increases. It is not expected to observe a very strong peak at the true quantum if σ is greater than 2.

It is now of our particular interest to investigate the same problem but using MCMC methods. Invoking plausible priors, the performance of MCMC methods is demonstrated in the sections below.

7.3.2. Prior Specifications

In addition to the contribution of the likelihood i.e. $f(x \mid \underline{m}, q, \sigma)$ as given in section 2.7, we assume that we have additional information available on the model parameters described by a prior distribution which takes the form

$$\pi(q, \underline{m}, \sigma) = \pi(q)\, \pi(\underline{m} \mid q)\, \pi(\sigma)$$

Discrete Uniform and Poisson distributions have formerly been considered by Freeman as possible priors for integers (see section 2.7 for details). In our analyses, we will use first a discrete Uniform prior with upper bound N=[x_{max}/q_{min}], then a truncated Poisson distribution. Truncation can be achieved in Bugs by the *I* function as

$$\pi(\underline{m} \mid q) \sim Pois(\mu)\, I(1, u)$$

where μ is as given in section 2.7 and the upper bound, u, being the integer part of x_{max}/q_{min} .

In addition to those, we will further adopt a Binomial prior in our analyses. That is,

$$\pi(\underline{m} | q, p) \sim Bin(p, n)$$

where $n = [x_{max}/q]$ and $\pi(p) \sim Be(1,1)$ defining a U(0,1) prior for *p*.

Moreover, for the parameter q, Freeman used a flat prior due to the lack of information about the distribution of q. In our analyses, we will however apply a

Uniform prior onto the reciprocal of q, say t, due to our knowledge that t is uniformly distributed. This seems a more natural choice than Freeman's. Note that in the previous chapters we have always used "τ" for the notation of the reciprocal of q. As this may be confused by the precision parameter of the Normal distribution (i.e. $\tau = \sigma^{-2}$) in Bayesian analyses, we prefer denoting the reciprocal by "t" in this chapter. Again in contrast to Freeman's analysis, we are now able to invoke a prior for the parameter σ when all the possible values of quantum are considered and perform the integration using MCMC. Therefore, we will first investigate Freeman's choice, that is

$$\pi\left(\sigma^{-2}\right) \sim Gam(1, 0.5)$$

where Gamma(1, 0.5) is of course equivalent to Freeman's prior $\chi^2_{(2)}$. (WinBugs provides facilities for modelling with the more general Gamma family rather than just the special cases of Chi–squared distributions).

We will also investigate the effect of other possible priors for the parameter σ within the framework of WinBugs.

7.3.3. Posterior Distributions

In order to investigate whether or not MCMC methods would perform well in estimating the quantum, we will make use of a small data set from circles, namely the Scottish good rings (n=16) throughout the following sections. It is our particular concern to repeat Freeman's analysis using these new techniques which allow us to apply his prior for σ when the full range of possible quantum values are investigated. Graphical representation of the BUGS model with the model specifications is illustrated in Fig 7.3. The data are again assumed to have $N(m_i q, \sigma^2)$ distribution. The precision parameter $\tau=\sigma^{-2}$ is given a Gamma prior which is equivalent to Freeman's prior $\chi^2_{(2)}$. The parameter t is given a prior U(0.1, 0.5) as it was the range of the gridsearch used so far. For the good rings data set, integers are given a discrete

Uniform prior with the upper bound being, at most, the integer part of the division x_{max}/q_{min} (or $x_{max}\, t_{max}$).

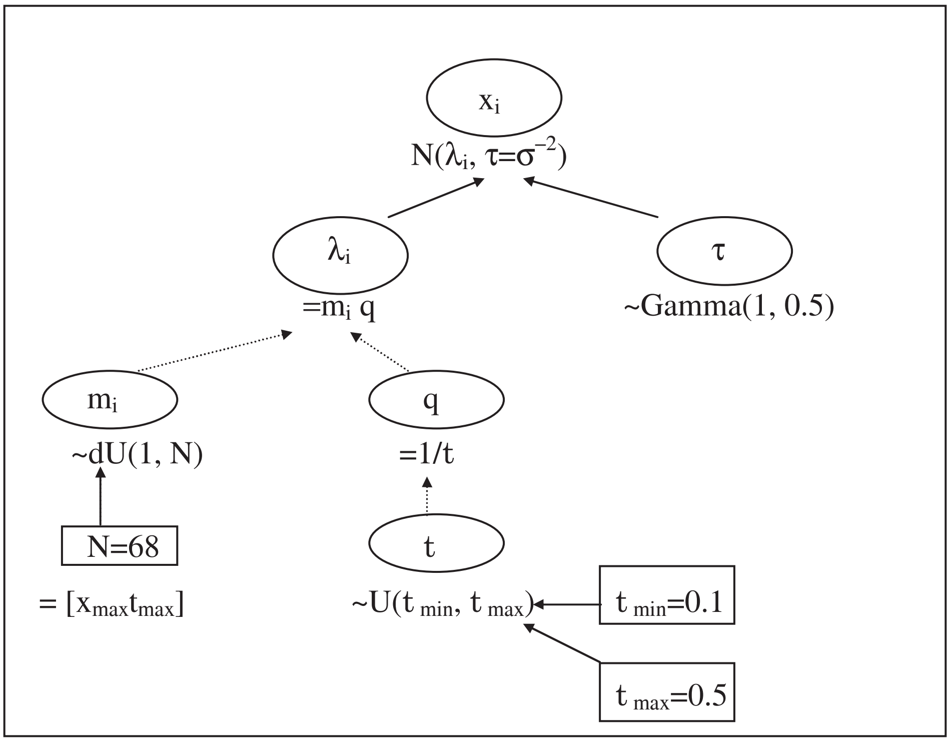

Fig 7.3. Graphical representation of simple quantal model in BUGS.

Table 7.1. Posterior summaries of each parameter (run 1).

par.	initial	pos. Mean	95% Prob.Int.	sd	# iter
t	0.16003	0.184	0.183–0.185	0.0005	5000
q	–	5.440	5.410–5.470	0.0153	5000
τ	0.67310	2.190	0.949–3.870	0.7520	5000
σ	–	0.709	0.509–1.030	0.1330	5000

A BUGS code of this graphical model which uses the Splus language received a burn–in of 500 iterates followed by a further 5000 iterations which took 2.25 minutes all together. Statistical summaries of the posterior distribution based on the last 5000 iterations for each variable have been obtained as given in Table 7.1. For the good rings, the best estimate of q is found to be 5.44 with $\sigma = 0.709$. Note that they were previously estimated as 5.44 and 0.635 respectively. True estimates of integers when q = 5.44 have also been obtained successfully but are not listed in the table. We must note that all integers were given the value of 1 as initials and this will remain the same throughout all analyses we will present in this chapter.

The next step is to assess the convergence of the estimates. Hence, the monitors of the 5000 iterations and kernel density plots of the sampled values of the model parameters are produced as in Fig 7.4. The chains seem to produce a good mixing for all. The results of the convergence diagnostic tests (see Table 7.2) suggested no convergence problems.

Table 7.2. Diagnostics of the estimates of the parameters from CODA (run 1)

	Geweke	**Raftery&Lewis**			**Heidelberger&Welch**			
Par.	***Z–score***	***M***	***N***	***I***	***test***	***# to keep***	***# to discard***	***CVM***
t	0.781	4	7032	1.88	passed	5000	0	0.155
q	–0.748	4	5215	1.39	passed	5000	0	0.152
τ	–0.830	2	3930	1.05	passed	5000	0	0.210
σ	1.160	2	3561	0.95	passed	5000	0	0.199

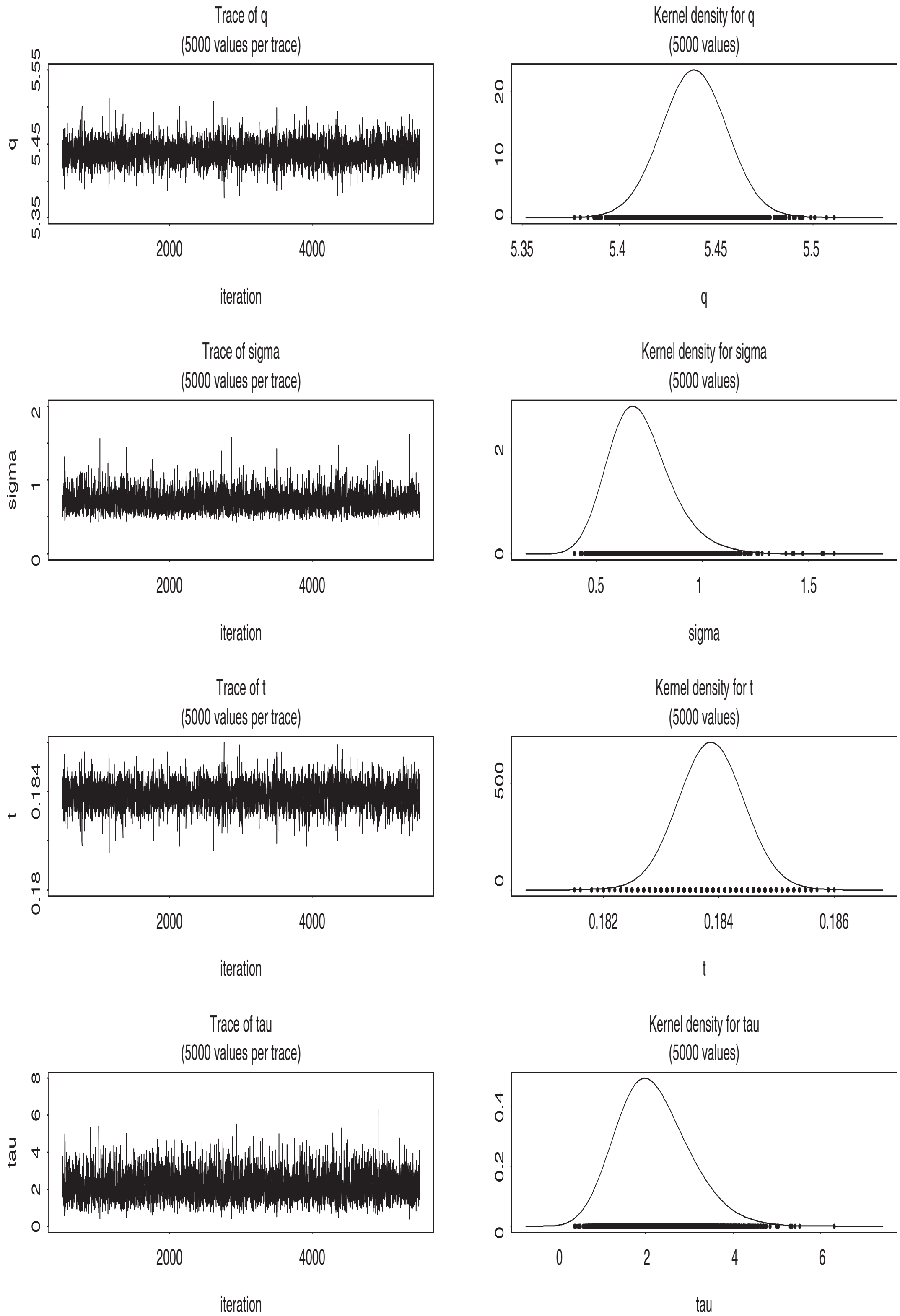

Fig 7.4. Convergence monitoring plots and kernel density plots of each variable for the Good Rings data (n=16)

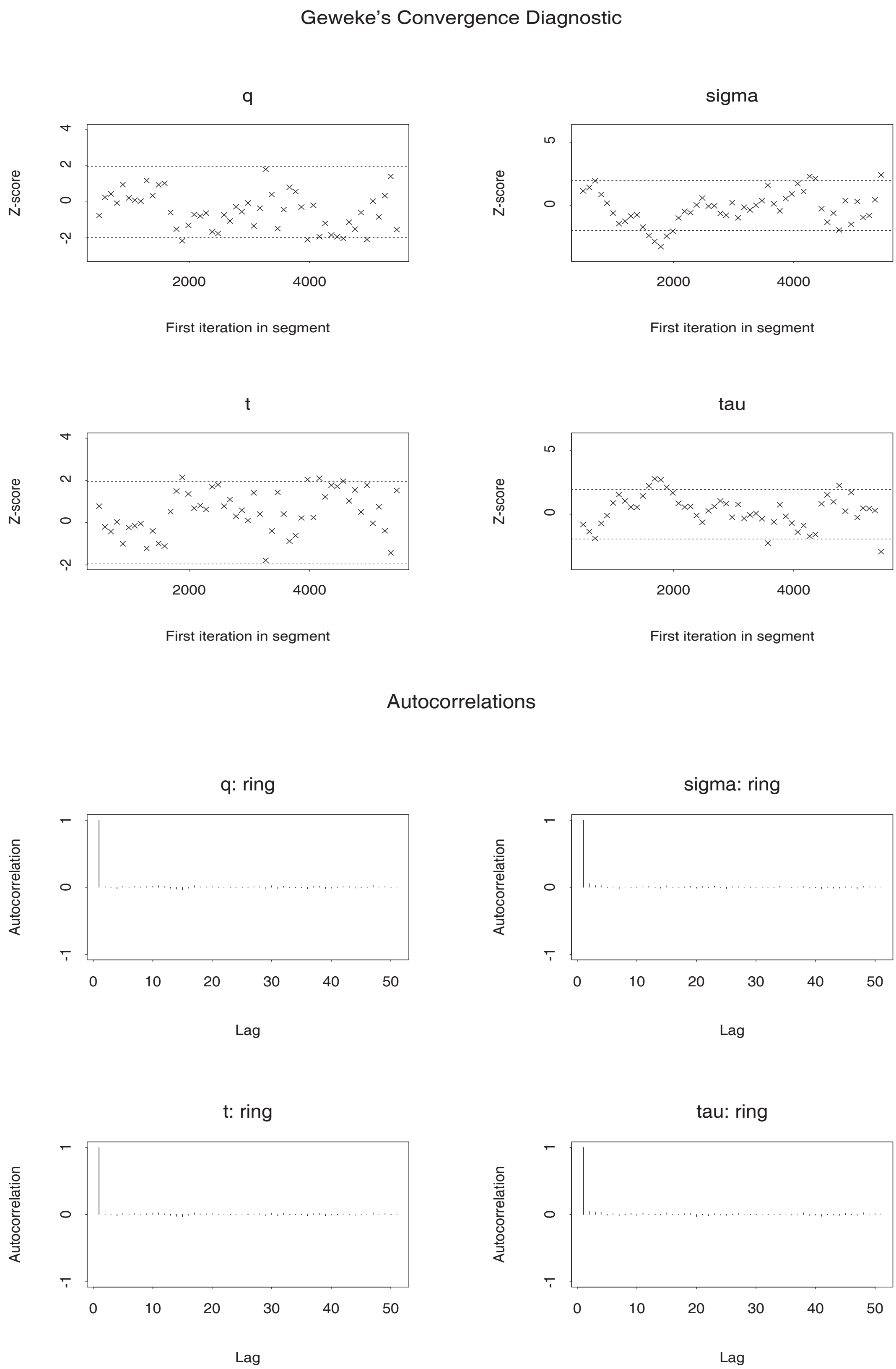

Fig 7.5. Plots of Z–scores and autocorrelations between sample values.

All Z–scores are between ± 2, and it is reported that the chain forgot its starting values, rather very quickly, after 2–5 iterations. Although the Cramer–von–Mises test accepts the convergence, the Raftery & Lewis diagnostics tool suggests an additional 2000 for t and 200 for q parameters. Note that following this suggestion did not change the estimates. Additionally, plots of Z–scores estimated in many segments of the chain are mostly within 95% probability limits and there does not appear to be any autocorrelation between sampled points.

Although the results from the diagnostic tools did not reveal any evidence against the convergence of the chains, we must note that it is not possible to say with certainty that the chains have fully converged to their stationary distributions. The basic philosophy of assessing convergence is to carry out a number of long runs from widely differing starting points and examine the result on the multiple sequences (Spiegelhalter et al, 1995). If they all lead to the same value and pass the diagnostic analyses, we can then be confident in the results obtained.

Following that, we have run the program by assigning different starting points to τ and t. This was achieved by changing the random number seed and generating an initial value for each within Bugs. Table 7.3 presents a summary of posterior means and approximate 95% probability intervals for various runs, as well as the convergence diagnostics obtained from the converged part of the chain (i.e. discarding first 500 iterations). A failure to pass a test is denoted by a cross or by a tick if otherwise.

An inspection of the results indicates that the chain does not always converge to the same value. This is not very surprising as any quantal problem may have multiple solutions. In fact, if there is any quantal effect in the data, then any posterior is expected to give some signs of quantality at some rational multiples (Freeman, 1976), which makes the posterior distribution multimodal. The results of five runs present this effect very clearly. First of all, an encouraging outcome is that 7.48 with σ=1.371 is estimated as a quantum, which is consistent with Freeman's conclusion that the value of 7.45 or 7.50 is an alternative quantum to 5.45 when σ is around 1.4. Convergence diagnostics for these estimates (in run 2) suggested that the chains for all the parameters have probably converged. In addition to 7.48, most of the additional runs have recovered the most probable value of quantum, 5.439, with good convergence results. For those, however, one must notice an important feature which is the closeness of the initial values of t =1/q to their real estimates. This implies that we can obtain the expected quantum values only if the chains get initialised very closely around them. We must emphasise here that all initial values used in this chapter were generated in Bugs, none of them are assigned by us.

Table 7.3. Posterior summaries and convergence diagnostics for different runs.
Geweke ✓⇨ |Z|–scores < 2, **R**aftery&**L**ewis ✓⇨ $I < 5$, **H**eidelberger&**W**elch ✓⇨ passed

Run	Burn–in	Par.	Initial	Mean	95% Prob.Int.	G	R–L	H–W
2	500	t	0.13414	0.1337	[0.1323,0.1352]	✓	✓	✓
		q	–	**7.480**	[7.395,7.559]	✓	✓	✓
		τ	0.33128	1.371	[1.034,1.707]	✓	✓	✓
		σ	–	0.5861	[0.3437,0.9346]	✓	✓	✓
3	500	t	0.17907	0.1839	[0.1829,0.1849]	✓	✓	✓
		q	–	**5.439**	[5.409,5.468]	✓	✓	✓
		τ	1.43805	2.194	[0.9525,3.951]	✓	✓	✓
		σ	–	0.7083	[0.5032,1.025]	✓	✓	✓
4	500	t	0.13357	0.1839	[0.1828,0.1849]	✓	✓	✓
		q	–	**5.439**	[5.409,5.469]	✓	✓	✓
		τ	0.34415	2.190	[0.9752,3.890]	✓	✓	✓
		σ		0.707	[0.5072,1.013]	✓	✓	✓
5	500	t	0.31345	0.4297	[0.3156,0.4986]	✗	✗	✗
		q	–	**2.395**	[2.006,3.168]	✗	✗	✗
		τ	0.57030	1.430	[0.087,4.058]	✓	✗	✗
		σ	–	1.172	[0.4965,3.387]	✓	✓	✓

The results of run 4 in Table 7.3 presents an interesting picture. Although the parameter t is initialised around 0.133 (i.e. q=7.48), we have obtained q as 5.439. A closer look at the trace of q from the first iteration in Fig 7.6. reveals that the chain stayed at around 7.5 for a while and then managed to jump to the state of q=5.44 at just about the burn–in time.

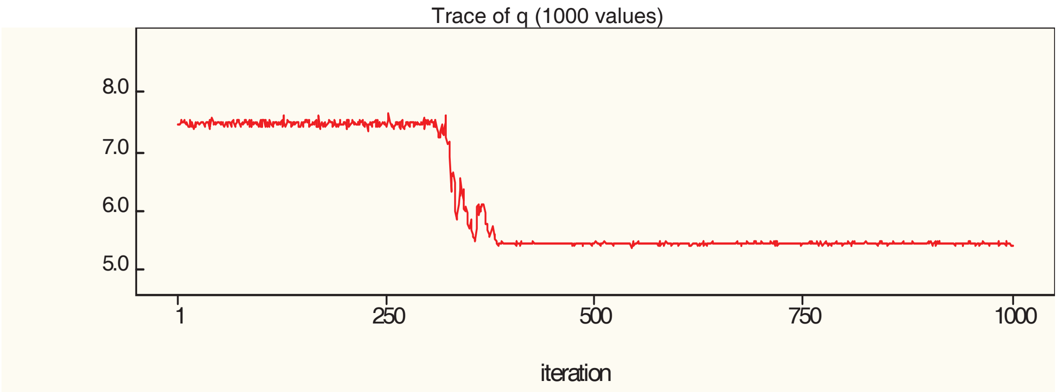

Fig 7.6. Trace of first 1000 iterations for q (4th run in table 7.3)

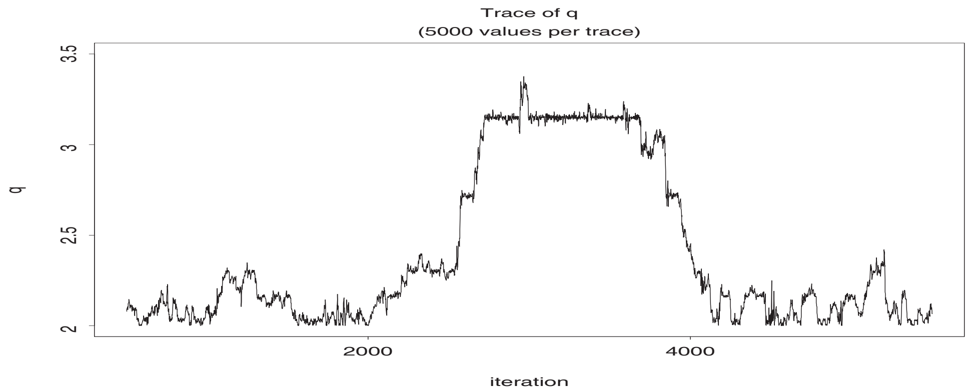

Fig 7.7. Trace of 501:5500 iterations for q (5th run in table 7.3)

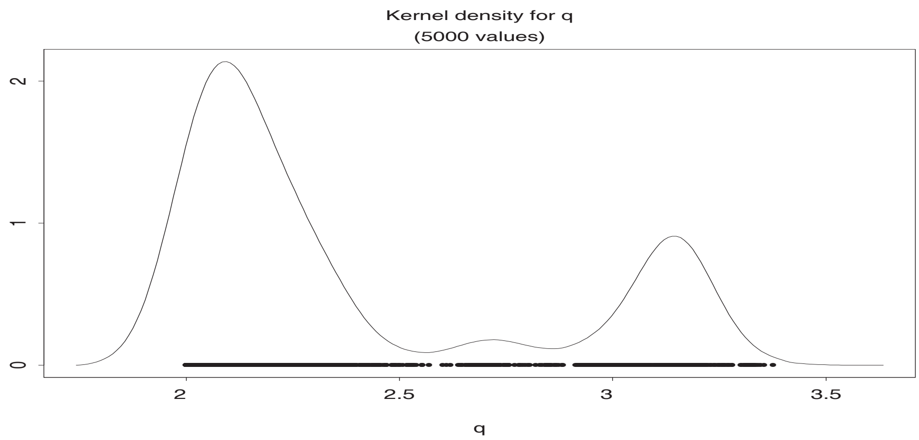

Fig 7.8. Kernel plot of 501:5500 iterations for q (5th run in table 7.3)

Moreover, run 5 shows that the analysis could lead us also to incorrect inferences when the initial value is far away from the true quantum value. In such cases, however, the chains fail the convergence diagnostic tests by producing poor mixing with high autocorrelation. The effect of multimodality again appears in the chain of q (see in Fig 7.7 and Fig 7.8), proving that the chain does not move freely in the q parameter space.

In order to investigate the impact of the discrete Uniform prior used for integers so far, we shall consider other discrete distributions as well. Poisson and Binomial distributions are chosen for that purpose and the rest of the model specifications are kept the same. As a result of various trials, we have observed that it is only possible to estimate q=5.44 or 7.5 if both $t=q^{-1}$ and $\tau=\sigma^{-2}$ are initialised very closely around the exact values of both q and σ. Otherwise, the chain for parameter τ tends to settle around a very small value (i.e. σ very big), which results in proposing the largest possible q value as the true estimate. Those values can however be ruled out by right truncating the Gamma prior of τ. However, we have encountered great difficulty in performing the analyses in WinBUGS (version 1.2) with a truncated Gamma prior, and this is perhaps not surprising since the manual warns against truncating the Gamma distribution. Therefore, it is necessary to choose another restricted prior for the precision parameter and one way of doing so is illustrated in the next subsection.

7.3.3.1. Uniform Prior on Standard Deviation (σ)

An alternative choice of informative prior distribution for σ can be made by taking a uniform distribution with a “sensible” range. This way, we can ensure that the posterior distribution is constrained to the same range.

In the discussion part of Freeman’s paper, Crawford (1976) pointed out that the maximum allowable value for σ is 1.5 rather than 2, otherwise true quantum can no longer be found for circles. Basing our choice of sensible range on this statement, we will adopt U(0, 1.5) prior on the parameter σ. The lower bound being equal to “0” causes crashes in BUGS, due to the calculation of $\tau = 1/[0,\ 1.5]^2$. One way of overcoming this problem is to assign a Pareto(1/2, 1.5^{-2}) distribution to the precision parameter τ instead. However, the Pareto distribution is not available yet in WinBUGS. In our application, we have therefore remedied this technical problem by replacing “0” with “0.00001”.

To begin with, we again assume a discrete Uniform prior for integers, m_i, but the Uniform prior for the standard deviation, σ as mentioned before. Table 7.4 summarises the results for several runs as before. The overall picture is very much the same as before. Signs of quantality at values q=7.479 and q=5.439 is again observed. However, it is clear that these values can be estimated only if the model is initialised closely around the actual values. The effect of the posterior distribution being multimodal is illustrated in run 3 in the same table. By just looking at the initial values, one may expect to estimate q=5.4 due to the initial value of t being very close to the reciprocal of q=5.4, at the same time q=7.5 seems to be also possible solution due to the initial of σ being very close to σ=1.4. As a result, run 3 has made an incorrect estimation that failed some of the convergence criteria.

Table 7.4. Posterior summaries and convergence diagnostics for different runs when integers are given discrete Uniform prior.

Geweke ✓⇨ |Z|–scores < 2, **R**aftery&**L**ewis ✓⇨ $I < 5$, **H**eidelberger&**W**elch ✓⇨ passed

Run	Burn–in	Par.	Initial	Mean	95% Prob.Int.	G	R–L	H–W
1	500	t	0.12391	0.1337	[0.1324,0.1352]	✓	✓	✓
		q	–	7.479	[7.399,7.553]	✓	✓	✓
		σ	0.7633	1.31	[1.025,1.491]	✓	✓	✓
		τ	–	0.6017	[0.4497,0.9519]	✓	✓	✓
2	1500	t	0.25515	0.1839	[0.1828,0.1849]	✓	✓	✓
		q	–	5.439	[5.408,5.469]	✓	✓	✓
		σ	0.7323	0.7351	[0.5079,1.0920]	✓	✓	✓
		τ	–	2.067	[0.8398,3.878]	✓	✓	✓
3	500	t	0.15795	0.165	[0.16,0.17]	✓	✗	✗
		q	–	6.070	[5.88,6.26]	✓	✗	✗
		σ	1.4023	1.390	[1.17,1.50]	✓	✓	✓
		τ	–	0.524	[0.446,0.729]	✓	✓	✓

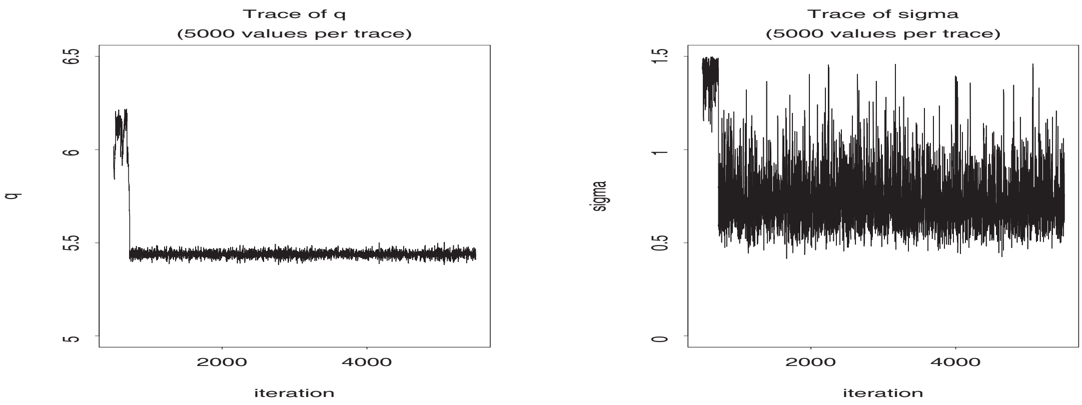

Fig 7.9. Trace of the chains for q and σ (run 4)

Since, not all the parameters of run 3 failed the convergence criteria, a next attempt could be to use these results as initial values of a new run and update the model using a new random number seed. The result of this approach is presented in Fig 7.9. Traces of the chains for q and σ show that the chains managed to escape the previous values and estimated real actual values that are $q \cong 5.4$ and $\sigma \cong 0.7$.

In order to investigate the impact of the priors for integers, we next adopt a truncated Poisson prior for them. Amongst many trial runs, we obtained the actual estimates only if the model was initialised very closely to the true values (see Table 7.5). Most of the time, it was observed that the chain for q tends to fall in the extreme bounds of the q values. We can conclude that it shows the weakest performance in detecting quantality.

Table 7.5. Posterior summaries and convergence diagnostics when integers are given a truncated Poisson prior

Geweke ✓⇨ $|Z|$–scores < 2, **R**aftery&**L**ewis ✓⇨ $I < 5$, **H**eidelberger&**W**elch ✓⇨ passed

Run	Burn–in	Par.	Initial	Mean	95% Prob.Int.	G	R–L	H–W
1	500	t	0.18496	0.1836	[0.1827,0.1845]	✓	✓	✓
		q	–	**5.446**	[5.421,5.474]	✓	✓	✓
		σ	0.10028	0.6195	[0.4584,0.8633]	✓	✓	✓
		τ	–	2.807	[1.342,4.762]	✓	✓	✓

Another possible prior for integers is a Binomial distribution. Table 7.6. demonstrates the statistical summaries of posterior distributions for various runs again as well as convergence diagnostics. It can be seen that the estimated quantum values are consistent with the ones previously obtained when integers were given discrete Uniform prior. One noticeable result is that the chains exhibit less dependency on the initial values. No matter how dispersed they are the Gibbs sampler was not prevented from reaching equilibrium, estimating the most probable values.

Table 7.6. Posterior summaries and convergence diagnostics for different runs when integers are given a Binomial prior.

Geweke ✓⇨ $|Z|$–scores < 2, **R**aftery&**L**ewis ✓⇨ $I < 5$, **H**eidelberger&**W**elch ✓⇨ passed

Run	Burn–in	Par.	Initial	Mean	95% Prob.Int.	G	R–L	H–W
1	500	t	0.3490	0.1843	[0.1838,0.1851]	✓	✓	✓
		q	–	**5.427**	[5.403,5.44]	✓	✓	✓
		σ	1.4985	0.731	[0.5102,1.0830]	✓	✓	✓
		τ	–	2.091	[0.8538,3.844]	✓	✓	✓
		p	0.4795	0.433	[0.3844,0.4803]	✓	✓	✓
2	500	t	0.4371	0.1337	[0.1326,0.1350]	✓	✓	✓
		q	–	**7.479**	[7.407,7.542]	✓	✓	✓
		σ	1.1882	1.311	[1.035,1.491]	✓	✓	✓
		τ	–	0.5999	[0.1326,0.1350]	✓	✓	✓
		p	0.62043	0.4378	[0.3818,0.4939]	✓	✓	✓

7.4. Hierarchical Bayesian Models for Structural Quantality

Many statistical applications involve multiple parameters that can be regarded as related or connected in some way by the structure of the problem, implying that a joint probability model for these parameters should reflect the dependence among them. Such parameters can be related to each other in a natural way if we use a prior distribution in which the parameters are viewed as a sample from a common population distribution. It is natural to model such a problem hierarchically, with observable outcomes modelled conditionally on certain parameters, which themselves are given probabilistic specification in terms of further parameters, known as *hyperparameters* (Gelman et al. 1995). In such a case, it is said that we have a hierarchical prior for unknown parameters.

Such hierarchical thinking helps in modelling our structural and subjective prior information at stages. The first stage prior description is used to model the structural relationship among the parameters, leading us to a class of hyperparameters. At the second stage, hyperparameters are chosen priors according to our subjective beliefs.

As an alternative way of constructing hierarchical quantality, we will therefore express our expectation that quantal values are close to each other through a Hierarchical Bayes model formulation which conditions that the values arise from a distribution whose variance is *a priori* formulated as being very small.

7.4.1. Model Specifications for Hierarchical Quantality

Suppose we have p data sets of equal size n (i.e. $\underline{x}=\left(\underline{x}_1,\ldots,\underline{x}_p\right)$) each of which is assumed to be quantal. Under the hierarchical quantum model 5.1, the data are distributed as

$$\underline{x}_j \mid q_j, \underline{m}_j, \sigma_j \sim N\left(q_j\, \underline{m}_j, \sigma_j^2 I_n\right)$$

where $j = 1, \ldots, p$.

Then the likelihood function is

$$f\left(\underline{x} \mid \underline{m}, q, \sigma\right) = \prod_{j=1}^{p}\left(\frac{1}{\sqrt{2\pi}\,\sigma_j}\right)^n exp\left\{-\sum_{i=1}^{n}\left(x_{ij}-m_{ij}\,q_j\right)^2 \Big/ 2\,\sigma_j{}^2\right\}$$

Prior distributions of integers and standard deviations could be defined as before. The q parameters from p experiments are however believed to be ‘close’ to each other. Assuming that q values are independently and identically distributed, this belief could be incorporated into the analyses through a hierarchical prior with π_1 and π_2 denoting the first and second stage priors respectively in the following form:

$$\pi_1(q|\lambda) \sim \prod_{j=1}^{p} N(\mu_q, \tau_q), \quad \text{where } \lambda = (\mu_q, \tau_q)$$

$$\pi_2(\lambda) = \pi(\mu_q)\,\pi(\tau_q), \text{ where } \pi(\mu_q) \text{ is vague and } \pi(\tau_q) \sim Ga(\alpha, \beta)$$

In the hierarchical prior above, we assumed that q values are drawn from a Normal distribution with hyperparameters μ_q and τ_q. It must be noted that the prior above needs to be restricted to the range of plausible quantum values (i.e. $[q_{min}, q_{max}]$) and this is achieved by the truncation function *I* in Bugs again (see Fig 7.10). The second stage priors are chosen such that we express our theory that quantum values vary closely around a mean value. Since the combined data from all p experiments would be highly informative about μ_q, we can afford to be vague about its prior. Thus, we invoked a $N(\mu, \tau)$ prior with $\mu=0$ and $\tau=0.001$. The α and β parameters however are to be chosen so that the variation amongst the q parameters is small. Following the Bayes theorem and combining the sampling distribution for observables (x_{ij}) and the prior distributions, the joint posterior distribution of all the parameters and the hyperparameters is obtained as

$$f\left(q, m, \sigma, \mu_q, \tau_q \,\middle|\, x\right) \propto f\left(x \,|\, q, \underline{m}, \sigma\right) \pi(\underline{m})\, \pi(\sigma)\, \pi_1(q\,|\,\lambda)\, \pi_2(\lambda)$$

$$\propto \prod_{j=1}^{p} \prod_{i=1}^{n} \sum_{m_{ij}}^{N} N\left(x_{ij} \,\middle|\, q_j, m_{ij}, \sigma_j\right) U(1, N)\, N_p\left(q_j \,\middle|\, \mu_q, \tau_q\right) N(0, 0.001)\, Ga(\alpha, \beta)$$

Marginal posterior densities of the individual parameters require us to integrate the product above, which is very difficult. Therefore, we again envisage to perform the analyses devising the MCMC methods within the framework of BUGS.

7.4.2. The Assumption of Exchangeability

If no information, other than the response data, is available to distinguish between the effects of each parameter (θ_i) from each unit, we must assume exchangeability (symmetry) among the parameters in their prior. That is to say that $P(\theta_1, \theta_2, \ldots, \theta_n)$ is invariant to permutations of the indexes $(1, \ldots, n)$. In other words, the distribution is exchangeable if reordering $(\theta_1, \theta_2, \ldots, \theta_n)$ does not change the probability distribution.

When attempting to construct a hierarchical model for the root spacings, there is no reason to think that quantum values of roots systematically differ from each other but we do not believe they are the same either. Therefore, it is sensible to think that the assumption of exchangeability holds in the forthcoming Hierarchical Bayesian analyses.

7.4.3. A Simulation Study

In pursuing an investigation of hierarchical quantality, we will present our proposal, the Hierarchical Bayesian model, on a simulated data. For this study, there are assumed to be 3 sets of data having three quantum values slightly differing from each other. Those are fixed as $q_1 = 5.35$, $q_2 = 5.44$ and $q_3 = 5.49$. Each set has an equal sample size that is chosen as 30 (i.e. 90 observations in total). Integers are again randomly selected from the Scotland good circles data set. Along with these model specifications, errors are generated from $N(0, 0.001^2)$ for each set and a hierarchical quantal data set is constructed in the form of (5.1).

Using this data set, we will now apply our ideas in constructing a Bayesian analysis and investigate the behaviour of the outcomes under different scenarios. Model specifications and relationships between parameters used in BUGS can be represented in a graphical form as in Fig 7.10.

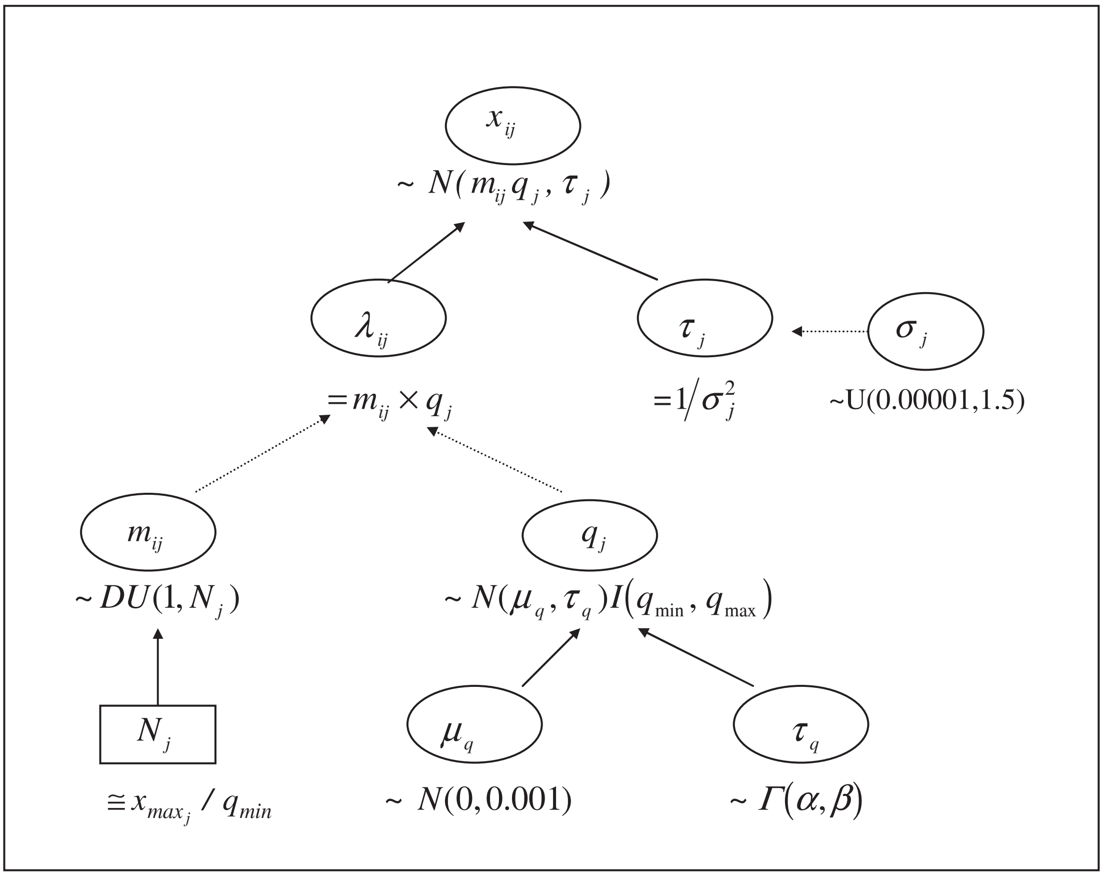

Fig 7.10. Graphical representation of the Hierarchical Bayesian model for the hierarchical quantality.

The data are again assumed to come from a Normal distribution. Integers are given a discrete Uniform distribution with upper bound depending on the maximum observation and lower bound of the quantum range. For the standard deviations σ_j, we adopt an informative Uniform prior as before. Since we have no *priori* knowledge about the distributional form of the set of quantum parameters, it is found reasonable to suppose that it has the most standard form. Therefore we choose a

Normal prior which is particularly suitable for performing the second stage analysis with hyperparameters on its parameters μ_q and τ_q. As mentioned before, the mean μ_q could be estimated using all the data, that is to assign a vague prior (i.e. N(0, 0.001)) to this parameter. Meanwhile, the precision parameter, τ_q, is given a Gamma prior with the hyperparameters α and β which are of interest mainly as tools in estimating q_j's as well as possible. This is the stage when we could express our subjective beliefs for the q parameters, that is they are close to each other.

To begin with, we choose α=160000 and β=400, which gives a mean of τ as 400 (i.e. σ=0.05) and a variance of 1. A WinBugs code of this Hierarchical model was initialised with the values listed in Table 7.7. Note that all integers were assigned an initial value of 1 as before. It must be also emphasised that initial values of q_1, q_2, q_3 and σ_1, σ_2, σ_3 were generated in WinBugs by changing the random number seed. This model then received a burn–in of 500 iterates followed by a further 5000 iterations. As well as statistical summaries of posterior distribution, convergence diagnostics for each variable, based on the last 5000 iterations, are demonstrated in Table 7.7.

The first run in the table shows that MCMC methods performed well in estimating the true quantum values as well as standard deviations (and also integers). Figures 7.11.(a), (b) and 7.12 presents the monitors of the chains and kernel density plots of the sampled values for the model parameters. All chains show good mixing and all the autocorrelations are negligible. In addition they passed all the convergence diagnostic provided by CODA (see Table 7.7 run 1), indicating that they have fully converged to their true posterior distributions.

The second run in the table has been performed by re–generating initial values for q_1, q_2, q_3 and σ_1, σ_2, σ_3 parameters. Inspection of the results shows that the estimated quantum values are varying around a mean value of 3.6 this time. Although we have not recovered the true values, it is noticeable that estimated mean value is equal to a rational fraction of the true mean value (e.g. 5.4 = 1.5×3.6). The chains from this run however indicates some convergence problems. Especially, the chains in relation to the quantum values fail convergence diagnostics. On the other hand, the Raftery and

Lewis convergence diagnostic indicates that these convergence problems can be alleviated by thinning the chain by 3 for q_j's and by 2 for μ_q. Thinning by n means recording the sampled values of the parameters every n^{th} iterations. This approach requires one to run the chain for much longer. Thus, we repeated the analysis by following this suggestion and also by performing 15000 iterations. As a result, almost the same values of the parameters have been estimated but with no convergence problems. This implies that 3.6 could provide a good fit as well. Although this result is encouraging, it is not fully satisfying as we have not recovered the true values.

Therefore, we continued the analysis from where it was left in the second run. In other words, a third run has been performed by initialising the parameters by the estimated values of the second run and updating the model parameters using different random number seed. It was of interest to investigate whether or not true values could be reached when starting from their some fraction which might also be considered as a possible solution. The outcome of this approach is remarkable. The chains achieved their correct values from slightly incorrect starting values. Additionally, the resulting chains have passed all the convergence diagnostics, leading us to the conclusion that they have fully converged.

In addition to the runs illustrated here, we have performed many repetitions of the same analyses, starting the sampling process from different initial values. Most of the time, we have either obtained the true estimates or a fraction of them (e.g. 3.6). In the latter case, we have applied the same approach as in run 3 and managed to reach back to the true values. Of course in practical situations where we do not know the true values, we would not be able to distinguish between the 'true' quantum and simple or rational fractions of it. This analysis would only suggest possible quantal effects but would not provide whether or not quantum model is appropriate. In practice, it would be desirable to examine which of the suggested values provide a better fit to the data. Gelman et al. (1992) suggest series of model checking functions which can be calculated for each observation, involving a comparison of the observation with a predictive distribution, however, this was not pursued here.

Table 7.7. Posterior summaries and their diagnostic test results for different runs when τ_q ~ Gamma(160000, 400).

Geweke ✓⇨ $|Z|$–scores < 2, **R**aftery&**L**ewis ✓⇨ $I < 5$, **H**eidelberger&**W**elch ✓⇨ passed

Run	Burn–in	Par.	Initial	Mean	95% Prob.Int.	G	R–L	H–W
1	500	mq	1	5.43	[5.37, 5.48]	✓	✓	✓
		q_1	3.5386	**5.35**	[5.35,5.35]	✓	✓	✓
		q_2	2.7351	**5.44**	[5.44,5.44]	✓	✓	✓
		q_3	2.0682	**5.49**	[5.49,5.49]	✓	✓	✓
		τ_1	–	852000	[462000, 1350000]	✓	✓	✓
		τ_2	–	884000	[473000, 1400000]	✓	✓	✓
		τ_3	–	227000	[124000, 356000]	✓	✓	✓
		σ_1	1.2313	0.0011	[0.00086,0.00147]	✓	✓	✓
		σ_2	0.7357	0.0010	[0.00084,0.00145]	✓	✓	✓
		σ_3	0.2154	0.0021	[0.0016,0.0028]	✓	✓	✓
		τ_q	1	400	[398, 402]	✓	✓	✓
		σ_q	–	0.05	[0.0499,0.0501]	✓	✓	✓
2	500	mq	1	3.60	[3.528,3.672]	✗	✓	✗
		q_1	3.1568	**3.573**	[3.541,3.633]	✗	✗	✓
		q_2	2.3372	**3.595**	[3.530,3.689]	✗	✗	✓
		q_3	2.2474	**3.635**	[3.516,3.689]	✗	✗	✗
		τ_1	–	1.18	[0.4977,2.061]	✗	✓	✓
		τ_2	–	1.02	[0.4697,1.952]	✓	✓	✓
		τ_3	–	1.08	[0.4791,1.919]	✗	✓	✓
		σ_1	1.4985	0.964	[0.6967,1.418]	✗	✓	✓
		σ_2	0.9338	1.046	[0.7158,1.459]	✓	✓	✓
		σ_3	0.1001	1.011	[0.7222,1.445]	✗	✓	✓
		τ_q	1	400	[398,402]	✓	✓	✓
		σ_q	–	0.05	[0.0498,0.0501]	✓	✓	✓
3	500	mq	3.60	5.426	[5.369, 5.484]	✓	✓	✓
		q_1	3.573	**5.35**	[5.35,5.35]	✓	✓	✓
		q_2	3.595	**5.44**	[5.44,5.44]	✓	✓	✓
		q_3	3.635	**5.49**	[5.49,5.49]	✓	✓	✓
		τ_1	–	859100	[484300, 1352000]	✓	✓	✓
		τ_2	–	890500	[494000, 1404000]	✓	✓	✓
		τ_3	–	225900	[126200, 358900]	✓	✓	✓
		σ_1	0.964	0.0011	[0.00086,0.00143]	✓	✓	✓
		σ_2	1.046	0.0010	[0.00084,0.00142]	✓	✓	✓
		σ_3	1.011	0.0021	[0.00167,0.00281]	✓	✓	✓
		τ_q	400	400	[398, 402]	✓	✓	✓
		σ_q	–	0.05	[0.0498,0.0501]	✓	✓	✓

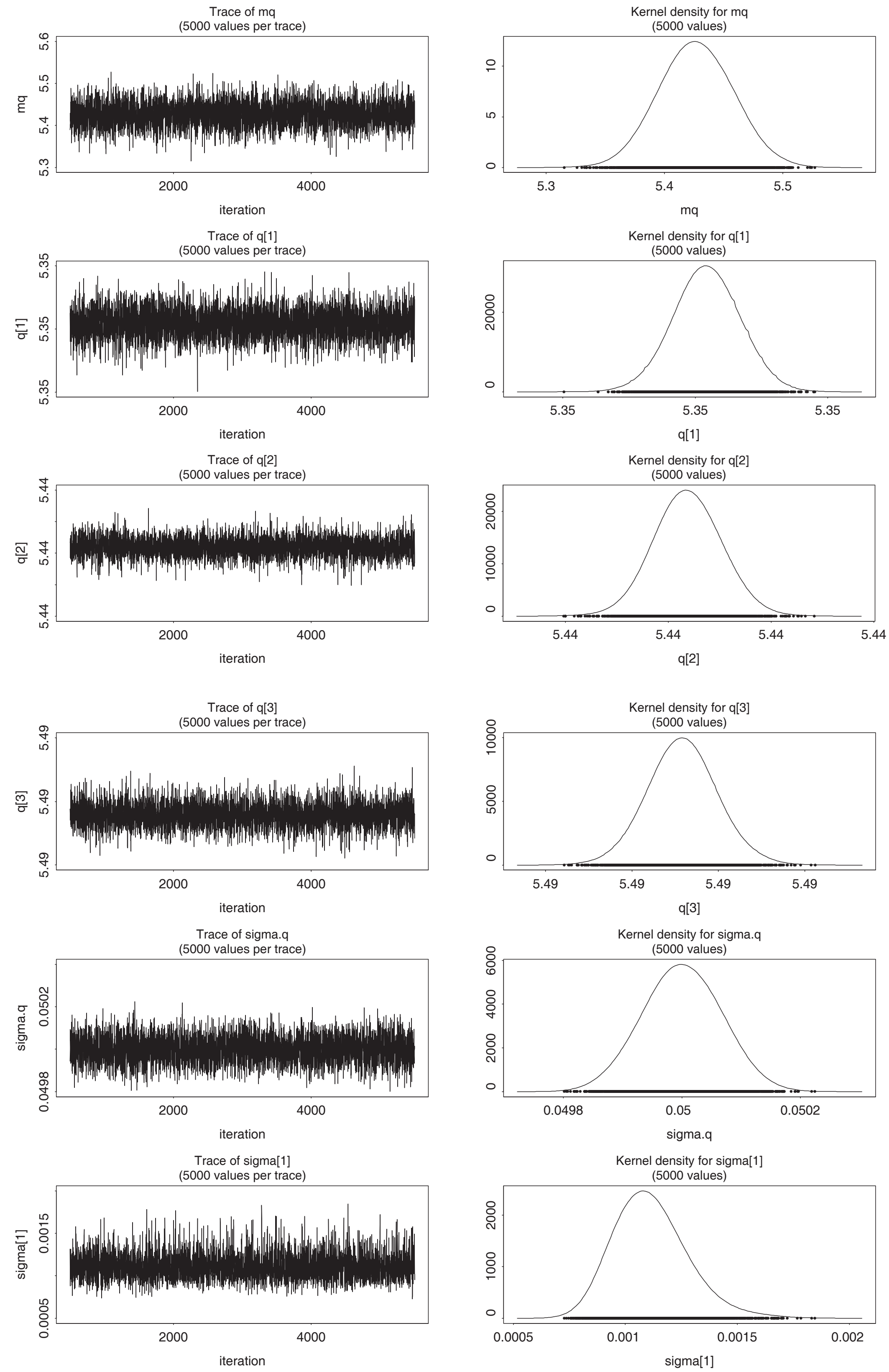

Fig 7.11. (a) Convergence monitoring plots and kernel density plots of each variable in Hierarchical Bayesian model for run 1 in table 7.7.

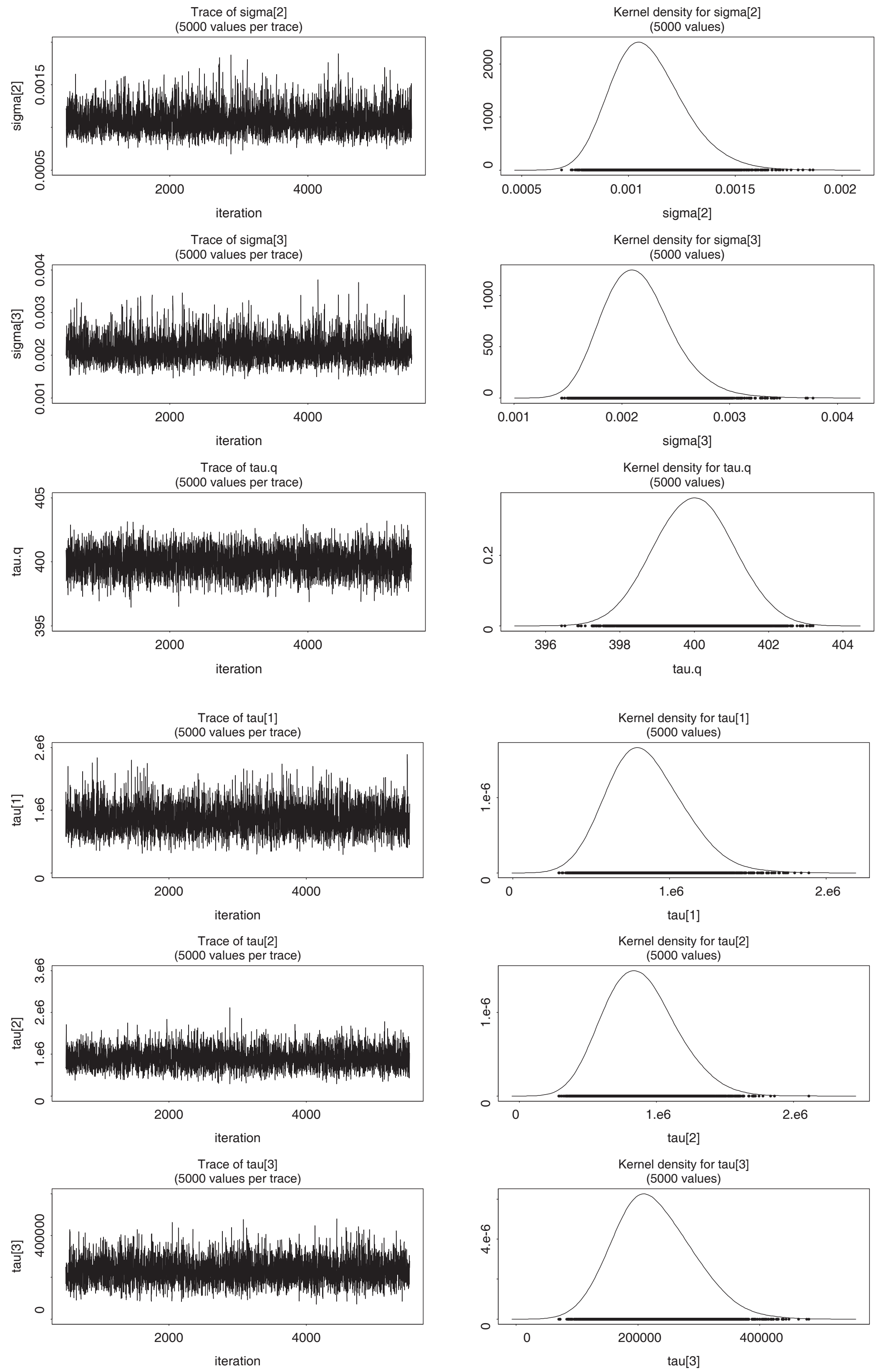

Fig 7.11. (b) Convergence monitoring plots and kernel density plots of each variable in Hierarchical Bayesian model for run 1 in table 7.7.

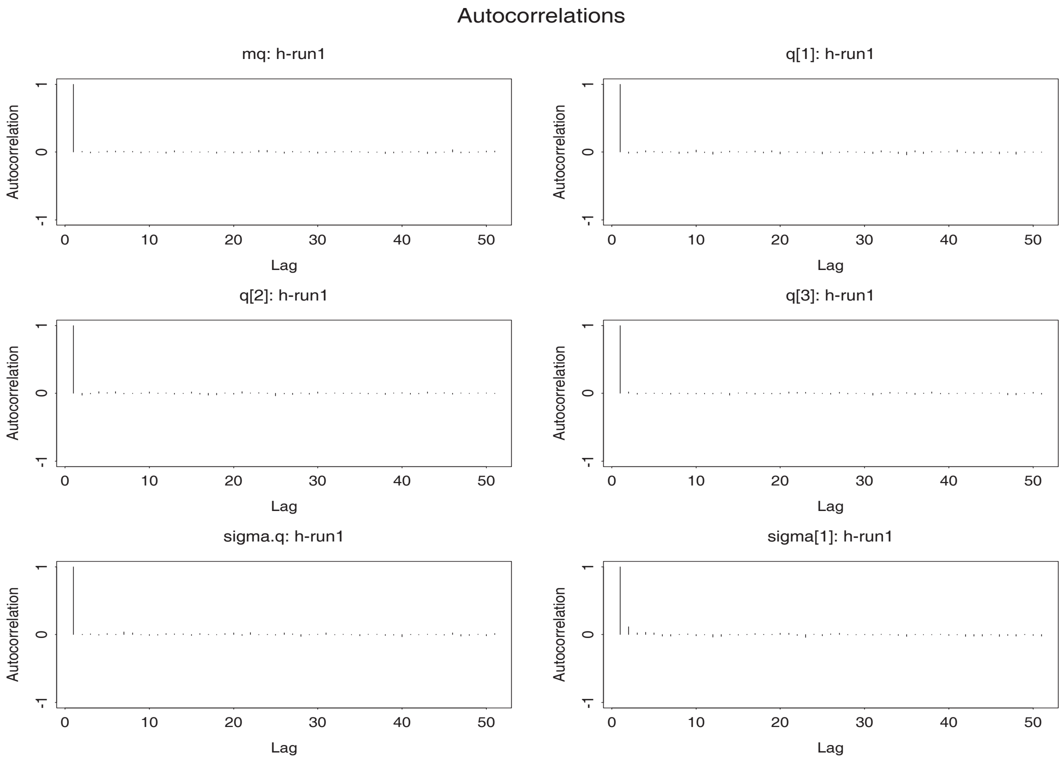

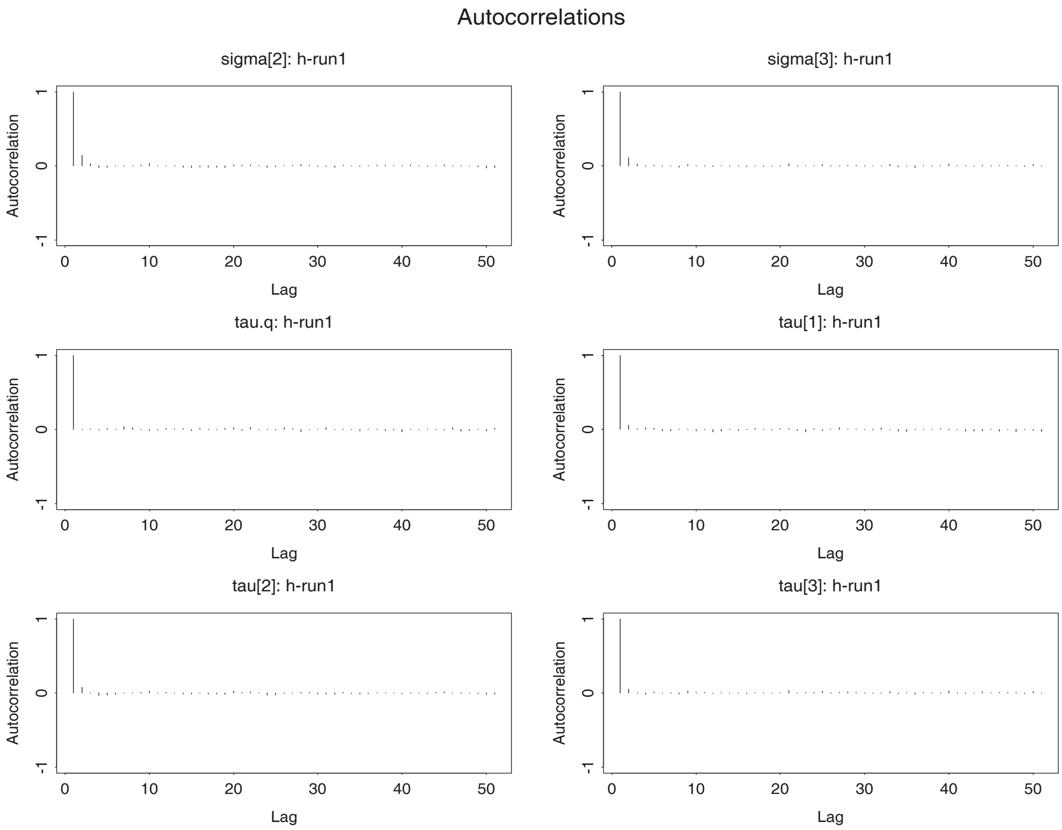

Fig 7.12. Plots of autocorrelations for each variable in Hierarchical Bayesian model for run 1 in table 7.7.

We have so far conducted a Hierarchical Bayesian Analysis assuming that the variation among any quantum values are around 0.05. In reality, however, we know neither where quantum values lie nor how large the variation among them could be. Therefore, we will now consider a smaller variation for quantum values and investigate the outcome when the same simulated data are used.

For this study, τ_q is hence given $Gam(400000, 625)$ defining approximately a variation of 0.04 instead. The model in Fig 7.10 with this new prior on τ_q is initialised and statistical summaries of the resulting posterior for each parameter are obtained as given in Table 7.8.

Table 7.8. Posterior summaries and their diagnostic test results for a run when τ_q ~ Gamma(400000, 625)

Geweke ✓⇨ $|Z|$–scores < 2, **R**aftery&**L**ewis ✓⇨ $I < 5$, **H**eidelberger&**W**elch ✓⇨ passed

Run	Burn–in	Par.	Initial	Mean	95% Prob.Int.	G	R–L	H–W
1	500	mq	1	2.713	[2.670,2.758]	✗	✗	✗
		q_1	2.1812	**2.675**	[2.675, 2.675]	✗	✗	✗
		q_2	2.9061	**2.720**	[2.72,2.72]	✗	✗	✗
		q_3	2.8043	**2.745**	[2.745,2.745]	✗	✗	✗
		τ_1	–	741700	[406400,984200]	✗	✗	✗
		τ_2	–	752300	[456400,985000]	✗	✗	✗
		τ_3	–	219200	[122300,348100]	✗	✗	✗
		σ_1	0.3281	0.00119	[0.001,0.0015]	✗	✗	✗
		σ_2	0.8589	0.00118	[0.001,0.0014]	✗	✗	✗
		σ_3	1.5859	0.00221	[0.0016,0.0028]	✗	✗	✗
		σ_q	–	0.039	[0.03947,0.03959]	✗	✗	✗
		τ_q	1	640	[638.1,641.8]	✗	✗	✗

It is clearly seen that the estimated values are again at around a fraction of the true values. In fact, the mean value 2.713 is almost half of the mean value of the actual quantum values. Since the simulated data are strongly quantal, it is not surprising to observe that half of the quantum fits the data as perfectly well as the actual quantum. That is also the reason why we could not recover the true quantum values when these estimated values of parameters were used as initials of a new run. The quantality at 2.72 is very strong, it stays at that state.

With the hierarchical Bayesian modelling, it must be noted that there were occasions when generated initial values caused the Bugs program to crash, which indicated some sort of dependency of the model performance on the starting values chosen.

7.4.4. Model Criticism

We have so far envisaged to device MCMC methods for use in estimating quantum feature, assuming it exists, firstly in its simplistic form and then structural form. Overall, the analyses indicated that the methods suffer from the multimodality problem. That is the stationary distribution of a Markov chain is multimodal with more or less separated modes which contain most of the probability content of the distribution.

The model implemented for the analysis of the simple quantal model presented this deficiency by its strong dependency on the initial values. This dependency is observed to be severe in such a way that correct inferences could be made only if the right combination of initial values are assigned to the most important parameters, namely σ and t (i.e. q). However, it is well known that any inference gained via MCMC sampling should be independent of the starting values.

Although we managed to obtain the same inferences as Freeman did, one must not forget that the data used for this practice was believed to have a strong quantal tendency, therefore Bugs achieved to initiate the model parameters around the actual values. This practice also involved many trivial runs some of which failed to converge.

Spiegelhalter et al. (1995) point out that if the target distribution is multimodal, or suspected to be multimodal, it is a good idea to start at least one sequence at each mode. However, a Metropolis algorithm proposing mainly local moves will mix poorly, since the chain will be trapped for long periods at one mode before escaping to another mode. Besides, if the number of modes is large, the simulation algorithm should be designed to jump between modes frequently.

One way of tackling the multimodality problem is known to be heating the target distribution – that is to place more probability between modes, so the modified MCMC sampler will travel more easily between modes and therefore explore the support of stationary distribution more easily. Another way could be the use of jumping algorithms commonly arise in mixture modelling, model choice and changepoint analysis, for example (Brooks, 1998).

Noting that Hierarchical Bayesian model for hierarchical quantality is also under the effect of multimodality problem, it is clear that some modification of these models are required. Implementation of above mentioned ways of tackling the problem is therefore suggested to be considered. At this stage, the models we proposed work only under certain conditions and will only be fully efficient as long as these conditions are satisfied.

7.5. Applications to the Root Spacings

Despite the problems we have highlighted so far, it is nonetheless of interest to know how the proposed Bayesian models, simple or hierarchical, would perform on the real data sets of root spacings. For this purpose, we will here apply them on some selected roots. To begin with, some crucial decisions on the choice of priors for the parameters t (i.e. q) and σ have to be made for the root spacings. For this study, we have decided to base our *a priori* belief for q on the information we have from previous studies of root spacings (Newson, 1993a and Barlow, 1988) which quoted the observed quantum values at around either 0.3 mm or 0.8 mm. Hence, we can consider a range of plausible q values as [q_{min}=0.2, q_{max}=1] which covers the previously estimated quantum values. Therefore, the prior for t is U(1,5). As the main assumption in the Bayesian formalism of quantality is that a quantum exists for some given data, the prior for σ should be chosen in connection with this choice of plausible range of q. Here, the fact that any quantum q must produce a σ^2/q^2 much smaller than 1/12 to be considered as the true quantum (see Broadbent's function in section 2.5.2) can be used as a rough guide on the decision of the largest attainable value of σ for the root spacings. Since the largest quantum value considered as a candidate is 1, we assign a prior distribution for σ as U(0.00001, 0.1). In addition, the integers are given a discrete Uniform prior as before.

Using the prior information above, a Bayesian analysis of the simple quantal model has been conducted for the root WR1, left series of which showed the strongest quantality with two quantum values: q_1=0.362 (σ_1=0.087) and q_2=0.240 (σ_2=0.059) [nominally] significant at 2% and 5% level respectively. The analysis involved many runs of the Bugs code using different initial values for the parameters σ and t. For the left series of the root, Figures 7.13 (a) and (b) present the behaviour of chains for q from two separate runs after a 500 burn-in followed by 5000 iterations. The first gives the posterior mean [95% probability interval] for q as 0.361 [0.358, 0.365] when σ is estimated as 0.087 [0.072, 0.091]. It must be emphasised that this result could be obtained *only if* the chain is initialised at closely around this quantum value. The second shows an indication of another possible value which is around 0.24 but the quantality is not so strong that the chain escapes from this value and drops down to the smallest value of the parameter q. In addition to these results, we obtained other quantum values at 0.581, 0.543, 0.5 and 0.4 which could be thought of as suggestive, perhaps not strong, quantal effects since they appeared as steps in the other runs of the program. Moreover, the similar analyses have also been carried out on the right series of the WR1 which was initially found to be not quantal. Fig 17.13 (c) gives an MCMC run for q, which is one of the many other runs that showed a very poor mixing and indicated no evidence of quantality. As clearly any non quantal random data would give more support to some values than the others, we observe some signs of multimodality in the graph.

(a)

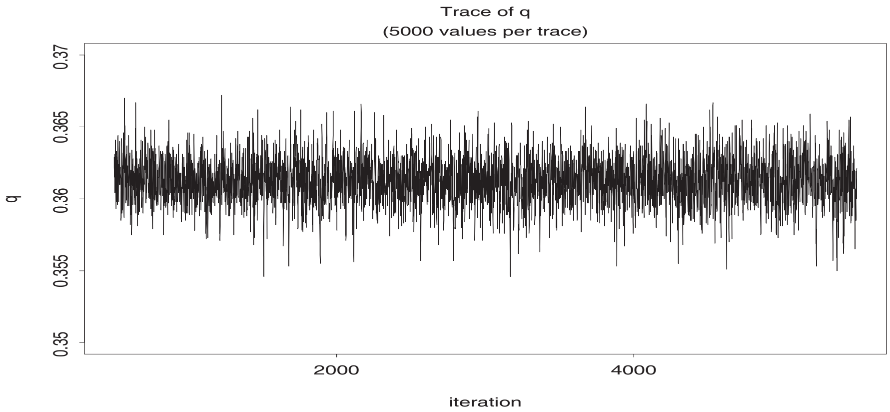

(b)

(c)

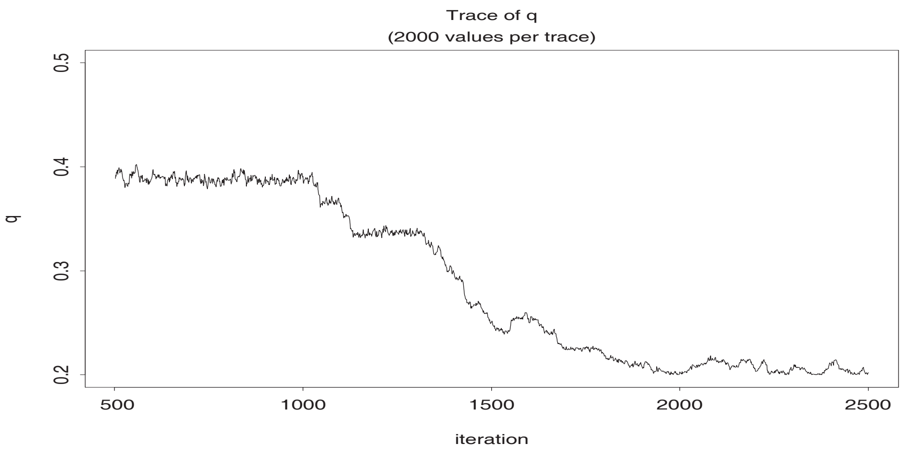

Fig 7.13. Convergence monitoring plots for q when (a) WR1–L; run 1, (b) WR1–L; run 2, (c) WR1–R are used.

Overall, we can conclude that the Bayesian analyses of the simple quantum model on the root spacings would strongly depend on the choice of the initial values. However, the strong quantality would be indicated by a good mixing of the chain with no convergence problems. In the case of weak quantality, the chain moves more freely in the q parameter space, giving some indications of quantality at various values and preferring the smallest possible value as an estimate eventually.

Since the basic philosophy behind the development of Bayesian modelling of quantality was to search for quantum values that are 'close' to each other, it is of our prime interest to investigate how well the Hierarchical Bayesian model would perform on the root spacings. Throughout applications of the model on the real data, we have however experienced considerable problems due to not only the existence of weak quantality which requires variety of trivial runs, but also the lack of knowledge about how much variation to expect. As a result, the number of crashes occasionally observed in the simulation study has increased in the analyses of the real data. Nevertheless, we will illustrate the behaviour of the posterior when this hierarchical thinking is applied to the root GR6 for which the algorithmic search showed a significant indication of hierarchical quantality at the level of its left and right series. It is here necessary to note that, at the second stage of modelling, the parameter τ_q will not be given a Gamma prior but assumed to be known so that many possible variations of quantum values could be examined.

To begin with, we initialised the hierarchical model with the results of the algorithmic search for the root GR6 which were q_1=0.280 (σ_1=0.068) and q_2=0.263 (σ_2=0.065) for the left and right series respectively. Additionally, the parameter σ_q that controls the variation among quantum values is assigned its exact value that is 0.01, and the parameter μ_q is given 0.1 arbitrarily. Run 1 in Figure 7.14 presents the chain obtained for q_1 and q_2 after 500 burn–in followed by 5000 iterations of the Bugs code constructed. Although both chain stays at the right values for a while, they both tend to decline down to the smallest quantum value.

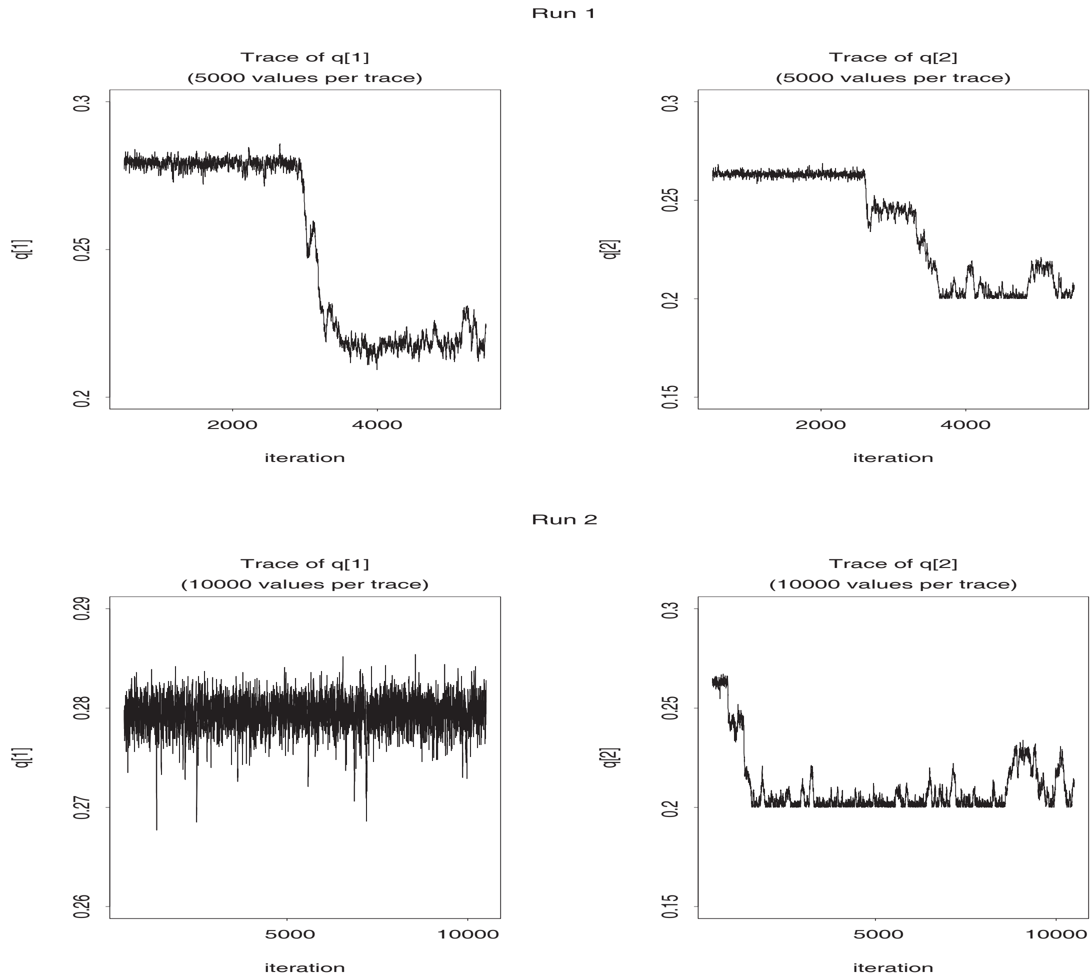

Fig 7.14. Convergence monitoring plots of q for run 1 (σ_q=0.01) and run 2 (σ_q=1).

Having the knowledge that quantality of the left series is stronger than the right series of the root (the first is significant at 5% and the second at 12%), it is surprising to observe that the chain for q_1 (of the left series) did not converge even though we provided very good starting conditions to the model. In order to check whether or not this is the influence of having the second group weakly quantal, we allowed a larger variation (i.e. σ_q=1) and re–ran the model keeping everything else the same. Run 2 in Figure 7.14 presents the chains for q_1 and q_2 after 500 burn-in followed by 10 000 iterations. It is clear that the true quantality can now be detected for the first group meanwhile the second group still shows the same behaviour as intuition would expect. That is to say that the small variation amongst quantum values can cause cross-correlation between them and having weak quantality for one group could destroy the quantality of the other. If we however increase the variation, then we loose the notion that quantum values are 'close' to each other.

Note that we have applied the proposed model on a root having the most significant evidence of hierarchical quantality and also we provided the most likely values as initial values to the parameters of the model. In additional runs of the model, we had a great difficulty in generating initial values for the q parameters, probably because of having a very restricted prior on the variation of them. Moreover, most of the values we provided cause the program to crash. In the simulation study of Hierarchical Bayesian modelling, we had this problem occasionally because we were dealing with a simulated data set that was strongly quantal and the program itself managed to initialise the parameters in the support of the likelihood. Whether it be simulated or real data, note that either μ_q or q had to be initialised by the user. As a result, it is clear that any further and more complex level of hierarchical quantality search via Bayesian analyses would be affected not only by the fact that most of the remaining data sets are either weakly or not quantal but also due to the multimodality problem. Therefore we will not proceed any further with the search of hierarchical quantality on the other data sets available.

7.6. Conclusions

In this chapter, we have investigated both simple and structural quantal problems from a Bayesian point of view, using the recent developments namely MCMC methods within the framework of the package WinBugs.

Much of the motivation for the development of a Bayesian approach has been driven by the question of how to express the notion of quantum values close to each other, which arises in the construction of hierarchical quantal models. As it is possible to incorporate this argument into a Bayesian analysis through prior probabilities, we proposed a Hierarchical Bayesian Model which allows us to formulate structural relationships between a set of parameters.

In the implementation phase, we began with repeating Freeman's Bayesian analysis on the stone circles. Refinements of his analysis has been achieved by allowing a full range prior distribution for the parameter σ, and also invoking alternative prior distributions for it. As a result, it was observed that MCMC methods perform well in uncovering the expected values only under certain conditions, that is when the model parameters are initialised closely around the actual values. This is because the posterior distribution is multimodal. Once the model is initialised, it may be difficult for the chain to jump from one mode to another and suggest the one which fits the data best. Inferences when a Binomial prior was invoked for integers were found to be less influenced by the initial values of parameters.

Despite this effect, we were able to recover the same values that Freeman suggested as possible quantum values which were 5.44 and 7.48. When estimated values were wrong inferences, this was indicated by the diagnostic tests in CODA. However, there were some suggestive values as well. As Freeman points out, this Bayesian analysis does not provide an overall assessment of whether the quantal model with q is appropriate or not. It provides only posterior distributions for the various parameters on the presumption that the data arise from the model. In practical situations, it is necessary to assess whether or not we are at the true quantum value or just some fraction of it or even maybe some secondary value. This could be done through a comparison of observed values with their predictive distributions. We note that, while the analytical approximations might be considered in obtaining predictive densities, the output from a MCMC simulation can also be utilized with some additional sampling for the same purpose.

Further, we have constructed a Hierarchical Bayesian model so as to investigate the existence of hierarchical quantality. Simulated data were used to examine the performance of MCMC methods for this purpose. Due to the effect of multimodality of the posterior, true values as well as some fractions of them are estimated. The latter was indicated by some, but not severe, convergence problems. In that case, we continued the analysis by initialising the model parameters with those estimated values which were suspected to be just fractions of the real estimate. In this way, we achieved to recover the true values. Applications of Hierarchical Bayesian model on the root spacings indicated that weak quantality that exists for majority of the roots prevents the model from performing well. It is believed the efficiency of the model depends on whether or not the degree of quantality remains the same within its hierarchy. In overall, these findings highlights the need to be cautious when considering MCMC methods for an investigation of both simple and structural quantality.

Chapter 8.
Summary and Conclusions

8.1. Introduction

Cyclic, or rhythmic, processes observed in natural phenomena have been the subject of considerable attention since the earliest times. A particular one comes to the notice in the form of quantal problems arisen by the questions whether or not there exists a "fundamental unit" that regulates such rhythmic processes. The prime objective of this thesis has been to investigate the problems which give rise to the quantal models and their possible extensions within the framework of Biological issues.

This thesis gives a full account of the development of existing methodology for simple forms of quantality, identifying some of the problems, advantages and drawbacks of different estimation and testing procedures. Further aspects of significance assessment of quantality have been examined within the context of the Megalithic Yard Problem.

Then, the simple models have been extended to the cases when any quantum has a non–constant feature. This was found particularly necessary in describing the quantality of root production mechanisms. That is to address the question of whether or not roots of plants produce their secondary roots (i.e. lateral roots) in a rhythmic fashion. The prime motivator for the current interest in developing new quantum models can be attributed to the expectation of variable quantality in structural forms.

The first extension – Hierarchical quantum model – hence not only suggests the expectation of root lateralization *per se* to be rhythmic (i.e. quantal) but also defines a system within which coherent rhythms occur at various levels determined by lateral root series, roots and treatments. Attention is here given to the quantality at one level as well as how they relate to the quantal patterns at another level.

The second extension – Regression quantum model – has been brought particularly by the biological process of root growth that raises the question of whether the rhythm of lateral root production changes as the individual root grows.

Within the scope of this thesis, new methodological tools have been developed so as to screen, extract and also test hierarchical and regression quantal patterns with particular applications on the available roots of plants; onions, tomatoes and ferns.

On the basis of outcomes of analyses proposed in this thesis, we can conclude that onion root spacings show little tendency to be pure quantal, however treated roots indicate some evidence of hierarchical quantality with most evidence coming from the Strong treatment group for quantum values varying around 0.462 mm. Moreover, tomato roots provide good evidence in favour of both simple and hierarchical quantality. The latter form is constructed around common quantum values of 0.36 mm (or 0.24 mm) and 0.23 mm. In addition, the question of quantality of spacings has been extended with the total series and target positions of the spacings and it is concluded there is little evidence to suggest quantal model for those.

Furthermore, fern root spacings appeared to be "too regular" that paradoxically destroyed the simple quantality. However, the analyses of fern roots using the regression quantum model concluded to be suggestive of this new form, particularly for the C-type ferns. We must here note that further analyses are required to draw a stronger conclusion.

8.2. New Features of the Existing Methodology

Kendall's method has been central to our studies to develop new models and methodologies. Therefore, a full description of his technique together with its theoretical justification is provided in the first part of the thesis. Further insights have been developed by examining some of the issues of quantum estimation method and the significance assessment for the estimated quantum. New features extracted and conclusions drawn can be summarised as follows:

⇒ Kendall's cosine quantogram and modular quantogram can be formulated as Likelihood Ratio Tests, utilising circular structure of the errors.

⇒ The 'frequency measure' of reciprocal of quantum, τ, should be used as the natural scale for the gridsearch of quantogram analyses.

⇒ The best increment which determines how finely a gridsearch is to be done have been suggested to be chosen by the halving method we proposed and used as in section 2.6.4.

⇒ The supremum of the process $\{\phi(\tau): \tau_{min} < \tau < \tau_{max}\}$, under the null hypothesis

a) are better represented by a three parameter Generalised Extreme Value distribution than by a two parameter Gumbel distribution. Later in the Chapter 6, this finding is proved to be useful in approximating the significance probabilities when calculating the power of Fisher's combined test.

b) are independent of τ, for not too big τ_{max} or too small τ_{min}. That is to say that they show a random pattern, indicating no tendency towards any particular values of the τ–range.

⇒ Kendall's suggestion that significance formalism is not sensitive to the underlying 'non-quantal' distribution has been confirmed by examining many distributions as underlying distributions.

⇒ Selected random number generators used to generate non-quantal data sets have been proved to be adequate

⇒ The violation of the assumption of independence for the data points indicates no serious effect on the significance assessment for quantality.

8.3. Methodological Developments

In addition to the features outlined above, this study has also provided methodological developments within the framework of not only the simple quantality but also extended forms of quantality as given below:

***Power Assessment for the Simple Forms of Quantality*:** A comparative study on the power of the test statistics for "pure" or "shifted" quantality, denoted respectively as $\phi(\tau)$ and $\chi(\tau)$, concluded that there would be little loss in power if $\chi(\tau)$ is utilised to search for pure quantality instead of $\phi(\tau)$. This result improves the quantality assessment by providing protection against unsuspected 'shifted' quantality if there is doubt as to whether any quantality that may exist is "pure" or "shifted".

In the power assessment, the simulation study has been conducted taking into account the effect of the sample size. We believe that it would be beneficial to carry out additional simulation studies to test whether or not different ranges (i.e. wider or narrower) of gridsearch would result in any influence on the power. These studies might contribute a better power assessment of the two test statistics.

***Proposal of Hierarchical Quantal Models*:** A distinctive nature of the current quantal problem with root spacings appeared to be that each root has its own periodic lateralization and this varied from root to root. With inclusion of levels of spacings such that there exists rank series on the same root, roots within the same treatment group and different treatments, it is expected to observe some sort of hierarchy in quantality. A hierarchy for quantality is here considered to be "sensible" if each of its levels is supported by the sub-levels with an expectation that any variation amongst quantum values are the most at first level but the least at the highest level. That is in general to claim that any hierarchical quantality should present its values close to each other. For the evaluation of this claim, we have established various methods.

Our first approach has been to develop a graphical tool in order to screen the existing structures. The approach is analogous to one used in the analysis of one-way Anova models. Essentially, we asked what would happen if data come from one-way quantal model but we fit a common quantum. Residuals from such a wrongly fitted model hence appeared in clusters indicating real structures. The quality of performance is however found to depend critically on the magnitude of variation among quantum values and the degree of quantality in the individual groups.

The next key contribution to the solution of hierarchical quantal problems has been achieved in an algorithmic fashion using the complete data of one level in order to investigate its quantum value and that of sub-levels adaptively around this initial value. For the evaluation phase, this is performed by starting the search of quantality for the first level of hierarchy over a very large range and by reducing the range around the estimated quantum value for the other data sets. The quantitative synthesis of evidence from different data sets on each level is then accomplished through a composite test as we proposed in section 6.2.1. To begin with, Fisher's combined test is used as the governing criterion for testing the validity of this new composite test. A simulation study has been conducted in order to compare the power of two procedures for combining the evidence and we concluded that new test has nicer properties over Fisher's method as far as hierarchical quantality is concerned.

As a result, we developed a graphical tool that served as a useful diagnostic for determining the presence of the hierarchical quantality and proposed not only an algorithmic method that proved to be a viable means of quantifying this structure but also a test statistic that was found to be powerful in the verification of the new form of quantality.

A Bayesian formulation of hierarchical quantality has also been considered in the thesis. To begin with, Freeman's initial Bayesian analysis on the simple quantum model has been re–examined with some extensions which were achieved by taking advantage of advances, known to be MCMC methods, in Bayesian methodology since his original analysis. Then a hierarchical Bayesian model is proposed as another way of expressing our beliefs about hierarchical quantum values. In both attempts, the full implementation of the Bayesian analyses has been limited by the multimodality problem created by the nature of quantal problems. Despite the limitations, we have been able to obtain the same inferences as Freeman and also obtain the correct estimates of hierarchical quantum values from simulated data. However, it is believed that some modifications of the models in order to overcome the multimodality problem would lead to more reliable estimates in real applications.

***Proposal of Regression Quantal Models*: ** In the thesis, another novel model as we named Regression quantal model has been derived from the argument that the root may change its rhythmic process as it grows. The difficulty with construction of this model is caused by the question of how much a quantum could be allowed to vary along the root. Our solution was to restrict the of the variation parameter by the total length of the root i.e. covariate. With a modification of quantogram analysis, a two-dimensional gridsearch provided an efficient method so as to estimate not only quantum but also the new parameter.

We believe that the development of such procedures will have an impact on the newer methods towards the solution of similar problems.

8.4. Suggestions for Practical Use

Two important problems have hampered the practical use of the methods in the investigation of either simple, or structural forms of quantality, particularly for Onion roots. These impracticalities are caused firstly by the low accuracy that the experimenter used to measure the spacings. This resulted in simple fractions of the accuracy to be suggested as a candidate quantum and also any true underlying effect to be concealed. Secondly, having two different accuracies for the same sort of measurements inhibited us from searching for a quantum within the similar areas. To achieve greater consistent accuracy, it would therefore be reasonable to suggest experimenters (or Biologists) to measure the root distances using an accuracy of, at most, 0.1 mm, and furthermore, to keep the accuracy constant throughout the experiment if the purpose of the investigation is to search for regularity in the root production (or any other system of plants).

A visual examination of the data may suggest a non-uniform distribution of final digits, indicating perhaps a digit preference by the experimentalist. In particular, there is a suspicion of preference for even digits over odd. This problem is similar to that of rounding or accuracy of measurement discussed above and would result in an indication of a possibly spurious quantum corresponding to the "effective accuracy", or simple fraction of it, just as with the accuracy, though the problem is less severe.

8.5. Possibilities for Further Research

The methodological tools we proposed and used were solely for the purpose of detecting a "pure" form of the structural quantality. We have not addressed the issue of how to proceed in the case when shift components are added to the coherent system of new quantal models. This will obviously complicate any analyses in great amount. We avoided this complication by subtracting the first observation (i.e. shift) from all the measurements. In another application, this may however not be the most plausible thing to do. It might further be of more interest to know what the value of shift would be. For such cases, the model needs to receive further considerations and adjustments. We leave this as a future work.

Another possible future research is created by the Bayesian analysis of quantal problems via the MCMC method. Remember that multimodality of quantal problems inhibited the method from producing a chain that converges to the true value of quantum. Hence, the very next step should be towards the solution of this problem. In Chapter 7, no attempt was made to give more than an outline of the possible solutions of multimodality problem within Bayesian inference. It must be emphasised that the suggested methods are yet problem specific and not proved to work for all problems. The implementation of them also requires one to involve with a very heavy programming and this was beyond the scope of this thesis and therefore it is left as a possible future work. However, the key advantage of the Bayesian approach is that it allows incorporation into the analysis in a natural way of the less specific aspects of complex models such as the feature of hierarchical quantal models that quantum values should be “close”. Likewise, the essential feature of regression quantal models that the regression parameter is “small” in relation to the base value could be expressed in a Bayesian framework in a similar way. However this will probably give rise to problems of multimodality similar to those encountered in hierarchical models and so the idea was not pursued but could be another possibility for a future work.

APPENDICES

APPENDIX A.

List of the Computer Programs

This appendix gives the list of all computer program that have been written throughout this study. The programs are not given here but can be obtained on request.

Program	Language	Function
QSEARCH.F	Fortran	Performs basic quantogram (cosine or modular) with significance assessment of first desired number of the highest peaks.
POWER1.F	Fortran	Computes the power of $\phi(\tau)$ and $\chi(\tau)$ for testing for 'pure' and 'shifted' quantality.
VMIS.F	Fortran	Generates a sample from von Mises distribution with a zero mean and κ concentration parameter
POWER2.F	Fortran	Computes the power of Fisher's combined test (T^F) and the new aggregrate test (T^*) using the output from the program–GEV.SCE written in S-Plus language and provided by Anderson (pers.comm.).
COMB.F	Fortran	Perform the algorithmic quantogram analyses in Chapter 6, combining the evidence by T^*
POLAR.S	S–Plus	Draws circular plots of residuals
FREE.ODC	WinBugs	Performs Bayesian analysis of simple quantum model
HIER.ODC	WinBugs	Performs Hierarchical Bayesian analysis for hierarchical quantum model when sample sizes of each group are equal
OFFHIER.ODC	WinBugs	Performs Hierarchical Bayesian analysis for hierarchical quantum model when sample sizes of each group are *not* equal

APPENDIX B.

Results of Initial Quantogram Analyses on Onion Roots

This appendix gives the full results of basic quantogram analyses on onion roots performed for all their series of raw spacings (in section B1) and positions (in section B2). Since all Control group roots are under the strong influence of the accuracy 0.5 and also their rank series have insufficient number of observations, no assessment of significance has been carried out for the observed peaks of them. Combined series of them however have been unrounded to the accuracy of 0.5 mm with U(–0.25, 0.25) and results are displayed in Fig B1.

For the rest of the groups, we present estimated quantum values, peak cosine quantogram values and their 'nominal' significance probabilities. In the case of positions, the results contain peak modular quantogram values as well as an estimate of β *only if* the observed peak is found to be significant (i.e. $P < 0.1$) and also the value of $\psi(\hat{q})$ regards the β-effect as being significant (i.e. $\psi(\hat{q})$ is outside the range ± 2).

All quantogram analyses have been performed with an increment of 0.001 over the τ–ranges converted from the q–ranges listed in table 5.6 in chapter 5. Significance probabilities have been assessed as described in section 5.4.1.3.

B1. Analyses of Raw Spacings

Table B1.1. Full results of gridsearch for Control root spacings.

Root	est.	r1	r2	r3	r4	r5	comb	total
C1	$\hat{q}$	0.8680	0.8382	0.8250	0.5875	0.6963	0.8375	0.6460
	$\phi(\hat{q})$	2.4955	1.6902	1.8895	2.7719	2.3853	2.4933	1.3902
C2	$\hat{q}$	0.7622	0.6261	0.7704	0.8576	0.5602	0.5882	0.8368
	$\phi(\hat{q})$	2.1651	2.3380	2.2066	2.4453	1.4140	2.5843	1.3685
C3	$\hat{q}$	0.5931	0.8561	0.8554	0.7309	0.7468	0.7352	0.7375
	$\phi(\hat{q})$	2.3681	1.9612	2.5000	2.2172	2.1842	2.7788	0.8382
C4	$\hat{q}$	0.6293	0.6146	0.7137	0.7657	0.7745	0.5834	0.6766
	$\phi(\hat{q})$	2.0462	2.4343	1.9277	2.8075	1.9996	1.6878	0.0461
C5	$\hat{q}$	0.8968	0.7518	0.8340	0.6035	0.5737	0.7132	0.5495
	$\phi(\hat{q})$	1.5388	3.1870	2.2968	2.1939	2.2211	1.4805	0.0653
C6	$\hat{q}$	0.5633	0.5580	0.7326	0.5984	0.8312	0.6854	0.8460
	$\phi(\hat{q})$	1.9836	1.9835	2.2709	2.3523	1.6443	2.7906	0.9651
C7	$\hat{q}$	0.6226	—	0.6835	0.7012	0.6120	0.6230	0.7067
	$\phi(\hat{q})$	2.3971		1.9779	2.8032	1.9716	2.8990	1.3074
C8	$\hat{q}$	0.8143	0.6711	0.8944	0.6192	0.5624	0.8103	0.8271
	$\phi(\hat{q})$	2.4975	2.1041	2.3368	2.1790	2.2609	2.5336	1.0147
C9	$\hat{q}$	—	0.6920	0.5970	0.6697	0.9000	0.6910	0.6649
	$\phi(\hat{q})$		1.6716	1.4408	2.3673	1.4142	2.0763	1.9171
C10	$\hat{q}$	0.7288	0.6406	0.8787	0.6464	0.8888	0.7309	0.8217
	$\phi(\hat{q})$	2.6317	2.0405	2.2372	2.3925	1.4142	2.8088	1.4289
C11	$\hat{q}$	—	0.6472	0.8517	0.7178	0.7462	0.7235	0.7032
	$\phi(\hat{q})$		2.2473	1.9183	2.8890	2.4285	3.5153	0.8143
C12	$\hat{q}$	0.6993	0.6978	0.6600	0.5834	0.6016	0.6978	0.6614
	$\phi(\hat{q})$	2.2710	1.9761	2.7154	2.1077	2.7231	2.6124	1.6061
C13	$\hat{q}$	0.6729	0.6901	0.8849	0.5865	0.7027	0.7042	0.5924
	$\phi(\hat{q})$	3.1782	2.5328	1.9543	2.2505	2.5397	2.4793	0.7575
C14	$\hat{q}$	0.5668	0.7622	0.7861	0.8569	0.7674	0.7674	0.6031
	$\phi(\hat{q})$	2.7848	2.0118	2.3539	3.1107	2.9842	2.5277	0.2122
C15	$\hat{q}$	0.6250	0.6788	0.6056	—	0.5552	0.7451	0.6702
	$\phi(\hat{q})$	1.4142	1.5791	1.9043		1.9043	1.9661	2.6309
C16	$\hat{q}$	0.8748	0.8605	0.8090	0.7552	—	0.8230	0.8130
	$\phi(\hat{q})$	1.4142	2.5648	1.9948	2.2632		2.0549	2.4925
C17	$\hat{q}$	0.9000	—	0.6269	0.7418	0.5707	0.7429	0.8811
	$\phi(\hat{q})$	1.4142		1.9210	2.5280	2.2141	2.1698	0.9734
C18	$\hat{q}$	0.7012	0.8510	0.6631	0.7722	0.7923	0.5552	0.8826
	$\phi(\hat{q})$	1.9792	1.9753	1.5827	2.1134	1.7366	1.3971	0.7887

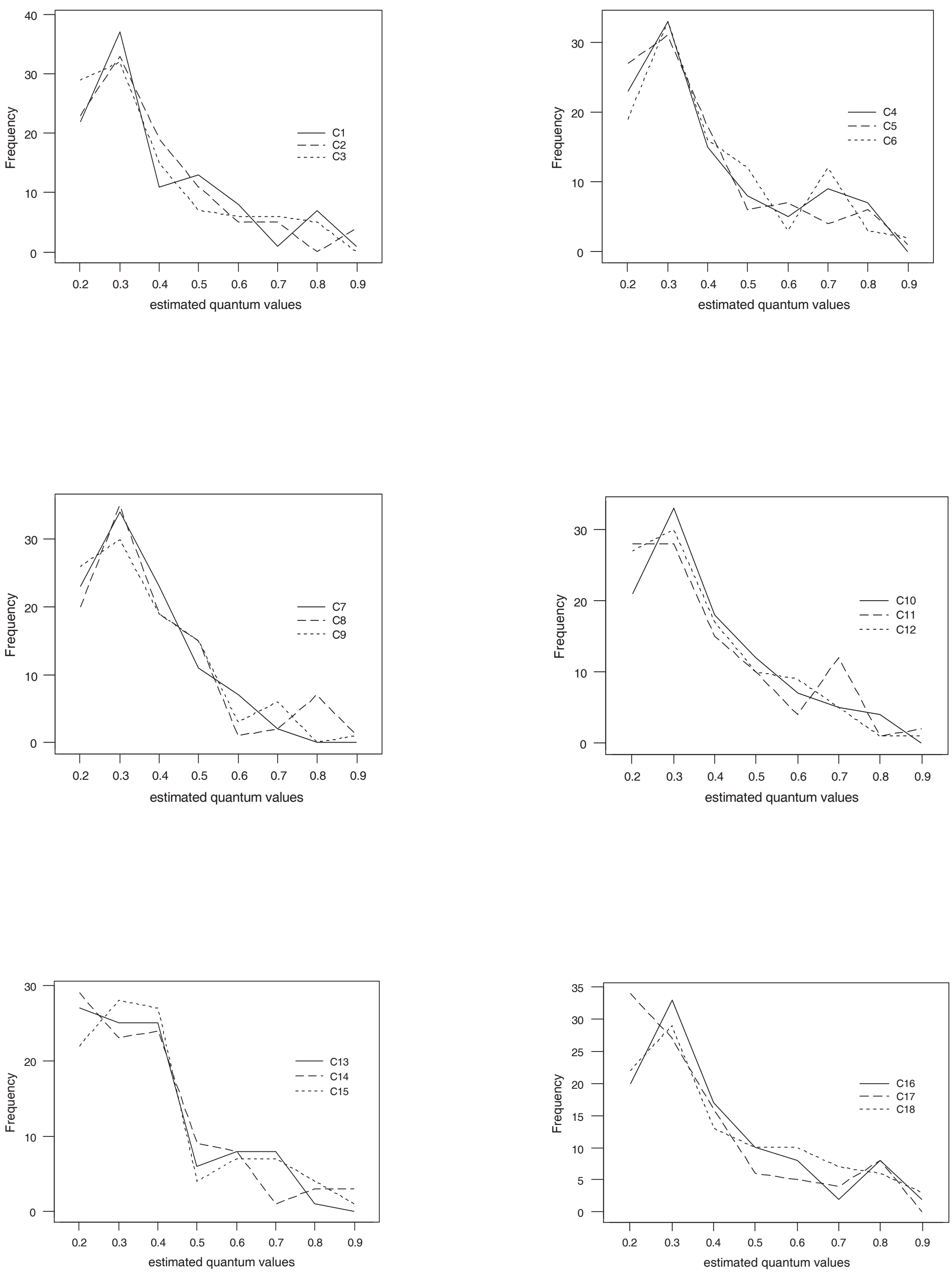

Fig B1. Gridsearch results from the Control group onion roots (combined rank series) after ‘unrounding’ with U(-0.25, 0.25) variate.

Table B1.2. Full results of gridsearch for Weak–treated root spacings.

Root	est.	r1	r2	r3	r4	r5	comb	total
W1	$\hat{q}$	0.2397	0.8285	0.8474	1.1600	1.4641	0.3305	0.2133
	$\phi(\hat{q})$	1.8802	2.4821	2.5152	2.4017	2.6249	2.7403	3.7851
	p	0.982	*	*	*	0.718	0.594	0.007
W2	$\hat{q}$	0.2417	2.5125	0.4032	0.6531	0.5125	0.3080	0.2240
	$\phi(\hat{q})$	2.7403	2.4069	3.3673	2.7812	2.4246	2.0270	2.2824
	p	0.269	*	0.064	*	0.621	0.997	0.558
W3	$\hat{q}$	0.2176	0.2437	1.6722	0.8298	0.9319	0.3154	0.2789
	$\phi(\hat{q})$	2.4247	2.8468	2.3554	1.9714	2.8389	2.5374	2.5388
	p	*	*	*	*	*	0.893	0.428
W4	$\hat{q}$	0.2588	0.4306	1.8832	0.2540		0.3852	0.2780
	$\phi(\hat{q})$	3.1611	2.6565	2.1608	3.0551		2.7310	1.8850
	p	*	*	0.783	*		0.784	0.938
W5	$\hat{q}$	0.2423	0.4444	0.2809	0.3599	0.8230	0.2425	0.2768
	$\phi(\hat{q})$	1.9644	2.1406	2.0021	2.0622	3.1463	2.8640	0.9814
	p	0.937	0.976	0.992	0.907	0.091	0.305	0.999
W6	$\hat{q}$	0.4022	0.2311	0.2519	1.0020	1.0193	0.2484	0.4938
	$\phi(\hat{q})$	2.5893	2.5179	2.4368	2.2022	3.2598	3.0309	2.2088
	p	0.782	0.444	*	*	*	0.495	0.815
W7	$\hat{q}$	0.6993	2.9154	0.3327	0.2623	1.1467	0.2605	0.7163
	$\phi(\hat{q})$	2.9711	2.4912	2.7048	2.4910	2.4418	2.8986	2.2965
	p	*	0.785	*	*	*	0.615	0.708

* sample size n < 10, no significance assessment has been made.

Table B1.3. Full results of gridsearch for Strong–treated root spacings.

Root	est.	r1	r2	r3	r4	r5	comb	total
S1	$\hat{q}$	0.3360	0.3958	0.2284	0.4826	0.2352	0.3400	0.5214
	$\phi(\hat{q})$	2.4426	2.0447	2.3713	3.2241	2.0101	2.0969	1.4329
	p	0.201	0.723	0.726	*	*	0.750	0.997
S2	$\hat{q}$	0.6988	0.8058	0.2581	0.4224	0.3152	0.2621	0.2278
	$\phi(\hat{q})$	2.6375	2.1962	2.4611	2.0027	1.8186	2.4944	–1.4314
	p	0.220	0.635	0.322	0.895	0.861	0.385	1.000
S3	$\hat{q}$	0.8741	0.2824	0.2675	0.3007	0.4636	0.4585	0.2132
	$\phi(\hat{q})$	2.2156	2.4323	2.3352	1.7994	3.4833	3.4715	1.4500
	p	0.710	0.478	0.336	0.985	0.019	0.025	0.965
S4	$\hat{q}$	0.2936	0.3527	0.3566	0.3049	—	0.3546	0.2603
	$\phi(\hat{q})$	2.0815	2.9089	2.0741	1.7692		3.4715	0.5545
	p	0.736	0.112	0.732	0.908		0.023	1.000
S5	$\hat{q}$	0.8496	0.2474	0.3272	0.2661	—	0.3304	0.2100
	$\phi(\hat{q})$	1.4730	2.7458	2.9172	2.0997		2.5481	0.1590
	p	0.986	0.289	0.097	0.776		0.407	1.000
S6	$\hat{q}$	0.2100	0.5032	0.4502	0.4921	—	0.4496	0.2100
	$\phi(\hat{q})$	2.1069	3.6225	3.9277	3.7205		5.3198	0.0205
	p	0.552	0.010	0.002	0.009		0.001	1.000

* sample size n < 10, no significance assessment has been made

B2. Analyses of Positions

Table B2.1. Full results of gridsearch for Weak–treated root positions.

Root	est.	r1	r2	r3	r4	r5	total
W1	$\hat{q}$	0.3439	0.3529	0.8489	0.2189	0.7576	1.3583
	$\chi(\hat{q})$	4.9482	3.8065	4.8383	2.9983	7.7019	9.9674
	$\psi(\hat{q})$	0.5012	0.7657	0.9716	–0.3195	–2.1071	–3.1289
	$\hat{\beta}$	—	—	—	—	—	–0.5112
	p	0.922	*	*	*	0.123	0.028
W2	$\hat{q}$	0.7380	0.7220	0.2325	0.5767	0.2443	0.3517
	$\chi(\hat{q})$	5.6385	4.4931	4.7375	3.9880	5.7189	5.7714
	$\psi(\hat{q})$	–3.1306	–2.6011	–3.0553	0.4067	0.3751	3.3404
	$\hat{\beta}$	—	—	—	—	—	—
	p	0.764	*	0.827	*	0.701	0.808
W3	$\hat{q}$	0.7981	0.2443	0.9001	0.5000	1.3298	0.3156
	$\chi(\hat{q})$	2.9989	5.7841	2.9999	2.0000	6.1450	5.5829
	$\psi(\hat{q})$	–0.5742	–2.9450	–0.8215	–1.1755	3.5042	3.2231
	$\hat{\beta}$	—	—	—	—	—	—
	p	*	*	*	*	*	0.837
W4	$\hat{q}$	0.2589	0.2364	0.8503	1.2077		0.2786
	$\chi(\hat{q})$	6.2757	5.5544	7.1861	5.7226		6.2660
	$\psi(\hat{q})$	–2.8730	–3.2268	3.1949	1.6974		–3.4611
	$\hat{\beta}$	—	—	—	—		—
	p	*	*	0.239	*		0.782
W5	$\hat{q}$	0.5583	0.2264	0.4751	0.6010	0.7639	0.6456
	$\chi(\hat{q})$	8.2939	5.2910	6.2973	7.6597	5.3869	8.0560
	$\psi(\hat{q})$	0.2244	–3.0315	–2.3762	1.8496	0.5729	2.7015
	$\hat{\beta}$	—	—	—	—	—	—
	p	0.108	0.856	0.585	0.222	0.893	0.213
W6	$\hat{q}$	0.7541	0.5900	0.9452	0.5695	1.0183	0.2508
	$\chi(\hat{q})$	6.7046	6.7346	3.9048	4.7574	5.8579	5.8641
	$\psi(\hat{q})$	–2.4336	–3.5726	2.7324	–0.4494	2.6876	0.5332
	$\hat{\beta}$	—	—	—	—	—	—
	p	0.335	0.262	*	*	*	0.834
W7	$\hat{q}$	0.6993	0.3510	0.8511	0.2128	2.2936	0.2452
	$\chi(\hat{q})$	6.5558	5.2483	5.3479	4.7455	2.9998	4.5967
	$\psi(\hat{q})$	3.4093	–3.0201	0.1919	0.2014	–0.1578	2.5781
	$\hat{\beta}$	—	—	—	—	—	—
	p	*	0.837	*	*	*	0.996

* sample size n < 10, no significance assessment has been made

Table B2.2. Full results of gridsearch for Strong–treated root positions.

Root	est.	r1	r2	r3	r4	r5	total
S1	$\hat{q}$	0.2390	0.3920	0.2245	0.4836	0.6010	0.6105
	$\chi(\hat{q})$	5.1030	8.3730	5.6123	5.9900	4.8032	6.0107
	$\psi(\hat{q})$	– 0.5848	– 3.1084	1.7540	– 1.3538	– 0.8361	– 3.4496
	$\hat{\beta}$	—	– 0.0538	—	—	—	—
	p	0.710	0.033	0.468	*	*	0.432
S2	$\hat{q}$	0.3089	0.7163	0.2806	1.2500	0.4677	1.2453
	$\chi(\hat{q})$	5.8168	5.8396	9.9617	6.7904	6.5184	5.2768
	$\psi(\hat{q})$	– 3.2370	3.3041	4.4345	– 3.2655	– 1.8492	1.2690
	$\hat{\beta}$	—	—	0.0752	—	—	—
	p	0.867	0.859	0.041	0.521	0.669	0.978
S3	$\hat{q}$	0.4645	0.2753	0.2755	0.3007	0.4539	0.2125
	$\chi(\hat{q})$	5.1578	7.0444	7.1373	8.4906	6.4062	5.4290
	$\psi(\hat{q})$	– 2.0722	1.3993	– 0.9851	– 1.2536	0.5846	– 0.3951
	$\hat{\beta}$	—	—	—	—	—	—
	p	0.937	0.298	0.409	0.106	0.621	0.937
S4	$\hat{q}$	0.6297	0.2239	0.2665	0.3081		0.4606
	$\chi(\hat{q})$	6.3430	7.4311	5.4444	7.8039		7.3935
	$\psi(\hat{q})$	– 3.4078	2.5295	– 1.9545	– 3.4327		– 1.7958
	$\hat{\beta}$	—	—	—	—		—
	p	0.357	0.197	0.650	0.185		0.057
S5	$\hat{q}$	0.3667	0.3240	0.3203	0.3282		0.2132
	$\chi(\hat{q})$	5.8478	6.2777	6.1507	5.8766		5.3978
	$\psi(\hat{q})$	– 3.1416	3.5017	– 0.6465	– 2.9516		– 3.0387
	$\hat{\beta}$	—	—	—	—		—
	p	0.657	0.504	0.614	0.652		0.857
S6	$\hat{q}$	0.4221	0.3445	0.3935	0.5507		0.4710
	$\chi(\hat{q})$	9.0685	6.812	7.6214	10.0936		4.8118
	$\psi(\hat{q})$	– 1.4103	3.3579	3.3935	1.0799		– 0.3216
	$\hat{\beta}$	—	—	—	—		—
	p	0.090	0.513	0.317	0.019		0.995

* sample size n < 10, no significance assessment has been made

APPENDIX C.

Results of Initial Quantogram Analyses on Tomato Roots

This appendix gives the full results of basic quantogram analyses on Tomato roots performed for all their series of raw spacings (in section C1) and positions (in section C2) with estimated quantum values, peak cosine quantogram values, standard deviations and their 'nominal' significance probabilities. In the case of positions, the results contain peak modular quantogram values instead as well as an estimate of β *only if* the observed peak is found to be significant (i.e. $P < 0.1$) and also the value of $\psi(\hat{q})$ regards the β-effect as being significant (i.e. $\psi(\hat{q})$ is outside the range ± 2).

All quantogram analyses have been performed with an increment of 0.001 over the τ–ranges converted from the q–ranges listed in table 5.9 in chapter 5. Nominal significance probabilities have been assessed as described in section 5.4.1.3.

C1. Analyses of Raw Spacings

Table C1.1. Full results of gridsearch for Wild type tomato roots

Root	*Series*	$\hat{q}$	$\phi(\hat{q})$	$\hat{\sigma}$	P-value
WR1	*Left*	0.3625	3.5875	0.0874	0.011
	Right	0.3003	1.9090	0.0869	0.890
	Total	0.2419	2.0916	0.0763	0.457
WR2	*Left*	0.3004	2.6773	0.0757	0.258
	Right	0.5670	2.5961	0.1433	0.455
	Total	0.7123	1.8269	0.2247	0.745
WR3	*Left*	0.2636	3.0476	0.0662	0.091
	Right	0.3032	1.9190	0.0860	0.871
	Total	0.3360	3.2127	0.0919	0.039
WR4	*Left*	0.4112	2.6920	0.0986	0.477
	Right	1.1097	2.3201	0.2859	0.630
	Total	0.3882	1.4145	0.1271	0.989
WR5	*Left*	0.2050	2.3942	0.0571	0.437
	Right	0.2070	2.5806	0.0546	0.455
	Total	0.2435	1.5670	0.0824	0.892
WR6	*Left*	0.2952	2.8040	0.0849	0.150
	Right	0.4212	2.2821	0.1245	0.681
	Total	0.2951	2.3914	0.0959	0.257
WR7	*Left*	0.7498	3.2928	0.1745	0.078
	Right	0.7110	2.4518	0.1829	0.567
	Total	0.7145	2.4556	0.2071	0.546
WR8	*Left*	0.2478	1.8854	0.0732	0.990
	Right	1.1695	2.7347	0.3101	0.175
	Total	0.2142	2.2573	0.0664	0.678
WR9	*Left*	0.3672	3.0891	0.0880	0.097
	Right	0.4625	2.0463	0.1338	0.839
	Total	0.3311	2.0685	0.1037	0.418
WR10	*Left*	0.3115	1.7027	0.0919	0.949
	Right	0.3135	2.1083	0.0855	0.679
	Total	0.6689	2.2523	0.1988	0.357

Table C1.2. Full results of gridsearch for Wild type, Naa treated tomato roots

Root	Series	$\hat{q}$	$\phi(\hat{q})$	$\hat{\sigma}$	P-value
NWR1	*Left*	0.2000	2.5193	0.0511	0.405
	Right	0.3487	2.3716	0.0965	0.464
	Total	0.2420	2.5035	0.0717	0.325
NWR2	*Left*	0.5292	3.4741	0.1272	0.017
	Right	0.5084	2.5660	0.1415	0.183
	Total	0.2637	1.2959	0.0942	0.870
NWR3	*Left*	0.2080	2.9232	0.0483	0.128
	Right	0.9296	1.9503	0.2622	0.759
	Total	0.2958	1.4187	0.0983	0.812
NWR4	*Left*	0.3156	3.0460	0.0868	0.075
	Right	0.4594	2.7873	0.1303	0.156
	Total	0.3911	1.8720	0.1343	0.589

Table C1.3. Full results of gridsearch for Gib–1 Mutant type tomato roots

Root	Series	$\hat{q}$	$\phi(\hat{q})$	$\hat{\sigma}$	P-value
GR1	*Left*	0.2307	2.2324	0.0537	0.334
	Right	0.2136	1.9418	0.0530	0.614
	Total	0.5941	1.9460	0.1766	0.586
GR2	*Left*	0.3155	2.8035	0.0630	0.186
	Right	0.2260	2.2030	0.0574	0.675
	Total	0.2470	2.8901	0.0619	0.085
GR3	*Left*	0.2774	2.9102	0.0699	0.097
	Right	0.4279	2.6649	0.1164	0.196
	Total	0.2262	2.0343	0.0724	0.389
GR4	*Left*	0.3282	2.6244	0.0867	0.203
	Right	0.8463	2.5071	0.2300	0.374
	Total	0.2205	2.1554	0.0691	0.354
GR5	*Left*	0.5014	3.2218	0.1167	0.068
	Right	0.3282	2.0396	0.0948	0.821
	Total	0.5180	2.4300	0.1547	0.181
GR6	*Left*	0.2801	3.2850	0.0684	0.043
	Right	0.2631	3.1041	0.0616	0.117
	Total	0.2948	1.6987	0.0977	0.813

Table C1.4. Full results of gridsearch for Gib–1 Mutant type, Naa treated tomato roots

Root	***Series***	$\hat{q}$	$\phi(\hat{q})$	$\hat{\sigma}$	**P-value**
NGR1	*Left*	0.3382	2.6912	0.0770	0.306
	Right	0.6258	2.0969	0.1696	0.582
	Total	1.5701	2.1181	0.4616	0.335
NGR2	*Left*	0.8693	2.9241	0.1992	0.070
	Right	0.2506	2.5020	0.0575	0.388
	Total	0.8576	2.2507	0.2422	0.293
NGR3	*Left*	0.2580	2.8005	0.0559	0.242
	Right	0.3033	2.7875	0.0627	0.274
	Total	0.3381	2.7466	0.0851	0.120
NGR4	*Left*	1.2952	1.9993	0.3192	0.861
	Right	0.2645	2.6556	0.0595	0.282
	Total	1.3353	3.4993	0.3050	0.012

C2. Analyses of Positions

Table C2.1. Full results of gridsearch for Wild type tomato positions

Root	***Series***	$\hat{q}$	$\chi(\hat{q})$	$\psi(\hat{q})$	$\hat{\beta}$	**P-value**
WR1	*Left*	0.3614	7.3801	3.6192	—	0.618
	Right	0.4225	6.7985	– 3.3658	—	0.824
	Total	0.4211	9.7093	– 3.0233	– 0.0506	0.078
WR2	*Left*	0.8477	6.7540	– 1.2998	—	0.765
	Right	0.2335	6.8534	– 2.1574	—	0.732
	Total	0.7509	9.8645	4.0555	0.1375	0.066
WR3	*Left*	0.3895	7.6401	2.6481	—	0.466
	Right	0.5416	6.5990	3.6328	—	0.817
	Total	0.2635	8.0895	2.4979	—	0.362
WR4	*Left*	0.2068	6.6024	– 3.4029	—	0.667
	Right	0.3486	6.9300	– 2.2692	—	0.624
	Total	1.0262	6.9331	0.4846	—	0.588
WR5	*Left*	0.6141	8.0567	– 2.8732	—	0.537
	Right	1.1375	6.8333	– 0.7595	—	0.916
	Total	0.5192	7.5264	– 3.8475	—	0.766

Table C2.1. (cont.)

WR6	*Left*	0.2135	7.5314	– 0.2091	—	0.808
	Right	0.5971	10.8340	2.5494	0.0550	0.070
	Total	0.2513	8.9635	4.1907	—	0.385
WR7	*Left*	0.4324	7.1503	– 2.9872	—	0.653
	Right	0.2267	8.2354	– 2.1327	—	0.268
	Total	0.7135	6.7347	– 2.7147	—	0.718
WR8	*Left*	0.9931	7.8768	– 2.7124	—	0.540
	Right	0.5782	6.8567	– 1.7248	—	0.829
	Total	0.9925	9.0592	– 2.2192	– 0.0866	0.094
WR9	*Left*	1.0241	8.1460	3.1672	—	0.374
	Right	0.2714	6.8946	– 0.6039	—	0.817
	Total	1.2005	6.2851	0.9674	—	0.964
WR10	*Left*	0.2247	6.6562	2.0198	—	0.783
	Right	0.2570	6.4065	3.5127	—	0.820
	Total	0.2570	7.0275	3.2689	—	0.672

Table C2.2. Full results of gridsearch for Wild type, Naa treated tomato positions

Root	*Series*	$\hat{q}$	$\chi(\hat{q})$	$\psi(\hat{q})$	$\hat{\beta}$	P-value
NWR1	*Left*	0.7896	9.3324	2.3588	0.0725	0.094
	Right	0.2438	9.9471	2.8329	0.0267	0.074
	Total	0.2438	6.4743	2.7405	—	0.873
NWR2	*Left*	1.2601	6.9706	– 3.7208	—	0.786
	Right	0.7351	10.7079	– 4.3155	– 0.1405	0.028
	Total	0.2472	7.9324	1.7675	—	0.517
NWR3	*Left*	0.2078	8.2373	2.0733	—	0.250
	Right	0.8541	7.7283	– 3.8924	—	0.341
	Total	1.3203	8.9451	0.4369	—	0.126
NWR4	*Left*	1.5177	9.1861	– 3.0528	—	0.261
	Right	0.2149	10.2801	– 4.5288	– 0.0554	0.037
	Total	0.2803	6.7374	– 3.6009	—	0.961

Table C2.3. Full results of gridsearch for Gib–1 Mutant type tomato positions

Root	*Series*	$\hat{q}$	$\chi(\hat{q})$	$\psi(\hat{q})$	$\hat{\beta}$	P-value
GR1	*Left*	0.3728	6.9308	– 0.4827	—	0.605
	Right	0.3676	5.9178	– 1.8839	—	0.923
	Total	0.2628	6.3722	– 2.7629	—	0.829
GR2	*Left*	1.9928	7.3499	– 3.7829	—	0.269
	Right	1.6337	5.9531	2.8133	—	0.902
	Total	0.9833	6.7272	– 3.2024	—	0.660
GR3	*Left*	0.4953	6.8871	– 3.6245	—	0.861
	Right	0.2114	10.1538	4.1662	0.0396	0.070
	Total	0.9809	7.7938	– 1.8380	—	0.609
GR4	*Left*	0.2002	6.2895	2.0389	—	0.959
	Right	0.3267	10.8046	– 1.8439	—	0.031
	Total	0.9025	10.9298	– 2.8645	– 0.3565	0.042
GR5	*Left*	0.4956	8.1622	2.7351	—	0.332
	Right	0.2219	8.5174	– 1.9420	—	0.252
	Total	0.3544	8.3963	3.9894	—	0.365
GR6	*Left*	0.5742	9.8192	3.9371	0.1871	0.084
	Right	0.2657	7.5623	0.1163	—	0.532
	Total	0.4030	9.7310	– 1.9787	—	0.101

Table C2.4. Full results of gridsearch for Gib–1 Mutant type, Naa treated tomato positions

Root	*Series*	$\hat{q}$	$\chi(\hat{q})$	$\psi(\hat{q})$	$\hat{\beta}$	P-value
NGR1	*Left*	1.7504	8.1251	3.5804	—	0.230
	Right	0.4070	6.0074	– 0.9566	—	0.932
	Total	1.7525	8.4210	2.5629	—	0.215
NGR2	*Left*	0.4112	6.7781	3.1134	—	0.643
	Right	0.2029	6.1124	– 2.7566	—	0.815
	Total	0.9003	6.3885	3.2463	—	0.790
NGR3	*Left*	0.2213	6.7840	2.9238	—	0.541
	Right	0.4207	8.1795	– 3.8203	– 0.1276	0.142
	Total	0.2694	6.7752	– 0.1645	—	0.609
NGR4	*Left*	0.4493	6.9349	– 3.1058	—	0.496
	Right	0.3254	8.2183	1.3526	—	0.151
	Total	0.2658	6.7278	– 1.9309	—	0.662

APPENDIX D.

Results of Simple and Regression Quantality Search for Fern Roots

D1. Results of Initial Quantogram Analyses

In this section, the full results of basic quantogram analyses on Fern roots performed for all their series of raw spacings and positions with estimated quantum values, peak cosine quantogram values, standard deviations and their 'nominal' significance probabilities are presented. In the case of positions, the results contain peak modular quantogram values instead as well as an estimate of β *only if* the observed peak is found to be significant (i.e. $P < 0.1$) and also the value of $\psi(\hat{q})$ regards the β-effect as being significant (i.e. $\psi(\hat{q})$ is outside the range ± 2).

All quantogram analyses have been performed over the ranges given in section 5.4.4 with an increment of 0.001. Significance probabilities have been assessed as described in section 5.4.1.3.

Table D1.1. Full results of gridsearch for Fern root spacings

Root	*Series*	$\hat{q}$	$\phi(\hat{q})$	P-value
CT1	*Left*	10.6383	4.7761	0.001
	Right	10.9890	4.2790	0.525
	Total	3.5211	4.9648	0.001
CT2	*Left*	10.4167	2.9544	0.771
	Right	0.6277	2.8608	0.501
	Total	0.4036	2.5724	0.696
CT3	*Left*	0.6468	2.4635	0.819
	Right	0.3022	2.7938	0.660
	Total	0.6576	2.7906	0.473
CT4	*Left*	10.6383	3.2515	0.192
	Right	0.3229	2.2936	0.924
	Total	0.2130	2.8081	0.504
MQ	*Left*	1.0137	3.0498	0.104
	Right	0.2268	1.8843	0.913
	Total	0.6417	2.3283	0.203

Table D1.2. Full results of gridsearch for Fern root positions

Root	*Series*	$\hat{q}$	$\chi(\hat{q})$	$\psi(\hat{q})$	$\hat{\beta}$	P-value
CT1	*Left*	10.7527	7.9839	– 0.3546	—	0.848
	Right	10.7527	8.5441	3.5097	3.64	0.169
	Total	3.3670	7.6054	3.0529	—	0.500
CT2	*Left*	0.2904	5.6302	– 1.9905	—	0.957
	Right	0.3152	6.3189	3.5446	—	0.825
	Total	0.3632	7.2687	– 0.5589	—	0.588
CT3	*Left*	0.6469	7.2307	– 0.7847	—	0.385
	Right	0.3013	5.4181	– 3.2716	—	0.983
	Total	2.4091	6.0370	3.3563	—	0.955
CT4	*Left*	10.7527	6.4668	–1.5232	—	0.774
	Right	0.8725	5.8127	– 1.6804	—	0.914
	Total	0.2920	7.7143	1.8874	—	0.331
MQ	*Left*	1.1328	10.1017	– 1.0721	—	0.085
	Right	0.2342	6.3843	1.6080	—	0.971
	Total	0.2474	9.1433	3.4349	—	0.247

D2. Results of Regression Quantality Search

This section gives the full results of 2D gridsearches performed as described in section 6.6.2 in order to estimate the parameters of regression quantal model. Note that P-values have been obtained performing 99 simulations.

Table D2.1. Full results of 2D gridsearch for Fern root spacings

Root	*Series*	$\hat{q}$	$\hat{\gamma}$	$\phi(\hat{q},\hat{\gamma})$	P-value
CT1	*Left*	2.6999	0.0171	3.8103	0.53
	Right	0.2073	0.0075	3.9530	0.46
	Total	3.5273	0.0000	4.9648	0.02
CT2	*Left*	0.2549	0.0126	3.9824	0.12
	Right	0.2421	0.0107	4.2241	0.04
	Total	0.2245	0.0068	3.2248	0.85
CT3	*Left*	1.4779	0.0671	3.8086	0.42
	Right	0.2893	0.0094	3.8312	0.45
	Total	0.2577	0.0015	4.1632	0.05
CT4	*Left*	0.5667	0.0300	3.7750	0.46
	Right	0.3940	0.0150	4.0102	0.11
	Total	0.2116	0.0002	3.3989	0.83
MQ	*Left*	1.0106	0.0049	3.2932	0.49
	Right	0.2245	0.0014	2.6444	0.90
	Total	0.5948	0.0043	2.7929	0.36

APPENDIX E.

Additional Results of Hierarchical Quantality Search

This appendix is the addendum to the section 6.4 in Chapter 6 to present the alternative hierarchical quantum values obtained for some groups of tomato roots. The results are obtained by applying the algorithmic approach as described in section 6.2.4, however with different quantum values which are the second indicative values of each treatment groups, and around which the level 2 analyses have been initiated. Here we only present the solutions which give some indication of hierarchical quantality. It must be noted that additional analyses have been performed by following a different setup for the algorithmic search. That is basically to search for a quantum value on the combined data of one treatment group and narrow the range for the other treatments of the same level around this initial value. If we repeat this analysis for each treatment group starting from a different one each time, we only discover possible combinations that are close to each other at the level 1. Note that previously we began the analysis for each treatment group independently. For the sub-levels of hierarchy, we applied the same setup. Note that we reduced the original ranges in different fractions by making sure that the smallest range of search was again a quarter of the original range. Results of the analyses with this new setup agreed with the results we have presented in the thesis and this appendix. Therefore, we can confidently conclude that we have recovered all possible solutions in our analyses.

For the reader to follow results below, it is necessary to point out that $\hat{q}$ values in the first highlighted columns in Tables E1–E3 were obtained by initiating the analyses around 0.2409, 0.4994 and 0.3544 respectively.

Table E1. Results of hierarchy level 2 analyses for Wild type roots and also level 3 analyses for their corresponding L and R series

root	$\hat{q}$	$\hat{q}_L$	$\hat{q}_R$	P*
WR1	0.2412 (0.086)	0.2405 (0.007)	0.2259 (0.437)	**0.027**
WR2	0.2369 (0.296)	0.2347 (0.197)	0.2376 (0.526)	0.285
WR3	0.2640 (0.019)	0.2636 (0.036)	0.3032 (0.754)	**0.159**
WR4	0.2944 (0.233)	0.2982 (0.917)	0.2637 (0.376)	0.744
WR5	0.3087 (0.723)	0.3084 (0.770)	0.3586 (0.763)	0.735
WR6	0.2947 (0.024)	0.2952 (0.032)	0.3433 (0.585)	**0.133**
WR7	0.2378 (0.948)	0.2118 (0.941)	0.2685 (0.918)	0.987
WR8	0.2360 (0.236)	0.2478 (0.787)	0.2358 (0.109)	0.315
WR9	0.2401 (0.147)	0.2403 (0.084)	0.2300 (0.718)	0.308
WR10	0.3113 (0.223)	0.3115 (0.730)	0.3135 (0.416)	0.623
P*	**0.008**			

Table E2. Results of hierarchy level 2 analyses for Gib–1 Mutant roots and also level 3 analyses for their corresponding L and R series

root	$\hat{q}$	$\hat{q}_L$	$\hat{q}_R$	P*
GR1	0.3664 (0.745)	0.3703 (0.985)	0.3626 (0.898)	0.932
GR2	0.3512 (0.364)	0.3155 (0.071)	0.3502 (0.714)	0.303
GR3	0.4297 (0.251)	0.4908 (0.179)	0.4279 (0.088)	**0.066**
GR4	0.3307 (0.194)	0.3239 (0.902)	0.3283 (0.130)	0.446
GR5	0.5008 (0.012)	0.5014 (0.028)	0.4993 (0.425)	**0.052**
GR6	0.4080 (0.559)	0.4092 (0.305)	0.4029 (0.864)	0.623
P*	**0.098**			

Table E3. Results of hierarchy level 2 analyses for Gib–1 Mutant roots and also level 3 analyses for their L and R series (positions used)

root	$\hat{q}$	$\hat{q}_L$	$\hat{q}_R$	P*
GR1	0.3732 (0.801)	0.3731 (0.199)	0.3675 (0.267)	**0.177**
GR2	0.3898 (0.307)	0.4725 (0.904)	0.3558 (0.423)	0.764
GR3	0.4374 (0.718)	0.4951 (0.307)	0.4375 (0.525)	0.323
GR4	0.4617 (0.508)	0.5668 (0.753)	0.4278 (0.566)	0.730
GR5	0.4984 (0.077)	0.4961 (0.555)	0.4983 (0.362)	0.501
GR6	0.4031 (0.034)	0.4032 (0.348)	0.3972 (0.548)	0.450
P*	**0.164**			

Appendix F.

Data Sets

This appendix presents the data sets used for the current study of quantality. Data consist of measurements of distances between laterals on the roots of Onions, Tomatoes and Ferns. Section F1 gives Onion roots with their rank series, "r", as well as total series. Measurements are in *millimetres* as originally provided. Section F2 and F3 give Tomato and Fern roots respectively with their left, right and total series. Measurements are in *centimetres* as originally provided.

F1. Onion Data Set

Table F1.1. Control group root spacings (mm)

Root	r1	r2	r3	r4	r5
C1	12.0, 9.5, 2.5, 4.5, 10.5, 6.0	2.5, 36.0, 31.0, 2.0, 4.5, 1.5, 1.0, 8.5, 16.0	14.0, 1.5, 2.5, 1.5, 3.0, 2.5, 4.0, 2.5, 2.0, 1.5, 0.5, 11.0, 2.5, 4.0, 2.0, 2.5, 5.0	3.5, 13.5, 13.5, 67.0	32.0, 62.0, 3.5
Total	2.5, 1.0, 4.5, 4.0, 5.0, 4.5, 2.5, 4.5, 0.5, 1.5, 8.0, 0.5,1.0, 3.0, 1.5, 2.5, 1.5, 3.0, 2.5, 4.0, 2.5, 2.0, 1.5, 0.5, 5.0, 2.0, 4.0, 0.5, 1.5, 0.5, 0.5, 3.5, 2.0, 2.5, 0.5, 4.5, 6.0, 4.5, 1.0, 2.0, 0.5				
C2	23.0, 3.0, 20.5, 19.0	27.0, 4.5, 5.0, 7.5, 3.0, 15.5, 7.5	30.0, 7.0, 17.0	9.5, 6.0, 6.0, 3.5, 30.0, 4.0	46.5
Total	5.0, 0.5, 1.0, 3.0, 6.0, 6.0, 3.5, 3.0, 3.0, 1.5, 4.0, 0.5, 5.0, 1.5, 6.0, 2.0, 1.0, 2.5, 4.0, 1.5, 7.5, 2.5, 5.0				
C3	3.0, 25.5, 6.5	6.0, 26.5, 7.0	5.0, 6.0, 18.0, 15.5, 17.0	1.5, 19.0, 8.0, 1.5, 3.5, 4.0, 4.5, 3.0	7.5, 3.0, 3.0, 7.5, 3.0, 3.5, 2.0

Table F1.1. (cont.)

Total	1.0, 5.0, 6.0, 2.0, 7.5, 2.0, 1.0, 0.5, 2.5, 2.5, 1.0, 1.5, 1.5, 1.0, 3.0, 1.5, 2.0, 2.0, 0.5, 1.5, 6.5, 1.5, 3.5, 2.5, 1.5, 1.5, 3.0, 0.5, 2.5				
C4	4.5, 7.0, 7.5, 14.0, 17.5, 19.5	2.5, 2.0, 3.5, 10.5, 2.5, 9.0, 2.5, 10.5, 21.5, 13.5	1.5, 10.0, 9.0, 9.5, 10.0, 8.5, 4.0, 6.5, 5.0	4.0, 3.0, 7.5, 7.0, 11.5, 4.5, 24.5	7.0, 8.5, 14.0
Total	1.0, 2.5, 2.0, 0.5, 2.0, 1.0, 3.5, 0.5, 1.0, 0.5, 0.5, 3.5, 1.0, 2.0, 0.5, 0.5, 1.5, 5.0, 2.0, 2.0, 0.5, 2.0, 0.5, 0.5, 6.0, 1.5, 3.5, 4.5, 0.5, 1.5, 7.0, 4.0, 0.5, 6.0, 2.0, 3.0, 2.5				
C5	3.5, 1.0, 6.5, 5.5, 8.5, 25.0, 18.0	9.0, 8.5, 9.0, 4.0, 4.5, 4.5, 1.5, 13.5, 10.5, 1.5	6.5, 3.5, 1.0, 5.0, 7.5, 6.0, 18.5, 9.0, 5.5, 1.0, 5.0, 4.0, 22.5, 3.5, 6.5	4.0, 8.0, 3.0, 23.5, 6.0, 2.5, 1.0, 5.5, 16.5, 5.0, 5.0, 3.0, 3.5, 6.0, 3.0	1.5, 3.5, 3.0, 8.0, 11.5, 15.5, 11.5, 8.5
Total	4.0, 1.5, 1.0, 2.0, 1.5, 1.0, 1.0, 3.0, 0.5, 1.0, 1.0, 4.0, 1.5, 2.5, 0.5, 1.0, 2.0, 1.5, 1.0, 2.0, 1.5, 3.5, 0.5, 2.5, 2.0, 1.0, 2.5, 1.0, 1.5, 3.5, 0.5, 3.0, 6.0, 0.5, 5.0, 0.5, 0.5, 1.0, 3.5, 0.5, 0.5, 0.5, 3.0, 2.0, 5.0, 3.5, 1.5, 3.0, 3.5, 4.0, 2.0, 1.5, 1.5, 5.0				
C6	9.0, 44.5	14.5, 72.0	10.0,1.5, 15.5, 1.5, 11.0, 2.0, 11.0, 3.5, 3.5, 11.0	30.5, 5.0, 6.0	7.5, 3.5, 5.0, 10.0, 9.0, 2.0
Total	9.0, 2.0, 0.5, 3.0, 4.5, 1.5, 0.5, 1.5, 5.0, 2.5, 6.0, 1.5, 4.0, 5.0, 2.0, 2.0, 6.0, 5.0, 1.0, 2.5, 3.5, 6.0, 5.0, 7.0				
C7	23.0, 5.0, 5.5, 38.0	13.0, 7.5	4.5, 5.0, 12.5, 14.0, 12.5, 1.5, 15.5, 7.0, 7.0, 5.0, 12.0	2.5, 6.0, 3.0, 5.0, 5.5, 4.0, 22.0, 10.5, 4.5, 35.5	–
Total	2.0, 2.5, 5.0, 1.0, 3.0, 5.0, 1.5, 2.0, 2.0, 4.0, 8.0, 7.0, 5.0, 0.5, 1.5, 3.5, 7.0, 3.5, 1.0, 0.5, 7.0, 4.5, 2.5, 5.0, 3.0, 4.0, 5.0, 4.0				
C8	5.5, 15.5, 22.0, 2.5, 10.5, 5.0	5.5, 12.0, 15.5, 10.0, 4.0, 11.5, 6.5	3.5, 11.5, 13.5, 51.0	26.0, 3.0, 7.5, 2.0, 13.0	31.5, 5.0, 22.5
Total	3.0, 0.5, 1.0, 4.0, 1.5, 5.0, 5.5, 5.0, 3.0, 7.5, 10.0, 1.0, 2.0, 0.5, 2.0, 5.0, 2.0, 1.5, 1.0, 4.0, 2.5, 4.0, 7.5				
C9	12.5, 8.5, 2.0, 7.0, 1.0, 9.0, 29.0	3.5, 9.5, 12.0, 9.0, 7.5	41.5, 27.5, 2.0	4.5	–
Total	2.0, 3.5, 4.5, 0.5, 2.0, 2.5, 6.0, 2.0, 4.0, 3.0, 1.0, 5.0, 4.0, 3.5, 8.0, 6.0, 4.5, 7.0, 10.0, 2.0				
C10	9.5, 1.5, 12.5, 9.5, 22.5	5.0, 16.0, 6.5, 9.0	22.0, 15.0, 17.5	6.5, 15.5, 26.5	24.0
Total	5.0, 1.0, 3.5, 1.5, 1.5, 2.0, 9.0, 3.5, 1.0, 0.5, 2.0, 2.5, 4.0, 5.0, 4.0, 6.5, 2.0, 1.0, 4.0				
C11	6.5, 13.0, 4.5, 7.0	5.0, 9.5, 8.0, 3.5, 6.0, 6.5, 14.5, 13.5, 6.0	4.5, 5.0, 3.5, 6.5, 18.0, 2.0, 5.0, 2.0, 8.5, 5.0, 3.0	4.5, 50.0, 3.0	–
Total	1.5, 3.5, 1.0, 3.5, 1.0, 4.0, 2.5, 0.5, 5.0, 1.5, 2.0, 4.0, 2.0, 2.5, 4.0, 3.0, 0.5, 2.0, 5.0, 2.0, 2.0, 3.0, 3.0, 0.5, 5.0, 2.0, 1.0, 5.0				
C12	5.5, 10.5, 5.5, 16.0, 4.0, 2.0, 15.5, 12.0	7.0, 5.0, 5.5, 8.0, 19.5, 33.5, 5.0	2.0, 4.0, 4.5, 2.0, 35.0	10.5, 4.0, 13.5, 7.0, 6.0, 14.5	23.5, 26.5, 65.0, 80.0
Total	2.0, 2.0, 2.0, 4.5, 0.5, 0.5, 1.0, 2.0, 1.5, 1.5, 4.0, 1.5, 4.0, 2.5, 4.0, 5.5, 1.5, 7.0, 1.5, 4.0, 0.5, 1.5, 4.0, 2.0, 7.0, 8.5, 6.0, 5.0, 1.0				
C13	7.5, 12.0, 17.5, 2.0, 4.0, 2.0, 2.0, 7.5, 1.5	18.5, 23.5, 5.5, 12.5	7.0, 11.5, 3.5, 6.5, 10.5	17.0, 6.5, 3.5, 13.5	14.0, 12.0, 12.0
Total	1.0, 9.0, 0.5, 6.5, 0.5, 0.5, 6.5, 3.5, 0.5, 1.0, 2.5, 4.5, 2.0, 3.0, 5.5, 1.5, 0.5, 3.0, 1.0, 2.0, 2.0, 0.5, 7.0, 1.5, 4.0,				

Table F1.1. (cont.)

C14	89.0, 34.0, 12.0, 17.0, 4.5	2.5,7.5,2.5, 3.0,7.0, 36.5, 10.5, 4.5, 20.5, 20.0, 21.5, 8.5	4.0, 4.5, 11.0, 8.0, 22.0, 4.5, 3.0, 4.0, 5.5, 1.0,13.0, 13.5, 11.0,14.0, 11.0, 9.0, 15.0	6.0, 1.5, 2.5, 44.5, 13.0, 24.0, 3.5, 8.5, 1.0, 19.0	54.5, 7.0, 7.5, 6.0, 11.5, 7.0, 4.0, 7.0, 11.5, 26.0
Total	7.5, 4.0, 0.5, 4.0, 7.0, 2.5, 1.5, 6.0, 2.0, 0.5, 3.0, 6.0, 1.0, 0.5, 2.5, 8.5, 4.5, 3.0, 2.0, 2.0, 5.0, 0.5, 1.0, 6.0, 1.0, 5.0, 1.0, 1.0, 3.5, 0.5, 4.0, 1.5, 3.0, 4.0, 0.5, 3.5, 3.0, 4.0, 1.0, 5.5, 3.5, 1.5, 2.0, 3.5, 1.5, 2.5, 4.5, 1.0, 3.5, 5.5, 2.0, 2.5, 2.5, 2.5, 0.5, 5.5				
C15	17.5	2.0, 8.0, 5.0, 4.5, 1.5, 7.5, 3.5, 4.0, 8.0, 15.0,6.0, 9.0	74.5	20.0, 6.0, 15.0	-
Total	2.0, 2.0, 8.0, 1.5, 0.5, 3.0, 0.5, 4.0, 1.5, 7.5, 3.5, 4.0, 2.0, 6.0, 5.0, 4.0, 6.0, 6.0, 9.0, 12.0				
C16	3.5	13.0, 58.5, 12.0, 3.5	3.5, 4.0, 1.5, 5.0, 3.0, 2.5, 3.0, 5.0, 2.5, 4.0, 1.0, 3.5, 1.5, 4.0, 3.0, 9.0, 1.0, 3.0, 20.0, 1.5, 15.5	7.5, 1.5, 37.0, 4.0, 4.5	-
Total	13.0, 3.5, 4.0, 1.5, 5.0, 3.0, 2.5, 3.0, 2.0, 1.5, 1.5, 2.5, 4.0, 1.0, 3.5, 1.5, 4.0, 3.0, 9.0, 1.0, 1.5, 1.5, 3.0, 2.5, 1.5, 3.5, 1.0, 2.5, 6.0, 1.5, 5.5, 3.5, 6.5				
C17	4.5	7.5, 3.5, 2.5, 4.5, 4.5, 3.5, 2.5, 6.5, 3.0, 9.0, 5.5, 7.5, 10.0, 7.5, 5.0, 2.0	5.0, 1.5, 21.5, 46.0, 3.0, 4.0, 3.0, 1.5	16.5, 4.0, 3.5, 3.0, 9.0, 4.0, 15.5	-
Total	7.5, 3.5, 2.5, 2.0, 2.5, 2.5, 1.5, 0.5, 3.5, 2.5, 6.5, 3.0, 5.5, 3.5, 4.5, 1.0, 3.0, 3.5, 1.0, 2.0, 8.0, 1.0, 4.0, 2.5, 5.0, 2.0, 5.0, 1.0, 2.0, 3.0, 4.0, 1.5, 14.0, 1.0, 4.5				
C18	4.5	7.5, 3.5, 2.5, 4.5, 4.5, 3.5, 2.5, 6.5, 3.0, 9.0, 5.5, 7.5, 10.0, 7.5, 5.0, 2.0	5.0, 1.5, 21.5, 46.0, 3.0, 4.0, 3.0, 1.5	16.5, 4.0, 3.5, 3.0, 9.0, 4.0, 15.5	-
Total	8.0, 8.0, 1.0, 1.0, 0.5, 3.0, 0.5, 4.5, 1.5, 0.5, 2.0, 1.5, 0.5, 2.5, 2.0, 3.0, 1.0, 1.5, 1.5, 2.5, 5.0, 0.5, 1.0, 2.0, 5.0, 1.5, 3.5, 7.0, 4.5, 3.0, 3.0, 2.0, 3.5, 1.0, 4.0, 6.0, 1.5, 5.5, 2.5, 4.0, 4.5, 1.0, 4.0, 1.0, 6.0, 1.0, 7.0, 2.0, 1.0, 4.5, 5.5, 6.0, 1.0				

Table F1.2. Weakly–treated group root spacings (mm)

Root	R1	R2	R3	R4	R5
W1	1.9, 9.6, 2.4, 4.1, 5.2, 3.5, 1.3, 6.0, 0.2, 0.4, 6.7, 5.3, 1.0	29.8, 16.6, 4.2, 3.2	7.6, 3.6, 2.4, 2.6, 4.2, 1.7	6.9, 15.1, 11.6	26.4, 3.0, 1.0, 3.0, 4.2, 1.7, 2.3, 3.0, 2.3, 4.5, 1.0, 1.3, 2.7, 1.2, 1.4, 1.6, 2.9, 1.5, 0.9
Total	2.2, 6.4, 1.9, 9.6, 2.4, 3.9, 0.2, 2.8, 1.0, 1.4, 0.2, 1.4, 0.2, 1.7, 1.3, 1.0, 1.7, 1.2, 1.1, 1.0, 0.2, 0.4, 1.0, 0.4, 2.3, 1.7, 1.3, 1.5, 0.4, 0.6, 0.4, 0.9, 1.5, 0.2, 0.2, 0.4, 0.2, 0.2, 1.2, 0.2, 1.2, 1.4, 0.2, 2.9, 1.1, 0.4, 0.9, 0.4, 0.9				
W2	10.9, 2.9, 6.0, 4.3, 4.4, 3.6, 3.9, 3.4, 2.4, 3.8, 5.8, 2.8, 1.0,4.6, 2.0	7.7, 12.3, 2.8, 3.0, 5.0	25.0, 2.4, 2.8, 1.6, 10.5, 0.7, 0.4, 0.9, 0.5, 1.2, 1.6	32.0, 4.6, 5.2, 9.8	4.7, 6.2, 10.2, 4.9, 4.2, 1.0, 2.6, 2.0, 2.2, 2.2, 3.0, 3.6, 2.4, 5.6, 1.5
Total	0.4, 7.8, 2.7, 2.0, 0.9, 5.2, 0.1, 0.7, 4.3, 4.4, 0.8, 2.5, 0.3, 0.3, 1.8, 1.8, 1.0, 1.4, 1.0, 0.1, 2.3, 0.2, 0.2, 1.8, 1.6, 0.6, 0.2, 2.0, 0.8, 1.6, 0.6, 0.4, 0.2, 2.2, 0.4, 0.4, 0.2, 2.2, 0.2, 2.2, 1.5, 0.5, 0.2, 0.4, 0.2, 0.4, 0.3, 0.5, 0.7, 0.5, 1.6				
W3	12.4, 40.7, 2.4	15.1, 2.2, 8.8, 2.0, 3.4, 1.9, 1.5, 1.2	5.0, 1.8, 11.7	0.8, 2.5	5.7, 3.9, 18.6, 2.8, 9.2, 6.6, 2.5, 2.9, 5.6
Total	4.1, 1.6, 3.9, 6.9, 7.0, 4.7, 2.8, 7.6, 1.4, 0.2, 0.6, 4.2, 0.6, 0.8, 0.4, 2.1, 0.4, 0.3, 2.0, 0.6, 2.8, 1.9, 0.3, 0.6, 0.6, 0.1, 1.1				
W4	5.4, 25.1, 23.3, 6.2, 6.5, 4.9, 3.4	0.4, 35.7, 22.0, 5.2, 15.1, 1.2	9.5, 33.9, 1.9, 1.7, 1.6, 3.4, 4.0, 3.0, 3.1, 3.5, 4.2, 2.6, 3.6, 2.2, 2.0, 2.4	3.8, 2.3, 25.4, 9.7, 5.8, 2.5, 1.5, 2.3	–
Total	2.0, 0.4, 5.8, 1.3, 4.1, 8.1, 3.8, 2.3, 10.3, 0.6, 4.7, 1.9, 1.7, 1.6, 3.4, 1.2, 2.8, 3.0, 1.1, 1.9, 0.1, 0.8, 2.4, 0.3, 2.6, 0.5, 1.1, 1.4, 1.2, 0.3, 2.0, 0.3, 1.0, 2.2, 1.4, 0.6, 0.2, 1.2, 1.0, 0.4				
W5	1.4, 1.0, 0.7, 2.2, 1.2, 0.5, 6.5, 1.2, 2.3, 0.7, 7.6, 6.8, 2.9, 2.0, 2.4, 1.7, 1.1, 0.6, 2.6, 8.5, 2.1, 2.4, 4.5, 2.0	14.6, 1.6, 1.4, 8.0, 2.2, 2.7, 1.8, 3.2, 0.9, 13.8, 1.5, 1.0, 1.1, 1.8	2.2, 1.9, 4.2, 1.0, 5.8, 5.6, 13.8, 16.0, 2.6, 2.8, 6.2, 3.7	1.5, 1.0, 1.4, 8.3, 0.8, 1.2, 4.1, 3.6, 9.0, 2.5, 4.6, 1.3, 4.7, 2.5, 0.5, 2.2, 0.3, 1.8, 7.9, 1.7, 3.7, 3.1	2.4, 7.2, 2.5, 2.5, 6.1, 1.4, 1.0, 1.4, 0.9, 1.1, 0.8, 4.8, 1.6, 6.8, 0.7, 1.5, 2.4, 0.7, 2.5, 3.2, 2.6, 11.6, 2.4
Total	0.9, 0.5, 1.0, 0.5, 0.2, 0.2, 0.1, 1.4, 0.5, 0.2, 1.0, 0.5, 0.4, 4.2, 0.9, 0.1, 0.5, 0.4, 0.4, 0.8, 0.3, 0.1, 1.9, 0.5, 0.2, 0.7, 0.8, 3.6, 0.8, 0.4, 1.0, 0.3, 0.7, 1.4, 0.9, 1.1, 0.8, 1.4, 0.2, 0.3, 1.1, 1.1, 0.3, 0.4, 1.6, 0.4, 0.8, 1.1, 0.5, 0.8, 0.9, 1.1, 0.4, 0.2, 0.6, 0.7, 0.7, 0.1, 0.5, 0.2, 1.8, 0.1, 0.4, 0.1, 0.7, 0.6, 0.8, 0.3, 0.8, 1.0, 0.3, 0.9, 0.4, 0.1, 0.5, 1.6, 0.4, 0.6, 1.4, 0.8, 0.9, 1.7, 1.1, 2.0, 0.5, 0.1, 1.7, 1.4, 0.1, 0.4, 0.6, 1.1, 0.2, 1.6				
W6	2.0, 1.5, 18.1, 2.9, 18.9, 2.4, 3.6, 6.2, 1.6, 2.8, 0.7	2.2, 3.5, 3.0, 2.3, 3.7, 6.7, 2.6, 3.0, 3.5, 8.3, 2.3, 0.6	4.0,2.8, 18.9, 1.0	6.0, 9.1, 29.1, 5.0, 4.0, 8.7, 7.9, 0.4, 0.2	15.4, 58.1, 2.0, 2.0, 2.1, 1.0
Total	10.3, 6.0, 3.1, 4.9, 2.0, 1.5, 1.6, 13.8, 2.2, 0.5, 2.9, 0.1, 3.0, 2.3, 3.7, 0.6, 3.4, 1.6, 1.1, 0.1, 2.5, 0.3, 0.2, 2.4, 0.1, 3.5, 2.5, 1.3, 2.0, 0.4, 1.6, 0.5, 1.6, 0.5, 0.2, 0.2, 0.1, 0.1, 0.2, 0.1				
W7	13.5, 5.6, 25.8, 6.4, 15.4, 2.8, 2.1, 5.5, 0.6	20.3, 5.2, 1.8, 6.0, 2.8, 3.6, 2.4, 3.4, 3.2, 4.4, 3.0, 0.8, 0.2, 0.4, 0.3, 0.4	27.6, 7.0, 2.4, 3.4, 1.7, 11.0, 1.0	5.0, 38.3, 3.4, 1.3, 0.2	26.4, 34.4, 2.3
Total	13.5, 0.5, 5.1, 1.1, 3.7, 5.9, 5.0, 5.6, 0.1, 4.4, 0.8, 1.8, 3.8, 0.2, 2.0, 2.8, 2.2, 1.4, 1.0, 1.4, 2.0, 1.4, 0.3, 0.7, 2.2, 0.6, 2.1, 1.5, 0.2, 1.5, 1.5, 0.2, 0.5, 0.1, 0.2, 0.4, 0.1, 0.2, 0.4				

Table F1.3. Strongly–treated group roots spacings (mm)

<table>
<tr><th>Root</th><th>R1</th><th>R2</th><th>R3</th><th>R4</th><th>R5</th></tr>
<tr><td>S1</td><td>2.0, 1.6, 1.2,
0.4, 1.0, 0.7,
1.0, 0.9, 1.0,
1.4, 1.7, 2.4,
0.6, 0.7, 0.4,
0.7, 0.7, 0.9,
1.3, 0.3, 0.8,
0.5, 1.7,
1.2</td><td>1.1, 2.1, 1.0,
1.2, 2.0, 0.8,
3.9, 0.5, 0.7,
1.1, 0.8, 1.2,
1.0, 0.6, 0.8,
0.4, 0.7, 2.4,
0.7, 4.4</td><td>1.8, 1.6, 11.2,
3.2, 0.6, 0.7,
0.7, 2.5, 0.8,
0.5, 1.1</td><td>4.8, 5.3, 1.0,
3.4, 2.0, 0.4,
0.9, 1.0</td><td>1.2, 2.3, 1.4,
1.6, 3.8, 0.5,
0.5, 0.7, 0.6</td></tr>
<tr><td>Total</td><td colspan="5">1.1, 1.1, 0.4, 0.6, 1.0, 0.2, 1.0, 0.4, 0.2, 1.0, 0.4, 0.5, 0.3, 0.2, 0.7, 1.0, 0.1,
0.8, 0.4, 0.6, 0.1, 0.5, 0.2, 0.5, 0.1, 1.0, 0.7, 0.1, 0.3, 0.9, 0.1, 0.7, 0.2, 0.1,
0.5, 0.1, 0.1, 0.5, 0.1, 0.4, 0.7, 0.5, 0.1, 0.1, 0.4, 0.5, 0.2, 0.2, 0.4, 0.1, 0.4,
0.2, 0.1, 0.1, 0.7, 0.3, 0.2, 0.5, 0.8, 0.4, 0.1, 1.1, 0.1</td></tr>
<tr><td>S2</td><td>2.0, 0.7, 2.9,
0.5, 0.8, 0.8,
0.5, 0.8, 1.7,
1.2, 0.4, 0.6,
0.6, 0.6, 1.4,
3.0, 2.1, 5.0,
2.1, 2.2, 2.2,
0.3, 0.6, 0.6,
0.8, 2.2, 1.3,
0.6, 0.7, 3.4,
0.5, 1.1, 2.0,
0.7, 0.5, 0.6,
0.5, 0.5, 0.7,
1.1, 1.3, 0.9,
0.9, 0.4, 1.0,
0.8, 0.8, 1.2,
0.5, 0.7, 0.9,
2.1, 1.4, 0.5,
1.1, 0.8, 0.5,
4.0</td><td>1.6, 1.4, 1.6,
0.7, 2.0, 0.9,
0.5, 0.8, 0.5,
2.0, 4.7, 1.4,
0.8, 1.5, 0.4,
0.9, 4.9, 2.4,
1.6, 2.2, 0.5,
1.8, 1.6, 5.7,
2.5, 2.6, 0.7,
0.5, 1.0, 0.6,
1.1, 1.7, 0.8,
1.0, 0.6, 0.4,
1.1, 0.5, 2.2,
2.3, 4.0, 0.8,
2.5, 1.0, 0.9</td><td>0.7, 0.5, 2.0,
1.0, 0.7, 1.3,
0.6, 1.1, 0.6,
0.5, 0.3, 0.6,
0.5, 0.3, 0.6,
0.6, 0.5, 0.9,
0.5, 0.9, 0.9,
2.2, 1.8, 2.1,
1.9, 2.6, 1.8,
1.0, 1.3, 2.3,
2.7, 4.1, 0.8,
0.9, 0.3, 2.7,
0.8, 2.3, 2.3,
1.1, 1.3, 1.0,
0.5, 0.8, 0.9,
0.7, 0.5, 0.5,
0.8, 0.8, 0.6,
1.1, 0.6, 0.8,
1.2, 1.1, 1.0,
0.8, 2.8, 0.4,
1.1, 0.5, 0.9,
0.7, 0.5</td><td>0.4, 1.4, 0.4,
1.0, 1.7, 3.4,
0.5, 1.9, 1.4,
3.7, 0.3, 2.4,
9.7, 1.3, 1.6,
2.4, 0.9, 1.5,
1.3, 4.8, 3.6,
1.5, 1.3, 0.3,
0.9, 1.2,
11.0, 1.7,
2.1, 2.1, 3.4,
0.5</td><td>1.6, 0.6, 0.4,
1.9, 0.3, 0.7,
0.3, 0.7, 1.2,
0.5, 0.6, 0.8,
0.7, 2.1, 1.8,
1.1, 2.3, 1.4,
1.2, 2.1, 1.8,
3.8, 0.9, 1.0,
1.6, 6.0, 1.1,
2.8, 1.1, 1.3,
2.0, 0.5, 1.6,
0.7, 0.3, 0.9,
0.6, 0.6, 0.4,
0.5, 0.9, 0.5,
0.6, 1.1, 0.9,
1.3, 0.3, 1.9,
1.7, 2.0, 0.4,
1.3, 2.0, 0.9,
1.8, 0.6, 1.5,
0.6</td></tr>
<tr><td>Total</td><td colspan="5">0.3, 0.2, 0.2, 0.1, 0.1, 0.3, 0.1, 0.3, 0.3, 0.2, 0.2, 0.4, 0.2, 0.3, 0.1, 0.2, 0.2,
0.2, 0.2, 0.1, 0.6, 0.1, 0.5, 0.2, 0.2, 0.3, 0.1, 0.6, 0.3, 0.5, 0.1, 0.1, 0.1, 0.3,
0.3, 0.3, 0.3, 0.2, 0.3, 0.2, 0.3, 0.1, 0.2, 0.2, 0.1, 0.3, 0.2, 0.2, 0.1, 0.1, 0.3,
0.3, 0.4, 0.1, 0.2, 0.2, 0.5, 0.4, 0.1, 0.2, 0.4, 0.3, 0.3, 0.5, 0.1, 0.6, 0.1, 0.3,
0.4, 0.6, 0.2, 0.6, 0.5, 0.1, 0.2, 0.4, 0.7, 0.3, 0.1, 0.4, 0.4, 0.2, 0.3, 0.7, 0.9,
1.8, 0.8, 0.7, 0.8, 0.3, 0.7, 0.3, 0.2, 0.1, 0.5, 0.2, 0.1, 0.2, 0.6, 0.2, 0.5, 0.4,
0.6, 0.1, 0.4, 0.5, 0.3, 0.1, 0.5, 0.4, 0.2, 0.2, 0.1, 0.3, 0.7, 0.1, 0.5, 0.7, 1.0,
0.7, 0.4, 0.2, 0.2, 0.4, 0.5, 0.2, 0.1, 1.1, 0.1, 0.1, 1.0, 0.4, 0.6, 0.2, 0.1, 0.2,
0.9, 0.2, 0.7, 0.2, 0.3, 0.1, 0.2, 0.4, 0.1, 0.2, 0.4, 0.1, 0.2, 0.3, 0.5, 0.1, 0.5,
0.1, 0.4, 0.2, 0.4, 0.1, 0.1, 0.3, 0.7, 0.2, 0.3, 0.2, 0.6, 0.9, 0.1, 0.1, 0.5, 0.2,
0.2, 0.1, 0.1, 0.4, 0.5, 0.1, 0.1, 0.1, 0.2, 0.4, 0.2, 0.6, 0.7, 0.3, 0.1, 0.1, 0.5,
0.7, 0.1, 0.8, 0.4, 0.7, 0.4, 0.2, 0.4, 0.4, 0.3, 0.5, 0.2, 0.3, 0.3, 0.8, 0.3, 0.6,
0.2, 0.2, 0.3, 0.1, 0.8, 0.2, 0.1, 0.5, 0.2, 0.7, 0.2, 0.1, 0.3, 0.1, 0.1, 0.4, 0.2</td></tr>
<tr><td>S3</td><td>1.5, 1.2, 0.9,
0.9, 3.7, 1.8,
1.9, 1.7, 2.5,
1.1, 1.1, 1.9,
5.9, 5.8, 1.9,
4.2, 0.8, 1.8,
0.5, 0.9, 1.5,
7.0, 4.6, 1.9</td><td>1.6, 4.2, 1.7,
1.6, 5.7, 1.2,
0.8, 1.4, 0.8,
1.1, 2.8, 1.4,
3.0, 1.6, 1.4,
1.4, 3.3, 0.8,
0.9, 2.9, 6.8,
1.2, 1.2, 1.2,
3.4</td><td>0.6, 0.5, 0.4,
0.6, 0.8, 1.6,
0.2, 0.4, 0.8,
0.9, 2.1, 2.0,
1.4, 1.3, 0.4,
1.3, 1.2, 1.6,
1.4, 2.9, 3.7,
1.3, 2.0, 2.7,
1.4, 1.8, 0.8,
3.2, 1.0, 1.4,
0.4, 1.0, 0.5,
1.3, 1.6, 0.8,
0.5, 1.1, 1.4,
1.4, 0.8, 3.0,
1.4, 0.5, 0.3,
1.7, 0.5</td><td>0.2, 0.7, 0.3,
0.9, 2.7, 2.4,
3.6, 12.3,
8.5, 1.8, 4.1,
1.0, 3.9, 3.1,
0.5, 2.3, 1.3,
1.6, 0.4, 0.4,
1.2, 1.2, 2.4,
1.8</td><td>0.9, 1.8, 0.5,
0.4, 0.6, 3.5,
1.8, 3.2, 1.0,
2.3, 2.8, 1.0,
1.5, 2.7, 1.1,
1.2, 2.3, 0.9,
4.7, 1.7, 1.4,
0.8, 1.4, 0.9,
0.4, 5.1, 0.9,
0.6, 1.6, 0.6,
0.5, 1.5, 0.8,
1.4, 2.0, 1.4,
0.4, 0.4</td></tr>
<tr><td>Total</td><td colspan="5">0.6, 0.5, 0.4, 0.2, 0.2, 0.2, 0.5, 0.2, 0.1, 0.3, 0.6, 0.7, 0.1, 0.1, 0.4, 0.4, 0.4,
0.2, 0.2, 0.2, 0.3, 0.9, 0.2, 1.0, 0.7, 1.3, 0.5, 0.7, 0.2, 0.2, 0.7, 0.4, 0.2, 0.2,
0.6, 0.5, 0.2, 0.1, 0.2, 0.9, 0.3, 1.1, 0.2, 1.2, 0.2, 0.9, 0.3, 0.4, 0.4, 0.2, 0.6,
0.1, 0.7, 0.1, 0.2, 1.1, 0.3, 0.5, 0.6, 0.2, 0.3, 0.6, 0.4, 0.8, 1.0, 0.1, 0.1, 1.1,
0.1, 0.8, 0.7, 1.2, 0.2, 0.1, 1.5, 0.1, 0.1, 0.8, 0.5, 0.4, 0.8, 0.2, 1.2, 0.1, 0.7,
0.2, 0.1, 0.9, 0.1, 0.1, 0.3, 0.3, 0.1, 0.2, 0.4, 0.3, 0.1, 0.5, 0.2, 0.3, 0.2, 0.6,
0.3, 0.7, 0.6, 0.2, 0.5, 0.1, 0.4, 0.1, 0.9, 0.2, 0.4, 0.7, 0.3, 0.6, 0.4, 0.2, 0.2,
0.3, 0.5, 0.2, 0.2, 0.4, 0.2, 0.2, 0.2, 0.4 ,0.6, 0.2, 0.4, 0.2, 0.4, 0.2, 0.5, 0.5,
0.3, 0.6, 0.2, 0.6, 0.3, 0.1, 0.2, 0.2, 0.3, 0.1</td></tr>
</table>

Table F1.3. (cont.)

S4	5.0, 1.8, 0.7, 1.1, 1.4, 1.2, 1.2, 1.2, 2.0, 3.8, 3.2, 3.0, 2.1, 2.9, 0.4, 0.4	3.2, 6.0, 3.8, 1.8, 0.4, 2.0, 2.1, 1.3, 3.1, 1.2, 1.1, 1.4, 1.1, 1.3, 1.4, 1.6, 2.6, 0.9, 1.1, 0.8, 0.6, 0.8, 1.0, 0.4, 1.4, 1.0, 0.7, 5.0, 0.4, 0.7, 1.1, 0.4, 0.7	1.5, 5.0, 4.6, 3.3, 3.1, 1.1, 1.0, 0.8, 4.0, 1.3, 3.2, 1.7, 0.7, 0.3, 0.3	3.9, 1.5, 1.6, 1.2, 1.9, 0.9, 1.4, 0.8, 1.8, 1.8, 3.1, 1.3, 1.8, 2.2, 1.2, 1.2, 1.4, 4.2, 0.9, 3.6, 2.5, 4.6, 1.6, 3.8, 1.7, 1.0, 1.0, 0.9, 0.4, 0.4, 1.0, 0.6	–
Total	3.9, 1.5, 1.6 ,1.2, 1.0, 0.9, 0.9, 1.4, 0.8, 1.8, 1.8, 1.6, 1.5, 1.3, 1.0, 0.8, 1.0, 0.4, 0.8, 0.2, 1.0, 0.3, 0.9, 0.9, 0.5, 0.8, 0.6, 1.3, 0.5, 0.7, 0.3, 0.8, 0.1, 1.1, 0.2, 0.9, 0.3, 1.1, 0.1, 1.2, 0.6, 0.6, 0.2, 0.6, 1.0, 0.7, 1.1, 0.8, 0.2, 0.7, 0.1, 0.8, 0.2, 0.8, 0.6, 0.8, 0.8, 0.2, 0.4, 0.7, 0.1, 0.6, 0.3, 0.7, 0.3, 0.2, 0.2, 0.5, 0.1, 0.2, 0.1, 0.6, 0.1, 0.3, 0.4, 0.2, 0.2, 0.4, 0.1, 0.1, 0.2, 0.3, 0.1				
S5	1.1, 1.3, 2.5, 3.4, 3.5, 1.0, 1.4, 1.8, 1.5, 1.1, 0.6, 1.6, 4.4, 0.6, 3.2, 0.6, 1.1, 0.8, 0.7, 1.0, 0.8, 0.7, 0.8, 0.9, 1.3, 1.0, 0.8, 0.7, 0.6, 0.5, 0.4, 0.9	1.0, 3.7, 9.9, 2.4, 7.4, 3.2, 2.0, 1.0, 1.2, 4.0, 0.6, 3.2, 1.0, 1.5, 3.0, 2.3, 0.6, 0.7, 0.4	1.2, 0.8, 5.9, 7.9, 2.0, 0.9, 2.3, 1.2, 1.0, 1.0, 5.8, 0.6, 1.0, 0.6, 3.8, 0.7, 1.0, 0.7, 0.6, 0.6, 0.6, 1.6, 2.0, 1.4, 0.7, 0.6, 0.4	1.5, 5.6, 1.6, 7.0, 2.6, 2.6, 1.9, 1.1, 1.3, 0.9, 2.4, 1.2, 2.4, 2.6, 4.0, 3.4, 0.8, 0.6, 0.3	–
Total	1.0, 1.2, 1.2, 0.8, 0.5, 0.6, 1.5, 0.6, 1.1, 1.3, 0.3, 2.2, 0.1, 1.6, 0.6, 1.1, 1.3, 1.0, 1.2, 0.8, 0.2, 0.7, 0.1, 0.6, 1.6, 0.2, 0.2, 0.8, 0.5, 0.5, 0.6, 0.2, 0.2, 0.2, 1.0, 0.5, 0.1, 1.0, 0.4, 0.9, 0.1, 0.8, 0.4, 0.4, 0.4, 0.2, 0.4, 0.6, 0.6, 0.6, 0.8, 0.6, 0.6, 0.4, 0.7, 0.1, 0.7, 0.7, 0.3, 0.1, 0.5, 0.6, 0.2, 0.4, 0.3, 0.3, 0.5, 0.9, 0.2, 1.1, 0.9, 0.1, 0.8, 0.5, 0.2, 0.4, 0.1, 0.1, 0.5, 0.1, 0.3				
S6	0.9, 0.3, 0.4, 0.5, 0.9, 0.5, 0.3, 1.2, 0.9, 0.5, 0.4, 0.4, 0.8, 0.7, 0.2, 0.7, 0.9, 3.1, 0.7, 0.5, 1.0, 0.7, 1.7, 1.6, 0.4, 0.2, 0.8, 0.3, 0.7, 0.5, 0.5, 1.8, 1.0, 0.5, 0.8, 0.7, 0.6, 0.4, 0.4, 0.6, 0.8, 0.4, 0.6, 0.7, 0.8, 0.3, 0.6, 0.4, 0.3, 0.5, 0.6, 0.7, 0.7, 0.5, 0.5, 0.5, 0.2, 0.2, 0.6, 0.6, 0.4, 0.4, 0.4, 0.4, 0.4, 0.4, 0.6, 0.4, 0.6, 0.6, 0.6, 0.8, 0.4, 0.4, 0.6, 0.8, 0.6, 0.3, 0.8, 0.3, 0.4, 0.4, 0.3, 1.1, 0.6, 0.5, 0.7 0.5, 0.6, 0.6, 1.0, 0.7, 0.4, 0.4, 0.6, 0.5, 0.7, 0.5, 0.3, 0.6, 0.4, 0.4, 0.7, 0.5, 0.6, 0.4, 0.4, 0.4, 0.4, 0.8, 0.8, 0.6, 1.2, 0.6, 0.6, 0.4	1.0, 0.8, 1.0, 0.4, 4.5, 1.3, 1.4, 0.6, 0.9, 3.7, 1.0, 4.0, 2.0, 1.0, 1.0, 4.1, 0.6, 1.7, 0.4, 0.7, 0.3, 0.5, 0.6, 0.7, 0.7, 0.6, 0.7, 0.6, 0.4, 0.8, 1.3, 0.5, 0.6, 0.6, 0.8, 0.9, 0.5, 2.3, 0.5, 0.4, 0.4, 0.4, 0.4, 0.4, 0.6, 0.6, 0.6, 0.4, 0.4, 0.9, 0.5, 0.4, 0.4, 0.4, 0.6, 0.4, 0.5, 0.6, 0.5, 0.5, 0.5, 0.4, 0.5, 0.5, 0.4, 0.4, 0.6, 0.4, 0.6, 0.8, 0.5, 0.5, 0.4, 0.7, 0.5, 0.2, 0.6, 1.0, 0.6, 0.6, 0.6, 0.6, 0.8, 0.6, 0.4, 0.4, 0.4	1.2, 0.9, 0.9, 0.8, 0.6, 0.4, 0.7, 0.5, 4.0, 1.3, 0.9, 0.4, 0.8, 0.8, 0.9, 0.5, 0.8, 0.7, 1.0, 1.6, 1.3, 0.6, 0.5, 4.1, 0.5, 0.9, 0.4, 0.4, 0.6, 3.6, 6.0, 0.4, 0.5, 0.7, 0.4, 0.5, 0.6, 0.5, 0.8, 0.4, 0.8, 0.4, 0.4, 0.4, 0.8, 0.4, 1.5, 1.4, 0.3, 0.5, 0.5, 0.8, 0.7, 0.4, 0.4, 0.5, 1.2, 1.2, 0.8, 0.7, 0.5, 1.4, 1.4, 1.0, 1.2, 0.4, 0.4, 1.0, 0.9, 1.2, 0.5, 1.0, 1.4, 0.8, 1.5, 0.4, 0.3	2.9, 1.3, 1.6, 3.5, 8.9, 0.6, 3.3, 0.5, 1.6, 3.4, 0.5, 0.5, 0.6, 0.6, 0.6, 0.5, 0.9, 0.7, 0.3, 0.4, 0.5, 1.0, 0.5, 0.7, 0.4, 0.6, 0.4, 0.2, 0.5, 0.6, 1.2, 0.5, 0.9, 0.5, 0.5, 0.4, 0.4, 0.6, 0.4, 0.7, 0.5, 0.4, 0.5, 0.3, 0.4, 0.4, 0.5, 1.3, 0.4, 0.6, 0.6, 0.5, 0.8, 0.4, 0.6, 0.5, 0.4, 0.4, 0.5, 0.3, 0.6, 0.6, 0.5, 0.5, 0.8, 0.4, 0.7, 0.5, 0.6, 0.4, 0.5, 0.3, 0.4, 0.4, 0.8, 0.4, 0.5, 0.5, 0.4, 0.6, 0.4, 0.6, 0.3, 0.4, 0.3, 0.5, 0.3, 0.8, 1.0, 0.6, 0.4, 0.4, 0.3, 0.4	–
Total	0.8, 0.2, 0.2, 0.4, 0.3, 0.2, 0.1, 0.4, 0.4, 0.1, 0.3, 0.3, 0.1, 0.2, 0.4, 0.1, 0.3, 0.2, 0.5, 0.5, 0.6, 0.3, 0.5, 0.4, 0.4, 0.8, 0.3, 0.4, 0.2, 0.1, 0.1, 0.5, 0.7, 0.2, 0.5, 0.2, 0.4, 0.8, 0.1, 0.7, 0.4, 0.5, 0.2, 0.3, 0.2, 0.6, 0.4, 0.3, 0.1, 0.3, 0.6, 0.1, 0.8, 0.2, 0.4, 0.1, 1.1, 0.2, 0.2, 0.2, 0.2, 0.5, 0.1, 0.3, 0.4, 0.3, 0.2, 0.3, 0.5, 0.8, 0.2, 0.8, 0.2, 0.5, 0.3, 0.5, 0.1, 0.4, 0.3, 0.1, 0.5, 0.1, 0.4, 0.2, 0.4, 0.3, 0.1, 0.2, 0.3, 0.1, 0.2, 0.5, 0.1, 0.4, 0.4, 0.2, 0.2, 0.3, 0.2, 0.1, 0.1, 0.3, 0.3, 0.2, 0.1, 0.5, 0.1, 0.3, 0.1, 0.2, 0.2, 0.5, 0.2, 0.4, 0.6, 0.1, 0.3, 0.2, 0.2, 0.1, 0.2, 0.2, 0.2, 0.4, 0.1, 0.5, 0.2, 0.4, 0.2, 0.2, 0.1, 0.4, 0.1, 0.1, 0.3, 0.2, 0.3, 0.1, 0.4, 0.2, 0.2, 0.4, 0.2, 0.2, 0.2, 0.2, 0.2, 0.1, 0.1, 0.2, 0.2, 0.1, 0.1, 0.4, 0.2, 0.2, 0.2, 0.2, 0.1, 0.3, 0.2, 0.2, 0.1, 0.3, 0.1, 0.1, 0.3, 0.1, 0.4, 0.4, 0.1, 0.1, 0.2, 0.4, 0.1, 0.1, 0.4, 0.2, 0.3, 0.1, 0.2, 0.3, 0.1, 0.1, 0.2, 0.1, 0.3, 0.1, 0.3, 0.1, 0.3, 0.1, 0.1, 0.5, 0.4, 0.2, 0.2, 0.2, 0.2, 0.1, 0.2, 0.1, 0.2, 0.4, 0.4, 0.1, 0.1, 0.5, 0.5, 0.1, 0.4, 0.3, 0.2, 0.1, 0.1, 0.2, 0.4, 0.1, 0.3, 0.2, 0.2, 0.2, 0.2, 0.2, 0.2, 0.3, 0.1, 0.1, 0.3, 0.2, 0.2, 0.2, 0.1, 0.1, 0.2, 0.2, 0.2, 0.2, 0.3, 0.1, 0.4, 0.1, 0.1, 0.2, 0.2, 0.1, 0.3, 0.1, 0.1, 0.4, 0.2, 0.2, 0.2, 0.1, 0.1, 0.2, 0.2, 0.1, 0.1, 0.3, 0.1, 0.2, 0.2, 0.2, 0.1, 0.1, 0.2, 0.2, 0.4, 0.2, 0.4, 0.2, 0.2, 0.2, 0.4, 0.2, 0.4, 0.2, 0.1, 0.1, 0.3, 0.1, 0.2, 0.1, 0.1				

F2. Tomato Data Set

Table F2.1. Wild type tomato root spacings (cm)

Root	Right	Left
WR1	1.38, 0.09, 0.51, 0.23, 0.36, 0.12, 0.38, 0.29, 0.09, 0.34, 0.27, 0.31, 0.18, 0.31, 0.41, 0.20, 0.22, 0.12, 0.39, 0.36, 0.23, 0.37, 0.05, 0.20, 0.49, 0.35, 0.19, 0.61, 0.15, 0.21, 0.43, 0.24, 0.20, 0.32, 0.30, 0.33, 0.13, 0.47, 0.43, 0.40, 0.21, 0.21, 0.24, 0.48, 0.16, 0.14, 0.30, 0.54, 0.30, 0.38	0.87, 0.22, 0.12, 0.36, 0.36, 0.65, 0.08, 0.31, 0.12, 0.22, 0.20, 0.44, 0.10, 0.11, 0.55, 0.24, 0.25, 0.19, 0.13, 0.19, 0.31, 0.21, 0.25, 0.29, 0.26, 0.21, 0.28, 0.17, 0.14, 0.25, 0.24, 0.22, 0.08, 0.51, 0.21, 0.10, 0.22, 0.10, 0.30, 0.29, 0.29, 0.17, 0.14, 0.33, 0.07, 0.40, 0.33, 0.17, 0.09, 0.29, 0.08, 0.14, 0.14, 0.33, 0.03, 0.21, 0.24, 0.12, 0.15, 0.40, 0.66, 0.24, 0.29, 0.36
Total	0.87, 0.22, 0.12, 0.17, 0.09, 0.10, 0.36, 0.05, 0.23, 0.36, 0.01, 0.08, 0.03, 0.28, 0.10, 0.02, 0.22, 0.05, 0.09, 0.06 0.28, 0.16, 0.10, 0.01, 0.10, 0.21, 0.18, 0.16, 0.15, 0.09, 0.25, 0.07, 0.12, 0.08, 0.05, 0.17, 0.02, 0.10, 0.21, 0.18, 0.03, 0.25, 0.08, 0.21, 0.02, 0.24, 0.13, 0.05, 0.03, 0.17, 0.11, 0.17, 0.14, 0.07, 0.18, 0.17, 0.07, 0.12, 0.10, 0.08, 0.43, 0.08, 0.07, 0.14, 0.07, 0.03, 0.22, 0.10, 0.08, 0.22, 0.02, 0.20, 0.07, 0.25, 0.04, 0.17, 0.09, 0.05, 0.28, 0.05, 0.07, 0.01, 0.39 0.08, 0.25, 0.17, 0.01, 0.08, 0.29, 0.03, 0.05, 0.14, 0.02, 0.12, 0.09, 0.24, 0.03, 0.21, 0.24, 0.12, 0.04, 0.11, 0.03, 0.30, 0.07, 0.47, 0.19, 0.11, 0.13, 0.25, 0.04	
WR2	1.59, 0.53, 1.07, 0.34, 0.22, 0.24, 0.40, 0.12, 0.62, 0.22, 0.29, 0.25, 0.18, 0.16, 0.34, 0.20, 0.07, 0.28, 0.24, 0.36, 0.33, 0.22, 0.16, 0.21 0.23, 0.24, 0.23, 0.36, 0.85, 0.56, 0.43, 0.39, 0.19, 0.21, 0.37, 0.23, 0.12, 0.19, 0.12, 0.14, 0.23, 0.10	0.91, 0.57, 0.33, 0.76, 0.02, 0.43, 0.33, 0.42, 0.30, 0.48, 0.35, 0.22, 0.21, 0.09, 0.23, 0.07, 0.17, 0.27, 0.28, 0.06, 0.42, 0.23, 0.54, 0.15, 0.17, 0.33, 0.35, 0.19, 0.40, 0.26, 0.23, 0.28, 0.03, 0.30, 0.38, 0.21, 0.26, 0.06, 0.15, 0.24, 0.57, 0.54, 0.30, 0.44
Total	0.91, 0.57, 0.11, 0.22, 0.31, 0.45, 0.02, 0.43, 0.17, 0.16, 0.18, 0.22, 0.02, 0.22, 0.08, 0.32, 0.12, 0.04, 0.35, 0.22, 0.01, 0.20, 0.02, 0.07, 0.22, 0.01, 0.07, 0.17, 0.18, 0.09, 0.07, 0.21, 0.06, 0.07, 0.20, 0.07, 0.08, 0.20, 0.03, 0.21, 0.33, 0.03, 0.12, 0.17, 0.04, 0.22, 0.07, 0.09, 0.21, 0.05, 0.18, 0.01, 0.23, 0.17, 0.06, 0.20, 0.16, 0.07, 0.28, 0.03, 0.30, 0.17, 0.21, 0.21, 0.14, 0.12, 0.06, 0.15, 0.10, 0.14, 0.25, 0.19, 0.13, 0.08, 0.37, 0.09, 0.14, 0.12, 0.04, 0.15, 0.12, 0.14, 0.03, 0.20, 0.10	
WR3	2.88, 0.14, 0.18, 0.30, 0.61, 0.28, 0.13, 0.37, 0.37, 0.18, 0.21, 0.25, 0.33, 0.18, 0.34, 0.22, 0.31, 0.21, 0.16, 0.66, 0.49, 0.27, 0.69, 0.43, 0.38, 0.16, 0.17, 0.21, 0.12, 0.04, 0.23, 0.03, 0.47, 0.42, 0.08, 0.29, 0.11, 0.23, 0.21, 0.15, 0.07, 0.09, 0.18, 0.16	1.24, 0.61, 0.31, 0.27, 0.27, 0.13, 0.18, 0.47, 0.08, 0.31, 0.13, 0.14, 0.16, 0.35, 0.34, 0.31, 0.19, 0.14, 0.16, 0.18, 0.16, 0.15, 0.13, 0.53, 0.35, 0.63, 0.16, 0.39, 0.09, 0.29, 0.12, 0.32, 0.23, 0.08, 0.19, 0.07, 0.29, 0.11, 0.23, 0.17, 0.18, 0.10, 0.03, 0.37, 0.13, 0.32, 0.33, 0.27, 0.33, 0.28, 0.10, 0.10, 0.24, 0.09, 0.13, 0.26
Total	1.24, 0.61, 0.31, 0.27, 0.27, 0.13, 0.05, 0.13, 0.01, 0.18, 0.28, 0.02, 0.06, 0.31, 0.13, 0.11, 0.03, 0.16, 0.09, 0.13, 0.13, 0.24, 0.10, 0.27, 0.04, 0.14, 0.05, 0.14, 0.02, 0.14, 0.11, 0.07, 0.16, 0.10, 0.05, 0.13, 0.34, 0.19, 0.03, 0.31, 0.01, 0.20, 0.16, 0.27, 0.16, 0.23, 0.16, 0.09, 0.24, 0.05, 0.12, 0.10, 0.22, 0.23, 0.08, 0.16, 0.03, 0.07, 0.29, 0.04, 0.07, 0.23, 0.08, 0.09, 0.07, 0.11, 0.06, 0.04, 0.03, 0.14, 0.12, 0.04, 0.07, 0.13, 0.03, 0.03, 0.26, 0.21, 0.12, 0.27, 0.03, 0.08, 0.22, 0.07, 0.11, 0.10, 0.10, 0.03, 0.07, 0.14, 0.10, 0.05, 0.04, 0.03, 0.09, 0.01, 0.17, 0.09, 0.07	
WR4	1.32, 0.32, 0.31, 0.23, 0.30, 0.27, 0.41, 0.09, 0.58, 0.11, 0.79, 0.56, 0.04, 0.32, 0.33, 0.26, 0.13, 0.09, 0.23, 0.29, 0.18, 0.36, 0.29, 0.21, 0.48, 0.21, 0.26, 0.31, 0.34, 0.10, 0.21, 0.15, 0.10, 0.24, 0.11, 0.24, 0.14	2.18, 0.38, 0.19, 0.12, 1.07, 0.47, 0.24, 0.32, 0.28, 0.10, 0.37, 0.13, 0.12, 0.29, 0.12, 0.32, 0.16, 0.21, 0.21, 0.22, 0.21, 0.12, 0.25, 0.33, 0.27, 0.14, 0.29, 0.20, 0.14, 0.20, 0.11, 0.39, 0.33, 0.09, 0.24
Total	1.32, 0.32, 0.31, 0.23, 0.30, 0.08, 0.19, 0.12, 0.29, 0.09, 0.58, 0.11, 0.47, 0.24, 0.08, 0.24, 0.28, 0.04, 0.04, 0.02, 0.30, 0.07, 0.13, 0.12, 0.01, 0.26, 0.02, 0.11, 0.01, 0.08, 0.23, 0.01, 0.16, 0.12, 0.09, 0.09, 0.12, 0.22, 0.02, 0.19, 0.10, 0.02, 0.19, 0.06, 0.33, 0.09, 0.18, 0.03, 0.11, 0.15, 0.14, 0.17, 0.03, 0.14, 0.17, 0.03, 0.07, 0.04, 0.17, 0.15, 0.07, 0.03, 0.24, 0.06, 0.05, 0.04, 0.20, 0.04, 0.10	

Table F2.1. (cont.)

WR5	1.288, 0.058, 0.250, 0.212, 0.150, 0.328, 0.312, 0.344, 0.382, 0.430, 0.292, 0.382, 0.436, 1.514, 0.696, 0.424, 0.646, 0.414, 0.680, 0.288, 0.808, 0.352, 0.246, 0.430, 0.410, 0.580, 0.476, 0.772, 0.396, 0.326, 0.410, 0.412, 0.246, 0.638, 0.104, 0.240, 0.220, 0.160, 0.202, 0.534, 0.172, 0.432, 0.544, 0.142, 0.284, 0.398, 0.308, 0.366, 0.340, 0.354, 0.312, 0.036	0.638, 0.274, 0.666, 0.594, 0.512, 0.238, 0.140, 0.456, 0.198, 0.508, 0.276, 0.276, 0.182, 0.588, 0.188, 0.342, 0.242, 0.324, 0.272, 0.368, 0.276, 0.098, 0.326, 0.144, 0.738, 0.264, 0.248, 0.306, 0.330, 0.330, 0.612, 0.654, 0.154, 0.154, 0.470, 0.362, 0.616, 0.436, 0.684, 0.720, 0.204, 0.164, 0.386, 0.222, 0.318, 0.366, 0.720, 0.258, 0.374, 0.314, 0.154, 0.206, 0.122, 0.246, 0.494, 0.312, 0.122, 0.364, 0.130, 0.354, 0.166
Total	0.638, 0.274, 0.376, 0.058, 0.232, 0.018, 0.238, 0.020, 0.120, 0.262, 0.194, 0.198, 0.088, 0.094, 0.588, 0.188, 0.342, 0.242, 0.060, 0.098, 0.326, 0.144, 0.018, 0.414, 0.330, 0.322, 0.008, 0.344, 0.246, 0.022, 0.034, 0.362, 0.080, 0.536, 0.236, 0.200, 0.186, 0.018, 0.164, 0.386, 0.070, 0.104, 0.090, 0.534, 0.096, 0.076, 0.182, 0.250, 0.122, 0.050, 0.196, 0.202, 0.292, 0.016, 0.148, 0.206, 0.106, 0.036, 0.024	0.212, 0.150, 0.214, 0.114, 0.312, 0.086, 0.038, 0.292, 0.178, 0.204, 0.072, 0.276, 0.060, 0.264, 0.272, 0.160, 0.208, 0.216, 0.306, 0.264, 0.110, 0.138, 0.150, 0.156, 0.408, 0.246, 0.154, 0.010, 0.144, 0.436, 0.196, 0.326, 0.162, 0.248, 0.412, 0.060, 0.048, 0.192, 0.126, 0.094, 0.160, 0.112, 0.124, 0.314, 0.106, 0.048, 0.094, 0.112, 0.296, 0.070, 0.052, 0.288, 0.076, 0.130,
WR6	1.262, 0.176, 0.378, 0.682, 0.560, 0.340, 0.278, 0.210, 0.262, 0.276, 0.108, 0.250, 0.254, 0.166, 0.166, 0.122, 0.248, 0.298, 0.178, 0.550, 0.532, 0.174, 0.116, 0.084, 0.208, 0.180, 0.088, 0.346, 0.364, 0.324, 0.092, 0.168, 0.058, 0.416, 0.072, 0.596, 0.560, 0.322, 0.606, 0.760, 0.338, 0.372, 0.384, 0.660, 0.268, 0.256, 0.350, 0.328, 0.058, 0.542, 0.458, 0.648, 0.334, 0.548, 0.558, 0.406, 0.210, 0.410, 0.228, 0.420, 0.240, 0.198, 1.478, 0.702, 0.530, 0.400, 0.330, 0.244, 0.190, 0.446, 0.136, 0.174, 0.144, 0.220, 0.200, 0.518, 0.376, 0.472, 0.272, 0.924, 0.344, 0.960	1.178, 0.392, 0.152, 0.322, 0.080, 0.286, 0.272, 0.354, 0.348, 0.522, 0.228, 0.318, 0.314, 0.286, 0.326, 0.480, 0.026, 0.512, 0.468, 0.120, 0.334, 0.130, 0.294, 0.256, 0.234, 0.342, 0.124, 0.306, 0.754, 0.034, 0.228, 0.334, 0.326, 0.124, 0.196, 0.326, 0.318, 0.150, 0.684, 0.218, 0.036, 0.180, 0.322, 0.118, 0.024, 0.250, 0.032, 0.304, 0.132, 0.118, 0.106, 0.048, 0.188, 0.730, 0.480, 0.294, 0.298, 0.332, 0.422, 0.322, 0.148, 0.264, 0.036, 0.472, 0.386, 0.364, 0.378, 0.140, 0.164, 0.432, 0.424, 0.234, 0.148, 0.554, 0.006, 0.174, 0.272, 0.216, 0.152, 0.290, 0.018, 0.292, 0.234, 0.246, 0.064, 0.470, 0.626, 0.104, 0.146, 0.208, 0.204, 0.236, 0.178, 0.332, 0.196, 0.252, 0.356, 0.296, 0.860, 0.654, 0.524, 0.558, 0.166
Total	1.178, 0.084, 0.176, 0.132, 0.152, 0.094, 0.022, 0.326, 0.014, 0.278, 0.210, 0.020, 0.016, 0.254, 0.016, 0.150, 0.166, 0.010, 0.182, 0.368, 0.100, 0.120, 0.312, 0.022, 0.120, 0.060, 0.088, 0.086, 0.260, 0.082, 0.058, 0.260, 0.034, 0.122, 0.072, 0.034, 0.184, 0.138, 0.180, 0.150, 0.276, 0.408, 0.118, 0.024, 0.164, 0.086, 0.032, 0.266, 0.030, 0.268, 0.256, 0.176, 0.174, 0.306, 0.156, 0.266, 0.322, 0.060, 0.088, 0.246, 0.170, 0.236, 0.142, 0.068, 0.072, 0.164, 0.028, 0.148, 0.022, 0.532, 0.006, 0.174, 0.292, 0.228, 0.006, 0.246, 0.064, 0.214, 0.146, 0.032, 0.176, 0.204, 0.066, 0.136, 0.194, 0.002, 0.252, 0.264, 0.092, 0.284, 0.344, 0.038, 0.558, 0.166, 0.198	0.228, 0.080, 0.286, 0.088, 0.184, 0.354, 0.228, 0.014, 0.276, 0.028, 0.080, 0.234, 0.112, 0.248, 0.120, 0.026, 0.152, 0.178, 0.130, 0.022, 0.116, 0.084, 0.072, 0.136, 0.124, 0.158, 0.148, 0.176, 0.092, 0.168, 0.334, 0.228, 0.098, 0.124, 0.196, 0.142, 0.218, 0.036, 0.098, 0.082, 0.256, 0.066, 0.038, 0.132, 0.118, 0.106, 0.048, 0.188, 0.022, 0.058, 0.214, 0.298, 0.030, 0.302, 0.018, 0.036, 0.472, 0.022, 0.364, 0.194, 0.174, 0.228, 0.030, 0.390, 0.034, 0.206, 0.272, 0.216, 0.152, 0.126, 0.164, 0.018, 0.256, 0.144, 0.330, 0.152, 0.092, 0.012, 0.034, 0.140, 0.038, 0.106, 0.220, 0.006, 0.012, 0.460, 0.272, 0.128, 0.654, 0.142,
WR7	1.64, 0.91, 0.46, 0.42, 0.35, 0.09, 0.46, 0.15, 0.36, 0.22, 0.21, 0.21, 0.13, 0.32, 0.11, 0.16, 0.41, 0.16, 0.22, 0.28, 0.20, 0.36, 0.14, 0.12, 0.18, 0.47, 0.21, 0.26, 0.35, 0.29, 0.43, 0.29, 0.45, 0.30, 0.35, 0.45, 0.29, 0.43, 0.28, 0.33, 0.39	1.42, 0.26, 0.16, 0.18, 0.40, 0.34, 0.07, 0.23, 0.08, 0.13, 0.38, 0.22, 0.22, 0.17, 0.30, 0.31, 0.22, 0.30, 0.24, 0.23, 0.14, 0.27, 0.50, 0.22, 0.21, 0.18, 0.38, 0.24, 0.17, 0.19, 0.07, 0.17, 0.38, 0.23, 0.32, 0.53, 0.19, 0.15, 0.23, 0.37, 0.31, 0.57, 0.67, 1.27, 1.95, 0.35
Total	1.42, 0.22, 0.04, 0.16, 0.18, 0.40, 0.13, 0.22, 0.13, 0.09, 0.22, 0.17, 0.07, 0.15, 0.09, 0.13, 0.02, 0.23, 0.07, 0.07, 0.04, 0.11, 0.09, 0.29, 0.07, 0.14, 0.03, 0.09, 0.03, 0.23, 0.32, 0.03, 0.29, 0.21, 0.19, 0.01, 0.35, 0.21, 0.24, 0.29, 0.14, 0.29,	0.21, 0.07, 0.18, 0.05, 0.08, 0.13, 0.16, 0.08, 0.28, 0.03, 0.19, 0.03, 0.18, 0.12, 0.16, 0.07, 0.34, 0.16, 0.22, 0.21, 0.07, 0.08, 0.10, 0.09, 0.07, 0.17, 0.14, 0.21, 0.03, 0.12, 0.17, 0.06, 0.37, 0.02, 0.29, 0.28, 0.33, 0.37, 0.02, 1.93, 0.35
WR8	1.18, 0.33, 0.33, 0.14, 0.33, 0.26, 0.14, 0.32, 0.14, 0.21, 0.26, 0.29, 0.10, 0.06, 0.24, 0.23, 0.33, 0.57, 0.08, 0.23, 0.35, 0.24, 0.29, 0.24, 0.12, 0.15, 0.19, 0.15, 0.13, 0.21, 0.21, 0.17, 0.39, 0.18, 0.12, 0.22, 0.25, 0.33, 0.18, 0.35, 0.26, 0.30, 0.24, 0.17, 0.17, 0.61, 0.23, 0.54, 0.23, 0.36, 0.23, 0.19, 0.22, 0.13, 0.45, 0.33, 0.25, 0.73, 0.25, 0.34	0.26, 1.12, 0.19, 0.38, 0.44, 0.16, 0.14, 0.37, 0.30, 0.29, 0.21, 0.10, 0.22, 0.12, 0.22, 0.05, 0.60, 0.19, 0.33, 0.25, 0.18, 0.26, 0.15, 0.24, 0.10, 0.25, 0.42, 0.50, 0.50, 0.50, 0.28, 0.10, 0.29, 0.17, 0.18, 0.46, 0.47, 0.35, 0.29, 0.65, 0.13, 0.28, 0.42, 0.17, 0.30, 1.11, 0.20, 0.16, 0.23, 0.39, 0.52, 0.61, 2.55, 0.67, 0.14, 0.44

Table F2.1.(cont.)

Total	0.26, 0.92, 0.20, 0.13, 0.06, 0.27, 0.11, 0.03, 0.33, 0.08, 0.16, 0.02, 0.12, 0.02, 0.32, 0.03, 0.11, 0.19, 0.02, 0.26, 0.01, 0.21, 0.07, 0.03, 0.07, 0.06, 0.09, 0.12, 0.03, 0.19, 0.04, 0.01, 0.32, 0.28, 0.19, 0.10, 0.08, 0.15, 0.08, 0.17, 0.18, 0.24, 0.02, 0.15, 0.12, 0.12, 0.10, 0.02, 0.12, 0.11, 0.04, 0.19, 0.15, 0.04, 0.09, 0.21, 0.20, 0.01, 0.17, 0.32, 0.07, 0.18, 0.12, 0.13, 0.09, 0.19, 0.06, 0.04, 0.29, 0.17, 0.01, 0.17, 0.18, 0.26, 0.02, 0.28, 0.19, 0.05, 0.17, 0.13, 0.04, 0.25, 0.36, , 0.23, 0.06, 0.13, 0.28, 0.07, 0.23, 0.12, 0.17, 0.07, 0.23, 0.19, 0.22, 0.13, 0.45, 0.12, 0.20, 0.01, 0.15, 0.10, 0.13, 0.39, 0.21, 0.25, 0.06, 0.28, 0.33, 2.55, 0.67, 0.14, 0.44	
WR9	0.69, 0.29, 0.18, 0.30, 0.11, 0.10, 0.35, 0.05, 0.12, 0.27, 0.27, 0.33, 0.07, 0.32, 0.17, 0.19, 0.19, 0.14, 0.70, 0.39, 0.10, 0.27, 0.31, 0.84, 0.40, 0.11, 0.38, 0.17, 0.18, 0.35, 0.14, 0.22, 0.19, 0.23, 0.27, 0.39, 0.51, 0.14, 0.36, 0.20, 0.25, 0.17, 0.03, 0.21, 0.27, 0.37, 0.32, 0.19, 0.23, 0.28, 0.06, 0.24, 0.28, 0.18,0.38, 0.74, 1.32	0.55, 1.29, 0.27, 0.46, 0.12, 0.43, 0.30, 0.36, 0.26, 0.33, 0.05, 0.33, 0.11, 0.61, 0.59, 0.33, 0.41, 0.19, 0.51, 0.21, 0.51, 0.11, 0.24, 0.26, 0.23, 0.07, 0.36, 0.46, 0.26, 0.25, 0.17, 0.17, 0.41, 0.51, 0.29, 0.26, 0.26, 1.04, 0.19, 0.21, 0.72, 0.29, 0.48, 0.44, 0.36, 0.15
Total	0.55, 0.14, 0.29, 0.18, 0.30, 0.11, 0.10, 0.17, 0.18, 0.05, 0.04, 0.08, 0.27, 0.11, 0.12, 0.04, 0.33, 0.06, 0.01, 0.29, 0.03, 0.17, 0.16, 0.03, 0.19, 0.04, 0.10, 0.23, 0.05, 0.33, 0.09, 0.02, 0.37, 0.10, 0.14, 0.13, 0.31, 0.15, 0.33, 0.36, 0.05, 0.19, 0.16, 0.11, 0.24, 0.14, 0.07, 0.10, 0.18, 0.23, 0.11, 0.01, 0.14, 0.09, 0.13, 0.13, 0.06, 0.17, 0.06, 0.01, 0.26, 0.10, 0.29, 0.17, 0.26, 0.08, 0.14, 0.03, 0.17, 0.16, 0.01, 0.19, 0.22, 0.03, 0.17, 0.03, 0.21, 0.07, 0.20, 0.09, 0.26, 0.02, 0.24, 0.08, 0.19, 0.23, 0.28, 0.06, 0.20, 0.04, 0.15, 0.13, 0.08, 0.10, 0.38, 0.24, 0.29, 0.21, 0.27, 0.44, 0.36, 0.15, 0.10	
WR10	1.16, 0.29, 0.31, 0.25, 0.27, 0.32, 0.13, 0.47, 0.17, 0.21, 0.15, 0.31, 0.41, 0.16, 0.13, 0.42, 0.23, 0.37, 0.22, 0.10, 0.22, 0.22, 0.22, 0.19, 0.23, 0.23, 0.25, 0.33, 0.36, 0.21, 0.34, 0.20, 0.26, 0.20, 0.18, 0.22, 0.40, 0.49, 0.25, 0.29, 0.28, 0.31	1.06, 0.59, 0.42, 0.20, 0.20, 0.32, 0.20, 0.21, 0.31, 0.31, 0.07, 0.28, 0.19, 0.15, 0.18, 0.19, 0.06, 0.21, 0.18, 0.23, 0.15, 0.13, 0.14, 0.29, 0.34, 0.63, 0.40, 0.49, 0.50, 0.25, 0.22, 0.15, 0.05, 0.48, 0.31, 0.38, 0.14, 0.25, 0.30, 0.25, 0.15, 0.22, 0.12, 0.17, 0.27
Total	1.06, 0.10, 0.29, 0.20, 0.11, 0.25, 0.06, 0.20, 0.01, 0.19, 0.13, 0.13, 0.06, 0.20, 0.21, 0.17, 0.14, 0.07, 0.15, 0.09, 0.07, 0.15, 0.13, 0.19, 0.09, 0.06, 0.10, 0.08, 0.05, 0.14, 0.06, 0.21, 0.01, 0.17, 0.06, 0.17, 0.15, 0.05, 0.08, 0.14, 0.10, 0.19, 0.03, 0.22, 0.09, 0.13, 0.19, 0.23, 0.08, 0.15, 0.25, 0.33, 0.16, 0.20, 0.21, 0.09, 0.25, 0.20, 0.02, 0.15, 0.05, 0.04, 0.20, 0.18, 0.06, 0.16, 0.15, 0.25, 0.13, 0.14, 0.22, 0.03, 0.22, 0.08, 0.21, 0.04, 0.15, 0.09, 0.13, 0.12, 0.06, 0.11, 0.27	

F2.2. Gib1-Mutant type tomato root spacings (cm)

Root	Right	Left
GR1	0.612, 0.254, 0.358, 0.608, 0.354, 0.556, 0.158, 0.110, 0.220, 0.320, 0.032, 0.304, 0.018, 0.150, 0.300, 0.344, 0.280, 0.272, 0.290, 0.252, 0.114, 0.176, 0.108, 0.318, 0.338, 0.344, 0.290, 0.410, 0.554, 0.430, 0.238, 0.280, 0.228, 0.620, 0.188	0.144, 0.456, 0.338, 0.476, 0.506, 0.206, 0.438, 0.674, 0.300, 0.260, 0.228, 0.488, 0.500, 0.212, 0.442, 0.186, 0.520, 0.418, 0.208, 0.244, 0.468, 0.162, 0.326, 0.408, 0.532, 0.550, 0.180
Total	0.144, 0.456, 0.012, 0.254, 0.072, 0.286, 0.190, 0.418, 0.088, 0.206, 0.060, 0.378, 0.178, 0.158, 0.110, 0.220, 0.008, 0.300, 0.012, 0.032, 0.216, 0.088, 0.018, 0.122, 0.028, 0.300, 0.160, 0.184, 0.280, 0.036, 0.212, 0.024, 0.290, 0.128, 0.124, 0.062, 0.052, 0.176, 0.108, 0.184, 0.134, 0.284, 0.054, 0.154, 0.190, 0.054, 0.236, 0.232, 0.162, 0.016, 0.310, 0.244, 0.164, 0.266, 0.238, 0.028, 0.252, 0.228, 0.070, 0.180, 0.370, 0.188	
GR2	0.172, 0.660, 0.484, 0.632, 0.070, 0.290, 0.030, 0.298, 0.384, 0.104, 0.318, 0.048, 0.234, 0.252, 0.250, 0.540, 0.204, 0.620, 0.496, 0.394, 0.200, 0.432, 0.116, 0.312, 0.316, 0.154, 0.518, 0.494, 0.268, 0.014, 0.216,	0.352, 0.814, 0.384, 0.566, 0.444, 0.348, 0.414, 0.202, 0.374, 0.574, 0.320, 0.156, 0.122, 0.244, 0.430, 0.186, 0.420, 0.598, 0.344

Table F2.2. (cont.)

Total	0.172, 0.180, 0.480, 0.334, 0.150, 0.234, 0.398, 0.070, 0.098, 0.192, 0.030, 0.222, 0.076, 0.272, 0.112, 0.104, 0.198, 0.120, 0.048, 0.034, 0.200, 0.174, 0.078, 0.250, 0.246, 0.294, 0.026, 0.156, 0.022, 0.100, 0.244, 0.276, 0.154, 0.186, 0.156, 0.264, 0.130, 0.200, 0.268, 0.164, 0.116, 0.064, 0.248, 0.316, 0.154, 0.518, 0.494, 0.268, 0.014, 0.216	
GR3	0.110, 1.148, 0.350, 0.344, 0.184, 0.210, 0.344, 0.448, 0.226, 0.430, 0.348, 0.236, 0.236, 0.178, 0.220, 0.170, 0.274, 0.300, 0.162, 0.300, 0.254, 0.362, 0.544, 0.260, 0.290, 0.418, 0.060, 0.186, 0.280, 0.172, 0.252, 0.222, 0.296, 0.226, 0.306, 0.348, 0.266, 0.252, 0.210, 0.246, 0.084, 0.320, 0.294, 0.216, 0.214, 0.436, 0.120, 0.286, 0.272, 0.092, 0.164, 0.336, 0.216, 0.382, 0.250, 0.230, 0.148, 0.358, 0.382, 0.194, 0.210, 0.420, 0.264, 0.268, 0.224, 0.262	0.288, 0.086, 0.418, 0.194, 0.534, 0.638, 0.560, 0.338, 0.354, 0.472, 0.520, 0.132, 0.254, 0.378, 0.198, 0.414, 0.396, 0.096, 0.404, 0.380, 0.226, 0.298, 0.376, 0.410, 0.354, 0.396, 0.222, 0.312, 0.534, 0.250, 0.434, 0.692, 0.302, 0.582, 0.578, 0.442, 0.290, 0.306, 0.142, 0.112, 0.388, 0.304, 0.240, 0.358, 0.390, 0.158, 0.274, 0.242, 0.308, 0.588, 0.346, 0.504
Total	0.110, 0.178, 0.086, 0.418, 0.194, 0.272, 0.262, 0.088, 0.344, 0.184, 0.022, 0.188, 0.344, 0.028, 0.338, 0.082, 0.226, 0.046, 0.384, 0.088, 0.260, 0.236, 0.024, 0.132, 0.080, 0.174, 0.004, 0.220, 0.154, 0.016, 0.182, 0.092, 0.300, 0.022, 0.140, 0.256, 0.044, 0.052, 0.202, 0.202, 0.160, 0.220, 0.226, 0.098, 0.200, 0.060, 0.290, 0.026, 0.392, 0.018, 0.042, 0.186, 0.126, 0.154, 0.172, 0.070, 0.182, 0.040, 0.182, 0.130, 0.166, 0.226, 0.142, 0.164, 0.086, 0.262, 0.172, 0.094, 0.252, 0.210, 0.136, 0.110, 0.084, 0.108, 0.212, 0.294, 0.076, 0.140, 0.214, 0.224, 0.212, 0.120, 0.110, 0.176, 0.114, 0.158, 0.092, 0.056, 0.108, 0.034, 0.112, 0.190, 0.198, 0.018, 0.286, 0.096, 0.144, 0.106, 0.230, 0.022, 0.126, 0.264, 0.094, 0.064, 0.274, 0.044, 0.194, 0.004 0.206, 0.102, 0.318, 0.264, 0.006, 0.262, 0.084, 0.140, 0.262, 0.102	
GR4	0.148, 0.364, 0.758, 0.364, 0.506, 0.278, 0.156, 0.486, 0.238, 0.366, 0.166, 0.416, 0.390, 0.304, 0.214, 0.302, 0.096, 0.298, 0.318, 0.824, 0.032, 0.362, 0.260, 0.330, 0.378, 0.270, 0.262, 0.404, 0.136, 0.210, 0.428, 0.384, 0.396, 0.216, 0.086, 0.250, 0.292, 0.276, 0.418, 0.422, 0.132, 0.192, 0.292, 0.300, 0.326, 0.304, 0.322, 0.192, 0.356, 0.198, 0.250, 0.198, 0.158, 0.284, 0.230, 0.180, 0.334, 0.326	0.324, 0.332, 0.238, 0.588, 0.632, 0.352, 1.026, 0.356, 0.114, 0.320, 0.366, 0.022, 0.456, 0.068, 0.294, 0.158, 0.570, 0.580, 0.320, 0.332, 0.298, 0.424, 0.368, 0.178, 0.322, 0.254, 0.400, 0.156, 0.504, 0.178, 0.268, 0.616, 0.046, 0.182, 0.234, 0.196, 0.160, 0.346, 0.256, 0.240, 0.168, 0.434, 0.262, 0.094, 0.186, 0.280, 0.228, 0.410, 0.390, 0.676, 0.272, 0.330, 0.220, 0.198
Total	0.148, 0.176, 0.188, 0.144, 0.238, 0.376, 0.212, 0.152, 0.480, 0.026, 0.278, 0.048 0.108, 0.486, 0.238, 0.194, 0.172, 0.166, 0.018, 0.114, 0.284, 0.036, 0.354, 0.012, 0.022, 0.270, 0.186, 0.028, 0.040, 0.262, 0.032, 0.064, 0.094, 0.204, 0.318, 0.048, 0.580, 0.196, 0.032, 0.092, 0.270, 0.062, 0.198, 0.100, 0.230, 0.194, 0.184, 0.184, 0.086, 0.092, 0.170, 0.152, 0.252, 0.002, 0.134, 0.210, 0.056, 0.156, 0.216, 0.288, 0.096, 0.082, 0.268, 0.046, 0.216, 0.086, 0.250, 0.018, 0.046, 0.182, 0.046, 0.188, 0.088, 0.108, 0.160, 0.150, 0.196, 0.226, 0.030, 0.102, 0.138, 0.054, 0.114, 0.178, 0.256, 0.044, 0.218, 0.094, 0.014, 0.172, 0.132, 0.148, 0.174, 0.054, 0.138, 0.272 0.084, 0.198, 0.108, 0.142, 0.198, 0.158, 0.178, 0.106, 0.166, 0.064, 0.180, 0.086 0.220, 0.028, 0.170, 0.156	
GR5	0.192, 0.266, 0.562, 0.264, 0.340, 0.158, 0.058, 0.544, 0.258, 0.350, 0.226, 0.308, 0.400, 0.270, 0.088, 0.148, 0.402, 0.140, 0.352, 0.302, 0.162, 0.330, 0.156, 0.294, 0.262, 0.192, 0.434, 0.322, 0.134, 0.164, 0.238, 0.202, 0.462, 0.274, 0.194, 0.244, 0.316, 0.236, 0.066, 0.254, 0.286, 0.460, 0.120, 0.386, 0.362, 0.248, 0.484, 0.178, 0.204, 0.200, 0.284, 0.164, 0.140, 0.352, 0.432, 0.386,	0.256, 0.358, 0.632, 0.210, 0.402, 0.308, 0.336, 0.192, 0.370, 0.670, 0.396, 0.446, 0.210, 0.282, 0.508, 0.252, 0.460, 0.296, 0.502, 0.262, 0.252, 0.490, 0.592, 0.152, 0.218, 0.276, 0.248, 0.466, 0.142, 0.288, 0.356, 0.050, 0.188, 0.408, 0.298, 0.496, 0.434, 0.350, 0.252, 0.310, 0.332, 0.228, 0.452, 0.552
Total	0.192, 0.064, 0.202, 0.156, 0.406, 0.226, 0.038, 0.172, 0.168, 0.158, 0.058, 0.018, 0.308, 0.218, 0.118, 0.140, 0.052, 0.298, 0.072, 0.154, 0.308, 0.208, 0.192, 0.204, 0.066, 0.088, 0.148, 0.144, 0.210, 0.048, 0.140, 0.094, 0.258, 0.250, 0.052, 0.162, 0.038, 0.292, 0.156, 0.012, 0.282, 0.014, 0.248, 0.192, 0.062, 0.262, 0.110, 0.142, 0.180, 0.134, 0.164, 0.012, 0.226, 0.202, 0.164, 0.152, 0.146, 0.072, 0.202, 0.074, 0.120, 0.128, 0.116, 0.316, 0.034, 0.142, 0.060, 0.066, 0.162, 0.092, 0.264, 0.022, 0.028, 0.188, 0.244, 0.120, 0.044, 0.298, 0.044, 0.362, 0.090, 0.158, 0.276, 0.208, 0.142, 0.036, 0.204, 0.012, 0.188, 0.122, 0.162, 0.164, 0.006, 0.134, 0.094, 0.258, 0.194, 0.238, 0.314, 0.072	

Table F2.2. (cont.)

GR6	2.498, 0.158, 0.294, 0.498, 0.146, 0.358, 0.204, 0.522, 0.686, 0.442, 0.390, 0.390, 0.324, 0.502, 0.438, 0.496, 0.346, 0.436, 0.608, 0.178, 0.528, 0.270, 0.372, 0.508, 0.398, 0.238, 0.188, 0.366, 0.194, 0.318, 0.450, 0.320, 0.196, 0.256, 0.212, 0.418, 0.426, 0.102, 0.408, 0.288, 0.314, 0.240	0.152, 0.298, 0.826, 0.292, 0.570, 0.118, 0.158, 0.360, 0.192, 0.202, 0.256, 0.390, 0.452, 0.528, 0.162, 0.048, 0.306, 0.408, 0.450, 0.236, 0.278, 0.334, 0.228, 0.372, 0.330, 0.222, 0.166, 0.622, 0.138, 0.276, 0.286, 0.192, 0.312, 0.286, 0.272, 0.448, 0.280, 0.414, 0.254, 0.536, 0.048, 0.188, 0.338, 0.276, 0.182, 0.360, 0.110, 0.334, 0.302, 0.166, 0.228, 0.168, 0.440, 0.368, 0.030, 0.374, 0.396
Total	0.152, 0.298, 0.826, 0.292, 0.570, 0.118, 0.158, 0.084, 0.158, 0.118, 0.176, 0.016, 0.202, 0.256, 0.024, 0.146, 0.220, 0.138, 0.204, 0.110, 0.412, 0.116, 0.162, 0.048, 0.306, 0.054, 0.354, 0.088, 0.362, 0.028, 0.208, 0.182, 0.096, 0.228, 0.106, 0.228, 0.168, 0.204, 0.234, 0.096, 0.222, 0.166, 0.012, 0.346, 0.264, 0.138, 0.034, 0.242, 0.286, 0.080, 0.112, 0.066, 0.246, 0.282, 0.004, 0.266, 0.006, 0.366, 0.082, 0.280, 0.146, 0.268, 0.130, 0.124, 0.114, 0.188, 0.234, 0.048, 0.084, 0.104, 0.090, 0.248, 0.070, 0.206, 0.182, 0.062, 0.298, 0.022, 0.088, 0.108, 0.226, 0.030, 0.212, 0.060, 0.166, 0.192, 0.036, 0.168, 0.222, 0.102, 0.116, 0.292, 0.076, 0.030, 0.182, 0.192, 0.122, 0.240, 0.034	

F2.3. Wild type, Naa treated tomato root spacings (cm)

Root	Right	Left
NWR1	1.146, 0.174, 0.244, 0.154, 0.136, 0.096, 0.198, 0.288, 0.060, 0.238, 0.148, 0.214, 0.224, 0.124, 0.244, 0.234, 0.130, 0.310, 0.248, 0.174, 0.362, 0.128, 0.236, 0.174, 0.140, 0.348, 0.212, 0.258, 0.218, 0.088, 0.196, 0.174, 0.092, 0.276, 0.240, 0.138, 0.160, 0.138, 0.246, 0.138, 0.142, 0.252, 0.200, 0.174, 0.198, 0.332, 0.312, 0.144, 0.284, 0.232, 0.246, 0.252, 0.244, 0.312, 0.294, 0.500, 0.948, 0.820	1.062, 0.606, 0.318, 0.078, 0.298, 0.256, 0.286, 0.180, 0.378, 0.274, 0.388, 0.158, 0.362, 0.494, 0.278, 0.364, 0.512, 0.332, 0.472, 0.240, 0.400, 0.122, 0.292, 0.236, 0.242, 0.138, 0.418, 0.144, 0.326, 0.218, 0.554, 0.380, 0.514, 0.058, 0.546, 0.314, 0.162, 0.312, 0.160, 0.576, 0.382, 0.706
Total	1.062, 0.084, 0.174, 0.244, 0.104, 0.050, 0.136, 0.096, 0.036, 0.078, 0.084, 0.214, 0.074, 0.060, 0.122, 0.116, 0.148, 0.022, 0.180, 0.012, 0.224, 0.124, 0.018, 0.226, 0.048, 0.186, 0.130, 0.072, 0.158 0.080, 0.248, 0.034, 0.140, 0.354, 0.008, 0.128, 0.142, 0.094, 0.174, 0.096, 0.044, 0.348, 0.120, 0.092, 0.240, 0.018, 0.218, 0.088, 0.148, 0.048, 0.174, 0.018, 0.074, 0.276, 0.050, 0.122, 0.068, 0.138, 0.086, 0.074, 0.138, 0.024, 0.222, 0.020, 0.118, 0.020, 0.122, 0.252, 0.044, 0.144, 0.012, 0.174, 0.140, 0.058, 0.160, 0.172, 0.312, 0.070, 0.074, 0.284, 0.022, 0.210, 0.246, 0.058, 0.058, 0.136, 0.244, 0.166, 0.146, 0.168, 0.126, 0.036, 0.312, 0.152, 0.008, 0.576, 0.364, 0.018, 0.706, 0.096	
NWR2	0.436, 0.416, 0.312, 0.604, 0.216, 0.202, 0.068, 0.182, 0.134, 0.212, 0.166, 0.196, 0.162, 0.188, 0.176, 0.202, 0.144, 0.362, 0.042, 0.180, 0.228, 0.158, 0.144, 0.150, 0.244, 0.268, 0.360, 0.216, 0.432, 0.334, 0.194, 0.154, 0.144, 0.300, 0.148, 0.228, 0.232, 0.202, 0.422, 0.084, 0.110, 0.260, 0.238, 0.044, 0.250, 0.108, 0.216, 0.230, 0.314, 0.144, 0.080, 0.302, 0.150, 0.158, 0.466, 0.312, 0.070, 0.158, 0.396, 0.552, 0.352, 0.116, 0.356, 0.342, 0.310, 0.338, 0.402, 0.308, 0.216, 0.202	0.584, 0.540, 0.512, 0.956, 0.114, 0.314, 0.104, 0.260, 0.166, 0.214, 0.192, 0.288, 0.184, 0.214, 0.404, 0.180, 0.266, 0.274, 0.172, 0.308, 0.542, 0.364, 0.144, 0.358, 0.164, 0.124, 0.314, 0.078, 0.310, 0.374, 0.238, 0.204, 0.344, 0.216, 0.266, 0.254, 0.230, 0.164, 0.208, 0.262, 0.152, 0.152, 0.366, 0.222, 0.152, 0.366, 0.278, 0.342, 0.204, 0.322, 0.228, 0.258, 0.152, 0.138, 0.262, 0.490, 0.366, 0.374, 0.416

Table F2.3. (cont.)

<table>
<tr><td>Total</td><td colspan="2">0.436, 0.148, 0.268, 0.272, 0.040, 0.472, 0.132, 0.216, 0.202, 0.068, 0.182, 0.134,
0.022, 0.114, 0.076, 0.166, 0.072, 0.104, 0.020, 0.162, 0.078, 0.110, 0.056, 0.120,
0.094, 0.108, 0.084, 0.060, 0.228, 0.134, 0.042, 0.008, 0.172, 0.042, 0.186, 0.158,
0.060, 0.084, 0.096, 0.054, 0.212, 0.032, 0.242, 0.026, 0.146, 0.214, 0.094, 0.122,
0.420, 0.012, 0.334, 0.018, 0.144, 0.032, 0.154, 0.144, 0.028, 0.164, 0.108, 0.016,
0.132, 0.182, 0.046, 0.032, 0.200, 0.110, 0.092, 0.282, 0.140, 0.084, 0.014, 0.096,
0.108, 0.152, 0.192, 0.046, 0.044, 0.126, 0.124, 0.108, 0.034, 0.182, 0.072, 0.158,
0.072, 0.164, 0.078, 0.130, 0.014, 0.080, 0.168, 0.134, 0.018, 0.132, 0.020, 0.138,
0.228, 0.222, 0.016, 0.136, 0.176, 0.070, 0.120, 0.038, 0.240, 0.156, 0.186, 0.204,
0.162, 0.160, 0.192, 0.036, 0.080, 0.178, 0.152, 0.026, 0.112, 0.230, 0.032, 0.278,
0.212, 0.126, 0.240, 0.162, 0.212, 0.096, 0.216, 0.104, 0.098</td></tr>
<tr><td>NWR3</td><td>0.206, 0.372, 0.266, 0.750, 0.172,
0.156, 0.196, 0.264, 0.082, 0.172,
0.070, 0.268, 0.182, 0.224, 0.248,
0.266, 0.168, 0.120, 0.240, 0.192,
0.172, 0.222, 0.166, 0.286, 0.134,
0.274, 0.228, 0.186, 0.232, 0.114,
0.278, 0.258, 0.248, 0.472, 0.216,
0.158, 0.266, 0.382, 0.140, 0.296,
0.274, 0.368, 0.498, 0.684</td><td>1.016, 0.446, 0.074, 0.454, 0.296, 0.322,
0.214, 0.180, 0.242, 0.250, 0.268, 0.192,
0.204, 0.146, 0.146, 0.232, 0.350, 0.440,
0.270, 0.246, 0.186, 0.232, 0.244, 0.276,
0.542, 0.176, 0.336, 0.626, 0.410, 0.396,
0.436, 0.150, 0.332, 0.438, 0.272, 0.396</td></tr>
<tr><td>Total</td><td colspan="2">0.206, 0.372, 0.266, 0.172, 0.446, 0.074, 0.058, 0.172, 0.156, 0.068, 0.128, 0.168,
0.096, 0.082, 0.144, 0.028, 0.070, 0.116, 0.152, 0.028, 0.154, 0.088, 0.136, 0.114,
0.134, 0.134, 0.132, 0.060, 0.108, 0.096, 0.024, 0.122, 0.118, 0.028, 0.164, 0.068,
0.104, 0.222, 0.024, 0.142, 0.286, 0.012, 0.122, 0.148, 0.126, 0.120, 0.108, 0.078,
0.108, 0.124, 0.108, 0.114, 0.022, 0.256, 0.020, 0.238, 0.248, 0.056, 0.176, 0.240,
0.096, 0.120, 0.158, 0.266, 0.082, 0.300, 0.110, 0.030, 0.296, 0.070, 0.204, 0.232,
0.136, 0.014, 0.332, 0.152, 0.286, 0.272, 0.126</td></tr>
<tr><td>NWR4</td><td>1.248, 0.204, 0.282, 0.172, 0.276,
0.048, 0.368, 0.344, 0.230, 0.326,
0.324, 0.276, 0.026, 0.554, 0.238,
0.278, 0.150, 0.172, 0.636, 0.358,
0.378, 0.230, 0.270, 0.230, 0.132,
0.138, 0.210, 0.330, 0.398, 0.198,
0.160, 0.120, 0.108, 0.132, 0.142,
0.210, 0.272, 0.216, 0.378, 0.130,
0.320, 0.626, 0.368, 0.368, 0.210,
0.184, 0.248, 0.258, 0.140, 0.174,
0.308, 0.228, 0.106, 0.206, 0.266,
0.456, 0.158, 0.250, 0.744, 0.766,
0.066, 0.326, 0.380, 0.362, 0.194,
0.178, 0.274, 0.196, 0.136, 0.278,
0.208, 0.174, 0.146, 0.172, 0.224,
0.192, 0.314, 0.474, 0.284, 0.232,
0.148, 0.386, 0.460, 0.248, 0.356,
0.408, 0.234, 0.112, 0.166, 0.314,
0.184, 0.312, 0.220</td><td>1.380, 0.256, 0.258, 0.600, 0.216, 0.574,
0.156, 0.178, 0.518, 0.260, 0.400, 0.032,
0.276, 0.198, 0.218, 0.192, 0.162, 0.390,
0.220, 0.122, 0.414, 0.206, 0.306, 0.118,
0.184, 0.240, 0.152, 0.166, 0.154, 0.188,
0.186, 0.092, 0.214, 0.476, 0.432, 0.206,
0.326, 0.334, 0.304, 0.316, 0.164, 0.050,
0.270, 0.138, 0.380, 0.386, 0.360, 0.136,
0.388, 0.284, 0.310, 0.192, 0.198, 0.246,
0.258, 0.338, 0.192, 0.162, 0.096, 0.168,
0.194, 0.204, 0.350, 0.124, 0.242, 0.304,
0.102, 0.160, 0.162, 0.272, 0.188, 0.374,
0.352, 0.320, 0.438, 0.446, 0.188, 0.446,
0.624, 0.376, 0.492, 0.318, 0.260, 0.346,
0.174, 0.138, 0.478, 0.228, 0.160, 0.188,
0.468, 0.290</td></tr>
<tr><td>Total</td><td colspan="2">1.248, 0.132, 0.072, 0.184, 0.098, 0.160, 0.012, 0.276, 0.048, 0.264, 0.104, 0.112,
0.232, 0.230, 0.112, 0.156, 0.058, 0.120, 0.204, 0.276, 0.026, 0.012, 0.260, 0.282,
0.118, 0.032, 0.088, 0.188, 0.090, 0.108, 0.042, 0.172, 0.004, 0.192, 0.162, 0.278,
0.112, 0.220, 0.026, 0.096, 0.282, 0.132, 0.098, 0.108, 0.162, 0.144, 0.086, 0.032,
0.100, 0.084, 0.054, 0.186, 0.024, 0.128, 0.166, 0.036, 0.118, 0.188, 0.092, 0.094,
0.092, 0.012, 0.160, 0.042, 0.078, 0.108, 0.132, 0.142, 0.016, 0.194, 0.238, 0.034,
0.172, 0.044, 0.282, 0.096, 0.130, 0.108, 0.212, 0.092, 0.316, 0.164, 0.050, 0.004,
0.266, 0.102, 0.036, 0.332, 0.048, 0.162, 0.184, 0.040, 0.208, 0.152, 0.106, 0.030,
0.110, 0.174, 0.104, 0.204, 0.080, 0.148, 0.106, 0.056, 0.150, 0.042, 0.198, 0.026,
0.220, 0.236, 0.022, 0.136, 0.202, 0.048, 0.144, 0.162, 0.096, 0.168, 0.174, 0.020,
0.204, 0.350, 0.124, 0.068, 0.066, 0.108, 0.218, 0.086, 0.102, 0.160, 0.032, 0.130,
0.232, 0.040, 0.154, 0.034, 0.144, 0.230, 0.044, 0.196, 0.112, 0.024, 0.278, 0.018,
0.190, 0.174, 0.074, 0.072, 0.172, 0.202, 0.022, 0.166, 0.026, 0.314, 0.106, 0.368,
0.256, 0.028, 0.232, 0.116, 0.032, 0.386, 0.074, 0.318, 0.068, 0.192, 0.056, 0.290,
0.066, 0.108, 0.138, 0.162, 0.234, 0.082, 0.030, 0.166, 0.032, 0.160, 0.122, 0.066,
0.118, 0.312, 0.038, 0.182, 0.108</td></tr>
</table>

F2.4. Gib-1 Mutant type, Naa treated tomato root spacings (cm)

Root	Right	Left
NGR1	0.056, 0.220, 0.312, 0.430, 0.124, 0.370, 0.278, 0.198, 0.494, 0.048, 0.440, 0.248, 0.436, 0.304, 0.184, 0.160, 0.256, 0.156, 0.460, 0.320, 0.392, 0.170, 0.330, 0.674, 0.222, 0.196, 0.158, 0.198, 0.172, 0.298, 0.200, 0.132, 0.192, 0.174, 0.312, 0.128, 0.328, 0.116, 0.340, 0.402	0.238, 0.472, 0.438, 1.184, 0.332, 0.200, 0.144, 0.226, 0.262, 0.380, 0.238, 0.338, 0.136, 0.362, 0.382, 0.368, 0.958, 0.062, 0.368, 0.352, 0.298, 0.552, 0.472, 0.386, 0.404, 0.308, 0.496, 0.204
Total	0.056, 0.182, 0.038, 0.312, 0.122, 0.308, 0.124, 0.006, 0.364, 0.278, 0.198, 0.344, 0.150, 0.048, 0.134, 0.200, 0.106, 0.038, 0.210, 0.016, 0.262, 0.158, 0.222, 0.082, 0.156, 0.028, 0.160, 0.150, 0.106, 0.030, 0.126, 0.236, 0.224, 0.158, 0.162, 0.206, 0.186, 0.170, 0.330, 0.272, 0.062, 0.340, 0.028, 0.194, 0.158, 0.038, 0.158, 0.102, 0.096, 0.172, 0.284, 0.014, 0.200, 0.132, 0.126, 0.066, 0.174, 0.146, 0.166, 0.128, 0.110, 0.218, 0.090, 0.026, 0.340, 0.130, 0.204, 0.068	
NGR2	0.804, 0.642, 0.506, 0.388, 0.376, 0.308, 0.722, 0.158, 0.448, 0.254, 0.424, 0.264, 0.226, 0.402, 0.230, 0.456, 0.276, 0.126, 0.306, 0.380, 0.340, 0.252, 0.474, 0.622, 0.472	0.496, 0.430, 0.436, 0.246, 0.222, 0.178, 0.180, 0.274, 0.350, 0.198, 0.264, 0.338, 0.300, 0.096, 0.356, 0.160, 0.262, 0.202, 0.234, 0.260, 0.152, 0.260, 0.446, 0.244, 0.322, 0.250, 0.248, 0.214, 0.242, 0.456, 0.628, 0.152, 0.366, 0.164
Total	0.496, 0.308, 0.122, 0.436, 0.084, 0.162, 0.222, 0.122, 0.056, 0.180, 0.152, 0.122, 0.254, 0.096, 0.198, 0.014, 0.250, 0.338, 0.134, 0.158, 0.008, 0.096, 0.344, 0.012, 0.160, 0.082, 0.180, 0.202, 0.042, 0.192, 0.072, 0.188, 0.038, 0.114, 0.260, 0.028, 0.230, 0.188, 0.244, 0.024, 0.276, 0.022, 0.104, 0.146, 0.160, 0.088, 0.214, 0.078, 0.164, 0.176, 0.252, 0.028, 0.446, 0.182, 0.152, 0.288, 0.078, 0.164, 0.230	
NGR3	0.336, 1.000, 0.578, 0.302, 0.206, 0.344, 0.212, 0.244, 0.208, 0.304, 0.344, 0.324, 0.456, 1.228, 0.476, 0.330, 0.580, 0.380, 0.304, 0.154, 0.302	0.798, 1.316, 0.520, 0.230, 0.250, 0.212, 0.438, 0.364, 0.464, 0.358, 0.306, 0.196, 0.242, 0.180, 0.180, 0.396, 0.308, 0.288, 0.286, 0.198, 0.108, 0.166, 0.260, 0.224, 0.154
Total	0.336, 0.462, 0.538, 0.578, 0.200, 0.102, 0.206, 0.212, 0.132, 0.098, 0.114, 0.136, 0.108, 0.104, 0.104, 0.304, 0.030, 0.314, 0.050, 0.274, 0.190, 0.266, 0.092, 0.306, 0.196, 0.242, 0.180, 0.180, 0.032, 0.364, 0.112, 0.196, 0.134, 0.154, 0.286, 0.140, 0.058, 0.108, 0.166, 0.048, 0.212, 0.092, 0.132, 0.022, 0.132, 0.170	
NGR4	0.260, 0.262, 0.454, 0.390, 0.170, 0.128, 0.352, 0.302, 0.288, 0.292, 0.364, 0.184, 0.198, 0.234, 0.162, 0.348, 0.156, 0.208, 0.164, 0.506, 0.792, 0.674, 0.504, 0.658, 0.638, 0.132	0.802, 0.128, 0.456, 0.900, 0.496, 0.356, 0.614, 0.380, 0.536, 0.398, 0.326, 0.190, 0.112, 0.258, 0.244, 0.314, 0.398, 0.318, 0.516, 0.150, 0.280, 0.268
Total	0.260, 0.262, 0.280, 0.128, 0.046, 0.390, 0.020, 0.150, 0.128, 0.352, 0.270, 0.032, 0.288, 0.176, 0.116, 0.240, 0.124, 0.184, 0.198, 0.108, 0.126, 0.162, 0.092, 0.256, 0.156, 0.124, 0.084, 0.164, 0.150, 0.326, 0.030, 0.160, 0.112, 0.258, 0.244, 0.018, 0.296, 0.378, 0.020, 0.318, 0.166, 0.350, 0.150, 0.158, 0.122, 0.268, 0.248, 0.132	

F3. Fern Data Set

F3.1. Fern root spacings (cm)

Root	Right	Left
CT1	1.394, 1.084, 1.054, 1.016, 1.148, 1.082, 1.204, 1.234, 1.088, 0.932, 0.986, 1.012, 1.002, 1.066	2.130, 0.998, 1.058, 1.104, 1.120, 1.152, 1.248, 1.108, 1.016, 0.966, 0.934, 1.052, 1.032, 1.074
Total	1.394, 0.736, 0.348, 0.650, 0.404, 0.654, 0.362, 0.742, 0.406, 0.714, 0.368, 0.784, 0.420, 0.828, 0.406, 0.702, 0.386, 0.630, 0.302, 0.664, 0.322, 0.612, 0.400, 0.652, 0.350, 0.682, 0.384, 0.690	
CT2	0.828, 1.132, 1.046, 0.848, 0.754, 0.688, 0.832, 0.816, 0.940, 1.016, 1.188, 1.312, 1.244, 1.014, 1.004	1.274, 1.050, 0.982, 0.862, 0.854, 0.754, 0.840, 0.902, 1.018, 1.094, 1.262, 1.180, 1.138
Total	0.828, 0.446, 0.686, 0.364, 0.682, 0.300, 0.548, 0.314, 0.440, 0.414, 0.274, 0.480, 0.352, 0.488, 0.328, 0.574, 0.366, 0.652, 0.364, 0.730, 0.458, 0.804, 0.508, 0.672, 0.572, 0.566, 0.448, 1.004	
CT3	0.802, 0.756, 0.816, 0.602, 0.722, 0.762, 0.878, 1.006, 0.970, 1.026, 1.136, 2.114, 1.056, 0.666	1.226, 0.832, 0.654, 0.724, 0.710, 0.710, 1.146, 0.990, 0.962, 1.034, 1.746, 1.634, 0.690
Total	0.802, 0.424, 0.332, 0.500, 0.316, 0.338, 0.264, 0.460, 0.262, 0.448, 0.314, 0.396, 0.482, 0.664, 0.342, 0.648, 0.322, 0.640, 0.386, 0.648, 0.488, 1.258, 0.856, 0.778, 0.278, 0.412, 0.254	
CT4	0.486, 1.396, 1.226,1.576,0.960, 0.942, 1.124, 1.156, 1.198, 1.070, 0.974	0.948, 1.338, 2.018, 1.022, 0.912, 1.008, 1.232, 1.200, 1.052, 1.022
Total	0.486, 0.462, 0.934, 0.404, 0.822, 1.196, 0.380, 0.642, 0.318, 0.594, 0.348, 0.660, 0.464, 0.768, 0.388, 0.812, 0.386, 0.666, 0.404, 0.618, 0.356	
MQ	0.772, 1.040, 0.134, 0.204, 0.116, 0.274, 0.174, 0.160, 0.126, 0.138, 0.082, 0.090, 0.070, 0.092, 0.066, 0.082, 0.070, 0.108, 0.098, 0.112, 0.096, 0.140, 0.184, 0.156, 0.168, 0.082, 0.134, 0.132, 0.162, 0.146, 0.192, 0.200, 0.196, 0.210, 0.516, 0.866, 0.310, 0.356, 0.340, 0.190, 0.182, 0.276, 0.296, 0.340, 0.202, 0.152, 0.266, 0.286, 0.246, 0.118, 0.140, 0.182, 0.118, 0.094, 0.124, 0.110, 0.146, 0.178, 0.128, 0.094, 0.138, 0.106, 0.152, 0.114, 0.146, 0.172, 0.228, 0.118, 0.102, 0.190, 0.194, 0.186, 0.076, 0.114, 0.118, 0.158, 0.146, 0.180, 0.224, 0.102, 0.124, 0.152, 0.208, 0.230, 0.282, 0.134, 0.234, 0.242, 0.274, 0.170, 0.196, 0.270, 0.280, 0.346, 0.174, 0.226, 0.300	0.814, 0.310, 0.376, 0.294, 0.134, 0.108, 0.108, 0.120, 0.124, 0.142, 0.284, 0.138, 0.122, 0.102, 0.090, 0.106, 0.088, 0.088, 0.080, 0.091, 0.091, 0.104, 0.130, 0.166, 0.180, 0.114, 0.156, 0.122, 0.070, 0.126, 0.170, 0.184, 0.200, 0.336, 0.150, 0.182, 0.186, 0.204, 0.448, 0.362, 0.408, 0.568, 0.424, 0.618, 0.196, 0.202, 0.310, 1.290, 0.106, 0.110, 0.128, 0.152, 0.188, 0.124, 0.114, 0.118, 0.144, 0.140, 0.186, 0.098, 0.094, 0.122, 0.092, 0.130, 0.132, 0.156, 0.114, 0.128, 0.154, 0.110, 0.128, 0.182, 0.272, 0.118, 0.106, 0.140, 0.208, 0.236, 0.196, 0.154, 0.226, 0.240, 0.300, 0.144, 0.188, 0.230, 0.290, 0.188, 0.202, 0.234, 0.400, 0.276, 0.324
Total	0.772, 0.042, 0.310, 0.376, 0.294, 0.018, 0.116, 0.018, 0.090, 0.108, 0.006, 0.114, 0.002, 0.122, 0.142, 0.010, 0.174, 0.100, 0.060, 0.078, 0.048, 0.074, 0.064, 0.038, 0.044, 0.046, 0.044, 0.062, 0.008, 0.080, 0.012, 0.066, 0.010, 0.072, 0.008, 0.062, 0.029, 0.079, 0.012, 0.086, 0.018, 0.094, 0.036, 0.060, 0.106, 0.034, 0.146, 0.038, 0.076, 0.080, 0.076, 0.092, 0.030, 0.052, 0.018, 0.116, 0.010, 0.122, 0.048, 0.114, 0.070, 0.076, 0.124, 0.068, 0.200, 0.068, 0.128, 0.022, 0.182, 0.006, 0.180, 0.204, 0.132, 0.316, 0.362, 0.188, 0.220, 0.090, 0.356, 0.122, 0.218, 0.190, 0.016, 0.166, 0.276, 0.176, 0.120, 0.076, 0.202, 0.062, 0.202, 0.046, 0.106, 0.266, 0.286, 0.246, 0.118, 0.140, 0.128, 0.054, 0.052, 0.066, 0.044, 0.050, 0.078, 0.046, 0.106, 0.004, 0.146, 0.038, 0.124, 0.016, 0.098, 0.030, 0.088, 0.006, 0.138, 0.106, 0.034, 0.118, 0.068, 0.046, 0.052, 0.094, 0.122, 0.050, 0.042, 0.130, 0.056, 0.076, 0.042, 0.102, 0.012, 0.114, 0.064, 0.064, 0.130, 0.024, 0.110, 0.052, 0.076, 0.114, 0.068, 0.050, 0.158, 0.064, 0.082, 0.036, 0.106, 0.038, 0.102, 0.122, 0.086, 0.016, 0.124, 0.096, 0.056, 0.140, 0.068, 0.086, 0.144, 0.082, 0.200, 0.040, 0.094, 0.206, 0.028, 0.116, 0.126, 0.062, 0.212, 0.018, 0.152, 0.138, 0.058, 0.130, 0.140, 0.062, 0.218, 0.016, 0.330, 0.070, 0.104, 0.172, 0.054, 0.270, 0.030	

REFERENCES

Barlow, P. W. (1984). *Positional Controls in Root Development*. In Positional Controls in Plant Development (ed. P. W. Barlow and D. J. Carr), Cambridge University Press, pp. 281–318.

Barlow, P. W. (1989). *Meristem, metamers and modules and the development of shoot and root systems*. Botanical Journal of Linnean Society, **100**, pp.255–279.

Barlow, P. W. and Adam, J. S. (1988). *The Postion and Growth of Lateral Roots on Cultured Root Axes of Tomato*. Pl. Syst. Evol., **158**, pp. 141–154.

Best, D. J. and Fisher, N. I. (1979). *Efficient Simulation of the von Mises Distribution*. Appl. Statist., **28**, no. 2, pp. 152–157.

Best, N. G., Cowles, M. K. and Vines, S. K. (1995). *CODA: Convergence Diagnosis and Output Analysis Software for Gibbs Sampling Output. Version 0.4.* Cambridge: Medical Research Council Biostatistics Unit.

Brent, R. P. (1974). *Algorithm 488*. Comm. A.C.M., p. 704.

Broadbent, S. R. (1955). *Quantum Hypotheses*. Biometrika, **42**, pp. 45–57.

Broadbent, S. R. (1956). *Examination of a quantum hypothesis based on a single set of data*. Biometrika, **43**, pp.32–44.

Brooks, S. P. (1998). *Markov Chain Monte Carlo method and its application*. The Statistician, **47**, part 1, pp. 69–100.

Cramér, H. and Leadbetter, M. R. (1967). *Stationary and Related Stochastic Processes*. New York: John Wiley.

Crawford, G. I. (1976). *Discussion of Freeman's paper*. J. R. Statist. Soc. A, **139**, pp. 41–42.

Cryer, J. D. (1986). *Time Series Analysis*. Boston: Duxbury Press.

David, H. A. (1970). *Order Statistics*. New York: John Wiley & Sons.

Draper, N. R. and Smith, H. (1980). *Applied Regression Analysis*. New York: John Wiley & Sons.

Durand, D. and Greenwood, J. A. (1957). *Random Unit Vectors II: usefulness of Grame–Charlier and related series in approximating distributions*. Ann. Math. Statist., **28**, pp. 978–85.

Embrechts, P., Klüppelberg, C. and Mikosch, T. (1997). *Modelling Extremal Events*. Berlin: Springer.

Evans, M., Hastings, N. and Peacock, B. (1993). *Statistical Distributions*. second edition. New York: John Wiley & Sons.

Fieller, N. R. J. (1993). *Archaeostatistics: old statistics in ancient contexts*. The Statistician, **42**, pp. 279–295.

Fieller, N. R. J., Flenley, E. C., Gilbertson, D. D. and Hunt, C. O. (1990). *The UNESCO Libyan Valleys survey*. Libyan Studies, **21**, pp. 49–59.

Fisher, N. I. (1995). *Statistical Analysis of Circular Data*. Cambridge: Cambridge University Press.

Fisher, R. A. (1924). J. R. Statist. Soc., **87**, p. 442.

Fisher, R. A. (1950). *Statistical Methods for Research Workers No.5*. Edinburg: Oliver and Boyd.

Fowler, G. H. (1909). Trans. Linn. Soc. (Zool.), 2nd series, p. 9.

Freeman, P. R. (1976). *A Bayesian Analysis of the Megalithic Yard*. J. R. Statist. Soc. A, **139**, pp. 20–55.

Gamerman, D. (1997). *Markov Chain Monte Carlo, Stochastic Simulation for Bayesian Inference*. London: Chapman & Hall.

Gelfand, A. E., Dey, D. K. and Chang, H. (1992). *Model determination using predictive distributions with implementation via sampling-based methods*. In

Bayesian Statistics 4, (eds. Bernardo, J. M., Berger, J. O., Dawid, A. P. and Smith, A. F. M.), pp. 147-168, Oxford University Press.

Gelman, A., Carlin, J. B., Stern, H. S. and Rubin, D. B. (1995). *Bayesian Data Analysis*. London: Chapman & Hall.

Gelman, A. and Rubin, D. B. (1992). *Inference From Iterative Simulation Using Multiple Sequences*. Statistical Science, **7**, pp. 457–72.

Geweke, J. (1992). *Evaluating the Accuracy of Sampling–based Approaches to Calculating Posterior Moments*. In Bayesian Statistics 4, (eds. J.M. Bernardo, J.O. Berger, A.P. Dawid and A.F.M. Smith), Oxford University Press.

Gilbertson, D. D., Hunt, C. O. and Fieller, N. R. J. (1993). *The UNESCO Libyan Valleys Survey*. Libyan Studies, **24**.

Gilks, W. R., Richardson, S. and Spiegelhalter, D. J. (eds.) (1996). *Markov Chain Monte Carlo in Practice*. London: Chapman & Hall.

Grant, P. J. (1952). Proc. Phys. Soc. London, A, **65**, p. 150.

Grieve, R. A. F., Sharpton, V. L., Goodacre, A. K. and Garvin, J. B. (1985). *A Perspective on the evidence for periodic cometary impacts on Earth*. Earth and Planet Science Letters, **76**, pp. 1–9.

Gumbel, E. J. (1958). *Statistics of Extremes*. New York: Colombia University Press.

Guthrie, B. N. G. and Napier, W. M. (1991). *Evidence for Redshift Periodicity in Nearby Field* Galaxies. Mon. Not. R. Astr. Soc., **253**, p. 533.

Hammersley, J. M. and Morton, K. W. (1954). *Symposium on Monte Carlo Methods*. J.R.Statist.Soc. B, **16**, p. 23.

Harding, E. F. (1986). *Modelling: the classical approach*. The Statistician, **35**, pp. 135–142.

Hedges, L. V. and Olkin, I. (1985). *Statistical Methods for Meta–Analysis*. New York: Academic Press.

Heidelberger, P. and Welch, P. (1983). *Simulation Run Length Control in the Presence of an Initial Transient*. Operations Research, **31**, pp. 1109–1144.

Hewson, A. D. (1980). *The Ashanti Weights*. J. Archaeological Science, **7**, pp. 363–370.

Hochberg, Y. and Tamhane, A. (1987). *Multiple Comparison Procedures*. New York: John Wiley & Sons.

Johnston, J. P., Longuet–Higgins, H. C. and Ogston, A. G. (1945). *On the Distribution of the Molecular Weights of Proteins*. Trans. Faraday Soc., **41**, pp. 558–593.

Kendall, D. G. (1974). *Hunting Quanta*. Phil.Trans. R. Soc. A, **276**, pp. 231–266. See also the corrections and additions set out in the discussion following Mardia, K. V. (1975). *Statistics of Directional Data*. J. R. Statist. Soc. B, **37**, pp. 349–393.

Kent, J. T. (1975). *A Weak Convergence Theorem for the Empirical Characteristic Function*. J. Appl. Prob., **12**, pp. 515–523.

Kent, J. T. (1976). *Discussion of Freeman's paper*. J. R. Statist. Soc. A, **139**, pp. 39–40.

Kirk, T. H. (1994). *A Model for the Megalithic Yard*. Q. J. R. Astr. Soc., **35**, pp. 573–575.

Klein, R. G., Wolf, C., Freeman, L. G. and Allwarden, K. (1981). *The Use of Dental Crown Heights for Constructing Age Profiles of Red Deer and Similar Species in Archaeological Samples*. Journal of Archaeological Science, **8**, pp. 1–31.

Knox, I. (1994). *Quantal Redshifts.* Msc. Dissertation (unpublished), University of Sheffield.

Knuth, D. E. (1981). *Seminumerical Algorithms*, 2nd ed., vol.2 of *The Art of Computer Programming* (Reading, MA: Addison–Wesley), section 3.2–3.3.

L'Ecuyer, P. (1988). Communications of ACM, **31**, pp. 742–774.

Lin, B. L. and Raghavan, V. (1991). *Lateral Root Initiation in Marsilea Quadrifolia. I. Origin and Histogenesis of Lateral Roots*. Can. J. Bot., **69**, pp. 123–135.

Littell, R. C. and Folks, J. L. (1971). *Asymptotic Optimality of Fisher's Method of Combining Independent Tests*. Journal of the American Statistical Association, **66**, no. 336, pp. 802–806.

Lloret, P. G., Pulgarin, A., Casimiro, I., Molina, M. and Casero, P. J. (1998). *Effect of Treatment Naphthaleneactetic Acid on the Arrangement of Lateral Roots in Onion (Allium cepa L.): General Pattern and Coordination between Ranks*. Bot. Acta, **111**, pp. 55–61.

Marden, J. I. (1991). *Sensitive and Sturdy p–Values*. The Annals of Statistics, **19**, no. 2, pp. 918–934.

Mardia, K. V. (1972). *Statistics of Directional Data*. London: Academic Press.

Neave, R. H. (1973). *Miscellanea on Using the Box–Muller transformation with Multiplicative Congruential Pseudo–Random Number Generators*. Appl. Stats., **22**, pp. 92–97.

Newson, R. B., Parker, J. S. and Barlow, P. W. (1993a). *Are Lateral Roots of Tomato Spaced by Multiples of a Fundamental Distance?*. Annals of Botany, **71**, pp. 549–557.

Newson, R. B., Parker, J. S. and Barlow, P. W. (1993b). *Search for a "Fundamental Distance" that Determines the Spacing of Lateral Roots*. Poster Presentation, Long Ashton Research Station, Bristol.

Numerical Algorithms Group (1995). *NAG Library Manual*. Mark 15, routine G05CAF and G05CCF. Oxford: Numerical Algorithm Groups.

Olson, J. (1980). *The Roots of Stonehenge*. Publications of the Astronomical Society of the Pacific, **92**, no. 549, p. 548.

Park, S. K. and Miller, K. W. (1988). *Communications of the ACM.*, **31**, pp. 1192–1201.

Petruso, K. M. (1978). *Systems of Weight in the Bronze Age Aegean*. Ph.D. Diss., Indiana University.

Petruso, K. M. (1981). *Early Weights and Weighing in Egypt and the Indus Valley*. Bulletin of the Museum of Fine Arts, Boston, **79**, pp. 44–51.

Petruso, K. M. (1992). *Aya Irini: the Balance Weights: an analysis of weight measurement in prehistoric Crete and Cycladic Islands*. KEOS Part 8, Mainz on Rhine, Von Zabern.

Press, W. H., Flannery, B. P., Teukolsky, S. A. and Vetterling, W. T. (1992). *Numerical Recipes in FORTRAN: The Art of Scientific Computing*. Second edition. Cambridge: Cambridge University Press.

Prout, W. (1815). *On the Relation Between the Specific Gravities of Bodies in their Gaseous State and the Weights of their Atoms*. Annals of Philosophy, **6**, pp. 321–330.

Raftery, A. L. and Lewis, S. (1992a). How Many Iterations in the Gibbs Sampler? In *Bayesian Statistics 4*, (ed. J. M. Bernardo, J. O. Berger, A. P. Dawid and A.F.M. Smith), Oxford University Press, pp. 763–774.

Raftery, A. L. and Lewis, S. (1992b). Comment: One Long Run with Diagnostics: Implementation Strategies for Markov Chain Monte Carlo. *Statistical Science*, **7**, pp. 493–497.

Ripley, B. D. (1983). *Computer Generation of Random Variables: A Tutorial*. International Statistical Review, **51**, pp. 301–319.

Rosenthal, R. (1978). *Combining Results of Independent Studies*. Psychological Bulletin, **85**, pp. 185–193.

Rottländer, R. C. A. (1996). *New Ideas About Old units of Length*. Interdisciplinary Science Reviews, **21**, no. 3, pp. 235–242.

Rottländer, R. C. A. (1997). *The Development of Some Historical Units of Longitudinal Measurement from the Ell of Nippur*. PTB–Mitteilungen, **107**, no. 4, pp. 247–256.

Ruggles, C. L. N. (1984). *Megalithic Astronomy: A new archaeological and statistical study of 300 western Scottish sites.* B.A.R. British Series, p. 123.

Salisbury, D. (1994). *Letters: Remarkable Events*. New Scientist, **141**, no.1907, p.46.

Silverman, B. W. (1976). *Discussion of Freeman's paper*. J. R. Statist. Soc. A, **139**, pp. 44–45.

Spiegelhalter, D. J., Thomas, A., Best, N. G. and Gilks, W. R. (1995). *BUGS Manual and Examples: Version 0.6.* Cambridge: Medical Research Council Biostatistics Unit.

Stephens, M. A. (1963). *Random walk on a circle*. Biometrika, **50**, pp. 385–390.

Stewart, I. (1993). *Inside Science*. New Scientist, no. 1902, p. 1204.

Svedberg, T. (1939). *A discussion on the Protein Molecule*. Proc. Ro. Soc. A, **170**, p. 40.

Thom, A. (1955). *A Statistical Examination of the Megalithic Sites in Britain*. J. R. Statist. Soc. A., **118**, pp. 275–295.

Thom, A. (1967). *Megalithic Sites in Britain*. Oxford: Clarendon Press.

Tifft, W. G. and Cocke, W. J. (1984). *Global Redshift Quantization*. Astrophys. J., **287**, p. 492.

Turner, A. (1980). *The Paleoecology of the British Upper Pleistocene Large Predators and Their Prey*. Ph.D. Thesis, University of Sheffield.

Turner, A. and Fieller, N. R. J. (1981). *Detection of periodicity in crown heights of Devensian horse teeth*. Computer Applications in Archaeology, **9**, p. 120.

von Mises, R. (1918). Phys. Z., **19**, pp. 490–500.

Wichmann, B. A. and Hill, I. D. (1982). Algorithm AS 183. *An efficient and portable pseudo–random number generator.* Applied Statistics, **31**, no. 2, pp. 188–190.

Wigglesworth, V.D. (1942). *Principles of Insect Physiology*. 2nd ed. London: Methuen.